THE EFFECTS OF CHANGING REDOX CONDITIONS ON THE PHENOLIC DISTRIBUTIONS AND CARBON CYCLING AT BUTTERBURN FLOW

Kerry Lea Simcock

A thesis submitted to Newcastle University in partial fulfilment of the requirements for the degree of Doctor of Philosophy in the Faculty of Science, Agriculture and Engineering

School of Natural and Environmental Sciences
Drummond Building
Newcastle University
United Kingdom

February 2019

Declaration

I hereby certify that the work presented in this thesis is my original research work. Wherever contributions of others are involved, every effort is made to indicate this clearly, with due reference to the literature, and acknowledgement of collaborative research and discussions. No part of this work has been submitted previously for a degree at this or any other university.

Kerry Lea Simcock

Abstract

Northern peatlands store around 30% of soil carbon and 75% of atmospheric carbon and consist of a complex mixture of humic substances including recalcitrant phenolics such as lignins, tannins and sphagnum acid which make a significant contribution to the organic carbon content. Changes in water table regimes and vegetation inputs will impact the distributions and amounts of these phenols which will in turn significantly influence the carbon storage capacity. This study presents an exploration into the effects of water table fluctuations on redox conditions as well as the accumulation and degradation of lignin and *Sphagnum* phenols along a bog-fen gradient from Butterburn Flow, Cumbria UK. The insoluble residues of the living vegetation and associated roots as well as the peat were analysed using unlabelled and ^{13}C-labelled tetramethylammonium hydroxide thermochemolysis.

All *Sphagnum* mosses contained significant concentrations of sphagnum acid biomarkers not identified in either the above or below ground sections of any vascular plants. The chemical proxies σ and SR% which utilise these biomarkers proved useful indicators of *Sphagnum* abundance and were in no way distorted by the presence of other species, unlike the lignin proxy Λ. In some species, concentrations of both lignin-derived phenols and carbohydrates in vascular plant roots exceeded concentrations in above-ground sections of the same species. Therefore, for peats that contain dense and deep-reaching root systems, Λ and carbohydrate concentrations may be distorted. Bryophytes also contained lignin phenols, however, concentrations were minimal. The presence of such phenols is a result of the phenol-rich bog water in which the mosses reside.

Total organic carbon increased as a function of depth in all cores, despite concentrations of isosaccharinic acids, metasaccharinic acids and sphagnum acid biomarkers decreasing with depth. The carbon storage capacity of Butterburn Flow was estimated at 5.1 t ha^{-1}, which agrees with previous estimates for British bog habitats. Overall, sites with lowest water table tended to have lower phenolic content, higher oxidative stress and lower carbohydrate content. Therefore, increased climatic disturbance leading to water-table draw-down will lead to significant oxidative stress and chemical alteration of the peat.

Acknowledgements

I would firstly like to acknowledge my supervisors, Dr. Geoff Abbott and Dr. Chris Vane for providing this opportunity, help with fieldwork and collection of key results as well as supporting and encouraging me throughout the PhD. I also thank the British Geological Survey and Newcastle University NIReS Lord Adams Sustainability Studentship for funding this work. I would particularly like to thank the technical staff Bernie Bowler, Dave Early and Paul Donohoe who have been key to the success of this project, there to offer advice, support and comedy consistently no matter what the problem or setback. You have literally kept me going in the lab over the past 3 years!

I can't give all the credit to the Newcastle staff, however, and a special thank you goes to Dr. Daniel Stabler and Dr. Helen Gray who have put up with my never-ending questions, self-doubt, mood swings, anger, and minor mental breakdowns along with my infuriating inability to use technology correctly! Your understanding, advice, support and friendship is what has truly got me through this PhD, along with you telling me to man up, grow a pair, and get over myself!! Couldn't have done it without you!!

I would also like to give a big thank you to my dad, who has never doubted my abilities, always offered advice when needed, agreed with me on things he knew nothing about, and shared my anger and frustration even though he didn't have a clue what I was talking about or what it meant! Finally, a huge thank you also to my grandma, who has always been in my thoughts and has given me the motivation and drive to make it this far. You always made me feel like my best effort was good enough and that I could never fail. I dedicate this thesis to you.

Contents

Declaration i

Abstract ii

Acknowledgements iii

List of figures xvi

List of tables xviii

1 Introduction and literature review 1

1.1 Introduction 2

1.2 Literature review 4

1.2.1 Peatlands and organic carbon 4

1.2.2 *Sphagnum* mosses 7

1.2.3 Characterisation of sphagnum acid 10

1.2.4 Vascular plants and lignin 13

1.2.5 Characterisation of lignin 18

1.2.6 Thermally assisted hydrolysis and methylation (THM) in the presence of Tetramethylammonium hydroxide (TMAH) 20

1.2.7 ^{13}C labelled TMAH 22

1.2.8 Tannins 24

1.2.9 Carbohydrates 26

1.3 Aims and objectives 27

2 **Field site and methodology** **30**
2.1 Butterburn Flow 31
2.1.1 Hydrological analyses 33
2.1.2 Sample collection and preparation 34
2.2 Laboratory and extraction procedures 35
2.2.1 Chemical analysis 36
2.2.2 Quality control 39
2.2.3 Compound quantification and normalisation 40
2.2.4 Pyroprobe calibration 41
2.2.5 Unlabelled and ^{13}C labelled TMAH 43
2.2.6 Bulk density and elemental analyses 45
2.3 Statistical analysis 47

3 **Exploring the biochemistry of the dominant peat-forming vegetation across a range of environmental conditions at Butterburn Flow** **48**
3.1 Introduction 49
3.2 Methods 52
3.2.1 Sample collection and preparation 52
3.2.2 THM in the presence of TMAH 54
3.2.3 Chemical proxies 54
3.2.4 Exploration of carbohydrates 55
3.2.5 Statistical analyses 63
3.3 Results and discussion 63
3.3.1 Vegetation assessment 63
3.3.2 THM in the presence of TMAH 67
3.4 Conclusions 90

4 **Exploring the biogeochemistry of the peat across**

a range of environmental conditions at Butterburn Flow **92**

4.1 Introduction . . . 93
4.2 Methods . . . 95
4.2.1 Sample collection and preparation . . . 95
4.2.2 Chemical proxies . . . 96
4.2.3 Core dating . . . 96
4.2.4 Statistical analyses . . . 97
4.3 Results and discussion . . . 99
4.3.1 Water table dynamics . . . 99
4.3.2 Elemental analysis . . . 102
4.3.3 Bulk density . . . 107
4.3.4 Organic carbon storage . . . 110
4.3.5 THM in the presence of TMAH . . . 113
4.4 Conclusions . . . 149

5 An investigation into the presence of lignin-derived phenolics in *Sphagnum* mosses **153**

5.1 Introduction . . . 154
5.2 Methods . . . 157
5.2.1 Field site and sample collection . . . 157
5.2.2 Sample preparation and experimental design . . . 158
5.2.3 Chemical extraction and analytical analysis of the plants . . . 162
5.2.4 Chemical extraction and analytical analysis of the bog water . . . 162
5.2.5 Statistical analyses . . . 163
5.3 Results and discussion . . . 164
5.3.1 Lignin composition of the bog water . . . 165
5.3.2 Chemical composition of the *Sphagnum* mosses . . . 169
5.4 Conclusions . . . 178

6 General discussion and future work 180

6.1 Discussion and conclusions 181

6.1.1 Peatland vegetation 182

6.1.2 Peat chemistry and carbon storage 184

6.1.3 *Sphagnum* mosses 186

6.1.4 Recommendations for future work 187

References 190

Appendicies 222

List of Figures

1.1 A map displaying the global distribution of peatlands and their contribution to the total land area. Adapted from International Peat Society (2001) 5

1.2 Structure of galacturonic acid 9

1.3 A schematic of the structure of sphagnum acid (*p*-hydroxy-*β*-[carboxymethyl]- cinnamic acid) 10

1.4 A schematic of the four dominant sphagnum acid thermochemolysis products (I) methylated 4-isopropenylphenol (IUPAC: 1-methoxy-4-(prop-1-en-2-yl)benzene), (IIa) methylated *cis*-3-(4-hydroxyphen-1-yl)but-2-enoic acid (IUPAC: (Z)-methyl 3-(4-methoxyphenyl)but-2-enoate), (IIb) methylated *trans*-3-(4-hydroxyphen-1-yl)but-2-enoic acid (IUPAC: (E)-methyl 3-(4-methoxyphenyl)but-2-enoate) and (III) methylated 3-(4-hydroxyphen-1-yl)but-3-enoic acid (IUPAC: methyl 3-(4-methoxyphenyl)but-3-enoate), i and iii; methylated (Z) and (E)- 2-methyl-3-(4'-hydroxyphen-1-yl)but-2-enoic acid and ii; methylated 3-(4'-hydroxyphen-1-yl)pent-3-enoic acid (van der Heijden, 1994). Adapted from (Abbott et al., 2013) 12

1.5 Three main alcohol monomers that form the lignin bipolymer; *p*-coumaryl alcohol, coniferyl alcohol, and sinapyl alcohol. Adapted from (Weng and Chapple, 2010) 14

1.6 A schematic representation of a lignin polymer (adapted from Dorrestijn et al. (2000); L = lignin biomacromolecule. The box displays the dominant *β*-O-4 linkages found throughout the lignin bipolymer 15

1.7 A schematic representation of 6 linkage types found throughout the lignin bipolymer. a) = β-O-4 link, b) = β-5 link, c) = β-β link, d) = β-1 link, e) = 5-5 link and f) = 5-O-4 link. Adapted from Dorrestijn et al. (2000) 16
1.8 A schematic representation of the changes that occur from the fungal degradation of guaiacyl lignin. Adapted from Filley et al. (2000) 17
1.9 A schematic of the vanillyl and syringyl monomeric products formed from lignin during CuO oxidation (a) and TMAH thermochemolysis (b). The cinnamyl products formed in from both methods are identical, and so are not shown. Adapted from Wysocki et al. (2008) 20
1.10 Schematic demonstrating how intact lignin such as Syringic acid can be distinguished from tannins such as Gallic acid molecules that share a similar structure using ^{13}C TMAH. Asterisks indicate added ^{13}C methyl groups 23
1.11 Schematic Showing the chemical structure of a) condensed tannins and b) hydrolysable tannins. R = H; epicatechin, R = OH; epigallocatechin. Where PC = procyanidins and PD = prodelphinidins. Adapted from Nierop et al. (2005*b*). 25

2.1 Map of Butterburn Flow and sampling transect. Black circles indicate where cores were taken. 1 = Degraded Bog (DB), 2 = Bog Plateau (BP), 3 = Bog Margin (BM), 4 = Fen Lagg (FL) 33
2.2 Mean concentrations of each compound from 12 analyses of the bulk sample. Error bars show the standard error from 12 replicates. 40
2.3 Temperature calibration of the pyroprobe showing mean actual and mean observed melting points of five inorganic salts. Error bars represent standard error from three analytical replicates 43

2.4 Schematic of the methylation process of syringic acid (lignin compound, %1OH - 3,4,5-trimethoxybenzoic acid methyl ester) and gallic acid (tannin compound, %3OH - 3,4,5-trihydroxybenzoic acid) using both ^{12}C TMAH and ^{13}C TMAH, and the resulting change in molecular mass, allowing accurate identification of non-lignin compounds. 45

3.1 TMAH thermochemolysis formation of methylated metasaccharinic acids as proposed by Fabbri and Helleur (1999) and their associated epimers (Chiavari et al., 2007). These products are labelled as MC1-4 in this study. 56

3.2 TMAH thermochemolysis mass spectrum and fragmentation pathway of partially methylated isosaccharinic acid; peak 5. Modified from Schwarzinger (2004) 58

3.3 TMAH thermochemolysis formation of methylated isosaccharinic acids as proposed by Schwarzinger et al. (2002). These products are labelled as 1-4 in this study. Modified from Schwarzinger (2004) 59

3.4 Mass spectra for the polysaccharide derived compounds 1-5 as identified in this project 60

3.5 Mass spectra for the methylated carbohydrates (MC1-4) in the presence of both unlabelled and ^{13}C labelled TMAH. Red numbers indicate the number of methyl groups added during methylation. 62

3.6 Contribution of each plant type analysed to the σ, Λ chemical proxies, and their cellulose and methylated carbohydrate content 66

3.7 Partial total ion chromatogram (TIC) of the thermochemolysis products from *Sphagnum capillifolium, Sphagnum magellanicum, Sphagnum palustre, Sphagnum tenellum*. IS denotes internal standard. Peak identities are listed in Table 3.2. 73

3.8 Partial total ion chromatogram (TIC) of the thermochemolysis products from *Sphagnum cuspidatum, Sphagnum fallax* and *Sphagnum papillosum*. IS denotes internal standard. Peak identities are listed in Table 3.2. . . 74

3.9 Partial total ion chromatogram (TIC) of the thermochemolysis products from *Trichophorum cespitosum, Molinia caerulea, Hypnum jutlandicum* and *Pleurozium schreberi*. IS denotes internal standard. Peak identities are listed in Table 3.2. 76

3.10 Partial total ion chromatogram (TIC) of the thermochemolysis products from *Calluna vulgaris, Erica tetralix, Vaccinium oxycoccus* and *Potentilla erecta*. IS denotes internal standard. Peak identities are listed in Table 3.2. 78

3.11 Partial total ion chromatogram (TIC) of the thermochemolysis products from *Galium saxatile, Narthecium ossifragum, Deschampsia flexuosa* and *Eriophorum vaginatum*. IS denotes internal standard. Peak identities are listed in Table 3.2. 79

3.12 Partial total ion chromatogram (TIC) of the thermochemolysis products from the roots of *Calluna vulgaris, Erica tetralix, Vaccinium oxycoccus* and *Molinia caerulea*. IS denotes internal standard. Peak identities are listed in Table 3.2. 82

3.13 Contribution of shoots and roots from *Calluna vulgaris, Erica tetralix, Vaccinium oxycoccus* and *Molinia caerulea* to (a) the Λ chemical proxy and (b) their total carbohydrate content. Error bars represent the standard error from two analytical replicates. 85

3.14 Total amounts of σ, Λ and carbohydrate in the plant samples contributing to the peat at each coring site; Degraded bog (DB), Bog plateau (BP), Bog margin (BM) and Fen lagg (FL). 88

3.15 Total amounts of σ, Λ and carbohydrate in the surface peat (2-4 cm) at each coring site; Degraded bog (DB), Bog plateau (BP), Bog margin (BM) and Fen lagg (FL). 89

4.1 Water table (grey fill) and water temperature (solid black line) fluctuations over 12 months at Degraded Bog, DB (a), Bog Plateau, BP (b), Bog Margin, BM (c) and Fen Lagg, FL (d). The water table is presented as a distance from ground level (0 cm), dashed lines represent minimum and maximum values. Data for DB was recorded previous (Oct-Sep 2014-15) to the other 3 sites (Sep-Aug 2015-16). 100

4.2 Linear regression showing changes in total organic carbon (%) as a function of depth from the mean water table (Solid blue line) for a) Degraded Bog, b) Bog Plateau, c) Bog Margin and d) Fen Lagg. Dashed lines represent the minimum and maximum water table 104

4.3 Bulk density profiles at (a) DB, (b) BP, (c) BM and (d) FL sites. Depth is from the surface, and water table range is indicated by the dotted lines. Note the different scale used for DB 109

4.4 Cumulative organic carbon storage profiles at (a) Degraded Bog, DB, (b) Bog Plateau, BP, (c) Bog Margin, BM and (d) Fen Lagg, FL sites. Depth is from the surface, and water table range is indicated by the dotted lines. Note the different scales used. 112

4.5 Partial chromatogram for the total ion current (TIC) of the thermochemolysis products from DB (a), BP (b), BM (c) and FL (d) at 2-4 cm depth. Peak identities are listed in Table 4.3 116

4.6 Depth profiles of σ and SR% relative to the mean water table (MWT) for Degraded bog (a), Bog plateau (b), Bog margin (c) and Fen lagg (d) sites. Negative values on the y-axis indicate samples below the MWT, positive values indicate samples above the MWT. 0 and the solid blue lines indicate the MWT, with the dashed lines indicating the minimum and maximum water table levels. Note the different scale used. Error bars represent standard error for two analytical replicates. 118

4.7 Depth profiles of σ and SR% relative to the mean water table (MWT) for both hummock and hollow cores from (a), Bog plateau (a), Bog margin (b), Fen lagg (c) and Swamp forest (d) sites at Rygmossen, Sweden. Negative values on the y-axis indicate samples below the MWT, positive values indicate samples above the MWT. 0 and the solid blue lines indicate the MWT, with minimum and maximum water table levels indicated by the dashed lined for hollows and the solid black lines for hummocks. Error bars represent standard error for two analytical replicates. Adapted from Abbott et al. (2013) 121

4.8 Depth profiles relative to mean water table (MWT) of individual σ component yields (mg/100 mg OC) for Degraded bog (a), Bog plateau (b), Bog margin (c) and Fen lagg (d). Negative values on the y-axis indicate samples below the MWT, positive values indicate samples above the MWT. 0 and the solid blue lines indicate the MWT, with the dashed lines indicating the minimum and maximum water table levels. Note the different scales used. Error bars represent standard error of two analytical replicates. 126

4.9 Depth profiles relative to mean water table (MWT) of individual σ component yields relative to total σ (%) for Degraded bog (a), Bog plateau (b), Bog margin (c) and Fen lagg (d). Negative values on the y-axis indicate samples below the MWT, positive values indicate samples above the MWT. 0 and the solid blue lines indicate the MWT, with the dashed lines indicating the minimum and maximum water table levels. Note the different scale used. Error bars represent standard error for two analytical replicates. 130

4.10 Depth profiles for Λ (mg/100 mg OC) and $[Ad/Al]_G$ ratios at DB (a), BP (b), BM (c) and FL (d). Negative values on the y-axis indicate samples below MWT and positive values above MWT. Solid blue lines indicates the MWT, dashed lines indicate the minimum and maximum water table levels. Error bars represent the standard error from two analytical replicates. 133

4.11 S/G ratios as a function of depth from the mean water table (MWT) for DB (a), BP (b), BM (c) and FL (d). Negative values on the y-axis indicate samples below MWT and positive values above MWT. Solid blue lines indicates the MWT, dashed lines indicate the minimum and maximum water table levels. Error bars represent the standard error from two analytical replicates. 137

4.12 C/G ratios as a function of depth from the mean water table (MWT) for DB (a), BP (b), BM (c) and FL (d). Negative values on the y-axis indicate samples below MWT and positive values above MWT. Solid blue lines indicates the MWT, dashed lines indicate the minimum and maximum water table levels. Error bars represent the standard error from two analytical replicates. 139

4.13 Depth profiles relative to mean water table (MWT) of concentrations (mg/100 mg OC) of total carbohydrate pool, polysaccharide (cellulose) derived products, methylated carbohydrates and 1,2,4-trimethoxybenzene for a) DB, b) BP, c) BM and d) FL. Negative values on the y-axis indicate samples below MWT and positive values above MWT. Solid blue lines indicates the MWT, dashed lines indicate the minimum and maximum water table levels. Error bars represent the standard error of two analytical replicates. 142

4.14 Depth profiles relative to mean water table (MWT) of gallic acid and 1,3,5-trimethoxybenzene for a) DB, b) BP, c) BM and d) FL. Negative values on the y-axis indicate samples below MWT and positive values above MWT. Solid blue lines indicates the MWT, dashed lines indicate the minimum and maximum water table levels. 147

5.1 Map of Moor House National Nature Reserve. Sampling point represented by the orange diamond. Grid reference NY7527833361. 158

5.2 Pictures illustrating the experimental design. a) cross section of an extraction thimble filled with *Sphagnum* mosses, b) beakers filled with thimbles and treatment water c) aerial view of the extracted cellulose thimbles containing the glass wool control, d) aerial view of the extracted thimbles containing eight *Sphagnum capillifolium* plants each and e) illustrates how the thimbles were placed in the beaker and topped up to 50 mL with the treatment solution. 161

5.3 Partial total ion chromatogram (TIC) of the thermochemolysis products from bog water samples collected from Moor House peatland. Peak identities are listed in Table 5.1 168

5.4 The concentrations of Λ (a) and σ (b) in *Sphagnum* mosses and the bog water sampled at Moor House 169

5.5 Changes in Λ concentrations in the *Sphagnum* mosses between the Milli-Q, bog water and additional phenols treatments as measured at week 0 and week 4 171

5.6 Changes in concentrations of the phenols that were specifically added to the phenols treatment (P5, P18, G4 and G5) as well as the phenols that contribute to the Λ proxy (G6, G18 and S6) for the Milli-Q, bog water and additional phenols treatments as measured at week 0 (a) and week 4 (b) 172

5.7 Partial total ion chromatogram (TIC) of the thermochemolysis products from *Sphagnum capillifolium* samples collected from Moor House (a) and Butterburn Flow (b). The Moor House sample used here is from the Milli-Q water treatment collected at week 0. IS denotes internal standard. Peak identities are listed in Table 5.1 173

5.8 Partial total ion chromatogram (TIC) of the thermochemolysis products from *Sphagnum capillifolium* samples after 0 weeks in the Milli-Q water (a), bog water only (b), or bog water with additional phenols (c) treatment. IS denotes internal standard. Peak identities are listed in Table 5.1 175

5.9 Partial total ion chromatogram (TIC) of the thermochemolysis products from *Sphagnum capillifolium* samples after 4 weeks in the Milli-Q water (a), Bog water only (b), or Bog water with additional phenols (c) treatment. IS denotes internal standard. Peak identities are listed in Table 5.1 176

5.10 Changes in σ concentrations between the Milli-Q, bog water and additional phenols treatments as measured at week 0 and week 4 178

List of Tables

2.1 The main thermochemolysis products 38

3.1 Estimated percentage ground vegetation cover by eye from three randomly placed 1 m quadrats at each coring site. x = species present at the site, but no coverage data available. 64

3.2 The main thermochemolysis products 68

3.3 The yield (mg/100 mg OC) of the dominant lignin-derivatives, cellulose derivatives(1-3) and sphagnum acid derived products (I-III) within 7 Sphagnum moss samples. Values are an average taken from two analytical replicates. All samples have been analysed with 13C-labelled TMAH, and therefore are corrected for non-lignin phenols. n.d = not detected 70

3.4 The yield (mg/100 mg OC) of the dominant lignin derivatives, cellulose derivatives (1-4), and the corrected $[Ad/Al]_G$ ratio for 10 vascular plants and 4 root samples as well as 2 non-*Sphagnum* moss species. All samples have been analysed with 13C-labelled TMAH, and therefore are corrected for non-lignin phenols. n.d = not detected 80

4.1 Mean, minimum and maximum water table (cm) as a function of distance from the bog surface (0 cm). 101

4.2 The downcore% TOC, TN and C:N values for Degraded Bog (DB), Bog Plateau (BP), Bog Margin (BM) and Fen Lagg (FL) sites. Bold values represent the mesotelm. Values represent a 2 cm thick slice of peat. . . 106

4.3 The main thermochemolysis products 114

4.4 The average percentage yield of intact lignin (1 %OH), degraded lignin (2 %OH) and non-lignin (3 %OH) for the guaiacyl monomers G4, G5, G6 and G18 and the syringyl monomers S4, S5 and S6 at each site . . . 135

5.1 The main thermochemolysis products observed in all samples 165

6.1 The Λ concentrations (mg/100 mg OC) observed in above ground (shoot) and below ground (root) sections of *Calluna vulgaris*, *Erica tetralix*, *Vaccinium oxycoccos* and *Molinia caerulea* 183

6.2 The main thermochemolysis products 225

Chapter 1

Introduction and literature review

1. Introduction and literature review

1.1 Introduction

Over the period 1880-2012, the global average of land and ocean surface temperature has increased by approximately 0.85 °C (IPCC, 2014). This change is a result of increased anthropogenic greenhouse gas emissions such as; carbon dioxide (CO_2), methane (CH_4) and nitrous oxide (N_2O), in response to increased economic and population growth worldwide (IPCC, 2014). Between 1750-2011, anthropogenic CO_2 emissions were around 2040 ± 310 Gt, with around 40% of this remaining in the atmosphere, and the remainder absorbed by the ocean and on land via plants and soils (IPCC, 2014). Anthropogenic greenhouse gas (GHG) emissions have continued to increase dramatically in recent years, despite a growing number of policies focussed on curbing emissions from fossil fuel combustion (IPCC, 2014). Moreover, it is predicted that warming will continue beyond 2100, with many severe and irreversible impacts globally on a multi-century to millennial time scale (IPCC, 2014).

The ever-increasing threat of climate change led to the enactment of the Kyoto Protocol, an international agreement that committed Annex 1 (e.g UK) parties to reduce greenhouse gas emissions to an average of 5% below the 1990 average between 2008-2012, and 18% between 2013-2020. (UNFCCC, 2008). It was seen as in important first step towards a global emissions reduction scheme and allowed countries to use mechanisms such as Land Use, Land Use Change and Forestry (LULUCF) activities to help sequester carbon (UNFCCC, 2008). Following on from this, in November 2016, the Paris Agreement entered into force, an agreement uniting nations and aiming to keep global temperatures below 2°C above pre-industrial levels from 2020 UNFCCC (2017).

British vegetation and soils have been estimated to hold approximately 113 and 9838 Mt respectively of carbon, with peatlands accounting for almost 50% of the soil's total (Milne and Brown, 1997). Although well known for their capacity to sequester carbon

under the right climatic conditions, peatlands also have the ability to become significant carbon sources (Janssens et al., 2006). Moreover, several simulations investigating the fate of British blanket peats in a changing climate suggests a retreat of peat and significant shifts in their carbon storage capacities (Clark, Gallego-Sala, Allott, Chapman, Farewell, Freeman, House, Orr, Prentice and Smith, 2010; Clark, Billett, Coyle, Croft, Daniels, Evans, Evans, Freeman, Gallego-Sala, Heinemeyer, House, Monteith, Nayak, Orr, Prentice, Rose, Rowson, Smith, Smith and Tun, 2010).

Peatland organic matter is a complex mixture of humic substances consisting of a variety of both organic and inorganic components, including an abundance of recalcitrant phenolics such as lignins and tannins (Sarkanen and Ludwig, 1971; Verhoeven and Toth, 1995; Mason et al., 2009; Weng and Chapple, 2010; McClymont et al., 2011; Mason et al., 2012). Furthermore, the vegetation of many peatland ecosystems is often dominated by *Sphagnum* mosses which contain another phenolic compound; sphagnum acid (Verhoeven and Toth, 1995; Rasmussen et al., 1995; Verhoeven and Liefveld, 1997; McClymont et al., 2011). These compounds make a significant contribution to the organic carbon buried within peatland ecosystems and therefore make an interesting study. Due to its recalcitrance, previous studies have used lignin as an indicator of the turnover of organic carbon within soil and peat systems under a variety of environmental and climatic conditions (Yeloff and Mauquoy, 2006; Mason et al., 2009; Weng and Chapple, 2010; Mason et al., 2012). The methods by which this has been conducted vary, with high-temperature pyrolysis (Dijkstra et al., 1998; Schellekens et al., 2009; Van Campenhout et al., 2009; McClymont et al., 2011), tetramethylammonium hydroxide (TMAH) thermochemolysis (Filley et al., 1999; Nierop and Filley, 2007; Grasset et al., 2009; Mason et al., 2012; Abbott et al., 2013) and cupric oxidation (CuO) followed by gas chromatography (GC), gas chromatography/mass spectrometry (GC/MS) or high pressure liquid chromatography (HPLC) (Hedges and Parker, 1976; Hedges and Mann, 1979; Hedges and Ertel, 1982; Kögel, 1986; Goñi and Hedges, 1992) being among the most common methods. However, before 1999, tannins posed a problem for investigations using TMAH thermochemolysis as there was no reliable way of

fully distinguishing between lignin and tannin derived compounds (Filley et al., 1999; Filley et al., 2006). Thermally assisted hydrolysis and methylation (THM) used in conjunction with ^{13}C labelled tetramethylammonium hydroxide (TMAH) has been shown to overcome this analytical limitation (Filley et al., 1999; Filley et al., 2006).

The lignin content of soils and peats has been well studied, however, less attention has been paid to the role of tannins within the peat. Fewer studies still have focused on the fate of sphagnum acid, and only a handful of studies have performed a combined study on the fate all three polyphenolic compounds in peatland ecosystems (McClymont et al., 2011; Abbott et al., 2013; Swain and Abbott, 2013; Swain, 2013). In order to gain further insight into the fate of peat-based organic carbon, research on the processes controlling the sequestration and degradation of these phenolics is required.

1.2 Literature review

1.2.1 Peatlands and organic carbon

One of the first studies focussed on peatlands, and considered as the foundation for modern peatland science was conducted by Weber (1902) on the Aukštumala Raised Bog in Lithuania. It encompassed ecology, hydrology, and chemistry with an aim to investigate the interactions between peatlands, climate and sea level. Today, the effect of climate change on peatlands remains uncertain, and further research encompassing the ecology, hydrology and chemistry of peatland types in various environmental conditions is needed.

Peatlands are well known for their large carbon storage capacities holding approximately 612 Gt of carbon globally, with those situated in the northern hemisphere estimated to hold approximately 547 Gt of this total (Yu et al., 2010). Globally, the distribution of peatlands is very uneven (Figure 1.1), with most peatlands residing in

the northern hemisphere. This may be due to the combination of permanent snow and ice cover and less available land in the southern hemisphere (Zigang and Xintu, 2009).

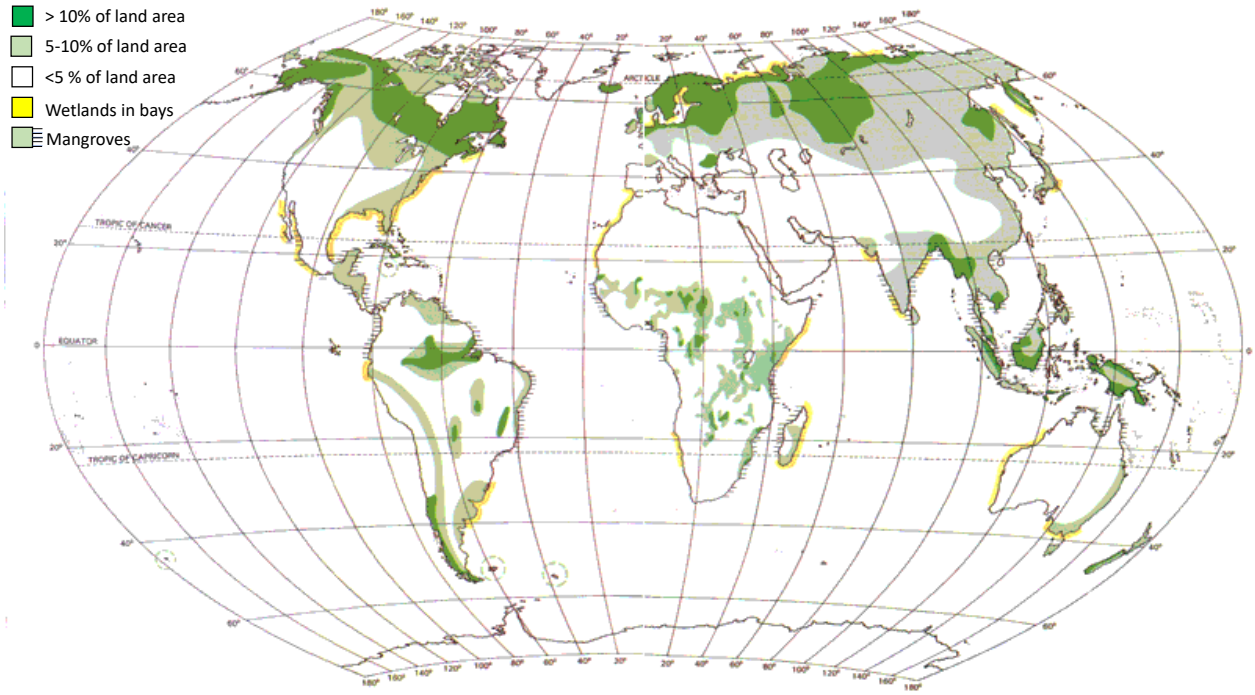

Figure 1.1: A map displaying the global distribution of peatlands and their contribution to the total land area. Adapted from International Peat Society (2001)

Peatlands store carbon by sequestering it in living and dead biomass, with peat formation dependant on rates of net primary production exceeding decay, resulting in peat which is rich in organic carbon (Moore, 1989). However, some of this carbon is returned to the atmosphere as CO_2 or CH_4 via the decay of the plant material and peat (Baird et al., 2009). Throughout the Holocene, peatlands have been a persistent sink for atmospheric CO_2 and a persistent source of CH_4 (Baird et al., 2009), and it is unknown what effect future changes in climate may have on this delicate equilibrium.

The classification of peatlands around the world is varied, and different countries have various ways of defining and classifying peatlands (Rydin et al., 2013). For example; in Finland, classification is based on the early work of Cajnder (1913) and requires

information on the water level and nutrient status of the peat. In Canada, classification is based mainly on hydrological regimes and must contain at least 40 cm of peat to be classified as a peatland (Tarnocai and Stolbovoy, 2006). In the UK, peatland classification is different again, based on the National Vegetation Classification (NVC), developed in the 1980's and covering all vegetation types in Britain (Rydin et al., 2013). It can then be further divided based on hydrological regimes into bogs; where water and nutrients are primarily received through precipitation, and fens; where water may be supplied by groundwater, or surface water (Reddy and DeLaune, 2008; Rydin et al., 2013). The word 'peatland' is, therefore, a generic term, the specifics of which will vary depending on which classification system is used.

The peat itself has a more straightforward definition than the ecosystem it resides in. Peat is defined as 'the partially decomposed remains of plant and soil organisms which have accumulated at the surface of the soil profile', and generally contains 50% or more total organic carbon (TOC) (Lindsay et al., 2010; JNCCC, 2011). Organic matter accumulates as primary productivity exceeds decay processes, and is regulated by the activity of decomposers such as bacteria, fungi and enzymes (Moore, 1989; Reddy and DeLaune, 2008). As the vegetation grows, decomposition continues at the surface, the organic matter quickly becomes buried and is soon transferred from a dry, oxygen-rich to a predominantly anoxic, water-saturated environment (Reddy and DeLaune, 2008). Within this anoxic environment, decomposition slows significantly, and the organic matter begins to accumulate (Reddy and DeLaune, 2008). Increased oxygen availability, sufficient nitrogen availability and energy-rich carbohydrates will allow rapid decomposition of plant material and peat until one of these parameters becomes a limiting factor (Bragazza et al., 2007; Reddy and DeLaune, 2008). For example, Freeman et al. (2004) investigated the role of phenoloxidase during peatland decomposition and observed oxygen constraints can directly reduce enzyme activity, which in turn slowed the depletion of phenolics within the peat.

The hydrology of peatlands is fundamental to peatland ecosystems and governs

both peatland ecology and decomposition processes (Clymo and Hayward, 1982). With reference to the water table, peatlands can be vertically split into 3 distinct layers; 1) the acrotelm - oxygen rich environment where decomposition is rapid, 2) the mesotelm - where water table fluctuates between minimum and maximum levels providing a wet, oxic environment allowing rapid decomposition and finally 3) the catotelm - below the minimum water level, and considered as a predominantly anoxic environment, although some trapped air or biogenic gasses may be present, decomposition is very slow (Rydin et al., 2013). As the peat accumulates and begins to grow, the water table rises with it due to its hydraulic conductivity, which can be significantly affected by macropores within the peat (Baird, 1997).

1.2.2 *Sphagnum* mosses

There are around 300 species of *Sphagnum* moss worldwide, the majority of which grow in boreal and northern temperate zones (Clymo and Hayward, 1982). They cover approximately 1.5 million km^2 and have stored around 150 Gt of carbon (Rydin et al., 2013). Clymo and Hayward (1982) suggested that there is more carbon stored in *Sphagnum* mosses than any other plant species, with *Sphagnum* litter forming the dominant carbon input on most ombrotrophic bogs. *Sphagnum* mosses are a key feature of many northern peatlands, adapted to cool, nutrient-poor, waterlogged and acidic conditions due to an abundance of uronic acids which can form 10-30% of the dry weight of *Sphagnum* species (Clymo, 1963; Spearing, 1972; Clymo and Hayward, 1982; Rydin et al., 2013). The combination of acidity, upward blanket-like growth, and waterlogging determines what other species, both plant and animal alike, can grow with them (Clymo and Hayward, 1982; van Breemen, 1995; Rydin et al., 2013).

In order to survive, *Sphagnum* mosses need a constant water supply with a low concentration of calcium, which is possible in areas with relatively high rainfall (Clymo and Hayward, 1982). *Sphagnum* species have a water content of around 700-1400% of the dry mass, although this is species dependent (Rydin, 1985; Schipperges and Rydin, 1998; Rydin et al., 2013). For example, Rydin (1985) placed four species of *Sphagnum*

in cylinders and measured water content at various water levels. At the beginning of the experiment, water content between different species could already be observed with *Sphagnum rubellum* and *Sphagnum tenellum* having an initial capitula water content of around 1400% whereas *Sphagnum balticum* and *Sphagnum fuscum* had an initial capitula water content of around 1100%. Bryophytes do not contain a root system, and so *Sphagnum* mosses retain water via mass flow through pores that occur on the water-holding hyaline cells (Clymo and Hayward, 1982). When the water table drops, these cells retain the water due to a high water potential, resulting in 90% of the space within a *Sphagnum* carpet being filled (Clymo and Hayward, 1982). The pendent branches of *Sphagnum* help the plant to move water, as opposed to the stem in vascular plants, allowing water to move sideways rather than upwards (Cavers, 1911; Clymo and Hayward, 1982; Rydin et al., 2013). If the water table is lowered, the *Sphagnum* will shrink, dry out and turn white which is a reversible effect (Clymo and Hayward, 1982).

It has been known for some time that *Sphagnum* species grow in acidic conditions which the plants themselves create (Clymo and Hayward, 1982). The plants contain a high cation exchange capacity due to an abundance of uronic acids, with plants growing further away from the water table e.g hummock forming species, containing a larger cation exchange capacity than hollow species which are often located around pools (Spearing, 1972; Clymo and Hayward, 1982). This high cation exchange capacity has been strongly correlated with the galacturonic acid (Figure 1.2) content of *Sphagnum* species and has also led to the use of *Sphagnum* species in the trapping and sampling of both air-borne and water-borne heavy metals and pollutants (Clymo and Hayward, 1982). These uronic acids e.g. Galacturonic acid are located in the cell wall and form a pectin-like polymer which can be referred to as 'Sphagnan' (Painter, 1991).

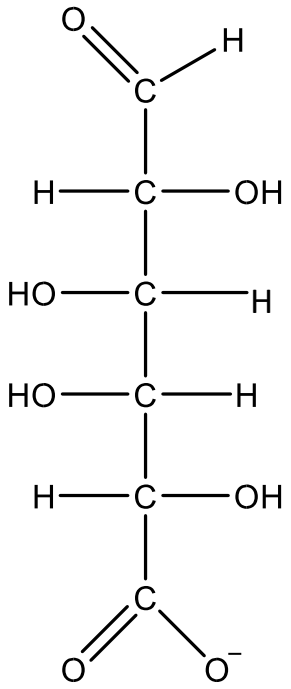

Figure 1.2: Structure of galacturonic acid

The growth of *Sphagnum* is similar to other moss species, however, the rate of decay is much slower, allowing the litter to accumulate as organic-rich peat (Clymo and Hayward, 1982; Rudolph and Samland, 1985; Rochefort et al., 1990; van Breemen, 1995). The exact reasons for this remain unclear, however, the low nitrogen (N) levels in the plants, the acidic conditions produced by the plants, or the very wet and anoxic conditions in which the plants live may all be contributing factors (Clymo and Hayward, 1982; Damman, 1988; Verhoeven and Liefveld, 1997). *Sphagnum* species also differ slightly in their chemical compositions, and this may be why within the *Sphagnum* genus, hollow species are more decay resistant compared to hummock species (Johnson and Damman, 1991; Hogg, 1993; Rydin et al., 2013).

It is generally accepted that *Sphagnum* mosses do not contain lignin (Weng and Chapple, 2010), however, they are considered unique in the biosynthesis of *trans* sphagnum acid (*p*-hydroxy-β-[carboxy-methyl]- cinnamic acid, Figure 1.3), (Rasmussen et al., 1995). This is a dominant phenolic in *Sphagnum* species, linked via ether bonds to the

cell wall thus forming a three dimensional polymeric network and providing both structural support and resistance to microbial decay (Rudolph and Samland, 1985; van der Heyden, 1994; Verhoeven and Liefveld, 1997; Freeman et al., 2001). Its high recalcitrance, due to the abundance of uronic acids and sphagnum acid, as well as its high carbon storage capacity is one reason why the distinctive biochemistry of *Sphagnum* species and the environments they inhabit needs to be better understood and requires further research.

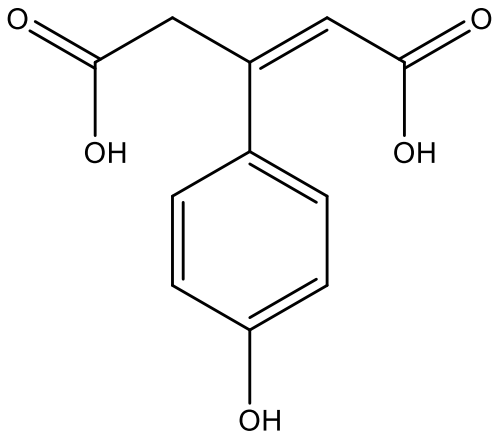

Figure 1.3: A schematic of the structure of sphagnum acid (p-hydroxy-β-[carboxy-methyl]- cinnamic acid)

1.2.3 Characterisation of sphagnum acid

Few studies have focused on the characterization of sphagnum acid when compared to other phenolics such as lignin. A study by van der Heijden et al. (1997) identified seven sphagnum acid products using thermally assisted hydrolysis and methylation (THM) in the presence of tetramethylammonium hydroxide (TMAH), including products with C3 side chains. Recently, these products were also identified by Abbott et al. (2013) and Swain and Abbott (2013), where the four dominant products I, IIa, IIb and III

were used during these studies as the remaining three (i ii and iii) are present only in trace amounts, below the limit of detection. Their structures are illustrated in Figure 1.4. These products have been found exclusively in several species of *Sphagnum* (McClymont et al., 2011; Swain, 2013; Schellekens et al., 2015a).

As previously mentioned, thermochemolysis retains the C3 side chain of sphagnum acid products. This is considered a large advantage over other methods that have been used to characterize *Sphagnum* mosses. For example, Williams et al. (1998) used alkaline cupric oxidation (CuO) to analyze 15 species of *Sphagnum* mosses along with other peatland vegetation. The results showed large quantities of unsubstituted *p*-hydroxyl phenols as well as sphagnum acid. CuO has commonly been used in the analysis of lignin in vascular plants, however, the C3 side chain is lost with this method, giving THM in the presence of TMAH method a great advantage in the analysis of *sphagnum* related substrates such as peat.

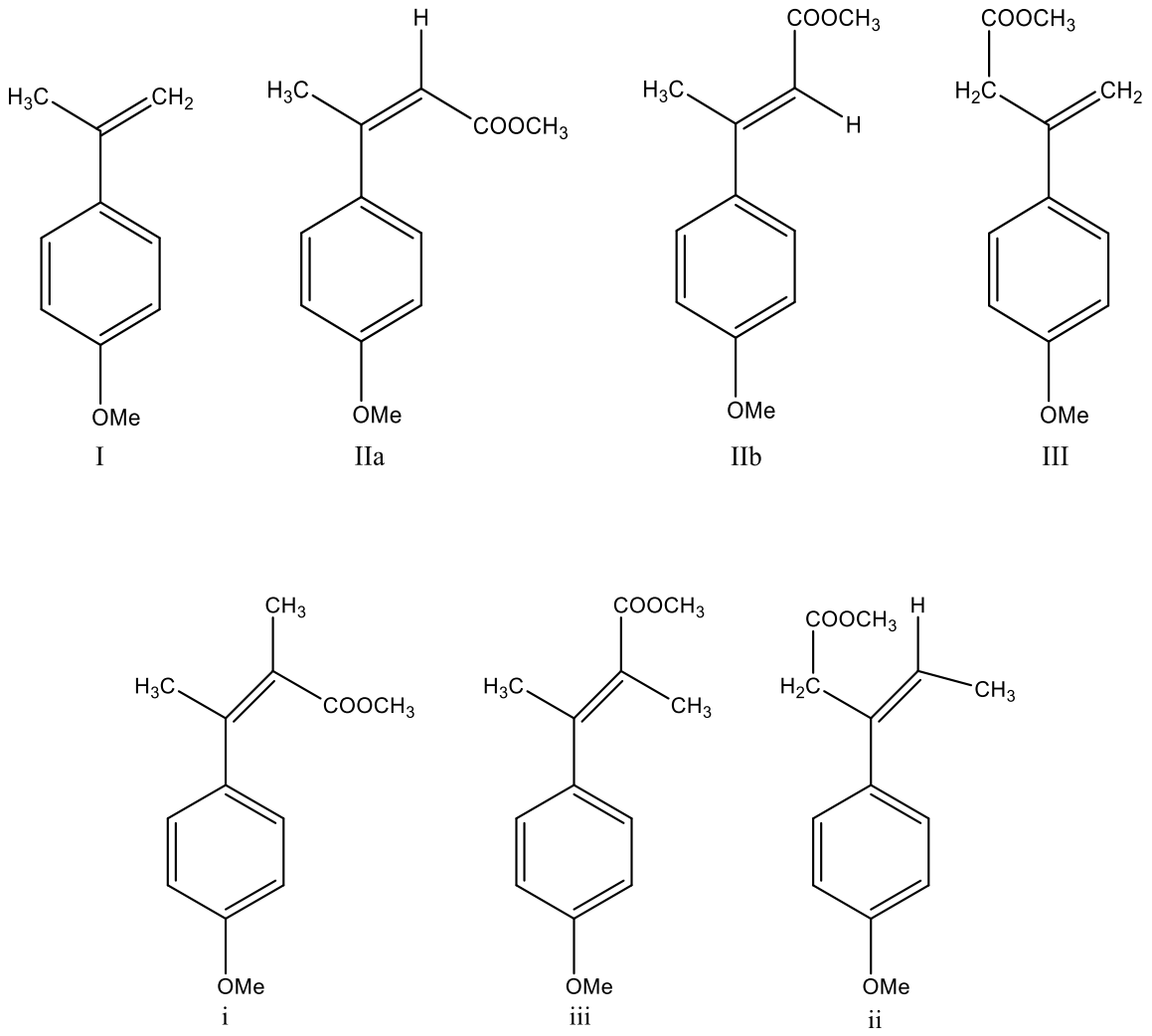

Figure 1.4: A schematic of the four dominant sphagnum acid thermochemolysis products (I) methylated 4-isopropenylphenol (IUPAC: 1-methoxy-4-(prop-1-en-2-yl)benzene), (IIa) methylated *cis*-3-(4-hydroxyphen-1-yl)but-2-enoic acid (IUPAC: (Z)-methyl 3-(4-methoxyphenyl)but-2-enoate), (IIb) methylated *trans*-3-(4-hydroxyphen-1-yl)but-2-enoic acid (IUPAC: (E)-methyl 3-(4-methoxyphenyl)but-2-enoate) and (III) methylated 3-(4-hydroxyphen-1-yl)but-3-enoic acid (IUPAC: methyl 3-(4-methoxyphenyl)but-3-enoate), i and iii; methylated (Z) and (E)- 2-methyl-3-(4'-hydroxyphen-1-yl)but-2-enoic acid and ii; methylated 3-(4'-hydroxyphen-1-yl)pent-3-enoic acid (van der Heijden, 1994). Adapted from (Abbott et al., 2013)

.

1.2.4 Vascular plants and lignin

The origin of lignin has been traced back to the rise of the vascular plants, which may have occurred around 700 million years ago (Heckman et al., 2001), and provides structural support, protection against pathogens and enhanced water transportation (Hon, 1995; Chabannes et al., 2001; Boerjan et al., 2003; Weng and Chapple, 2010). Deposited in the cell walls, lignin is connected to cellulose and hemicellulose and enabled vascular plants to stand upright and dominate the terrestrial biosphere (Sarkanen and Ludwig, 1971; Chabannes et al., 2001; Boerjan et al., 2003; Weng and Chapple, 2010). Lignin is the second most abundant bipolymer, succeeded only by cellulose, and is, therefore, a significant carbon sink, representing approximately 30% of organic carbon in the terrestrial biosphere (Boerjan et al., 2003; Weng and Chapple, 2010). It is considered to be unique to vascular plants and is therefore absent in bryophytes (Weng and Chapple, 2010).

Lignin is composed of three hydroxycinnamyl alcohols that each differ in their degree of methoxylation; *p*-coumaryl alcohol, coniferyl alcohol and sinapyl alcohol (Figure 1.5) (Freudenberg et al., 1968; Boerjan et al., 2003). Subsequently, via enzymic dehydrogenation, these monolignols produce *p*-hydroxyphenyl, guaiacyl, and syringyl monomer units respectively that form the lignin polymer (Adler, 1977; Boerjan et al., 2003). The exact mechanism of lignin polymerisation remains unclear (Dorrestijn et al., 2000), and the composition of lignin can vary between plant species. The distribution of different lignin units has been found to be specific to different plant groups e.g gymnosperms, angiosperms and grass lignin (Kirk et al., 1980; Clifford et al., 1995). The composition of the lignin found in complex mixtures such as soil and peat can, therefore, be used as a vegetation indicator, and has been successfully applied in several scientific studies (Hedges and Parker, 1976; Hedges and Mann, 1979; Kögel, 1986). Both syringyl and guaiacyl type lignin tends to be dominant in angiosperm species, whereas only guaiacyl type lignin dominates in gymnosperm species (Sarkanen and Ludwig, 1971; Boerjan et al., 2003; Weng and Chapple, 2010). This lignin type has also been found to be less susceptible to degradation in comparison to the syringyl type (Huang et al.,

1998). Cinnamyl lignin derivatives (*p*-coumaric and ferulic acid) dominate grass species, along with low concentrations of guaiacyl and syringyl derivatives (Clifford et al., 1995).

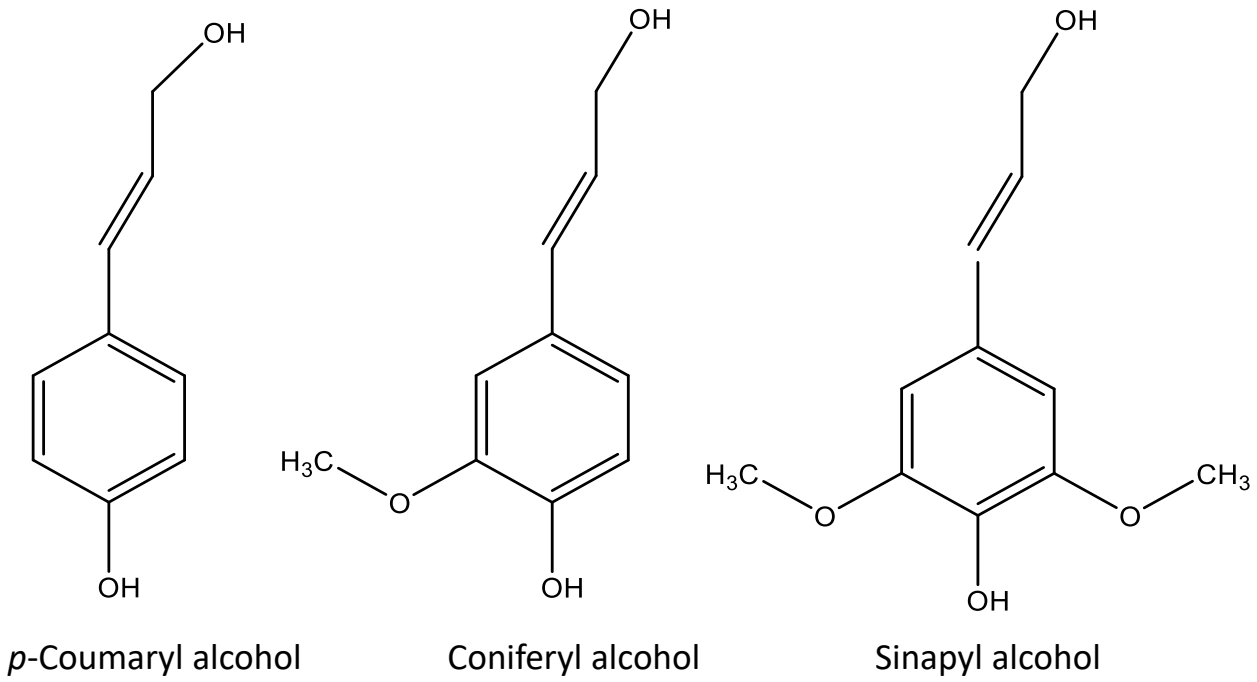

Figure 1.5: Three main alcohol monomers that form the lignin bipolymer; *p*-coumaryl alcohol, coniferyl alcohol, and sinapyl alcohol. Adapted from (Weng and Chapple, 2010)

As seen in Figure 1.6 lignin is a complex molecule, containing a diverse range of random linkages, which make it one of the hardest polymers to degrade, and provides an effective defence against pathogens and herbivores (Sarkanen and Ludwig, 1971; Crawford et al., 1981; Hon, 1995; Weng and Chapple, 2010). This recalcitrance is thought to be the reason why lignin appears stable in soil organic matter when compared to less structurally complex compounds e.g cellulose (Dignac et al., 2005). The most common link is the Arylglycerol--aryl ether (β-O-4) link illustrated in Figure 1.6. This particular link involves a covalent bond between the β carbon on the alkyl side chain and the oxygen bonded to the fourth carbon on the phenolic ring (Figure 1.6) (Adler, 1977), and accounts for approximately 46% and 60% of linkages in gymnosperms and angiosperms respectively (Dorrestijn et al., 2000). Other common links include carbon-

carbon bonds; β-5, β-β, β-1, and 5-5 (Figure 1.7) all of which are more difficult to chemically cleave (Boerjan et al., 2003; Kishimoto et al., 2010). Depending upon the distribution of monomers within the lignin polymer, the abundance of these different linkages will change (Boerjan et al., 2003). For example in a lignin polymer where guaiacyl units dominate, β-5, 5-5, and 5-O-4 linkages will be more abundant than if syringyl units were dominant due to the availability of the C_5 position for bonding (Boerjan et al., 2003; Kishimoto et al., 2010). There are more bond types that occur in lignin than listed here, however, the ones mentioned above can be observed in Figure 1.7.

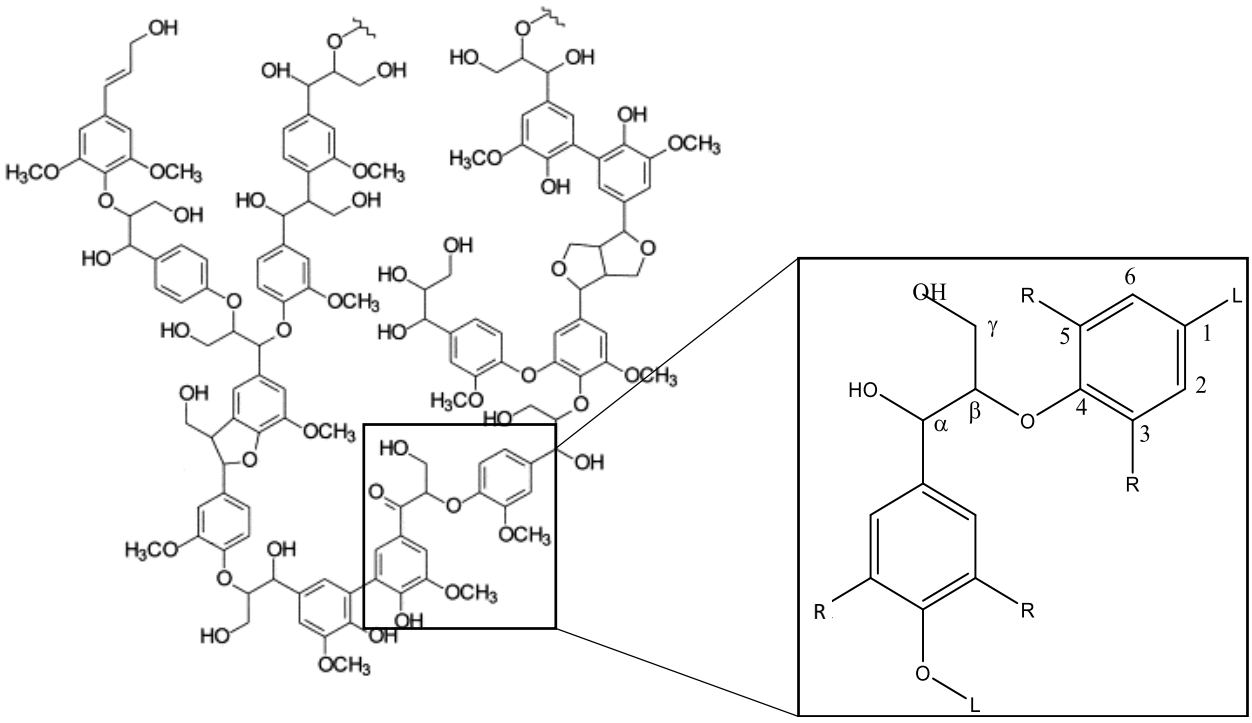

Figure 1.6: A schematic representation of a lignin polymer (adapted from Dorrestijn et al. (2000); L = lignin biomacromolecule. The box displays the dominant β-O-4 linkages found throughout the lignin bipolymer

Although the different linkages within lignin make it a recalcitrant organic compound, there are a small number of fungi and bacteria that are able to degrade it (Kirk and Farrell, 1987; Gold et al., 1989; Zimmermann, 1990; Hatakka, 1994; Vane et al., 2001). Lignin may therefore not be as stable long-term as expected, particularly in

aerobic soils where bacterial productivity is higher (Kiem and Kögel-Knabner, 2003; Dignac et al., 2005; Bahri et al., 2006; Dungait et al., 2012). In fact, Heim and Schmidt (2007) used compound-specific isotope analysis to investigate lignin input and stabilization in grassland and arable soils. The results suggested the residence time of lignin is shorter than that of bulk soil organic carbon, and therefore does not contribute to organic carbon stabilization in soils (Heim and Schmidt, 2007).

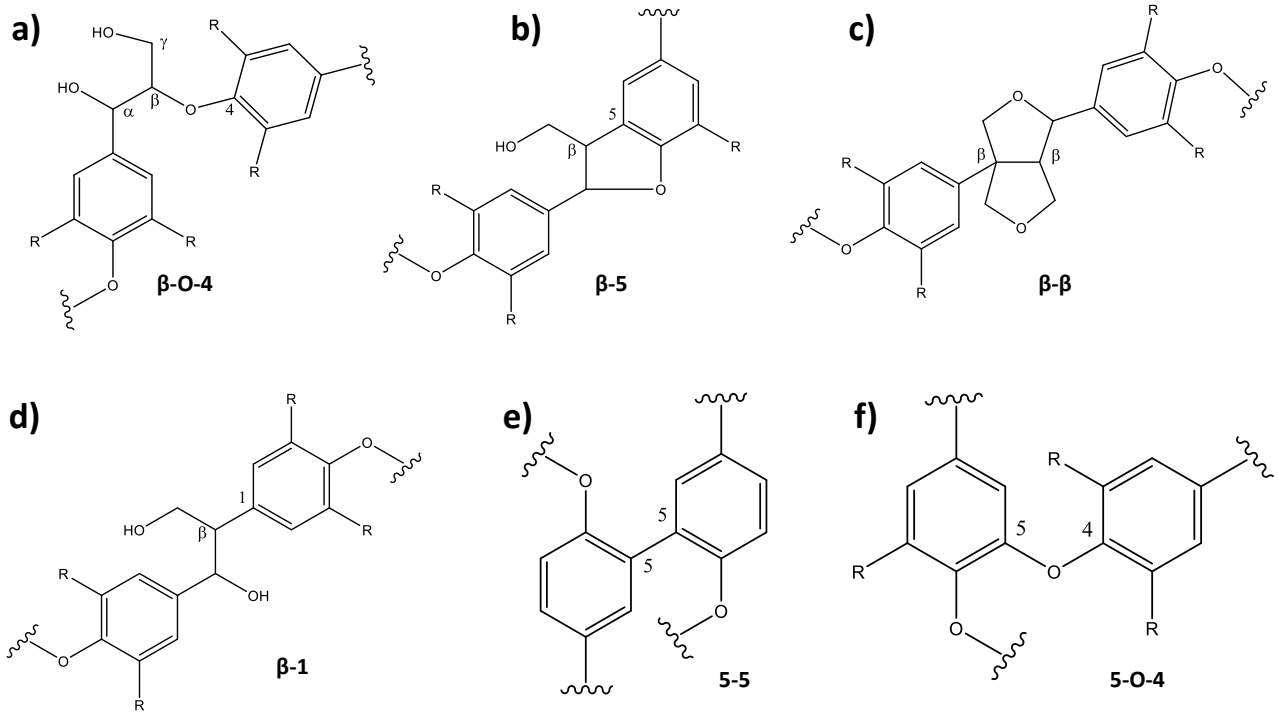

Figure 1.7: A schematic representation of 6 linkage types found throughout the lignin bipolymer. a) = β-O-4 link, b) = β-5 link, c) = β-β link, d) = β-1 link, e) = 5-5 link and f) = 5-O-4 link. Adapted from Dorrestijn et al. (2000)

The microbial degradation of lignin occurs most rapidly under aerobic conditions and is primarily performed by three groups of fungi; soft rot, brown rot and white rot (Kirk and Farrell, 1987). Brown rot fungi mineralise lignin methoxyl groups, which leads to the accumulation of hydroxylated phenyl derivatives (catechol derivatives) with only a small degree of side chain oxidation (Kirk and Farrell, 1987; Ander et al., 1988; Filley et al., 2000). On the other hand, white rot fungi are the most efficient lignin

degraders, able to convert all of the lignin macromolecule to carbon dioxide and water (Gold et al., 1989; Hatakka, 1994). Extensive aromatic ring cleavage and side chain oxidation of lignin is associated with residues following degradation by white rot fungi (Umezawa and Higuchi, 1987; Srebotnik et al., 1997). The processes involved in the fungal degradation of lignin are illustrated in Figure 1.8 below.

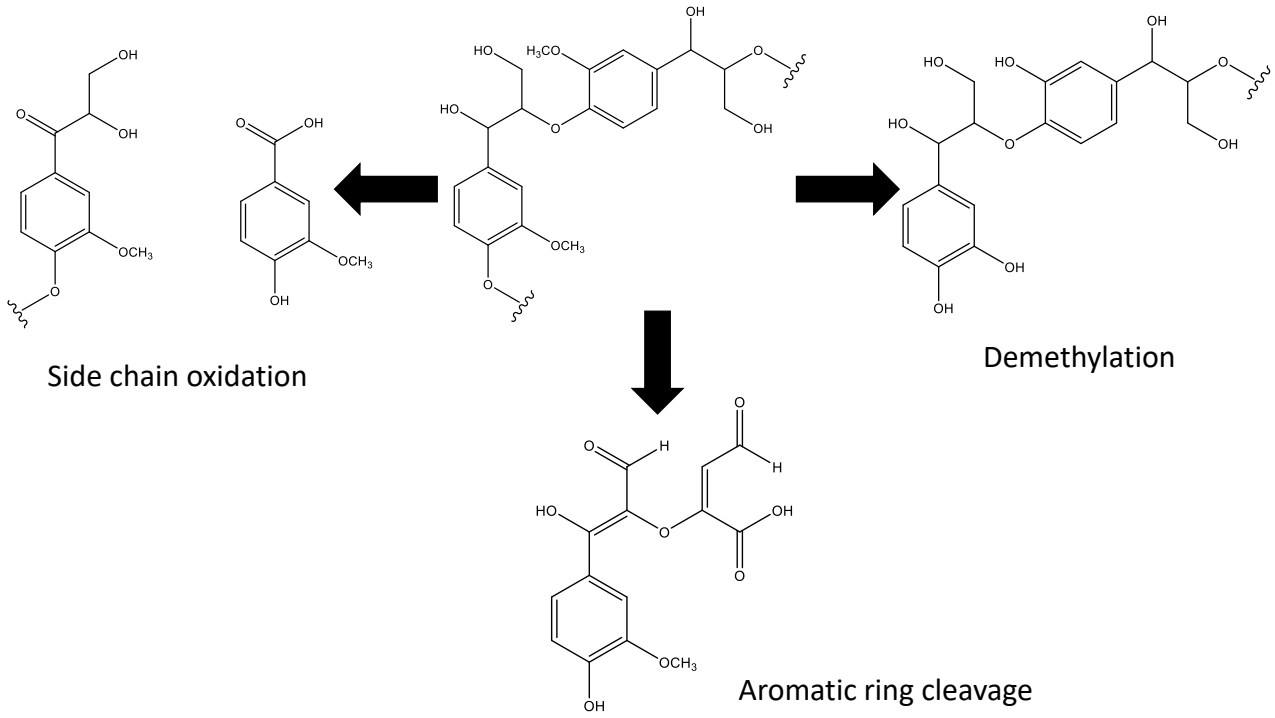

Figure 1.8: A schematic representation of the changes that occur from the fungal degradation of guaiacyl lignin. Adapted from Filley et al. (2000)

Although many studies have focussed on the role of Fungi in lignin biodegradation, they are not the only organisms able to degrade lignin (Sørensen, 1962; Zimmermann, 1990; Godden et al., 1992; Ahmad et al., 2010). For example, both *Rhodococcus, Streptomyces* and *Nocardia* bacterial species have been identified as lignin degraders in soils (Sørensen, 1962; Haider and Trojanowski, 1980; Antai and Crawford, 1981; Crawford et al., 1983; Zimmermann, 1990; Trojanowski, 2001). These species appear to break down lignocellulose into low molecular weight phenolic products, and some species show some specificity towards particular lignin types (Ahmad et al., 2010). Bacterial lignin degradation is still poorly researched and understood, however, and further research in

this area is needed.

1.2.5 Characterisation of lignin

Some of the many methods that have been used to investigate the structure and quantity of lignin in biomass include; nuclear magnetic resonance (NMR) (Park et al., 2013), ultraviolet resonance Raman (UVRR) spectroscopy (Saariaho et al., 2003), Fourier-transform infrared (FT-IR)(Stewart et al., 1997), near-infrared Fourier transform Raman spectroscopy (Agarwal and Ralph, 1997), analytical pyrolysis (Alves et al., 2006) and TMAH thermochemolysis (Filley et al., 1999; Kuroda and Nakagawa-izumi, 2006). However, the most common technique used to analyze lignin in geochemical studies is the cupric oxidation (CuO) method followed by GC, GC/MS or HPLC (Hedges and Parker, 1976; Hedges and Mann, 1979; Hedges and Ertel, 1982; Kögel, 1986; Goñi and Hedges, 1992).

Cupric oxidation of lignin involves one-electron oxidation of linkages in dilute alkaline solution resulting in the release of a range of phenolic monomers (Wysocki et al., 2008). Figure 1.9 shows six of the eight main monomers released during CuO which include three vanillyl and three syringyl products in the form of carboxylic acid, aldehydes and ketones as well as *p*-courmaric and ferulic acid (Hedges and Parker, 1976). They are formed from the three main monolignols presented in Figure 1.5 and can be used to provide information on lignin yield, plant source and degradation state of the lignin in peat (Hedges and Mann, 1979).

Although used relatively frequently, the CuO method for lignin analysis has a variety of drawbacks. Practically, the method is very time consuming and has been shown to be better suited to a low carbon, or very degraded sample such as ocean sediments (Wysocki et al., 2008). In addition, little structural information can be obtained following CuO as the propyl side chain which indicates intact lignin is not retained (Figure 1.9) (Hatcher et al., 1995; Dijkstra et al., 1998; Filley et al., 2000). Subsequently, the

use of this method has declined over the last two decades as new techniques have been introduced.

The more efficient technique of high-temperature pyrolysis followed by GC/MS (Py-GC/MS) is commonly used today, and has been used to identify lignin in plants, soils and peat (Dijkstra et al., 1998; Schellekens et al., 2009; Van Campenhout et al., 2009; McClymont et al., 2011; Schellekens et al., 2015a). In this method, lignin is thermally volatilized in the absence of oxygen, yielding smaller, volatile fragments amenable to GC (Kaal and Janssen, 2008). However, this method results in the decarboxylation of benzene-carboxylic acids, and so thermochemolysis in the presence of the methylating agent tetramethylammonium hydroxide (TMAH) was introduced to overcome this (Saiz-Jimenez, 1994; Klingberg et al., 2005). The presence of TMAH prevents the decarboxylation of products, and results in an in-situ methylation and stabilization of lignin products, producing the methyl ethers of carboxylic and hydroxyl groups (Challinor, 1989; Kaal and Janssen, 2008). These products can then be identified using a mass spectrometer to allow accurate identification.

The volatile lignin monomers are generated during thermochemolysis via heat induced bond dissociation, and the products reflect the composition of the original macromolecule (del Rio et al., 1996). The exact reaction mechanism for this is not fully understood, however, it has been demonstrated that the dominant reaction when TMAH is present is a thermally assisted chemolytic degradation as opposed to pyrolytic bond cleavage (Clifford et al., 1995). Therefore thermally assisted hydrolysis and methylation or THM is now used to refer to this method (Challinor, 2001; Tanczos et al., 2003). TMAH is currently the most widely used derivatizing agent coupled with THM (used in more than 90% of published studies), however, other methylating agents have been used to analyse lignin (Shadkami and Helleur, 2010). Examples include Tetraethylammonium hydroxide (TEAH) and teratbutylammonium hydroxide (TBAH), however, these methylating agents resulted in lower yields of polycarboxylic acids than TMAH and only partially alkylate the phenolic hydroxyl groups (Lehtonen et al., 2003).

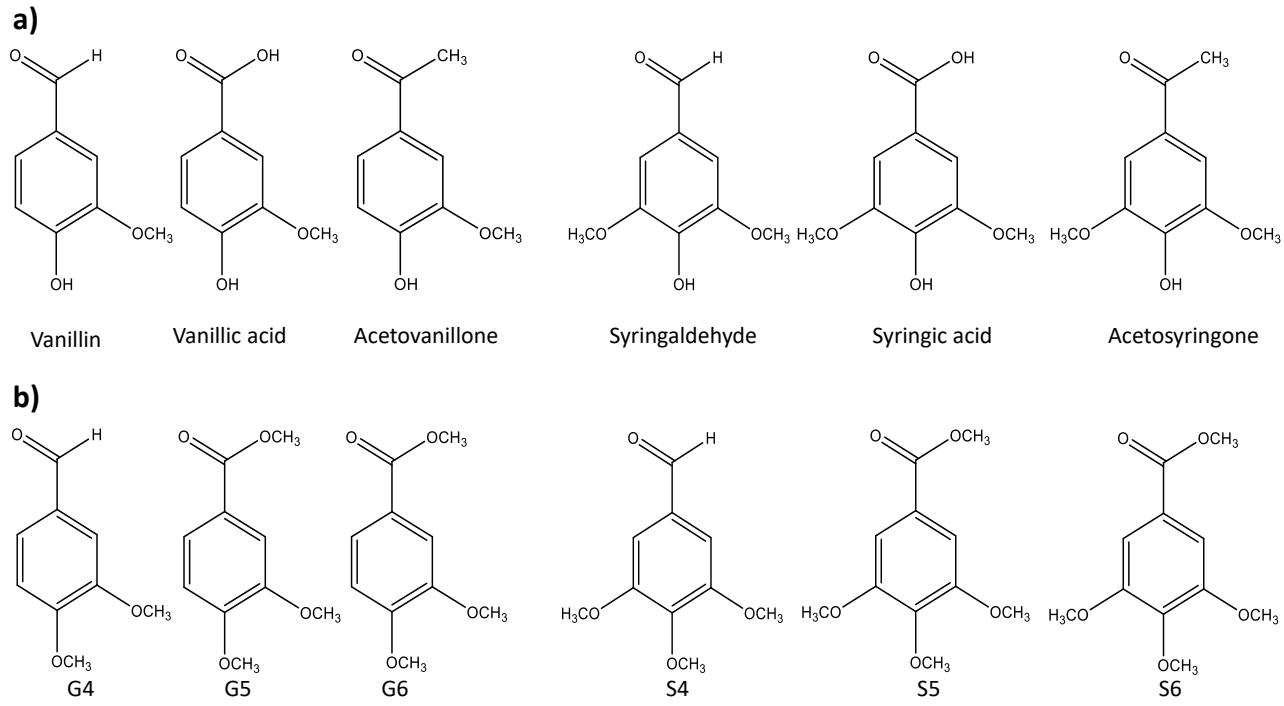

Figure 1.9: A schematic of the vanillyl and syringyl monomeric products formed from lignin during CuO oxidation (a) and TMAH thermochemolysis (b). The cinnamyl products formed in from both methods are identical, and so are not shown. Adapted from Wysocki et al. (2008)

1.2.6 Thermally assisted hydrolysis and methylation (THM) in the presence of Tetramethylammonium hydroxide (TMAH)

Thermally assisted hydrolysis and methylation (THM) in the presences of tetramethylammonium hydroxide (TMAH) has been shown to be a straightforward laboratory method involving small amounts of sample to provide important information on the chemical composition of soil humin (Fabbri et al., 1996; Filley et al., 1999). Products generally consist of an array of benzene-carboxylic acids, carbohydrate derivatives, as well as nitrogen-containing compounds, fatty acid methyl esters, alkenes and alkanols (Schulten and Sorge, 1995; Hatcher and Minard, 1995; Nierop et al., 2001). It is considered a useful technique due to its ability to cleave hydrolyzable bonds, forming car-

boxylic acids, which are then stabilized through methylation reactions (Challinor, 1991). This method produces all eight lignin phenols previously identified using CuO in addition to the *threo/erythro* 1-(3,4-dimethoxyphenyl)-1,2,3-trimethoxypropne (G14/15) and *threo/erythro* 1-(3,4,5-trimethoxyphenyl)-1,2,3-trimethoxypropane (S14/15) (Hedges and Parker, 1976). As the full process to THM is not completely understood, there is no mechanism by which to assess the quantitative recovery of lignin using this method (Kaal and Janssen, 2008), however, it remains the best method for organic-rich and humic substances such as peat (Saiz-Jimenez, 1994; Wysocki et al., 2008).

The mechanisms involved in THM analysis is described in Filley et al. (1999) and involves β-O-4 bond cleavage. Geib et al. (2008) used the THM in the presence of TMAH technique to investigate the digestion of lignin in insects, and noted the ability of TMAH to detect the chemical modification of the entire lignin molecule, therefore, TMAH provides information regarding the number of intact aryl ether linkages remaining (McKinney and Hatcher, 1996). The distribution of lignin monomers released following THM depends upon the extent of degradation as well as the proportion of β-O, β-5 and β-*beta* linkages, which will in itself influence degradation of lignin components (Vane et al., 2001).

Although THM in the presence of TMAH has many advantages and has been used successfully to analyze a variety of biological samples, some of the limitations of this method should be noted. Limitations include the methods inability to assess the number of methoxy groups originally present on analytical products prior to analysis (Filley et al., 2000; Challinor, 2001). Many non-lignin compounds, such as gallic acid, are soluble, and so can move through the water column and 'contaminate' lignin signals (Nierop et al., 2005*a*; Filley et al., 2006; Nierop and Filley, 2007). Significant efforts have been made to overcome this limitation, however, and are discussed in the next section.

1.2.7 ^{13}C labelled TMAH

The use of ^{13}C TMAH is relatively new and was first introduced in 1999 to investigate the mechanisms by which TMAH degrades the lignin bipolymer (Filley et al., 1999). It was developed as a technique to distinguish between the methoxyl groups present on the original lignin molecule prior to analysis and those added via transesterification processes during analysis (Filley et al., 2000). This distinction then allows for the identification of degraded lignin molecules as well as non-lignin products which can contribute significantly to the lignin signal (Filley et al., 1999; Filley et al., 2006). For example, Nierop and Filley (2007) found that lignin proxies such as Λ, [Ad/Al] and Γ were all significantly influenced by poly-hydroxyl and non-lignin phenols, with the total lignin yield reduced up to 46%. Because of this, ^{13}C TMAH has been used successfully in a variety of studies to analyze complex mixtures such as soil organic matter, peat, plant materials and dissolved organic matter (Filley et al., 2000; Vane et al., 2001; Filley et al., 2002; Frazier et al., 2005; Nierop et al., 2005*b*; Filley et al., 2006; Nierop and Filley, 2007; Mason, 2009; Mason et al., 2012; Abbott et al., 2013; Swain and Abbott, 2013).

A schematic illustrating how ^{13}C TMAH enables the identification of degraded and non-lignin phenols can be seen in Figure 1.10. Syringic acid (lignin derivative) and gallic acid (tannin derivative) both share a similar structure, and produce the same analytical product, 3,4,5-trimethoxybenzoic acid methyl ester (S6), with the molecular weight of 226 when analyzed with TMAH (Figure 1.10). However, four methyl groups have been added to gallic acid during thermochemolysis, which is where the labelled TMAH proves useful. With the ^{13}C labelled TMAH, the same 4 methyl groups are added, so the molecular weight of the analytical product changes from 226 to 230. This is different to the analytical product from the lignin-derived syringic acid, which only has two methyl groups added as it already contains two methyl groups naturally, and therefore gives a molecular weight of 228. The % of ^{13}C methyl groups added can then be calculated (Filley et al., 2006), and the % of intact lignin present calculated. This method does not allow distinction between fully demethylated lignin and non-lignin

products however as the same number of methyl groups would be added to a fully demethylated version of syringic acid and gallic acid, the main compound comprising hydrolyzable tannins (Nierop and Filley, 2007).

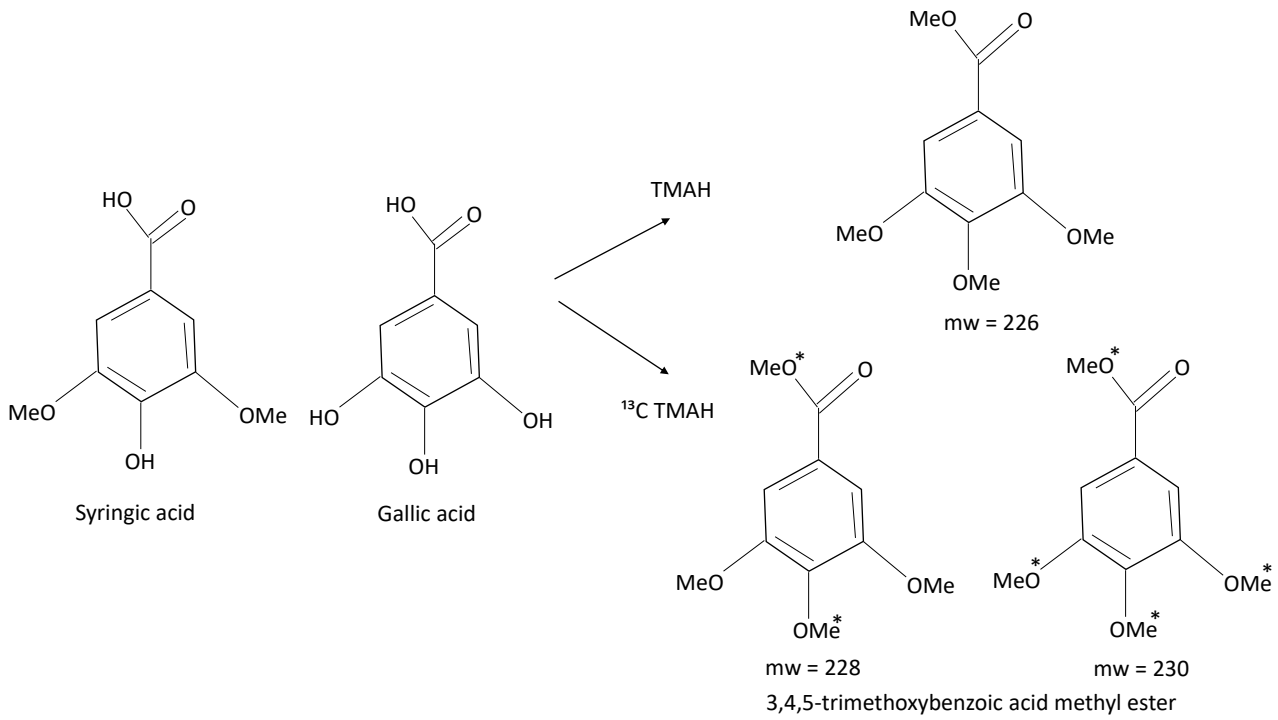

Figure 1.10: Schematic demonstrating how intact lignin such as Syringic acid can be distinguished from tannins such as Gallic acid molecules that share a similar structure using ^{13}C TMAH. Asterisks indicate added ^{13}C methyl groups

Other lignin derivatives are also affected by degraded and non-lignin sources, for example, the guaiacyl phenol 3-hydroxy-4-methoxy benzoic acid methyl ester (G6) and 3-(3-methoxy, 4-hydroxy-phenyl)-3-propenoic acid methyl ester (G18). G6 can be influenced by interference from demethylated lignin, or protocatechuic acid (3,4-dihydroxybenzoic acid methyl ester). Following methylation, in both instances, 3,4-dimethoxybenzoic acid methyl ester is produced (Nierop and Filley, 2007). In addition, G6 can also be affected by the Cannizzaro reaction in which a disproportionation of the aldehyde occurs, and the production of the methoxybenzoic acid methyl ester and methoxybenzyl alcohol methyl ether (Hatcher and Minard, 1995; Tanczos et al., 1999).

This could, in turn, affect the commonly used acid/aldehyde ratios [Ad/Al] to infer oxidation states (Hatcher and Minard, 1995). G18 is also affected by the microbially altered lignin (3-(3-dihydroxyphenyl)-3-propenoic acid methyl ester), or caffeic acid, both of which once methylated give the analytical product *trans* 3-(3,4-dimethoxyphenyl)-3-propenoic acid methyl ester (Nierop and Filley, 2007).

To date, there is no standardised method for THM in the presence of TMAH, and a variety of temperatures and procedures (e.g online, offline analysis, leaving TMAH to mix with the sample for varying amounts of time, adding the TMAH immediately before analysis) have been used within the literature (Hättenschwiler and Vitousek, 2000; Klingberg et al., 2005). This makes it exceptionally difficult to compare results between studies. However, the method still has many advantages over other analytical methods and is considered the best and fastest method for the analysis of complex mixtures such as peat (Saiz-Jimenez, 1994; Kaal and Janssen, 2008).

1.2.8 Tannins

Tannins are the fourth most abundant bipolymer on Earth and have been found to exceed lignin concentrations in some biological samples e.g bark (Hernes and Hedges, 2004). They are found primarily in two different forms; condensed tannins and hydrolyzable tannins (Bate-Smith, 1977; Hernes and Hedges, 2004). Condensed tannins are made up of flavanol monomers, connected via C4-C8 or C4-C6 linkages, whereas hydrolyzable tannins are an abundance of gallic acid molecules bound to a central sugar via ester bonds (Figure 1.11) (Kraus et al., 2004; Nierop et al., 2005*a*). The number of hydroxyl groups on the B ring of condensed tannins separates this tannin type into procyanidins (PC) or prodelphinidins (PD) for two or three hydroxyl groups respectively (Figure 1.11).

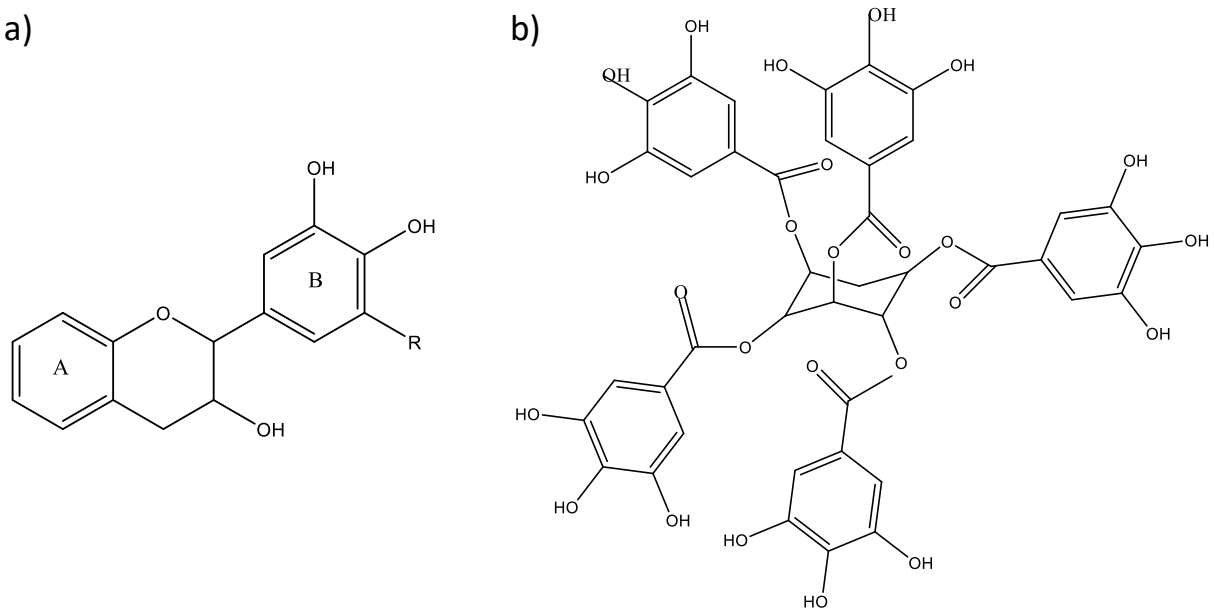

Figure 1.11: Schematic Showing the chemical structure of a) condensed tannins and b) hydrolysable tannins. R = H; epicatechin, R = OH; epigallocatechin. Where PC = procyanidins and PD = prodelphinidins. Adapted from Nierop et al. (2005*b*).

Tannins are defined as secondary metabolite, water-soluble polyphenolic compounds (Haslam, 1988). They can account for up to 40% dry weight of leaves, bark, and needles, and like lignin, are unique to vascular plants (Kraus et al., 2003). Their contribution to soil organic matter can, therefore, be significant. Condensed tannins can be found in ferns and half of the woody angiosperms, whereas hydrolyzable tannins only occur in dicots (Harborne, 1997; Nierop et al., 2005*a*). They are thought to be advantageous for vascular plants in relation to nutrient cycling, competitive advantage and herbivore defence (Kraus et al., 2003). However, the chemical structure of tannins, which is highly heterogeneous, acts as a controlling factor in relation to their function (Kraus et al., 2003). Studies have shown them to be involved in decay resistance and they may provide useful as an indicator for long-term soil degradation dynamics (Lorenz et al., 2000; Loranger et al., 2002; Coq et al., 2010).

Although tannins may play a vital role in soil organic matter diagenesis, the fate of tannins within soil is unclear, due to a difficulty in accurate analysis as a result of their similarity with lignin and other phenolic compounds (Filley et al., 1999; Nierop et al., 2005*b*). However, following the introduction and successful application of ^{13}C TMAH by Filley et al. (1999), the contribution and diagenetic fate of tannins in soils and peats con now be pursued without hindrance.

1.2.9 Carbohydrates

Carbohydrates are abundant and useful compounds, and a primary source of energy for many organisms (Brett and Waldron, 1996). They can occur in different forms, for example, monosacchrides (simple sugar monomers) and polysaccharides (large carbohydrate polymers) (Brett and Waldron, 1996). Polysaccharides comprise the largest photosynthetically derived carbon pool on Earth and are useful indicators of organic matter turnover and degradation in soils (Jia et al., 2008). Moreover, they are also components of bacteria, fungi, and algae (Peberdy, 1990; de Leeuw and Largeau, 1993)

Cellulose is a polysaccharide associated with hemicellulose and composed solely of glucose units linked by β-(1-4) glycosidic bonds (Kögel-Knabner, 2002). Hemicellulose is another polysaccharide but differs from cellulose in the fact that it contains a variety of sugar monomers as opposed to just glucose e.g pentoses, hexoses, hexuronic acids and deoxyhexoses (Kögel-Knabner, 2002). These units are also linked by glycosidic bonds, however, are often branched polymers, and the ratio of monomer types may vary depending upon the source (Kögel-Knabner, 2002).

Studies suggest that soil carbohydrates can typically account for 5-25% of soil organic matter (Angers et al., 1988; Murata et al., 1999). They have a relatively simple structure when compared to recalcitrant structures such as lignins and tannins, and can, therefore, be more rapidly degraded (Derrien et al., 2006; Coq et al., 2010). Increasingly, however, research suggests that this theory is too simple and that some sugars are physically protected (i.e structural carbohydrates) and therefore preserved for much longer

time frames (de Leeuw and Largeau, 1993; Derrien et al., 2006; Estournel-Pelardy et al., 2011). Such physical protection may be from recalcitrant compounds such as lignin and sphagnum acid (Verhoeven and Liefveld, 1997; Derrien et al., 2006; Abbott et al., 2013), however to confirm this, further research is needed.

The most common method for carbohydrate analysis involves acid hydrolysis to investigate the distribution of neutral monosaccharides (i.e xylose) in peat and plant samples (Amelung et al., 1996; Hu et al., 1995; Prietzel et al., 2013; Rumpel and Dignac, 2006; Bourdon et al., 2000; Rovira and Vallejo, 2007). Although acid hydrolysis produces a full suite of monosaccharides from soils, other techniques such as TMAH thermochemolysis are well suited to the chemical analysis of complex mixtures. This technique has been highly successful in the analysis of lignin, tannin and carbohydrate derivatives otherwise locked in a macromolecular structure (Fabbri et al., 1996; Filley et al., 1999; Challinor, 2001; Grasset et al., 2009). Although thermochemolysis of carbohydrates does not allow the identification of individual carbohydrates, it does allow access to a cellulose pool hidden to acid hydrolysis (Estournel-Pelardy et al., 2011), and has been used successfully to investigate the carbohydrate content of samples in several studies (Fabbri and Helleur, 1999; Schwarzinger et al., 2002; Tanczos et al., 2003; Schwarzinger, 2004; Abbott et al., 2013; Black, 2016; Younes and Grasset, 2017).

1.3 Aims and objectives

The effects of climate change upon peatlands are likely to be complex and there is evidence of an already intensified hydrological cycle (Durack et al., 2012). Changes in water table regimes and vegetation inputs will have an impact upon oxygen availability as well as the distributions and amounts of Sphagnum and vascular plant derived phenols (Clymo, 1984; Abbott et al., 2013). This will in turn significantly influence the carbon storage capacity of peatlands (Rydin et al., 2013). This study presents an exploration of the above and below ground organic carbon across a range of environ-

mental conditions at Butterburn Flow, Cumbria UK. This allows the complete picture of the carbon cycle at Butterburn Flow to be established and will give clues as to the fate of peatland organic carbon stocks under future climate regimes. This study was divided into three sections, each with specific aims;

1. Exploring the biochemistry of the dominant peat-forming vegetation across a range of environmental conditions at Butterburn Flow (Chapter 3). This first section includes an in-depth vegetation survey and an investigation into the chemical composition of the dominant plant species across four micro-habitats at Butterburn Flow. The specific objectives were;

a) To establish the dominant plant types and peat-forming species

b) To explore the chemical contribution of different plant types to chemical proxies such as Λ, σ and SR%

c) To confirm the presence of the sphagnum acid biomarkers (I-III)(see Figure 1.4) in *Sphagnum* mosses as observed in van der Heijden et al. (1997) and Abbott et al. (2013)

d) To understand the phenolic make-up and contribution of vascular plant roots to the peat and chemical proxies mentioned above

2. Exploring the biochemistry of the peat across a range of environmental conditions (Chapter 4). This study uses a multi-proxy approach to establish the degree of organic matter decomposition within 1 m of peat across a variety of peatland micro-habitats at Butterburn Flow. The specific objectives were;

a) To characterise the carbon storage and geochemical profile of each micro-habitat up to a depth of 1 m, in an attempt to understand carbon cycling under different hydrological regimes

b) To investigate down core changes in chemical composition and degradation using lignin (Λ, $[\mathrm{Ad/Al}]_G$) and *Sphagnum* (σ, SR%) proxies to establish the long-term persistence of such products and their role in peatland carbon cycle.

c) To evaluate whether the distribution of *Sphagnum* thermochemolysis products

can be used as an indicator for redox conditions in peatlands

d) To establish the effects of sphagnum acid and lignin degradation on the vulnerable carbohydrates and overall carbon contents of the peat.

3. An investigation into the presence of lignin-derived phenolics in *Sphagnum* mosses (Chapter 5). This is a laboratory-based study that uses the species *Sphagnum capillifolium* to establish whether lignin phenols from the dissolved organic carbon (DOC) in the peat water can be incorporated into *Sphagnum* tissue. The specific objectives were:

a) To understand the effects of exposing *Sphagnum* moss to; a) lignin-derived phenol enriched water, b) normal bog water collected from the peatland, or c) phenol free water, on the concentrations of lignin-derived phenols identified in *Sphagnum* tissue

b) To establish whether lignin-derived phenols can be incorporated into *Sphagnum* tissues via external water sources, as suggested by Abbott et al. (2013).

Chapter 2

Field site and methodology

2. Field site and methodology

2.1 Butterburn Flow

Vegetation samples and peat cores were collected from Butterburn Flow (NY 68001 77438), a designated Site of Special Scientific Interest (SSSI) since 1959 (see Figure 2.1). Located near Spadeadam Royal Air Force station (mean annual precipitation 1252.8 mm, mean annual temperature 7.35 °C), it covers 409.3 ha, the largest within the Border Mires Special Area of Conservation (SAC). This area consists of 58 wetlands situated on the border of Northumberland and Cumbria. After decades of restorative work, these mires are among the best in the UK, forming islands of deep ombrotrophic peat, within a forest matrix. (Lunn and Burlton, 2010).

The site represents a transitional mire between hummock-hollow topography and a true patterned mire with a network of soak ways and open water pools. Due to the instability of the area, a short 500 m transect was used for sampling (see Figure 2.1). The following 4 sampling sites were identified based on vegetational and hydrological differences, covering the diversity of environmental conditions at Butterburn Flow; (for full species composition at each site refer to Chapter 3, Table 3.1).

1. Degraded bog (DB) - Small dry area raised approximately 279 m above sea level. pH 4.47, peat is less than 1 m deep. Plant community consists mainly of *Molinia caerulea, Hypnum jutlandicum, and Pleurozium schreberi.*

2. Bog Plateau (BP) - Larger area showing a hummock-hollow topography, approximately 278 m above sea level. pH 4.25, peat deeper than 1 m. Plant community consists of mainly *Calluna vulgaris, Erica tetralix, Trichophorum cespitosum, Molinia caerulea, Sphagnum capillifolium, Sphagnum magellanicum and Sphagnum papillosum.*

3. Bog margin (BM) - Very wet site consisting of a complex network of soak ways and open water pools. Approximately 278 m above sea level. pH 4.10, peat

deeper than 1 m. Plant community consists mainly of *Erica tetralix, Narthecium ossifragum, Eriophorum vaginatum, Trichophorum cespitosum, Sphagnum capillifolium, Sphagnum cuspidatum, Sphagnum magellanicum, Sphagnum papillosum,* and *Sphagnum tenellum.*

4. Fen Lagg (FL) - Dry site, a possible nutrient provision from flooding of the nearby river after extreme precipitation. Approximately 275 m above sea level. pH 4.02, peat deeper than 1 m. Plant community mainly consists of *Eriophorum vaginatum, Sphagnum capillifolium, Sphagnum papillosum and Sphagnum tenellum*

Plant community composition at each site was determined via quadrat surveys. Three 1 m quadrats were randomly placed within each sampling site and species percentage area covered by eye was recorded (Sutherland, 2006). For a more in-depth description of these methods see Chapter 3, section 3.2.1.

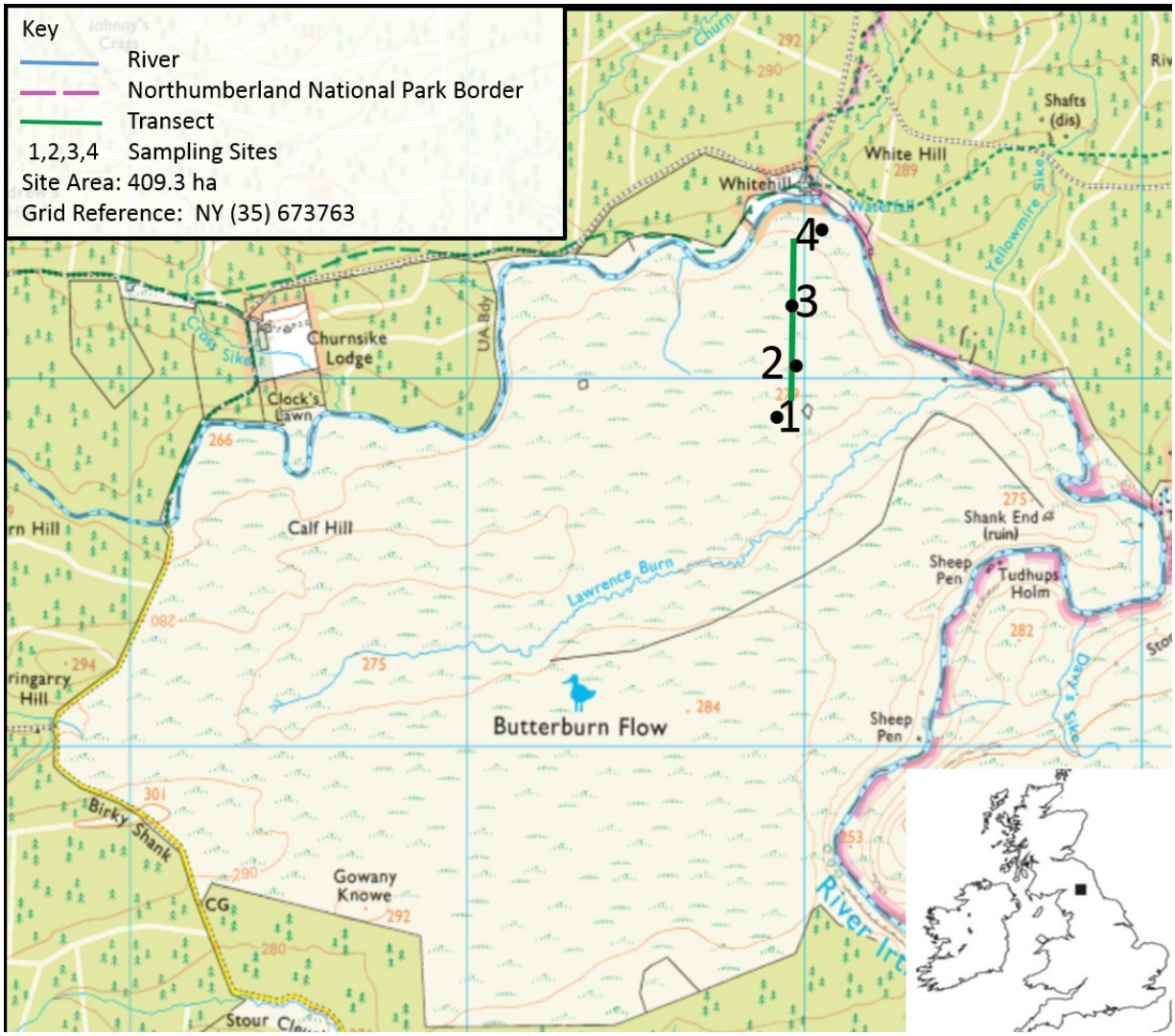

Figure 2.1: Map of Butterburn Flow and sampling transect. Black circles indicate where cores were taken. 1 = Degraded Bog (DB), 2 = Bog Plateau (BP), 3 = Bog Margin (BM), 4 = Fen Lagg (FL)

2.1.1 Hydrological analyses

For hydrological analysis, Solonist leveloggers were placed at a depth of approximately 1 m at each coring site during core collection. Loggers were programmed to take a reading of water level and temperature every 30 min over 12 months to ensure accurate and detailed records of water table fluctuations. A Solonist barologger at DB was also

installed with the same recording programme to measure changes in air pressure and temperature. This was then used in conjunction with the water data to compensate for air pressure changes on water table fluctuations.

2.1.2 Sample collection and preparation

At each site, living vegetation samples were collected with the help of ecologist Helen Adamson (Newcastle University) for plant species identification. 1 m peat cores were then collected with the help of Dr Christopher Vane (British Geological Survey) and an assessment of stratigraphy made. A detailed description of these methods can be found in Nikitina et al. (2014). For illustrations of core stratigraphy refer to Appendix A.

All *Sphagnum* plant species identified at each site were collected, and the whole plant (living sections of capitulun, stem, and branches) used for chemical analysis. In total the following seven species were analysed; *Sphagnum palustre, Sphagnum capillifolium, Sphagnum cuspidatum, Sphagnum magellanicum, Sphagnum papillosum, Sphagnum fallax and Sphagnum tenellum*

Non-*Sphagnum* and vascular plant species were also collected and separated where possible into above ground (shoot) and below ground (root) sections to obtain a more detailed chemical understanding of each plant species as some studies have found significant differences between above and below ground sections (Huang et al., 2011; Ronkainen et al., 2013). The following plant species were analysed; *Calluna vulgaris, Erica tetralix, Vaccinium oxycoccus, Potentilla erecta, Galium saxatile, Narthecium ossifragum, Deschampsia flexuosa, Eriophorum vaginatum, Trichophorum cespitosum, Molinia caerulea, Hypnum jutlandicum and Pleurozium schreberi.* For all plant samples, an attempt was made to separate individual species, however, trace amounts of fungi, vascular plant roots and bryophytes may remain.

In total, eight peat cores of 1 m depth were collected using a Russian corer from the selected sites (DB, BP, BM, FL), and placed into plastic half-pipe, then covered in plastic wrap to retain their shape for transportation and storage. The cores were then returned to the laboratory within 24 hours and stored at -20 °C until processed. Processing began by removing the piping and cutting into approximately 2 cm thick samples using an electric hacksaw. For each sample, the outer edge was removed to minimise external contamination. For geochemical analysis, the remainder of the peat sample and all plant samples were freeze-dried, and then ground to a fine powder using a Glen Creston 6750 freezermill and stored at -20 °C until extraction.

2.2 Laboratory and extraction procedures

All solvents used in laboratory procedures were technical grade purchased from Leading Solvent Supplies and then distilled through a 30 plate Oldershaw fractionation column. All glassware was initially washed in a laboratory dishwasher and then triple rinsed with MeOH and DCM. Teflon extraction tubes were scrubbed with warm soapy water, rinsed and placed on top of a drying cabinet. Once dry, they were sonicated with 1 : 1 DCM : MeOH for 1 h. Immediately prior to use, they were triple rinsed with MeOH and DCM.

Both plant and peat samples were extracted in a 50 mL Teflon tube (Fisher Scientific) using 30 mL of a 1 : 1 DCM : MeOH solvent mixture. Recovery standards (5α-Androstane (Sigma-Aldrich), for n-alkane extracts and 2-Nonadecanone (Sigma-Aldrich), for ketone extracts were added to the dry peat before adding solvent and sonicating for 2 h. Samples were then centrifuged (Sorvall Lynx 4000, Thermo Scientific) at 17,226 g for 15 min. The supernatant was removed and placed into a 100 mL round bottom flask. 30 mL of fresh solvent mixture was added and samples were sonicated again for a further 2 h, centrifuged, and the supernatant removed and added to the same 100 mL round bottom flask. The remaining soil particulate was then placed on top of a drying cabinet overnight. Once dry, approximately 1 mg was taken and

placed into a quartz tube (Analytix, UK) plugged with extracted glass wool ready for Py-GC/MS analysis.

2.2.1 Chemical analysis

Online thermally assisted hydrolysis and methylation (THM) in the presence of Tetramethylammonium Hydroxide (TMAH) was conducted using a CDS Pyroprobe 1000 unit with a platinum coil and sealed into a CDS 1500 valved interface. Immediately prior to analysis, an internal standard of 5α-androstane (Sigma-Aldrich) was added for quantification purposes alongside an aqueous solution of either unlabelled or ^{13}C labelled TMAH (25% w/w)(Sigma-Aldrich). THM was carried out at 610 °C for 10 s with a 20 °C/ms temperature ramp and then products were passed into a Hewlett-Packard 6890 gas chromatograph (GC) with a split injector (30mL/min) linked to a Hewlett-Packard 5973 mass spectrometer (electron voltage 70eV, emission current 35 uA, source temperature 230 °C, quadrupole temperature 150 °C, multiplier voltage 2200 V, interface temperature 320 °C). Acquisition was controlled by a HP kayak xa chemstation computer, in full scan mode (50-650 amu). Product separation was performed on a fused silica capillary column (60 m x 0.25 mm internal diameter) coated with 0.25 μm 5% phenyl methyl silicone (HP-5MS). Initially the GC was held at 50 °C and then heated at a rate of 1.5 °C/min to 220 °C and held for 1 minute,then raised up to a temperature of 320 °C at a rate of 15 °C/min where it was finally held for 16 minutes with Helium as the carrier gas (constant flow 1mL/min, initial pressure of 120 kPa). Each acquired data run was stored for later data processing, integration, and printing. Data was interrogated using DGMS OpenChrom community edition 1.1.0 software, and compound identification were based on the NIST98 mass spectral library, ion fragmentation patterns and published data. In particular, data and traces presented in del Rio et al. (1998) and Abbott et al. (2013) were used heavily as a reference. Table 2.1 contains the full range of THM products identified throughout this thesis and their peak assignments. The naming system used for lignin-derived compounds is the same as that used in works by Clifford et al. (1995); del Rio et al. (1998); Chefetz et al. (2000); Vane et al.

(2001) and Frazier et al. (2003)

Table 2.1: The main thermochemolysis products

Peak label	Tentative assignment	Molecular formula	Molecular ion (M^+)	Characteristic fragment ions and relative abundances (%)
P1	methoxybenzene	C_7H_8O	108	65(75), 77(60), 108(100)
P2	4-methoxytoluene	$C_8H_{10}O$	122	91(20), 107(35), 122(100)
G1	1,2-dimethoxybenzene	$C_8H_{10}O_2$	138	95(50), 123(38), 138(100)
P3	4-methoxybenzeneethylene	C_8H15O	134	91(100), 119(45, 134(100)
1	methylated isosaccharinic acid	$C_{11}H_{22}O_6$	250	142(100), 127(35), 113(30)
2	methylated isosaccharinic acid	$C_{11}H_{22}O_6$	250	156(100), 141(50), 125(30)
G2	3,4-dimethoxytoluene	$C_9H_{12}O_2$	152	109(45), 137(60), 152(100)
4	methylated isosaccharinic acid	$C_{11}H_{22}O_6$	250	154(100), 146(60), 125(35)
I	4-isopropenylphenol	$C10H_{12}O$	148	105(20), 133(70), 148(100)
P4	4-methoxybenzaldehyde	$C_8H_8O_2$	136	77(15), 135(100), 136(70)
S1	1,2,3-trimethoxybenzene	$C_9H_{12}O_3$	168	110(30), 153(65), 168(100)
P5	4-methoxyacetophenone	$C_9H_{10}O_2$	150	107(20), 135(100), 150(40)
P6	4-methoxybenzoic acid methyl ester	$C_9H_{10}O_3$	166	77(15), 135(100), 166(40)
1,2,4-TMB	1,2,4-trimethoxybenzene	$C_9H_{12}O_3$	168	125(50), 153(90), 168(100)
S2	3,4,5-trimethoxytoluene	$C_{10}H_{14}O_3$	182	139(40), 167(85), 182(100)
1,3,5-TMB	1,3,5-trimethoxybenzene	$C_9H_{12}O_3$	168	109(20), 139(80), 168(100)
1,2,3,4-TETMB	1,2,3,4-tetramethoxybenzene	$C_{10}H_{14}O_4$	198	140(40), 83(55), 198(100)
G4	3,4-dimethoxybenzaldehyde	$C_9H_{10}O_3$	166	151(20), 165(50), 166(100)
5	methylated isosaccharinic acid	$C_{11}H_{22}O_6$	250	75(100) 141(60), 173(80)
MC1	methylated metasaccharinc acid	$C_{11}H_{22}O_5$	250	75(40), 101(35), 129(100)
MC2	methylated metasaccharinc acid	$C_{11}H_{22}O_5$	250	101(35), 191(20) 129(100)
MC3	methylated metasaccharinc acid	$C_{11}H_{22}O_5$	250	75(40), 101(35), 129(100)
MC4	methylated metasaccharinc acid	$C_{11}H_{22}O_5$	250	101(35), 191(20), 129(100)
G5	3,4-dimethoxyacetophenone	$C_{10}H_{12}O_3$	180	137(15), 165(100), 180(55)
P17	*cis*-3-(4-dimethoxyphenyl)-3-propenoic acid methyl ester	$C_{11}H_{13}O_3$	193	133(35), 161(100), 192(75)
G6	3,4-dimethoxybenzoic acid methyl ester	$C_{10}H_{12}O_4$	196	165(90), 181(15), 196(100)
S4	3,4,5-trimethoxybenzaldehyde	$C_{10}H_{12}O_4$	196	125(30), 181(50), 196(100)
IIa	*cis*-3-(4-hydroxyphen-1-yl)but-2-enoic acid methyl ester	$C_{12}H_{14}O_3$	206	174(40), 175(100), 206(95)
III	3-(4-hydroxyphen-1-yl)but-3-enoic acid methyl ester	$C_{12}H_{14}O_3$	206	133(40), 148(100), 206(95)
G7	*cis* 1-(3,4-dimethoxyphenyl)-2-methoxyethylene	$C_{11}H_{14}O_3$	195	151(35), 179(65), 194(100)
G8	*trans* 1-(3,4-dimethoxyphenyl)-2-methoxyethylene	$C_{11}H_{14}O_3$	195	151(35), 179(65), 194(100)
P18	*trans*-3-(4-dimethoxyphenyl)-3-propenoic acid methyl ester	$C_{11}H_{13}O_3$	193	133(35), 161(100), 192(75)
IIb	*trans*-3-(4-hydroxyphen-1-yl)but-2-enoic acid methyl ester	$C_{12}H_{14}O_3$	206	174(40), 175(100), 206(95)
S5	3,4,5-trimethoxyacetophenone	$C_{11}H_{14}O_4$	210	139(18), 195(100), 210(85)
S6	3,4,5-benzoic acid methyl ester	$C_{11}H_{14}O_5$	226	195(30), 211(50), 226(100)
S7	*cis* 1-(3,4,5-trimethoxyphenyl)-2-methoxyethylene	$C_{12}H_{16})O_4$	225	181(20), 209(100), 224(92)
S8	*trans* 1-(3,4,5-trimethoxyphenyl)-2-methoxyethylene	$C_{12}H_{16})O_4$	224	181(20), 209(100), 224(92)
G14	*threo/erythro* 1-(3,4-dimethoxyphenyl)-1,2,3-trimethoxypropane	$C_{14}H_{22}O_5$	270	166(15), 181(100), 270(5)
S10	*cis*-1-(3,4,5-trimethoxyphenyl)-methoxyprop-1-ene	$C_{14}H_{20}O_5$	268	195(20), 223(100), 238(90)
G15	*threo/erythro* 1-(3,4-dimethoxyphenyl)-1,2,3-trimethoxypropane	$C_{14}H_{22}O_5$	270	166(15), 181(100), 270(5)
S11	*trans*-1-(3,4,5-trimethoxyphenyl)-methoxyprop-1-ene	$C_{14}H_{20}O_5$	268	195(20), 223(100), 238(95)
G18	*trans*-3-(3,4-dimethoxyphenyl)-3-propenoic acid methyl ester	$C_{12}H_{15}O_4$	223	191(45), 207(15), 222(100)
G19	*trans* 1-(3,4-dimethoxyphenyl)-1,3-dimethoxyprop-1-ene	$C_{13}H_{18}O_4$	238	176(35), 207(50), 238(100)
S14	*threo/erythro* 1-(3,4,5-trimethoxyphenyl)-1,2,3-trimethoxybenzene	$C_{15}H_{24}O_6$	300	181(10), 211(100), 300(8)
$C_{16:0}$ FAME	C_{16} fatty acid methyl ester	$C_{17}H_{34}O_2$	270	74(100), 87(75), 270(15)
S15	*threo/erythro* 1-(3,4,5-trimethoxyphenyl)-1,2,3-trimethoxybenzene	$C_{15}H_{24}O_6$	300	181(10), 211(100), 300(8)
IS	5α-androstane	$C_{19}H_{32}$	260	203(65), 245(100), 260(90)
S17	*cis* 3-(3,4,5-trimethoxyphenyl)-3-propenoic acid methyl ester	$C_{13}H_{17}O_5$	253	221(15), 237(55), 252(100)

2.2.2 Quality control

To maintain a high quality and reliable dataset, two blank samples of extracted glass wool were used and passed through the same laboratory procedures as peat samples. This ensured any data that may be generated due to cross-contamination of samples were discarded, reducing contamination effects on the final results. Also, a bulk sample was run with every batch of samples extracted to ensure there were no issues with extraction efficiencies/analytical procedures. The bulk sample was a combination of sub-samples taken from 5 randomly selected pre-cut peat samples. They were placed together, freeze dried, crushed and extracted in the same way as all other samples. The reason for combining samples was to ensure there was enough volume of sample to extract and analyze multiple times to test analytical accuracy. These two controls to check for analytical inaccuracies and contamination effects ensures the data presented within this thesis is of both high quality and accuracy and is extremely reliable.

In total, 12 bulk samples were run, one at the beginning, one in the middle and one at the end of every batch of samples where each full core of samples considered to be a batch. Specific peaks were then picked to cover a range of concentrations and the percentage variance calculated. All data were normalised to 100 mg OC before analysis began as described in the following section. 9 peaks were chosen for analysis and their associated compounds were P2, G1, P3, G5, G6, P18, S6, G18 and 16:0 fatty acid methyl ester (16:0 FAME).

Figure 2.2 shows the mean concentrations of each compound from the 12 replicates. Mean values were 0.0002, 0.0002, 0.0001, 0.0001, 0.0004, 0.0003, 0.0002, 0.0004 and 0.0001 $\pm$ 0.00005, 0.00004, 0.00003, 0.00002, 0.00006, 0.00006, 0.00004, 0.00008 and 0.00002 for P2, G1, P3, G5, G6, P18, S6, G18 and 16:0 FAME respectively. Analytical replicates were within 10.34% of each other.

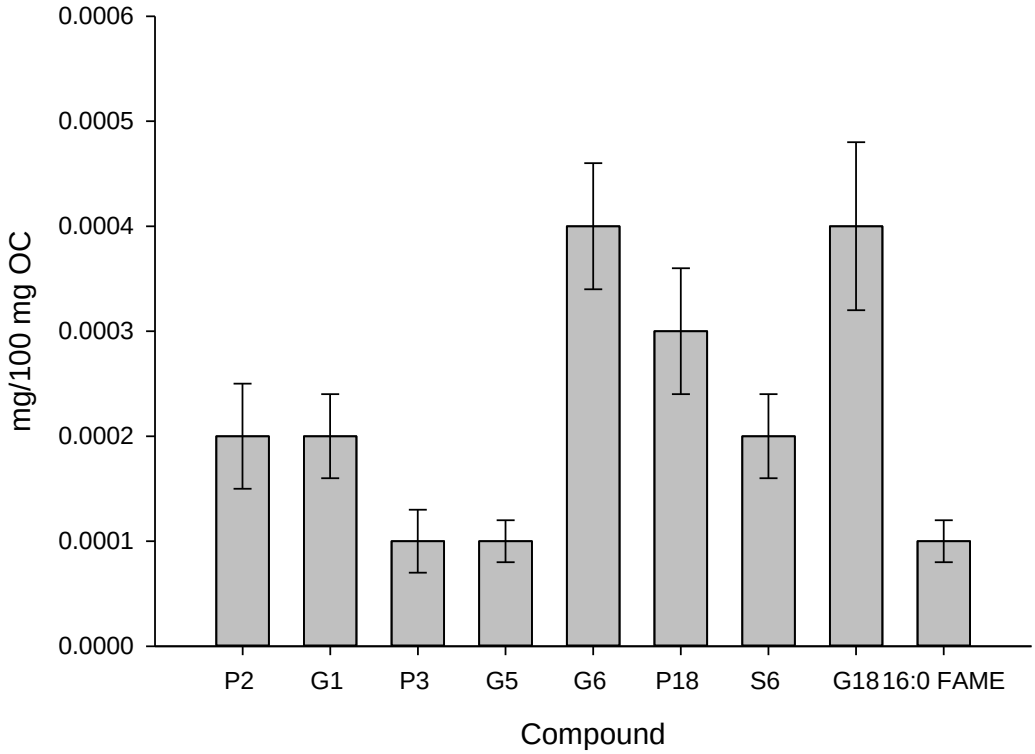

Figure 2.2: Mean concentrations of each compound from 12 analyses of the bulk sample. Error bars show the standard error from 12 replicates.

2.2.3 Compound quantification and normalisation

For THM analysis, all compounds were quantified using an internal standard of 5α-androstane and the following equation to calculate the mass of the compound (CM) in mg;

$$CM = (C_{pa}/S_{pa}) \times MS \tag{2.1}$$

Where C_{pa} is the peak area of the compound, S_{pa} is the peak area of the internal standard and MS is the mass (mg) of the internal standard added to the sample. After

this, compounds were normalised to mg/100 mg OC using the following equation;

$$mg/100mgOC = CM \times 100\ mg\ OC \tag{2.2}$$

Where the 100 mg OC was calculated using the equation below;

$$100\ mg\ OC = 100/OC \tag{2.3}$$

Where OC is the mass (mg) of organic carbon in the sample and was calculated using the following equation;

$$OC = (SW/100) \times TOC \tag{2.4}$$

Where SW is the weight of the sample analysed (mg) and TOC is the total amount of organic carbon (%) obtained using the methods described below in Section 2.2.6.

2.2.4 Pyroprobe calibration

Temperature calibration of the pyropobe is an important task to carry out periodically, particularly if the pyroprobe coil is renewed and ensures THM is carried out at the same, known temperature for all samples. The temperature displayed on the control unit will not reflect the actual temperature the sample is exposed to during analysis due to the insulating properties of the quartz tube and glass wool in which the sample is placed.

To ensure pyrolysis was carried out at the optimal temperature of 610 °C, calibration of the pyroprobe was carried out using the methods described by Bashir (1999). Calibration involved the use of five inorganic salts with known melting points. The salts were prepared in the quartz tubes in the same way as the peat samples, with extracted glass wool used to plug each end. The tubes were then placed in the pyroprobe coil, which was placed into a brass heating block kept at a constant temperature of 340 °C. Helium was used as a carrier gas and kept at a constant rate of 2-10 mL/min. The salts could be observed through a glass window under a microscope, and the programmed temperature at which they were observed melting was measured. The pyroprobe was flashed at increasing temperatures until the salts were fully melted, and the temperature displayed on the pyroprobe control unit was recorded (Figure 2.3). The salts used for the calibration were lead chloride (M.P 501 °C), barium nitrate (M.P 592 °C), lithium chloride (M.P 605 °C), potassium iodide (M.P 681 °C) and magnesium chloride (M.P 714 °C).

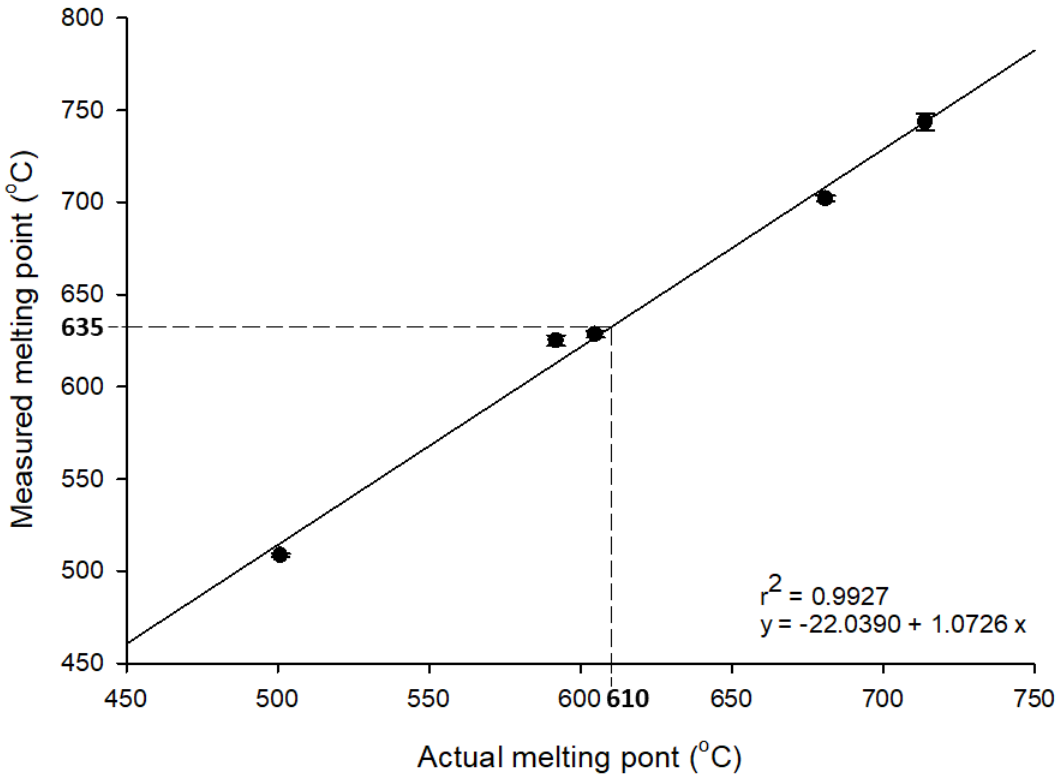

Figure 2.3: Temperature calibration of the pyroprobe showing mean actual and mean observed melting points of five inorganic salts. Error bars represent standard error from three analytical replicates

Calibration of the pyroprobe illustrated that pyrolysis at 610 °C inside the quartz tube was equivalent to a programmed temperature of 632 °C on the pyroprobe control unit. Previous calibrations indicated a programmed temperature of 686 °C (Swain, 2013) and 735 °C (Mason, 2009). These differences may be due to the use of different coils, or the use of a different carrier gas. Nevertheless, they demonstrate the need for periodic calibration to ensure consistent pyrolysis temperatures.

2.2.5 Unlabelled and ^{13}C labelled TMAH

Thermochemolysis with TMAH results in the addition of methyl groups to the acidic hydroxyl groups of the thermochemolysis products. When ^{13}C-labelled TMAH is used,

this changes the molecular mass of the compounds depending upon how many methyl groups are added. The number of ^{13}C-labelled methyl groups should be equal to the number of acidic oxygen functional groups, and can, therefore, be measured as the difference in the mass of the molecular ion between the unlabelled and labelled product (Filley et al., 1999; Filley et al., 2006).

Using this information, the percentage aromatic hydroxyl content of thermochemolysis products can be determined as described in (Filley et al., 1999; Filley et al., 2006). The main equations used in this thesis are shown in Appendix B and are taken from (Filley et al., 2006). Samples treated with unlabelled TMAH were used for identification and quantification purposes, and the ion fragment ratios were used to calculate ^{13}C percentage along with those of labelled samples.

The percentage hydroxyl content of thermochemolysis products is a valuable tool to assess the percentages of intact ($\%1OH$), degraded and non-lignin products (%2OH or more). The degree of methylation of these products can vary, depending on the number of hydroxyl groups present, this then allows the percentage of one, two or three hydroxyl groups present (%1OH, %2OH, %3OH respectively) to be calculated. A peat sample will produce a complex mixture of compounds, including but not limited to lignin compounds, and this method, therefore, allows us to differentiate between non-lignin compounds, such as gallic acid, that may contribute to lignin signals (Figure 2.4) The ^{13}C-labelled TMAH used for this thesis was synthesised in-house following published methods (Filley et al., 1999) then tested for both contamination and functionality with a standard of gallic acid (Sigma-Aldrich) (see Appendix B and C).

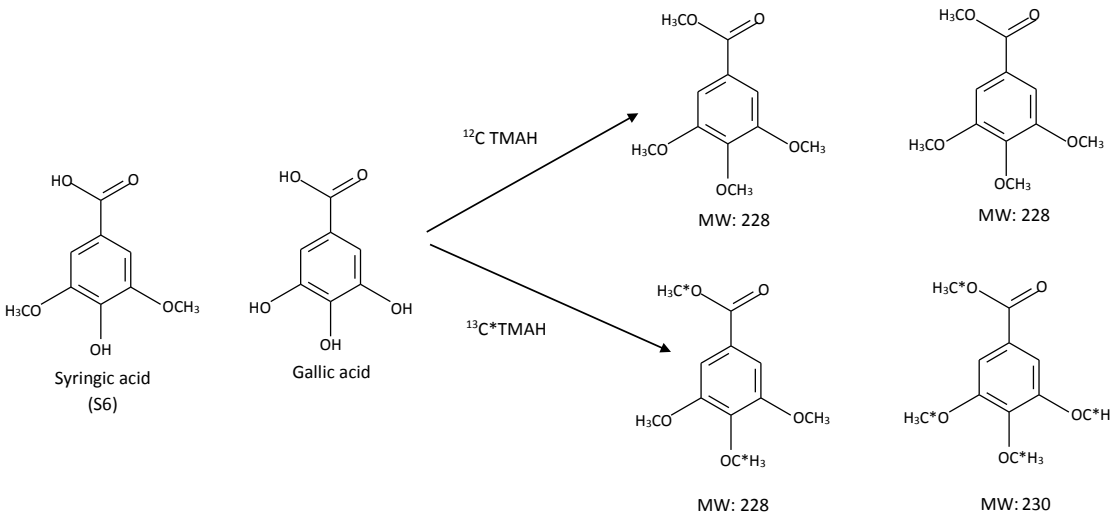

Figure 2.4: Schematic of the methylation process of syringic acid (lignin compound, %1OH - 3,4,5-trimethoxybenzoic acid methyl ester) and gallic acid (tannin compound, %3OH - 3,4,5-trihydroxybenzoic acid) using both ^{12}C TMAH and ^{13}C TMAH, and the resulting change in molecular mass, allowing accurate identification of non-lignin compounds.

2.2.6 Bulk density and elemental analyses

The bulk density of peat is a good indicator of the physical properties of peat and can provide information related to soil compaction, the degree of decomposition and organic matter content (Boelter, 1969; Grigal, 1989). It is expressed in this study as the weight per unit volume of dry soil and includes solids and pore spaces. A modification of the method outlined in Chambers et al. (2011) was used throughout this study. 10 cm of peat of known volume were taken from each frozen core and placed into a weighed aluminium tray. Samples were weighed, and then oven dried at 100 °C overnight. They

were removed from the oven, allowed to cool for 15 minutes and weighed. Samples were placed back in the oven for a further 4 hours, left to cool for 15 minutes and then weighed a second time to ensure there was no significant weight change and that the sample was completely dry. It should be noted, however, that bulk density measurements here are only semi-quantitative as core extraction, transportation and freezing will have already slightly changed the volume of the peat. The bulk density of the peat is finally calculated using the following equation;

$$D_b = W_d / V_w \tag{2.5}$$

Where D_b is the bulk density of the peat (g cm^3), W_d is the weight of the oven dry peat and V_w is the volume of the wet peat (cm^3). No correction for stone content was used as stone content was not significant.

Total organic carbon analysis was carried out according to BS7755 (Section 3.8, 1995). Approximately 10 mg of freeze-dried, ground, soil and plant material were weighed into porous crucibles. 1 mL of HCl (4 M) was added to remove carbonates. Samples were left for 4 hours before being placed in an oven at 70 °C overnight. AR077 iron chips and SL266 tungsten accelerators were added and the TOC content was measured using the LECO-CS230 Carbon - Sulphur analyser (Leco Corporation, USA). The analyser was calibrated using 1 g standard steel rings of certified carbon content (Leco Corporation, USA) and evolved CO_2 was quantified using infrared detection. A reference soil (ISE reference soil 999) was analysed periodically to confirm the accuracy of measurements. The weight of organic carbon (t ha^{-1}) was calculated for each soil horizon using data from bulk density and TOC measurements in the following equation to evaluate the organic carbon storage capacity (OCsc) of Butterburn Flow down to 100 cm depth:

$$OCsc = d \times D_b \times TOC \tag{2.6}$$

Where d represents the depth of peat analysed (cm), D_b is the measured bulk density (g cm^3) and TOC is the measured total organic carbon content (%).

Total carbon (TC), nitrogen (TN) and sulphur (TS) analyses were conducted on an Elementar VarioMAX CNS analyser. Approximately 30 mg of freeze-dried, ground, soil and plant material were weighed into clean (pre-combusted) ceramic crucibles and analysed for carbon, nitrogen and sulphur content. Samples were combusted at 1145 °C in an oxygen-enriched helium atmosphere. Sulfadiazine (%N = 22.37; %C = 47.99; %S = 12.81) was used as the calibration standard and was analysed at the start and end of the sample sequence and after every 10 samples. Raw data were corrected for analytical drift (based on the calibration standard data) during the analysis using the Elementar software.

2.3 Statistical analysis

All statistical analysis was carried out using the IBM SPSS Statistics 22 software package. All significant differences between values were evaluated using a significance level (P-value) less than 0.05, allowing a 95% confidence interval. All data were first tested for normal distribution using the Shapiro-Wilk test of normality. If the P-value was above 0.05, then the data was considered to be normally distributed and the appropriate test was then selected to further analyse the data. The standard error of the mean was calculated and displayed on graphs using error bars, or within the text using (±).

Chapter 3

Exploring the biochemistry of the dominant peat-forming vegetation across a range of environmental conditions at Butterburn Flow

3. Exploring the biochemistry of the dominant peat-forming vegetation across a range of environmental conditions at Butterburn Flow

3.1 Introduction

Peat formation is a process requiring rates of net primary production to exceed decay, resulting in the sequestration of carbon-rich organic material, peat (Moore, 1989). Changes in climate will significantly influence organic carbon sequestration due to changes in vegetation cover, water table and resulting microbial and enzyme activity (Hättenschwiler and Vitousek, 2000; Freeman et al., 2001; Yeloff and Mauquoy, 2006). Changes to the C input will also occur due to ecological changes in plant species and community compositions (Farmer and Morrison, 1964; van Breemen, 1995). In order to understand the effects of climate change on carbon cycling within these ecosystems, it is important to elucidate the biochemistry of the peat-forming vegetation.

A vast amount of geochemical research has been focussed on linking specific compounds identified within soils and sediments to the plants from which they originated (Hedges and Parker, 1976; Hedges and Mann, 1979; Kögel, 1986; Gallet and Lebreton, 1995; Pancost et al., 2002; Andersson et al., 2011; Huang et al., 2011). Lignin is the second most abundant biopolymer on Earth (Boerjan et al., 2003), and a geochemical biomarker for vascular plants (Weng and Chapple, 2010). Key compositional differences between lignin phenols from gymnosperms (non-flowering plants and conifers) and angiosperms (flowering plants including grasses, shrubs, and hardwood trees) have been observed, allowing lignin to be used as an indicator of vascular plant type in complex mixtures such as soils and sediments (Hedges and Parker, 1976; Hedges and Mann, 1979; Kögel, 1986).

Vascular plants contribute carbon to the peat via both above (leaves, stems, flowers) and below (roots) ground biomass. Vascular plant roots play an important role in the

C cycle (Silvola et al., 1992, Silvola et al., 1996*a*, Joabsson et al., 1999; Kögel-Knabner, 2002; Zerva et al., 2005; Wiesenberg et al., 2010) and can therefore significantly influence the carbon balance within soils and peat. Several studies analysing lipid extracts have documented key chemical differences in root and shoot material obtained from vascular plants and stress the importance of accounting for this root-derived OM in chemical analysis of peat (Pancost et al., 2002; Andersson et al., 2011; Huang et al., 2011). However few studies (Gallet and Lebreton, 1995) have explored the phenolic composition of root material and their significance on the sedimentary organic matter, and further research is desperately needed in this area.

However, vascular plants are not the only plant types growing in peatland habitats. Northern peatlands are often dominated by bryophyte species such as *Sphagnum* (Shaw et al., 2003*a*). Bryophytes differ from vascular plants in a variety of ways including their lack of roots and synthesis of lignin, in addition to their exceptional tolerance for low nutrient environments (Hornibrook et al., 2000; Weng and Chapple, 2010). Several studies have also demonstrated moss tissue to be more decay resistant than that of vascular plants (Verhoeven and Toth, 1995; Bragazza et al., 2007).

Sphagnum mosses, like other bryophytes, are able to regulate their environment by increasing the acidity as a result of their high cation exchange capacity and slowing decay (Spearing, 1972; Clymo and Hayward, 1982). However, these interesting species are generally regarded as rather unique for a variety of reasons. Firstly, *Sphagnum* mosses are considered to store more carbon in both dead and living biomass than any other genus of plant (Clymo and Hayward, 1982). Secondly, they have a rather distinctive geochemical profile and appear to be exclusive in their ability to synthesise the recalcitrant phenolic sphagnum acid (*p*-hydroxy-β-[carboxymethyl]-cinnamic acid) (Rudolph and Samland, 1985). Finally, they also contain large concentrations of carbohydrates such as uronic acids (e.g galacturonic acid) which form a large polymeric network known as 'sphagnan' (Verhoeven and Liefveld, 1997). These cell wall polysaccharides display lignin-like properties and may contribute to decay resistance within

the peat (Hájek et al., 2011). These combined features have made *Sphagnum* mosses an interesting species to study.

Thermally assisted hydrolysis and methylation (THM) in the presence of tetramethylammoniumhydroxide (TMAH) can be used to establish the chemical composition of *Sphagnum* mosses. This results in the formation of specific products (I-III) due to the partial decarboxylation of sphagnum acid, that then become stabilised by methylation (van der Heijden et al., 1997). The formation of these products have been explained by Dallinga et al. (1984) and van der Heijden et al. (1997) and will be summarised here and thier structures can be found in Chapter 1, Figure 1.4. The formation of compounds II and III from sphagnum acid involves 1,3H and 1,5H shifts followed by the loss of CO_2 in both cases. These elimination steps can be repeated to form I, however, THM interrupts this second step due to transesterification processes, resulting in the stabilization of IIa/b and III (van der Heijden et al., 1997). The analysis of all four sphagnum acid products using THM in the presence of TMAH may, therefore, be able to reveal the degree of decarboxylation occurring in the peat with an increase in I above that of fresh *Sphagnum* representing decarboxylation *in situ* (Abbott et al., 2013; Swain and Abbott, 2013). A number studies have investigated the presence and abundance of these phenolic compounds within a variety of *Sphagnum* species (Rasmussen et al., 1995; Verhoeven and Liefveld, 1997; Williams et al., 1998). However, to date, only Abbott et al. (2013) have used this method to compare the chemical composition of *Sphagnum* mosses with other common peat forming vascular species.

Alkaline cupric oxidation (CuO) is a method that has commonly been used to analyse lignin in vascular plants (Hedges and Mann, 1979; Hedges and Ertel, 1982; Goi and Hedges, 1990; Opsahl and Benner, 1995). However, Hatcher et al. (1995) and Filley et al. (2000) demonstrated THM in the presence of TMAH was a more sensitive indicator of lignin degradation products than CuO as the C3 side chain is preserved. Three of the four thermochemolysis products identified by van der Heijden et al. (1997) contain C3 side chains (See Chapter 1, section 1.2.3 for product structures), which make THM

in the presence of TMAH an ideal method to track these products within complex mixtures. In addition, Wysocki et al. (2008) suggest that the CuO method was not suited to carbon-rich substrates with a significant plant input, which is the very definition of peat.

The aim of this chapter is to explore the chemical composition of the dominant peat-forming plant species across various microhabitats at Butterburn Flow, Cumbria and understand what this means in terms of the surface peat chemical composition. A selection of the dominant species (with roots where possible) was collected from each coring site for this analysis. The specific objectives were;

1. To survey the vegetation cover, and establish the dominant plant types e.g (*Sphagnum* mosses, non-*Sphagnum* mosses, grasses, and shrubs) and peat-forming species

2. To explore the chemical contribution of different plant types to chemical proxies such as lignin (Λ) and *Sphagnum* proxies (σ and SR%) used in peat analysis and confirm the presence of the characteristic sphagnum acid biomarkers (I-III) in *Sphagnum* mosses as observed by van der Heijden et al. (1997) and Abbott et al. (2013)

3. To understand the phenolic make-up and contribution of vascular plant roots to the peat and chemical proxies mentioned above

4. To use the chemical proxies in conjunction with the vegetation survey to understand what the chemical signatures should look like in surficial present day peat at each microhabitat

3.2 Methods

3.2.1 Sample collection and preparation

In-depth vegetation surveys were conducted and an estimate of % vegetation cover by eye was made, as described in Sutherland (2006). Living plant matter from the dominant vegetation was collected from four different coring sites at Butterburn Flow, Cumbria. These sites were located across a 500 m transect spanning a range of environ-

mental conditions which include; Degraded bog (DB), Bog plateau (BP), Bog margin (BM) and Fen lagg (FL) (see chapter 2, section 2.1 for more detailed descriptions). Species identification was carried out by research ecologist Helen Adamson (Newcastle University).

All *Sphagnum* species identified at each site were collected, and the whole living plant (capitulun, stem, and branches) used for chemical analysis. In total the following seven species were analysed; *Sphagnum palustre, Sphagnum capillifolium, Sphagnum cuspidatum, Sphagnum magellanicum, Sphagnum papillosum, Sphagnum fallax and Sphagnum tenellum*

The following non-*Sphagnum* moss and vascular plant species were also analysed (above ground whole plant sections were selected); *Calluna vulgaris, Erica tetralix, Vaccinium oxycoccus, Potentilla erecta, Galium saxatile, Narthecium ossifragum, Deschampsia flexuosa, Eriophorum vaginatum, Trichophorum cespitosum, Molinia caerulea, Hypnum jutlandicum* and *Pleurozium schreberi*. All plant species were separated and cleaned in deionised water, however, trace amounts of fungi, vascular plant roots and bryophytes may remain.

In addition to above ground sections, root samples were collected from 4 different plant species (*Calluna vulgaris, Erica tetralix, Vaccinium oxycoccus* and *Molinia caerulea*). In comparison to plant shoots, only a small number of root samples were collected due to difficulties in obtaining samples, confirming species origin and permit restrictions on sampling techniques in the field.

Once collected, samples were brought back to Newcastle University, separated and cleaned in deionised water before being stored at -20 °C. When ready for analysis, samples were freeze-dried and crushed to a fine powder before being extracted with a 1 : 1 DCM : MeOH mixture. For a more detailed description see chapter 2, section 2.2.

3.2.2 THM in the presence of TMAH

Around 1 mg of the extracted residue was placed in the middle of a quartz tube plugged on either side with extracted glass wool. On-line THM was carried out at 610°C for 10s. 5α-androstane was used as an internal standard for quantification of compounds, and the NIST 98 library was used for compound identification. For a more detailed description of analytical methods see chapter 2, section 2.2.

3.2.3 Chemical proxies

The chemical proxy Lambda (Λ) is used throughout this chapter for lignin content where Λ represents the sum of the 8 dominant lignin-derived phenols;

$$\Lambda = (G4 + G5 + G6 + S4 + S5 + S6 + P18 + G18) \tag{3.1}$$

All yields are normalised to mg/100 mg OC and corrected for non-lignin phenols unless otherwise stated.

In addition, there are 2 sphagnum acid proxies used within this chapter; Sigma (σ) and the sphagnum ratio (SR%). σ represents the sum of all sphagnum acid derivatives (I, IIa, IIb and III) normalised to 100 mg OC;

$$\sigma = (I + IIa + IIb + III) \tag{3.2}$$

SR% provides an indication of the relative amounts of *Sphagnum*- (σ) and lignin-derived (Λ) phenols contributing to the soil organic matter (SOM). The calculation is expressed below, with all compound masses normalised to 100 mg OC

$$SR\% = [\sigma/(\sigma + \Lambda)]^{*}100 \tag{3.3}$$

3.2.4 Exploration of carbohydrates

Acid hydrolysis is an easy, yet time-consuming technique commonly utilised in the analysis of neutral monosaccharides in many natural environments, including soils (Hu et al., 1995; Amelung et al., 1996; Bourdon et al., 2000; Rumpel and Dignac, 2006; Rovira and Vallejo, 2007; Prietzel et al., 2013). TMAH thermochemolysis is well suited to the analysis of complex mixtures, allowing analysis of lignin, tannin and carbohydrate derivatives otherwise locked in a macromolecular structure (Fabbri et al., 1996; Filley et al., 1999; Challinor, 2001; Grasset et al., 2009). Although thermochemolysis of carbohydrates does not allow the identification of individual carbohydrates, it does allow access to a cellulose pool that is hidden to acid hydrolysis (Estournel-Pelardy et al., 2011).

Several studies have identified THM products in the presence of TMAH derived from individual sugars. For example, Fabbri and Helleur (1999) identified pairs of C6 methylated metasaccharinic acid (3-deoxy-aldonic acid) isomers that display similar mass spectra with a base peak of m/z 129 and a fragment ion of m/z 101 (labelled as peaks MC1-4 in this study). 1,2,4-Trimethoxy benzene was also identified as a product of carbohydrates after analysis of monosaccharide standards. The formation of these methylated metasaccharinic acids and their epimers are shown in Figure 3.1.

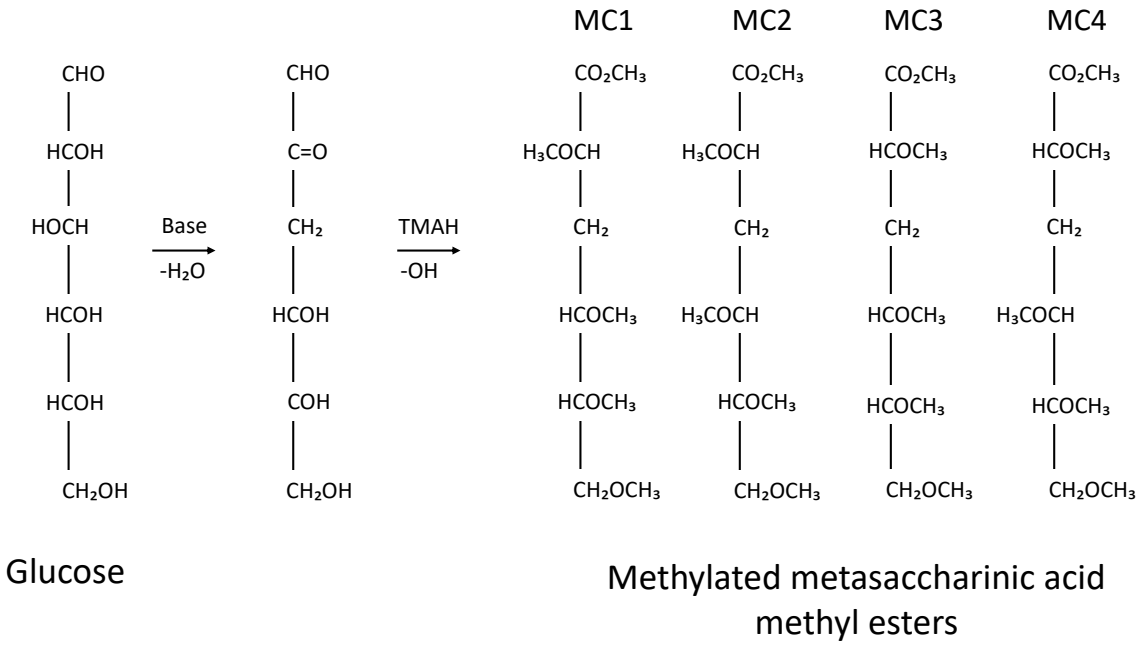

Figure 3.1: TMAH thermochemolysis formation of methylated metasaccharinic acids as proposed by Fabbri and Helleur (1999) and their associated epimers (Chiavari et al., 2007). These products are labelled as MC1-4 in this study.

The origin of these metasaccharinic acids is debated however as several studies have observed a microbial contribution to the carbohydrate pool in soils (Kandeler et al., 2000; Amelung et al., 2001; Glaser et al., 2004). Amino sugars are present in the cell walls of bacteria and fungi and have therefore been used as biomarkers, indicating microbial and fungal contributions to SOM (Amelung et al., 1999; Zhang et al., 1999; Amelung, 2001; Solomon et al., 2001; Turrión et al., 2002; Glaser et al., 2004). Concentrations of amino sugars in soils can be considerable, particularly following the cessation of the microbial community, and appear to be stable compounds in the long term (Kandeler et al., 2000; Kiem and Kögel-Knabner, 2003; Glaser et al., 2004). 1,2,4-trimethoxybenzene (1,2,4-TMB) has also been discovered to have multiple origins, identified in analyses of monosaccharides, polysaccharides, tannins and amino sugars (Fabbri and Helleur, 1999; Schwarzinger et al., 2002; Black, 2016). Findings should, therefore, be interpreted with care, and for this study, 1,2,4-TMB and metasaccharinic

acids (MC1-4) have been separated from polysaccharide analysis.

The products formed by the polysaccharide cellulose have been explored using THM in the presence of TMAH and found to produce a different chromatographic profile to the monosaccharides, with the exception of 1,2,4-TMB (Fabbri and Helleur, 1999). This difference is explained by the difference in the formation mechanism of the products. Cellulose degrades under alkaline conditions and undergoes a peeling reaction leading to the formation of carboxylic acid products (Knill and Kennedy, 2003). The peeled end can then go through similar reactions to the monosaccharide units, however, rather than a hexonic acid being produced, cellulose produces a 2-hydroxylmethyl pentonic acid isomer (commonly called an isosaccharinic acid) (Fabbri and Helleur, 1999). The first set of methylated isosaccharinic acid isomers were identified by Fabbri and Helleur (1999) after analysis of cellulose using electron ionization (EI) mass spectroscopy and show a characteristic m/z 173 fragment ion (labelled as peaks 5 in this study). The fragmentation pathway for these products is illustrated in Figure 3.2. In addition, two major products with a base peak of m/z 142 and m/z 154 (labelled as peaks 1 and 4 respectively in this study) were identified by Schwarzinger et al. (2002) after analysis of a cellulose standard, and by Bardy et al. (2011) in the analysis of soils from the Amazon basin (Figure 3.3). More recently studies by Abbott et al. (2013) and Swain and Abbott (2013) identified an additional two products after the thermochemolysis of a cellulose standard with a base peak of m/z 156 (labelled as peaks 2 and 3 in this study). The mass spectra for these products are shown in Figure 3.4 following analysis with ^{12}C-TMAH, and the combination of these products (labelled as products 1-5 in this study) have been used in this study to assess the cellulose content of plant and soil samples.

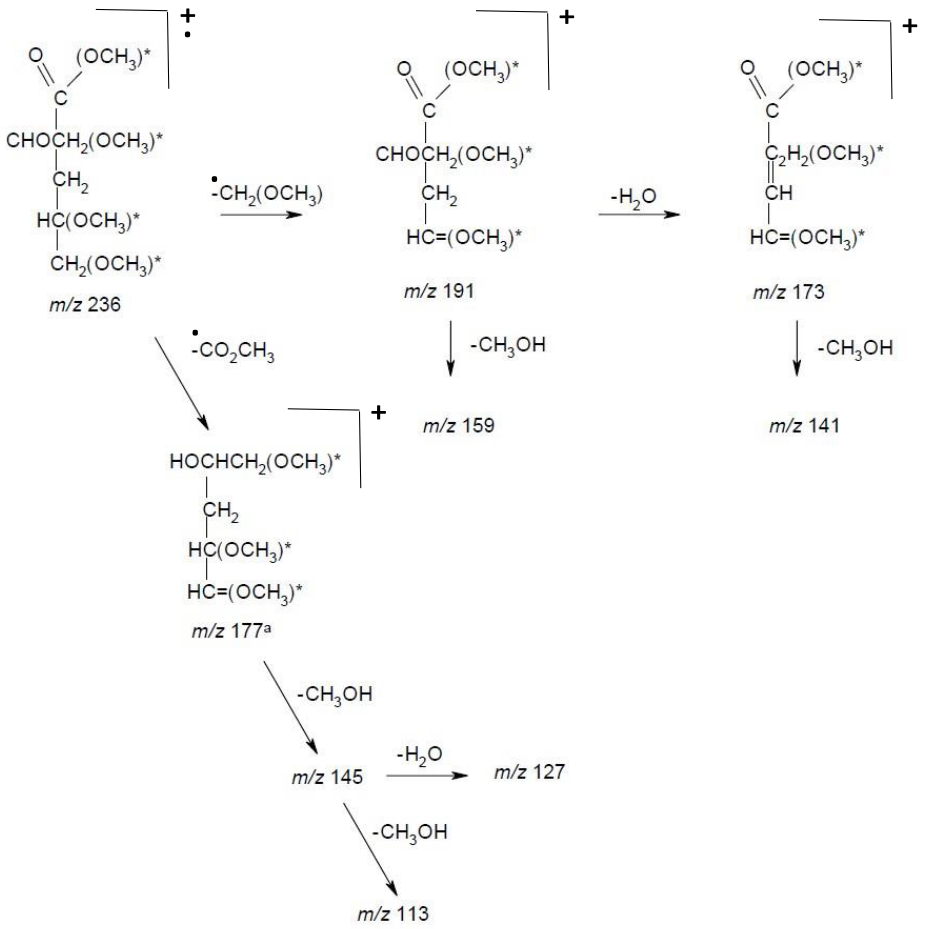

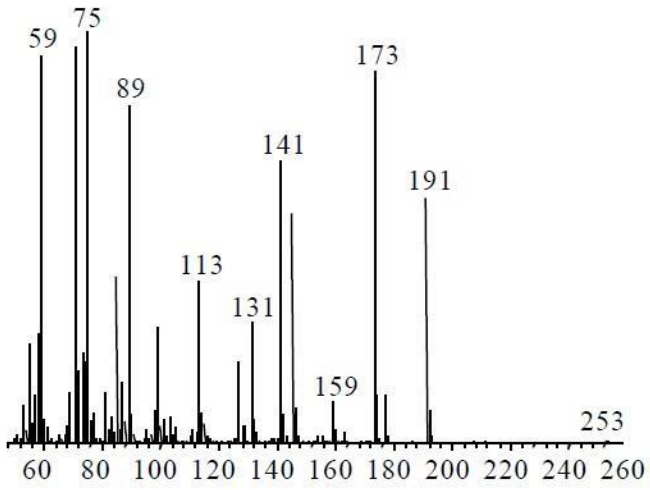

Figure 3.2: TMAH thermochemolysis mass spectrum and fragmentation pathway of partially methylated isosaccharinic acid; peak 5. Modified from Schwarzinger (2004)

.

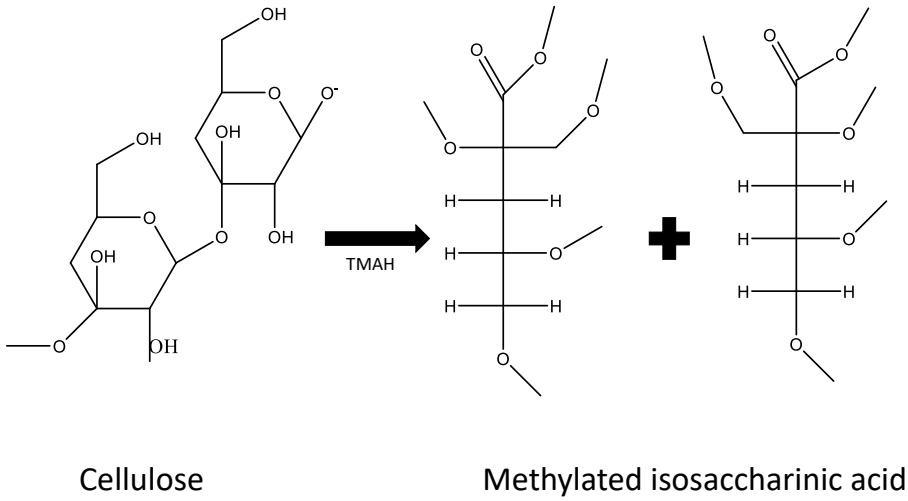

Figure 3.3: TMAH thermochemolysis formation of methylated isosaccharinic acids as proposed by Schwarzinger et al. (2002). These products are labelled as 1-4 in this study. Modified from Schwarzinger (2004)

.

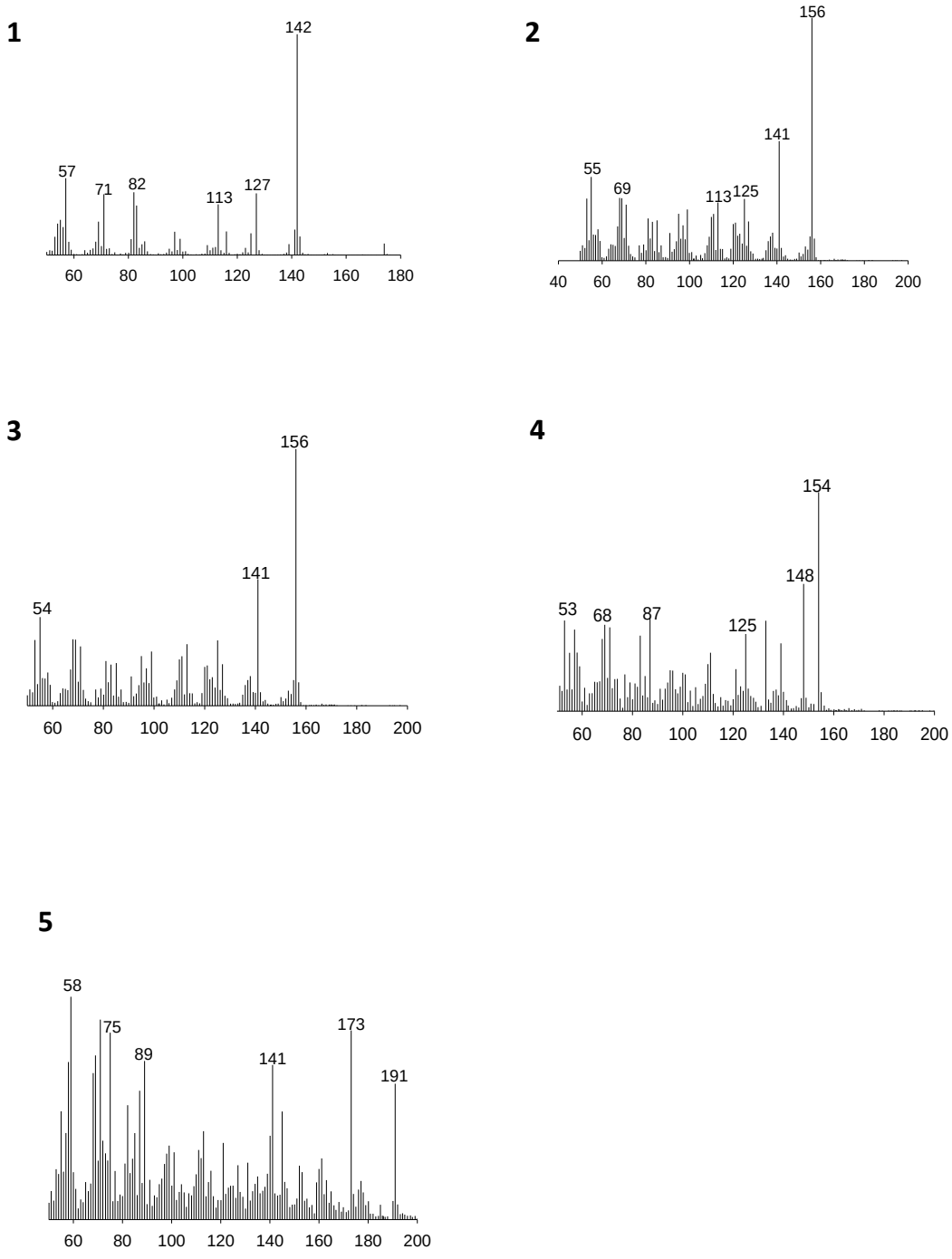

Figure 3.4: Mass spectra for the polysaccharide derived compounds 1-5 as identified in this project

.

The mass spectra of the methylated carbohydrate isomers as observed in this study are shown in Figure 3.5. In previous studies (e.g Schwarzinger et al., 2002; Abbott et al., 2013), incomplete methylation of the monosaccaharide derivatives (MC1-4) has been observed, with larger amounts of TMAH needed for full methylation. The mass spectra generated from this study provide further support for this. From the spectra for MC1 and MC3, it can be seen that only 2 or 3 functional groups have been methylated as opposed to the 3 or 4 that are available. The m/z 147 fragment ion produces a m/z 149 fragment ion with labelled TMAH and the m/z 177 fragment ion gives a m/z 180 fragment ion when in fact what should be seen is a m/z 150 and m/z 182 fragment ion instead. There is also difference in weight of 14 between the m/z 147 and m/z 177 fragment ion of MC1 and 3 compared to the m/z 161 and m/z 191 of MC2 and 4 which confirms the presence of an unmethylated oxygen functional group. It is this difference in methylated that results in the formation of 4 different products.

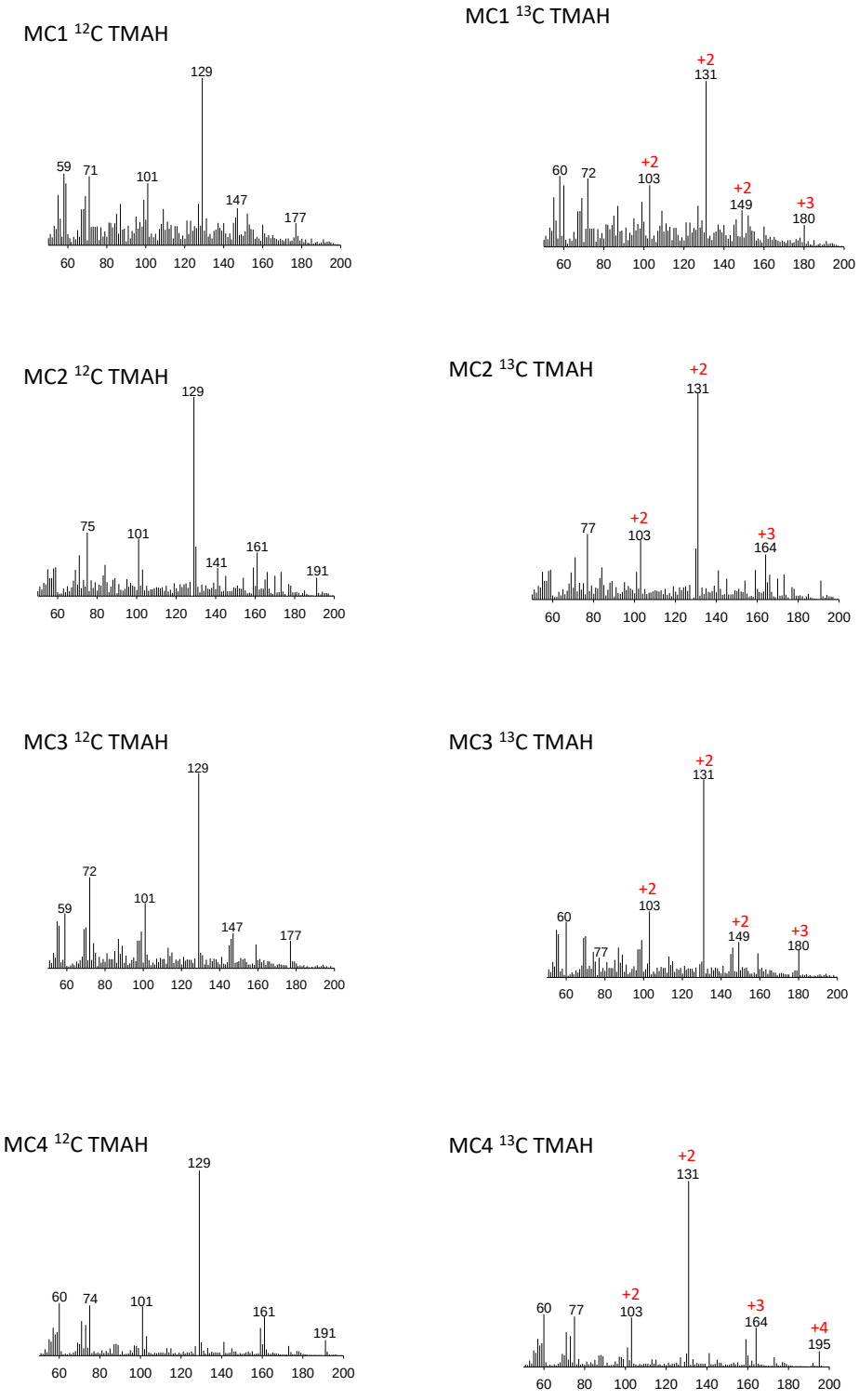

Figure 3.5: Mass spectra for the methylated carbohydrates (MC1-4) in the presence of both unlabelled and ^{13}C labelled TMAH. Red numbers indicate the number of methyl groups added during methylation.

3.2.5 Statistical analyses

All statistical analyses were carried out on IBM SPSS Statistics 23 software. All data were normalised to 100 mg OC and tested for normality using the Shapiro-wilk test as well as visual data assessments. Data could not be made normal by transformations and so non-parametric analyses were used throughout this chapter. A generalized linear model (GZLM) with Fishers Least Significant Difference (LSD) post-hoc tests were used to investigate significant differences in the abundance of the selected chemical proxies; Λ, σ and carbohydrate content (compounds 1-5 for cellulose and MC1-4 for methylated carbohydrate content) between different plant types (e.g *Sphagnum* mosses, Non-*Sphagnum* mosses, grasses, or Shrubs and herbs). The same test was used to investigate the concentrations of the individual *Sphagnum* biomarkers (I, IIa, IIb and III) identified in the *Sphagnum* mosses. Analyses were considered to show significant differences if $p<0.05$.

3.3 Results and discussion

3.3.1 Vegetation assessment

Table 3.1 illustrates the plant species diversity and distribution as observed in the field across the four coring sites at Butterburn Flow. Liverwort species were identified, however, covered so little ground they have only been marked as present (x) or absent (). DB was the only site where *Sphagnum* species were not observed and instead contained an abundance of purple moor grass (*Molinia caerulea*) as well as the non-*Sphagnum* mosses *Hypnum jutlandicum* and *Pleurozium schreberi*, species commonly found on heathland, indicating drier or drained conditions. This is consistent with the presence of several drainage ditches that were observed close to this site.

Table 3.1: Estimated percentage ground vegetation cover by eye from three randomly placed 1 m quadrats at each coring site. x = species present at the site, but no coverage data available.

Site	Degraded bog			Bog plateau			Bog margin			Fen lagg		
Grid reference	NY 67926, 76923			NY 67936, 76963			NY 67934, 77059			NY 68013, 77413		
Shrubs and herbs												
Calluna vulgaris					14	1						
Erica tetralix				40	21	9	10	4	26	4	6	9
Empetrum nigrum				1	1	1						
Vaccinium oxycoccos				2	1	6				8	7	4
Narthecium ossifragum				3		9	50	54	9	1	1	1
Potentilla erecta			3							5	18	5
Galium saxatile	5	9	4									
Grasses and sedges												
Deschammpsia flxuosa	7		4							5	2	
Eriophorum angustifolium					1	1						
Eriophorum vaginatum		4	6	7	18	5	34	18	17	26	1	31
Trichophorum cespitosum				35	25	21	4	9	45			
Molinia caerulea	36	23	64							26	15	31
Festuca ovina	4		1							6	2	2
Carex nigra		1								1		
Andromeda				1	1	1			1			
Mosses												
Aulacomnium plaustre	1				1					2	2	2
Hypnum jutlandicum	34		4							5	3	4
Pleurozium schreberi	7	61	12							1		
Polytrichum alpestre		1			4					1	1	2
Polytrichum commune	4	1	1			2						
Rhytidiadelphus loreus											1	1
Rhytidiadelphus squarrosus	2		1							1		
Sphagnum capillifolium					4	2			1	8	33	4
Sphagnum cuspidatum								1			1	
Sphagnum fallax					1							
Sphagnum magellanicum				4	3			5				
Sphagnum plaustre											4	
Sphagnum papillosum				7	5	42	1	9	1		3	2
Sphagnum tenellum							1					2
Total	100	100	100	100	100	100	100	100	100	100	100	100
Liverworts												
Calypogia fissa												x
Calypogeia muellerana					x	x						
Diplophyllum albicans				x								
Kurzia pauciflora						x	x		x			
Lophozia ventricosa										x		
Odontoschisma sphagnii								x	x	x	x	

BM had the largest *Sphagnum* species diversity and these mosses made up the majority of the understory vegetation at this site. Other classic peat-forming species such as Hares tail cotton grass (*Eriophorum vaginatum*) and Bog asphodel (*Narthecium ossifragum*) were also present in high abundance. Overall, DB and FL were most similar in terms of both species diversity and water table dynamics, although some *Sphagnum* mosses were present at FL (see chapter 4, section 4.3.1 for water table dynamics).

There have been several scientific studies conducted on Butterburn flow (e.g Hendon et al., 2001; Smith et al., 2003; Charman et al., 2004; Hendon and Charman, 2004; Yeloff et al., 2007a,b; Yeloff and Van Geel, 2007; McClymont et al., 2008), all of which observed *Sphagnum* species, and many observed similar vegetation compositions to those observed here. For example, Smith et al. (2003) carried out vegetation surveys in 1988, 1992 and 2002 across 10 different sites at Butterburn Flow. Their surveys showed 14 key species covered up to 66% of the quadrats across all survey years, 11 of which correspond to the dominant species in this study that were selected for chemical analysis. In addition, Yeloff et al. (2007a) sampled at 3 sites very close to the coring sites selected here and observed a dominance of *Sphagnum magellanicum* and *Sphagnum papillosum* as well as constant vascular species *Erica tetralix, Narthecium ossifragum, Vaccinium oxycoccos* and *Calluna vulgaris*. This suggests that the vegetation, and therefore water table and climatic conditions have remained similar within the last 30 years, which should be reflected in the surficial peat.

3.3.1.1 Contribution of plant types to chemical proxies

Figure 3.6 provides an overview of how the various plant types (i.e *Sphagnum* mosses, Non-*Sphagnum* mosses, Grasses, and Shrubs/herbs) identified in the vegetation survey above and selected for chemical analysis contribute to the chemical proxies used in peat analysis. Different plant types contained different amounts of σ, Λ, cellulose derivatives and methylated carbohydrates (GLZM, interaction, plant type x chemical proxy, $\chi^2(6) = 80.626$, $p<0.01$). σ was present only in *Sphagnum* mosses (GLZM,

LSD, p<0.01) due to the absence of I, IIa/b and III in any other plant type (Figures 3.10, 3.11, 3.9). This study, therefore, provides further support to the exclusivity these biomarkers to *Sphagnum* mosses as has been previously suggested e.g (van der Heijden et al., 1997; McClymont et al., 2008; Abbott et al., 2013).

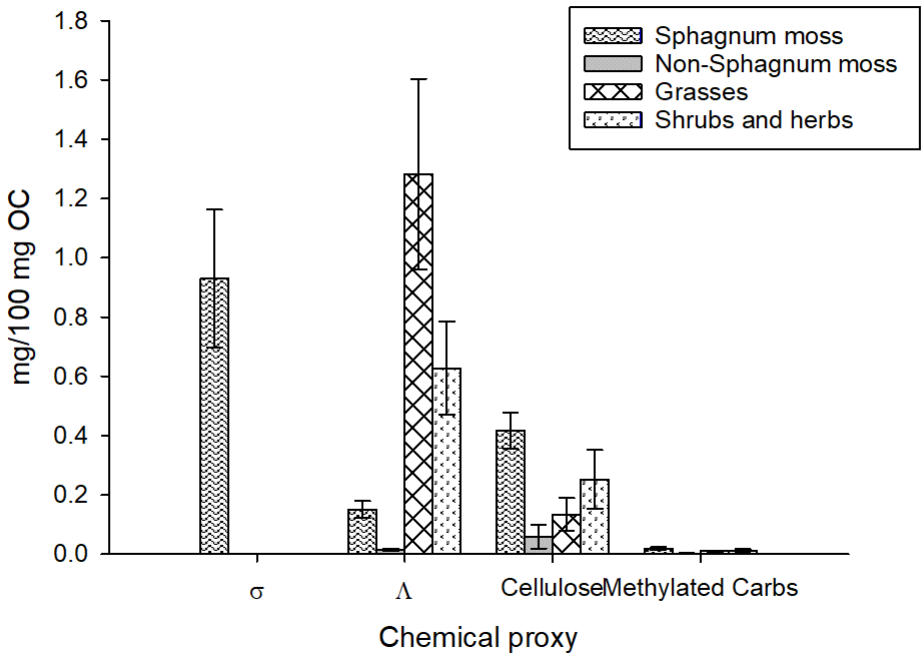

Figure 3.6: Contribution of each plant type analysed to the σ, Λ chemical proxies, and their cellulose and methylated carbohydrate content

Both *Sphagnum* and non-*Sphagnum* mosses contained small amounts of Λ and this was significantly lower compared to the grasses and the shrubs/herbs (GLZM, LSD, p<0.01 for all). Overall, grasses contained the most Λ (GLZM, LSD, p<0.01) with a two-fold increase from shrubs/herbs. There was no difference in either cellulose or methylated carbohydrate derivatives between any plant types (GLZM, LSD, p>0.05), however, cellulose biomarkers were consistently in higher abundance than the methylated carbohydrate derivatives.

The high concentrations of Λ in the vascular plants (grasses and shrubs and herbs)

was expected and authenticates the validity of the Λ as a vascular plant proxy (Weng and Chapple, 2010). The presence of lignin phenols in mosses, however, is highly controversial, and several studies have stated that lower plants are unable to biosynthesise lignin, (e.g Weng and Chapple (2010); Espiñeira et al. (2011)). In addition, McClymont et al. (2011) noted the absence of lignin biomarkers in the pyrolysates of several bryophyte species including *Sphagnum*. In contrast, Xu et al. (2009) provide evidence of the genetic ability for moss lignin biosynthesis, and several studies are in agreement that mosses contain lignin-like structures in their cell walls (Ros et al., 2007; Ligrone et al., 2008). Moreover, Schellekens et al. (2009); Abbott et al. (2013) and Schellekens et al. (2015a) identified low concentrations of lignin phenols such as the cinnamyl phenols *p*-courmaric acid (P18) and ferulic acid (G18), the guaiacyl lignin phenols; 3,4-dimethoxybenzaldehyde (G4), 3,4-dimethoxyacetophenone (G5), and 3,4-dimethoxybenzoic acid methyl ester (G6), and the syringyl lignin phenol 3,4,5-benzoic acid methyl ester (S6) in *Sphagnum* pyrolysates, which have also been observed in this study (See Figure 3.7 and Figure 3.8). It is possible, however, that the mosses are not biosynthesising these compounds, but instead these compounds migrate into the plant via the peat water, or via contamination with *Ericaceae* rootlets, and then are incorporated into the plant (Smeerdijk and Boon, 1987; Abbott et al., 2013; Schellekens et al., 2015a). The mechanisms for this are unknown, however, and further research in this area is needed.

3.3.2 THM in the presence of TMAH

THM thermochemolysis of the solvent-extracted dominant vegetation yielded a range of methylated phenolic products alongside other oxygenated compounds as listed in Table 3.2. The naming system used for lignin derived compounds is the same as that used in works by del Rio et al. (1998); Clifford et al. (1995); Chefetz et al. (2000); Vane et al. (2001) and Frazier et al. (2003).

Table 3.2: The main thermochemolysis products

Peak label	Tentative assignment
P1	methoxybenzene
P2	4-methoxytoluene
G1	1,2-dimethoxybenzene
P3	4-methoxybenzeneethylene
1	methylated isosaccharinic acid
2	methylated isosaccharinic acid
G2	3,4-dimethoxytoluene
4	methylated isosaccharinic acid
I	4-isopropenylphenol
P4	4-methoxybenzaldehyde
S1	1,2,3-trimethoxybenzene
P5	4-methoxyacetophenone
1,2,4-TMB	1,2,4-trimethoxybenzene
S2	3,4,5-trimethoxytoluene
1,3,5-TMB	1,3,5-trimethoxybenzene
1,2,3,4-TETMB	1,2,3,4-tetramethoxybenzene
G4	3,4-dimethoxybenzaldehyde
5	methylated isosaccharinic acid
MC1	methylated metasaccharninc acid
MC2	methylated metasaccharninc acid
MC3	methylated metasaccharninc acid
MC4	methylated metasaccharninc acid
G5	3,4-dimethoxyacetophenone
G6	3,4-dimethoxybenzoic acid methyl ester
S4	3,4,5-trimethoxybenzaldehyde
IIa	*cis*-3-(4-hydroxyphen-1-yl)but-2-enoic acid methyl ester
III	3-(4-hydroxyphen-1-yl)but-3-enoic acid methyl ester
G7	*cis* 1-(3,4-dimethoxyphenyl)-2-methoxyethylene
G8	*trans* 1-(3,4-dimethoxyphenyl)-2-methoxyethylene
P18	*trans*-3-(4-dimethoxyphenyl)-3-propenoic acid methyl ester
IIb	*trans*-3-(4-hydroxyphen-1-yl)but-2-enoic acid methyl ester
S5	3,4,5-trimethoxyacetophenone
S6	3,4,5-benzoic acid methyl ester
S7	*cis* 1-(3,4,5-trimethoxyphenyl)-2-methoxyethylene
S8	*trans* 1-(3,4,5-trimethoxyphenyl)-2-methoxyethylene
G14	*threo/erythro* 1-(3,4-dimethoxyphenyl)-1,2,3-trimethoxypropane
G15	*threo/erythro* 1-(3,4-dimethoxyphenyl)-1,2,3-trimethoxypropane
G18	*trans*-3-(3,4-dimethoxyphenyl)-3-propenoic acid methyl ester
G19	*trans* 1-(3,4-dimethoxyphenyl)-1,3-dimethoxyprop-1-ene
S14	*threo/erythro* 1-(3,4,5-trimethoxyphenyl)-1,2,3-trimethoxybenzene
$C_{16:0}$ FAME	C_{16} fatty acid methyl ester
S15	*threo/erythro* 1-(3,4,5-trimethoxyphenyl)-1,2,3-trimethoxybenzene
IS	5α-androstane
S17	*cis* 3-(3,4,5-trimethoxyphenyl)-3-propenoic acid methyl ester

3.3.2.1 *Sphagnum* biomarkers

Overall, the distribution of thermochemolysis products for the *Sphagnum* mosses were very similar. Sphagnum acid biomarkers (I, IIa/b or III) were absent in all species except Sphagnum mosses (see Table 3.3 and Figures 3.7, 3.8, 3.10, 3.11 and 3.9), reinforcing their use as a biomarker for Sphagnum species. There were significant differences between concentrations of these four compounds (GZLM, $\chi^2(3) = 20.462, p<0.01$), with I and IIb present in significantly higher concentrations than IIa and III in all Sphagnum species (LSD, $p<0.05$ for all), which has been observed in previous studies (van der Heijden et al., 1997; Abbott et al., 2013). For example, Abbott et al. (2013) analysed nine *Sphagnum* species in addition to eight non-*Sphagnum* bryophytes and vascular plants from Ryggmossen peatland, central Sweden. Following thermally assisted hydrolysis and methylation, the sphagnum acid derivatives I-III were identified in *Sphagnum* mosses only, confirming their reliability as a *Sphagnum* biomarker, and the dominance of compounds I and IIb was clear in all species. Moreover, the same compound dominance was observed from an authentic sphagnum acid standard that was also analysed in the same study, confirming these products as thermochemolysis products of bound sphagnum acid.

In this study, the relative proportion of the *Sphagnum* biomarkers I-III contributing to the sum of Sphagnum phenols (σ) were 36.6, 8.5, 11.7 and 43.3% ($\pm$ 8.1, 2.5, 3.2 and 11.3%) for I, IIa, IIb and III respectively, which closely resembles the results obtained by Swain (2013) following analysis for 5 *Sphagnum* species collected from Ryggmossen bog, Sweden and, again, reflect the dominance of I and IIb to the σ signal. *Sphagnum palustre* contained overall the highest concentrations, particularly of IIb, but of all sphagnum acid compounds. Average yields of I, IIa, IIb and III across the 7 Sphagnum species analysed were 0.343, 0.079, 0.402 and 0.108 mg/100 mg OC ($\pm$ 0.075, 0.023, 0.105 and 0.030) respectively (Table 3.3).

Table 3.3: The yield (mg/100 mg OC) of the dominant lignin-derivatives, cellulose derivatives(1-3) and sphagnum acid derived products (I-III) within 7 Sphagnum moss samples. Values are an average taken from two analytical replicates. All samples have been analysed with 13C-labelled TMAH, and therefore are corrected for non-lignin phenols. n.d = not detected

Species	P1	P2	P3	P18	G1	G4	G5	G6	G18	S1	S6	1	2	3	I	IIa	III	IIb	SR%
								mg/100mg OC											
Sphagnum fallax	0.144	0.215	0.242	0.050	0.084	0.014	0.002	0.002	0.001	0.042	0.002	0.254	0.032	0.099	0.351	0.088	0.122	0.459	89.6
Sphagnum cuspidatum	0.094	0.118	0.116	0.036	0.055	0.001	n.d	0.003	0.001	0.023	0.004	0.266	0.094	0.189	0.251	0.027	0.052	0.175	86.5
Sphagnum magellanicum	0.122	0.151	0.197	0.047	0.088	0.029	0.010	0.008	0.001	0.037	0.009	0.172	0.023	0.102	0.261	0.078	0.095	0.359	78.4
Sphagnum palustre	0.227	0.294	0.496	0.113	0.193	0.006	0.004	0.006	0.003	0.074	0.005	0.422	0.066	0.168	0.781	0.212	0.279	0.996	88.8
Sphagnum papillosum	0.062	0.087	0.121	0.035	0.051	0.002	0.003	0.004	0.002	0.020	0.004	0.159	0.026	0.068	0.212	0.044	0.056	0.220	79.7
Sphagnum tenellum	0.063	0.091	0.174	0.054	0.076	0.005	0.005	0.007	0.001	0.029	0.006	0.225	0.039	0.088	0.293	0.049	0.083	0.311	84.9
Sphagnum capillifolium	0.068	0.099	0.174	0.032	0.077	0.002	0.002	0.003	0.001	0.036	n.d	7 0.216	0.044	0.090	0.233	0.054	0.070	0.295	88.6
Mean	0.112	0.151	0.217	0.053	0.089	0.045	0.006	0.031	0.010	0.038	0.004	0.245	0.046	0.115	0.340	0.079	0.108	0.402	85.2
S.E	0.023	0.033	0.051	0.011	0.019	0.008	0.001	0.007	0.004	0.007	0.001	0.038	0.008	0.019	0.075	0.023	0.030	0.105	1.705

The sphagnum ratio (SR%) remained high in all species (Table 3.3), ranging from 78.4-89.6% and indicating a strong σ signal although some intact lignin was present (Figures 3.7 and 3.8). Large quantities of *p*-hydroxy phenols; methoxybenzene (P1), 4-methoxytoluene (P2), 4-methoxybenzeneethylene (P3) as well as 4-methoxyacetophenone (P5) were identified, which have been observed in other studies (see (Schellekens et al., 2009; McClymont et al., 2011; Swain, 2013; Schellekens et al., 2015a).The vascular plant-derived phenols identified included methylated guaiacyl (G) lignin phenols; 1,2-dimethoxybenzene (G1), 3,4-dimethoxybenzaldehyde (G4) and 3,4-dimethoxybenzoic acid methyl ester (G6) as well as the syringyl (S) derivatives; 1,2,3-trimethoxy benzene (S1) and 3,4,5-trimethoxybenzoic acid methyl ester (S6). Not all of these compounds were derived from degraded lignin, however, with an average of 80.2% of guaiacyl structures (G4, G5, G6 and G18) and only 18.0% of the syringyl structures (S6) derived from intact lignin. All Sphagnum mosses were completely devoid of the lignin derivatives 3,4-dimethoxytoluene (G2), 3,4,5-trimethoxybenzaldehyde (S4) and 3,4,5-trimethoxyacetophenone (S5) (Figures 3.7 and 3.8).

As mentioned above, low concentrations of vascular plant-derived phenolics in *Sphagnum* tissues are not unusual and have been observed in several other studies (Bland et al., 1968; Smeerdijk and Boon, 1987; Schellekens et al., 2009; Swain, 2013; Schellekens et al., 2015a). For example, Smeerdijk and Boon (1987) observed small amounts of some guaiacyl and syringyl lignin phenols from the pyrolysates of subfossil *Sphagnum* leaves from a freshly cut peat profile from the Assendelver Polders in the western Netherlands. More recently, Schellekens et al. (2015a) observed minor concentrations of guaiacyl lignin in pyrolysates of living *Sphagnum centrale* and *Sphagnum magellanicum* collected from a peatland in northern Sweden. Although it is currently debated as to how *Sphagnum* species accumulate such phenolics, one line of thought suggests the source may be the bog water used by and surrounding the plants (Abbott et al., 2013; Schellekens et al., 2015a). Nichols et al. (2010) demonstrated that the water from the surface of the peat is used by the living *Sphagnum* which is then held in the large water holding hyaline cells (Clymo and Hayward, 1982). Couple this with the solubility of

vascular plant phenols (Hernes and Benner, 2003) it is possible that migration of these phenols has occurred via the dissolved organic matter (DOM) in the peat water, which have then been incorporated into the plant tissues (Abbott et al., 2013).

There were several other dominant inputs to the Sphagnum mosses, including cellulose derivatives 1, 2 and 3, as well as 1,2,4-trimethoxybenzene (1,2,4-TMB) which reflect a high cellulose content (see Figures 3.7 and 3.8). The input from the methylated carbohydrate derivatives (MC1-4) was minimal in all samples.

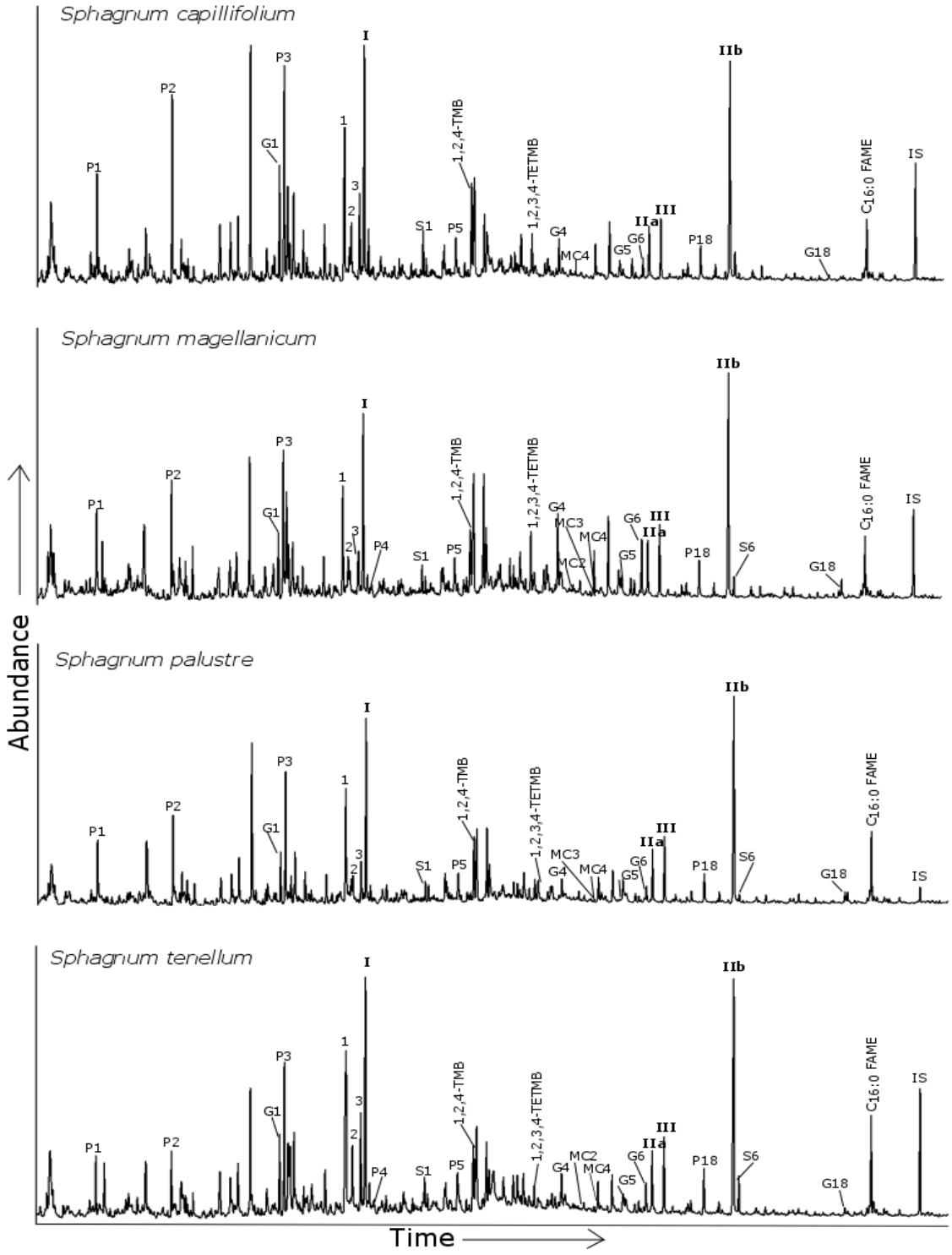

Figure 3.7: Partial total ion chromatogram (TIC) of the thermochemolysis products from *Sphagnum capillifolium, Sphagnum magellanicum, Sphagnum palustre, Sphagnum tenellum*. IS denotes internal standard. Peak identities are listed in Table 3.2.

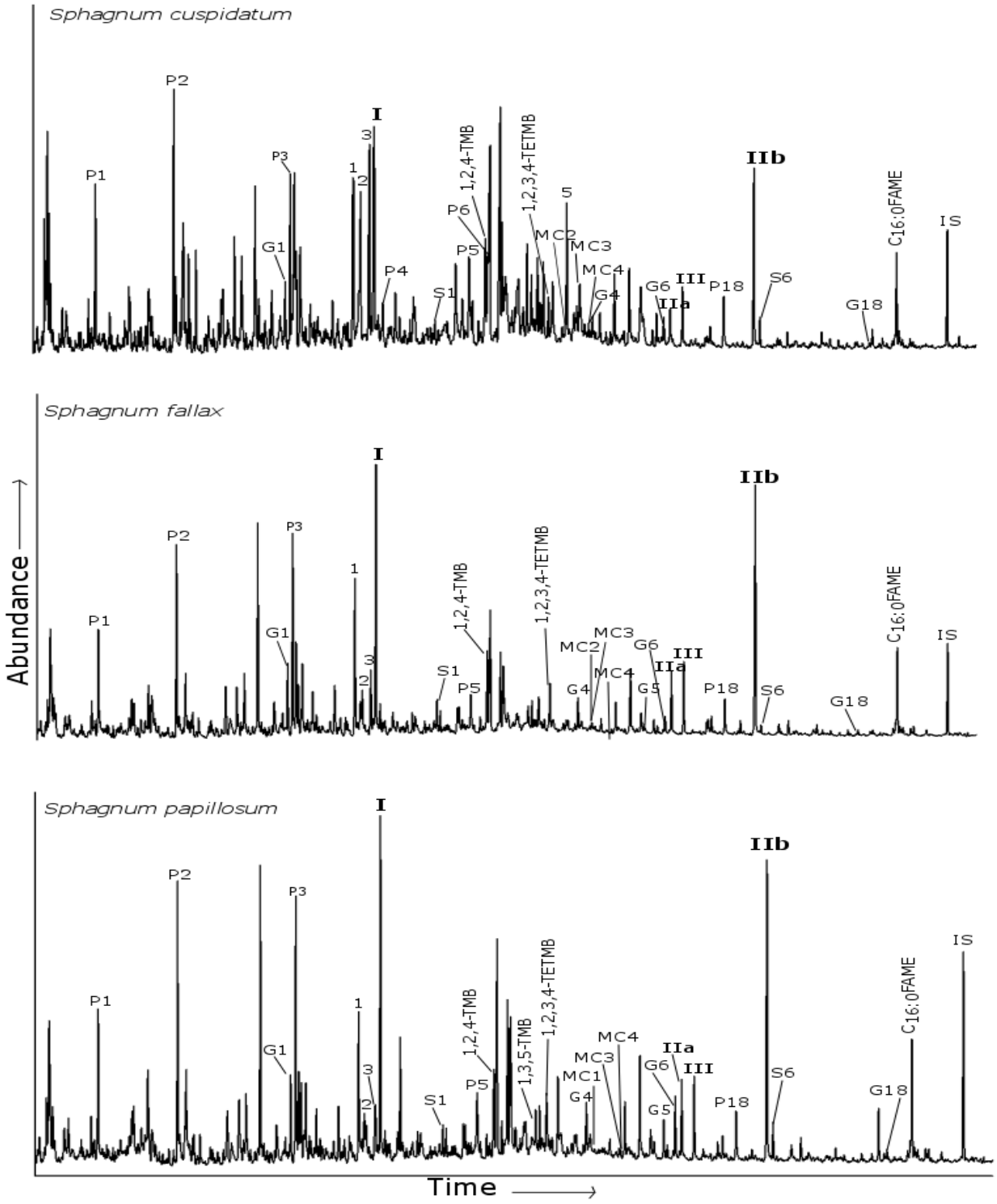

Figure 3.8: Partial total ion chromatogram (TIC) of the thermochemolysis products from *Sphagnum cuspidatum, Sphagnum fallax* and *Sphagnum papillosum.* IS denotes internal standard. Peak identities are listed in Table 3.2.

3.3.2.2 Non-sphagnum mosses

Overall, the non-Sphagnum mosses (*Hypnum jutlandicum* and *Pleurozium schreberi*) contained the lowest concentrations of all compounds identified and, like the *Sphagnum* mosses, contained no 3,4,5-trimethoxybenzaldehyde (S4) or 3,4,5-trimethoxy acetophenone (S5) (Table 3.4, Figure 3.9). The lignin yield (Λ) was also very low (0.020 mg/100 mg OC for *Pleurozium schreberi* and 0.010 mg/100 mg OC for *Hypnum jutlandicum*) for these species after correction for non-lignin phenols.^{13}C TMAH revealed that 84.4% of the guaiacyl and only 15.4% of the syringyl phenols were derived from methoxylated phenolic subunits for these non-*Sphagnum* mosses. *Sphagnum* biomarkers were completely absent and analyses showed a limited range of thermochemolysis products in general (Figure 3.9). *Pleurozium schreberi* was dominated by the *p*-hydroxy phenols 4-methoxyacetophenone (P5) and 4-methoxybenzoic acid methyl ester (P6), whereas $C_{16:0}$ FAME dominated *Hypnum jutlandicum* (Figure 3.9).

The absence of *Sphagnum* markers, as well as a low Λ and phenolic yield, is expected and consistent with other studies of non-*Sphagnum* mosses (McClymont et al., 2011; Swain, 2013). However, the results obtained for *Pleurozium schreberi* in this study are dissimilar to those obtained by Swain (2013) who observed G5 and G6 as dominant compounds as opposed to P5 and P6 observed here. This may suggest that the phenolic composition of some mosses may change depending upon location and, if mosses do incorporate lignin into their tissues via DOC, the phenolic composition of the peat water may be a controlling factor here.

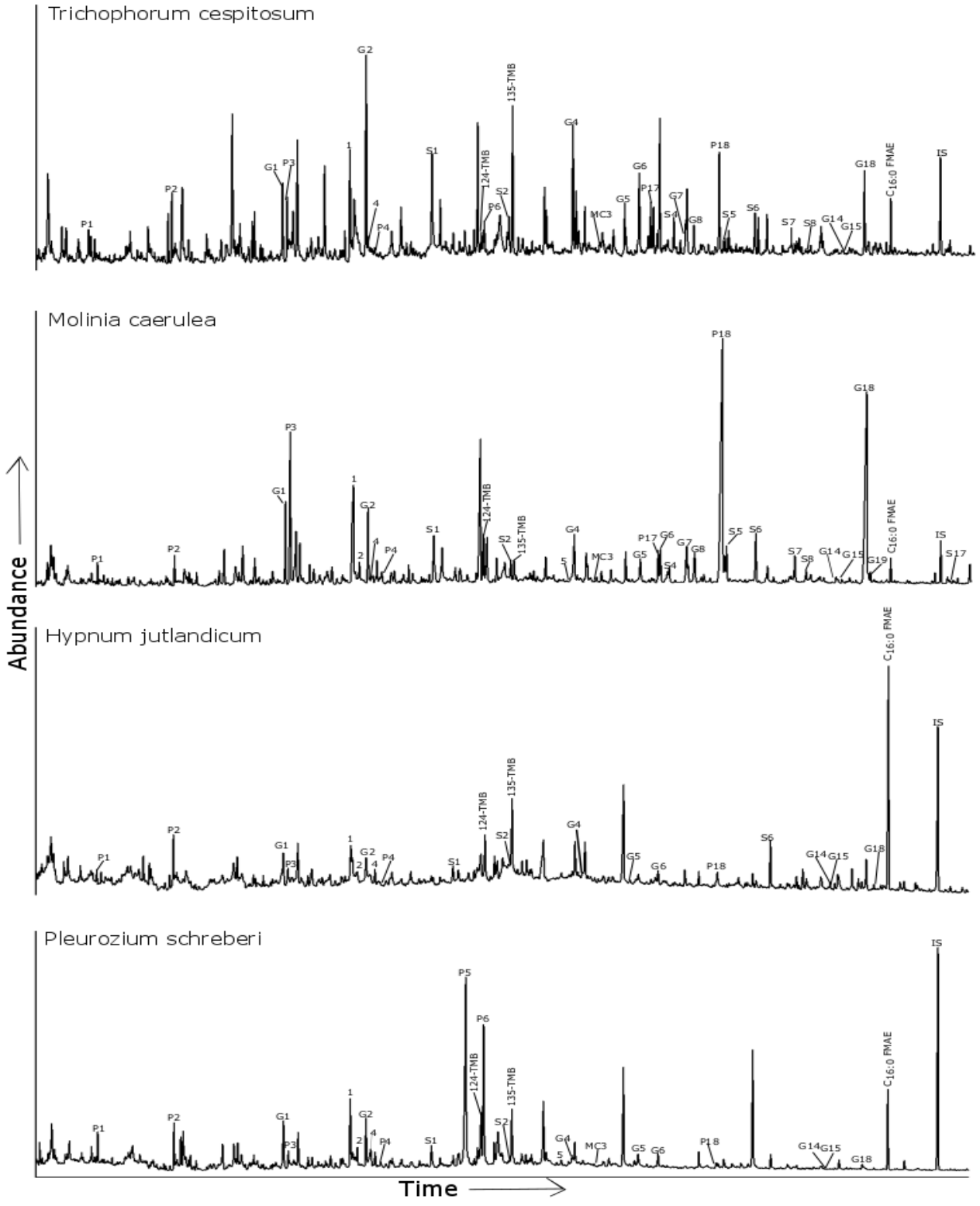

Figure 3.9: Partial total ion chromatogram (TIC) of the thermochemolysis products from *Trichophorum cespitosum, Molinia caerulea, Hypnum jutlandicum* and *Pleurozium schreberi*. IS denotes internal standard. Peak identities are listed in Table 3.2.

3.3.2.3 Vascular plants

The vascular plants overall showed large, but similar, distributions of thermochemolysis products, however concentrations of *p*-hydroxy, guaiacyl and syringyl structures varied between species and plant type (Table 3.4 and Figures 3.10, 3.11, 3.9). The 'shrubs and herbs' analysed tended to show dominance of 1,2-dimethoxybenzene (G1), 3,4-dimethoxytoluene (G2), 3,4-dimethoxybenzoic acid methyl ester (G6), *trans* 3-(3,4-dimethoxyphenyl)-3-propenoic acid methyl ester (G18), 3,4,5-trimethoxyacetophenone (S6). *Vaccinium oxycoccus* also had a dominant input of 4-methoxybenzeneethylene (P3) and *trans* 3-(4-methoxyphenyl)-3-propenoic acid methyl ester (P18). *Narthecum ossifragum* showed the strongest dominance from guaiacyl and syringyl structures than any other species (Figures 3.10, 3.11 and 3.9). These results are in accordance with the mixture of guaiacyl and syringyl phenols identified in angiosperms (Hedges and Mann, 1979), and results appear similar to those presented in studies by both Mason et al. (2012) and Abbott et al. (2013) who observed a mixture of lignin-derived phenols following TMAH thermochemolysis in plant species such as *Andromeda polifolia, Calluna vulgaris, Empetrum nigrum, Rhododendron tomentosum and Vaccinium microcarpum.*

Grasses tended to be dominated by *p*-courmaric acid (*trans* 3-(4-methoxyphenyl)-3-propenoic acid methyl ester (P18)) and ferulic acid (*trans* 3-(3,4-dimethoxyphenyl)-3-propenoic acid methyl ester (G18)), and match the product composition found in other studies (Nierop, 2001; Mason et al., 2012; Abbott et al., 2013) (Figures 3.9 and 3.11). For example,Mason et al. (2012) analysed grass samples using TMAH thermochemolysis from a grassland dominated by *Festuca ovina, Deschampsia flexuosa* and *Eriophorum vaginatum* species. The traces obtained show a clear dominance of P18 and G18, which were observed here, in addition to a significant input of G3 which differs from this study where G3 is absent, but a considerable input from G2 can be observed Figure 3.9 and 3.11. A significant input from P18 ad G18 is expected as these monomers are indicative of a gramineous input (Hedges and Mann, 1979) and are therefore expected to dominate the surface peat at DB and FL where there is a significant grass input.

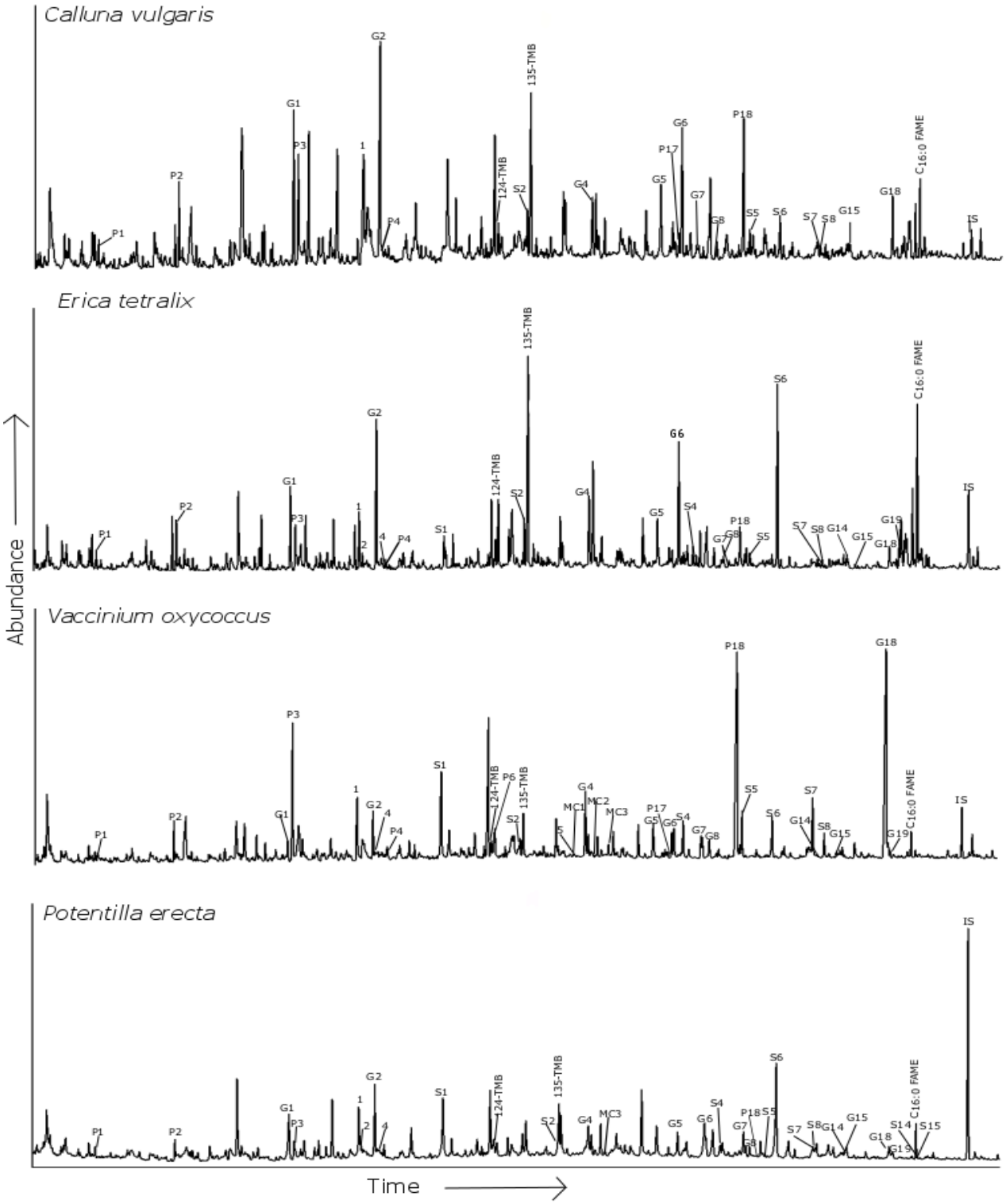

Figure 3.10: Partial total ion chromatogram (TIC) of the thermochemolysis products from *Calluna vulgaris, Erica tetralix, Vaccinium oxycoccus* and *Potentilla erecta*. IS denotes internal standard. Peak identities are listed in Table 3.2.

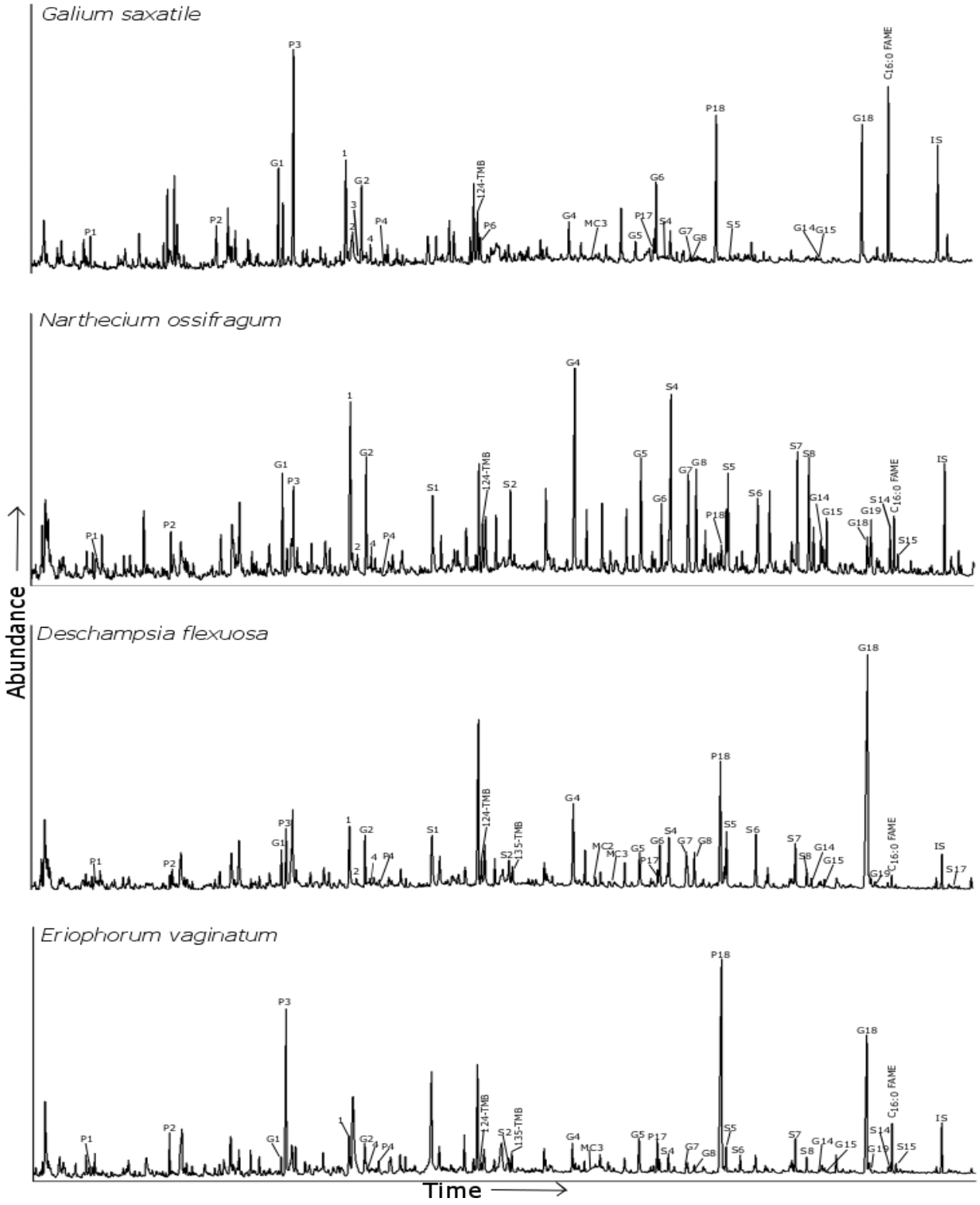

Figure 3.11: Partial total ion chromatogram (TIC) of the thermochemolysis products from *Galium saxatile, Narthecium ossifragum, Deschampsia flexuosa* and *Eriophorum vaginatum*. IS denotes internal standard. Peak identities are listed in Table 3.2.

Table 3.4: The yield (mg/100 mg OC) of the dominant lignin derivatives, cellulose derivatives (1-4), and the corrected $[Ad/Al]_G$ ratio for 10 vascular plants and 4 root samples as well as 2 non-*Sphagnum* moss species. All samples have been analysed with 13C-labelled TMAH, and therefore are corrected for non-lignin phenols. n.d = not detected

Species	P1	P2	P3	P18	G1	G2	G4	G5	G6	G18	S4	S5	S6	1	2	4	$[Ad/Al]_G$
	mg/100mg OC																
Shrubs and herbs																	
Calluna vulgaris	0.052	0.133	0.164	0.270	0.352	0.514	0.059	0.134	0.038	0.016	0.0169	0.0352	0.0151	0.2015	n.d	n.d	2.788
Calluna vulgaris roots	0.030	0.054	0.031	0.060	0.202	0.536	0.177	0.222	0.098	0.016	0.102	0.086	0.013	0.316	0.017	0.034	2.947
Erica tetralix	0.018	0.062	0.041	0.028	0.134	0.233	0.027	0.038	0.021	0.002	n.d	0.011	0.011	0.088	0.007	0.008	3.517
Erica tetralix roots	n.d	0.034	n.d	n.d	0.163	0.374	0.110	0.134	0.028	0.004	0.002	0.039	0.012	0.227	0.019	0.023	2.267
Vaccinium oxycoccus	0.012	0.045	0.199	0.518	0.028	0.060	0.039	0.007	0.034	0.447	0.001	0.054	0.004	0.096	n.d	0.003	0.869
Vaccinium oxycoccus roots	0.006	0.028	0.025	0.021	0.090	0.335	0.123	0.032	0.234	0.068	0.000	0.016	0.020	0.236	0.015	0.007	1.909
Potentilla erecta	0.007	0.033	0.016	0.037	0.039	0.039	0.008	0.002	0.014	0.010	0.000	0.002	0.007	0.049	0.006	0.002	1.674
Galium saxatile	0.012	0.047	0.040	0.109	0.053	0.055	0.025	0.006	0.044	0.090	0.00	0.001	n.d	0.105	0.009	0.007	1.723
Narthecium ossifragum	0.051	0.257	0.151	0.337	0.112	0.152	0.106	0.003	0.099	0.072	0.002	0.049	0.004	0.724	0.031	0.045	0.933
Grasses																	
Deschampsia flexuosa	0.029	0.059	0.190	0.502	0.101	0.109	0.047	0.007	0.064	0.056	0.004	0.047	0.007	0.234	0.018	0.010	1.380
Eriophorum vaginatum	0.013	0.066	0.358	0.841	0.029	0.048	0.026	0.010	0.021	0.370	0.003	0.044	0.003	0.070	n.d	0.003	0.788
Trichophorum cespitosum	0.017	0.057	0.051	0.120	0.085	0.229	0.087	0.021	0.154	0.096	0.000	0.012	0.010	0.147	n.d	0.006	1.763
Molinia caerulea	0.031	0.068	0.392	1.300	0.089	0.115	0.059	0.024	0.040	0.565	0.001	0.074	0.011	0.256	0.012	0.012	0.675
Molinia caerulea roots	0.020	0.064	0.362	0.740	0.107	0.115	0.048	0.008	0.11	0.055	0.001	0.022	0.005	0.237	0.016	0.025	0.226
mosses																	
Hypnum jutlandicum	0.006	0.014	0.004	0.003	0.026	0.010	0.001	0.002	0.003	0.001	n.d	n.d	0.001	0.008	0.005	0.002	4.250
Pleurozium schreberi	0.016	0.018	0.006	0.002	0.034	0.030	0.003	0.006	0.007	0.002	n.d	n.d	n.d	0.041	0.010	0.013	2.448

3.3.2.4 Vascular plant roots

The TIC of the roots from *Calluna vulgaris, Erica tetralix,* and *Vaccinium oxycoccus* (shrubs/herbs) appear similar to each other (see Figure 3.12) and contained a range of *p*-hydroxyl, guaiacyl, and syringyl lignin monomers. However, there are differences in product abundances, particularly between these samples and the grass roots analysed from *Molinia caerulea* (Figure 3.12).

Overall, the root samples from the shrubs/herbs displayed dominance from the guaiacyl structures; 1,2-dimethoxybenzene (G1), 3,4-dimethoxytoluene (G2), 3,4-dimethoxybenzaldehyde (G4), 3,4-dimethoxyacetophenone (G5), and 3,4-dimethoxybenzoic acid methyl ester (G6) (Figure 3.12), as well as the syringyl structures; 1,2,3-trimethoxybenzene (S1) and 3,4,5-trimethoxybenzoic acid methyl ester (S6). 1,3,5-Trimethoxy benzene (1,3,5-TMB), a known biomarker for tannins and cutan (McKinney et al., 1996; Nierop et al., 2005*a*) was also a very dominant product (Figure 3.12). The phenolic content of the roots appear to be different to the above-ground sections of the same species (Figures 3.10, 3.12 and Table 3.4) confirming that different plant sections are compositionally different (Nierop et al., 2001; Nierop, 2001; Kögel-Knabner, 2002). For example, Nierop (2001) analysed the roots and shoots of a variety of plant species using Py-GC/MS including pine roots and observed a different distribution of products compared to the needles. In addition, the roots of both *Empetrum* and *Fagus* species showed a significantly lower abundance of syringols. These samples were also analysed using THM thermochemolysis and showed the same trend, with a distinct lack of syringyl lignin in *Empetrum* and *Fagus* roots.

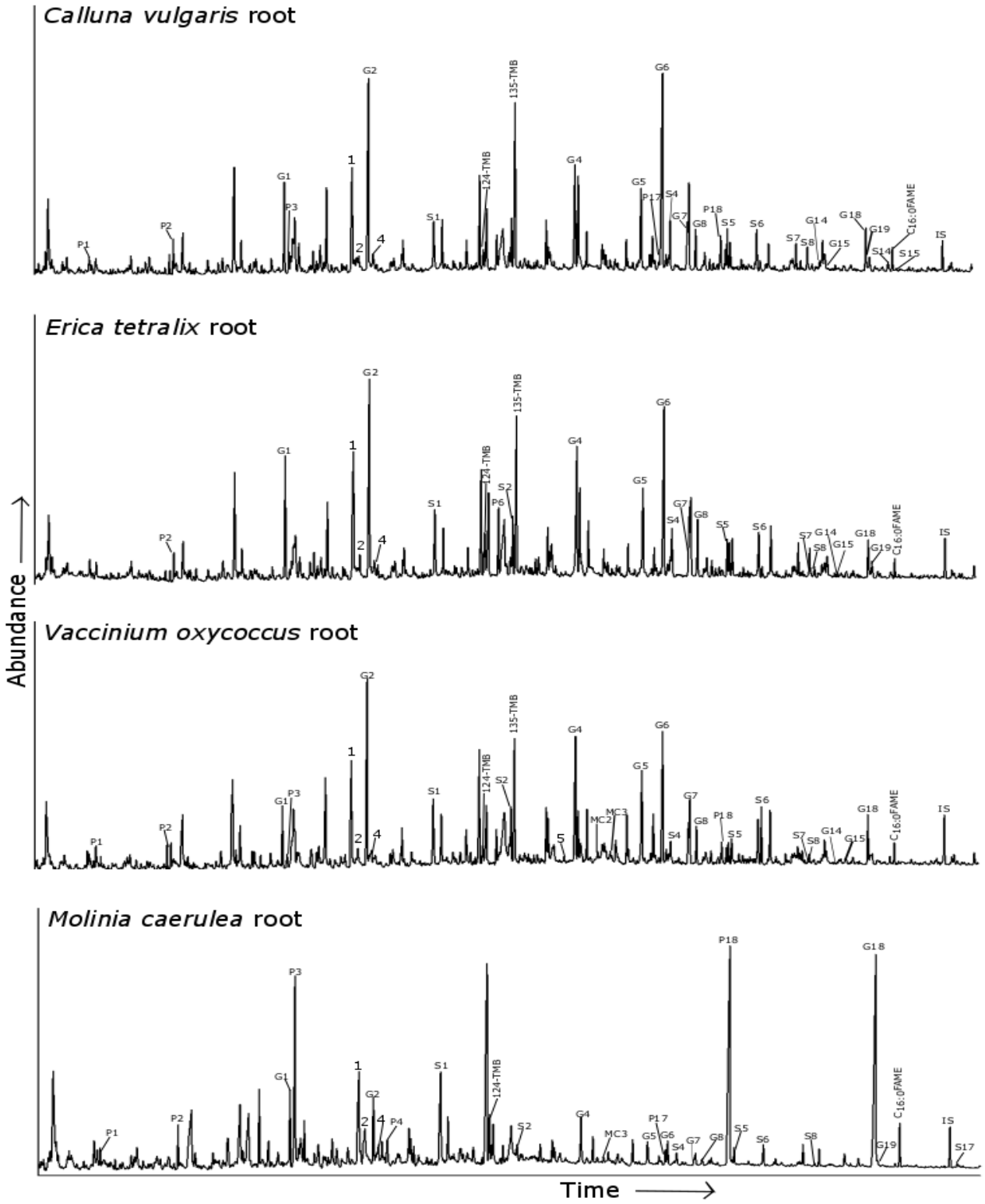

Figure 3.12: Partial total ion chromatogram (TIC) of the thermochemolysis products from the roots of *Calluna vulgaris, Erica tetralix, Vaccinium oxycoccus* and *Molinia caerulea*. IS denotes internal standard. Peak identities are listed in Table 3.2.

Analysis of the above-ground portion of *Calluna vulgaris* (Figure 3.10) shows the presence of 4-methoxybenzaldehyde (P4) which is absent from the roots, and suggests a larger input from *trans* 3-(4-methoxyphenyl)-3-propenoic acid methyl ester (P18) and C_{16} fatty acid methyl ester ($C_{16:0}$ FAME) than in the roots. The increased abundance of this latter compound is also seen in the analysis of the above-ground section of *Erica tetralix*. In addition, for the roots for this species products methoxybenzene (P1), 4-methoxybenzeneethylene (P3) and 3-(4-methoxyphenyl)-3-propenoic acid methyl ester (P18) were absent, unlike the above ground sections. However, the species that shows the most noticeable differences in THM product composition between above and below ground sections is *Vaccinium oxycoccus*. The above ground analysis for this species produced a very different ion chromatogram with increased dominance from 4-methoxybenzeneethylene (P3), *trans* 3-(4-methoxyphenyl)-3-propenoic acid methyl ester (P18) and *trans* 3-(3,4-dimethoxyphenyl)-3-propenoic acid methyl ester (G18) than is observed in the roots (Figures 3.12 and 3.10). The roots also contain more 3,4-dimethoxytoluene (G2), 3,4-dimethoxybenzaldehyde (G4) and 3,4-dimethoxybenzoic acid methyl ester (G6) than above ground parts for this species.

The root sample from the grass *Molinia caerulea* produced a similar distribution of THM products to the other roots analysed, however, concentrations varied (Figure 3.12). This sample was dominated by the *p*-hydroxyl phenols; 4-methoxybenzeneethylene (P3), *trans* 3-(4-dimethoxyphenyl)-3-propenoic acid methyl ester (P18), the guaiacyl phenolic subunits; 1,2-dimethoxybenzene (G1), *trans* 3-(3,4-dimethoxyphenyl)-3-propenoic acid methyl ester (G18) and finally the syringyl phenolic subunit; 1,2,3-trimethoxybenzene (S1) (Figure 3.12). This species produced a very similar ion chromatogram to the above-ground part of the plant in terms of both compound distribution and abundance (Figures 3.9 and 3.12), with generally low levels of lignin phenols in comparison to the shrubs/herbs which agrees with results obtained from roots from the grass *Lolium multiflorum* (Kögel-Knabner, 2002), and maybe a common feature of grass roots, however, more research using a variety of species is needed to confirm this. The dominance of the cinnamyl phenols P18 and G18 was also observed by Nierop

(2001) in the roots and leaves of the grass *Deschampsia* which provides further support to the dominance of these products being a commonality among grasses regardless of whether it is root or shoot material.

Figure 3.13 demonstrates roots from all species analysed contributed a considerable amount to the Λ and carbohydrate signal. Many of the monomers that contribute to the Λ signal (e.g P18, G6 and G18) have been observed as dominant products in all root samples. The differences observed between root and shoot chemical composition for the four species analysed highlights the need for careful interpretation of lignin THM product concentrations in the peat, and particularly what effect deep-reaching root systems may have on the chemical proxies such as Λ and carbohydrate concentrations (1-5 and MC1-4). Moreover, depending on species, plant roots can present a stronger Λ signal than above ground sections (shoots). Both *Calluna vulgaris* and *Erica tetralix* roots suggest a stronger Λ signal than above ground sections. This differs from what is suggested by Nierop et al. (2001) who, after pyrolysis of *Calluna vulgaris* roots, wood and flowers + leaves, observed much lower peak intensities for the lignin phenols in the roots. In addition, many lignin phenols observed in above ground sections were absent in the roots. In comparison, *Vaccinium oxycoccus* and *Molinia caerulea* roots contribute much less to Λ even though the ion chromatograms (Figures 3.9 and 3.12) for the root and shoot of *Molinia caerulea* appeared very similar. Therefore, areas with a strong vascular plant input e.g DB the Λ proxy could be significantly distorted in the surface peat where root systems make a significant contribution to the organic matter.

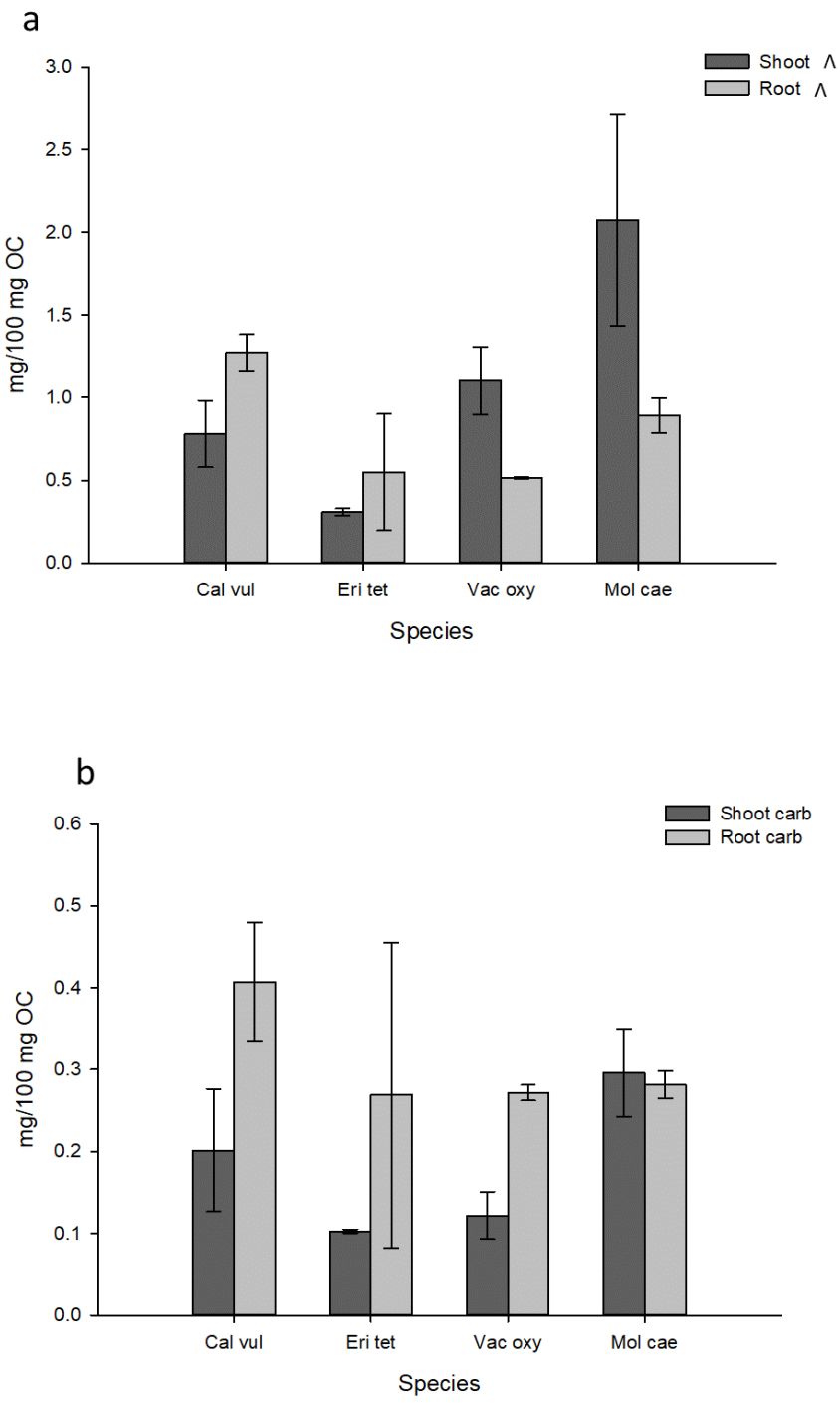

Figure 3.13: Contribution of shoots and roots from *Calluna vulgaris, Erica tetralix, Vaccinium oxycoccus* and *Molinia caerulea* to (a) the Λ chemical proxy and (b) their total carbohydrate content. Error bars represent the standard error from two analytical replicates.

For carbohydrate derivatives 1-6 and MC 1-4 similar trends can be seen. All samples contributed a considerable amount to the carbohydrate signal (Figure 3.13), with *Calluna vulgaris, Erica tetralix* and *Vaccinium oxycoccus* all suggesting roots could add more to this signal than above ground sections. *Molinia caerulea* was the only species in which a similar concentration of carbohydrate was found in both root and shoot sections.

Jackson et al. (1996) observed, on average, 75% of root biomass occurs in the top 40 cm, with an annual turn over rate of approximately 55% (Gill and Jackson, 2000). Perhaps a record of the % of fresh root material physically observed in peat samples after core extraction could be noted to enable a greater understanding of the depth of peat that may be affected by root inputs, and to what degree the chemical proxies obtained from peat samples may be affected. From the results obtained here, it is clear that future research needs to further investigate the geochemistry of roots from various peatland species and the effects of this on the chemical analysis of surface peats.

The roots from the shrubs/herbs species analysed here differ from above ground sections, however, do not contain characteristics associated with other plant types e.g graminoids which are dominated by the monolignols P18 and G18. Moreover, the analysis of the grass roots closely resembled above ground sections in terms of phenolic product distribution, however, more roots from grasses need to be analysed to establish whether this is standard across this plant type. Therefore, although root systems may distort the Λ signal, the phenolic distributions of the roots analysed in this study should not significantly disrupt phenolic plant source proxies such as the C/G and S/G ratios proposed by Hedges and Mann (1979). The input of fresh phenolics into deeper peat layers is something that should be considered, however, during the chemical analysis of peat samples.

Sphagnum biomarkers (I-III) were absent from all root samples analysed in this study, and so did not contribute in any way the σ chemical proxy (Figure 3.12). This

further reinforces the use of these compounds as biomarkers for *Sphagnum* mosses only. They can, therefore, be reliability used in palaeoecological reconstructions as they produce a plant source signal that is not influenced by deep running vascular plant roots.

3.3.2.5 Distribution of THM products at each coring site

Plant biodiversity on a peatland has a significant effect on the peat SOM and can change chemical biomarker presence, distribution and concentration. In order to understand chemical input to the top layers of the peat, the total amount of σ, Λ and carbohydrate present in the present-day plant species at each site, and therefore contributing to the peat, is displayed in Figure 3.14. The present-day vegetation suggests there should be no *Sphagnum* biomarkers contributing to the surface peat at DB, and so any σ found during peat analysis will indicate a change in plant biodiversity, and therefore palaeoecological and climatic change. This result was expected as there were no *Sphagnum* mosses found at this site during the on-site vegetation survey. All other sites have σ as an input, with FL showing the highest concentrations and BP the least. Again, this was expected as the vegetation survey showed that this site had the lowest coverage and diversity of *Sphagnum* species (Table 3.1).

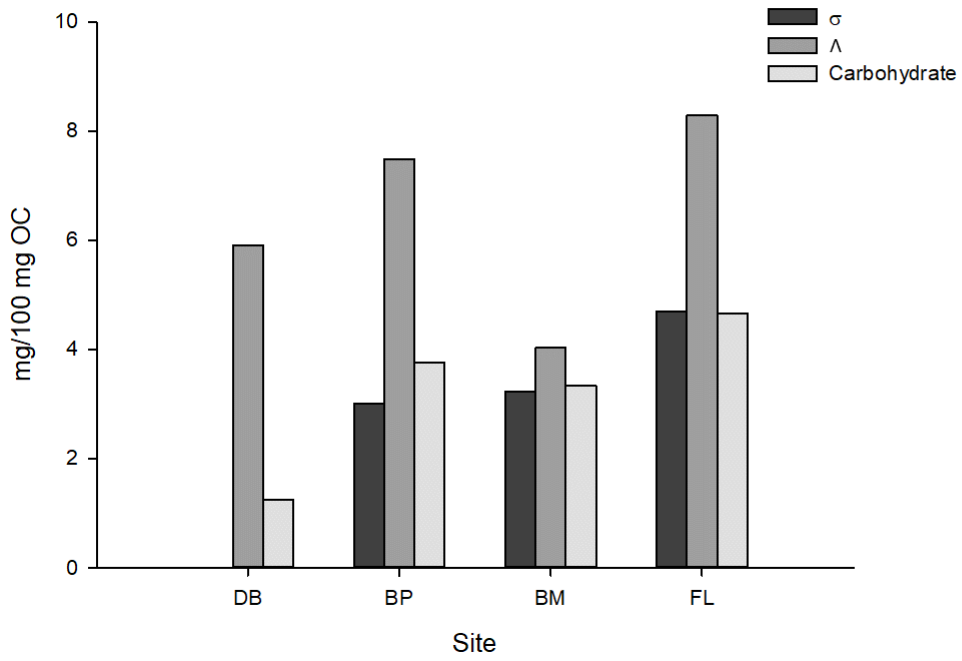

Figure 3.14: Total amounts of σ, Λ and carbohydrate in the plant samples contributing to the peat at each coring site; Degraded bog (DB), Bog plateau (BP), Bog margin (BM) and Fen lagg (FL).

All sites show considerable Λ deposition, with FL showing the most, and BM showing the least. This can be explained due to the diversity of vascular plant species present being the smallest at the BM site and the largest at FL (Table 3.1). Although DB did not contain any *Sphagnum* mosses, the amount of Λ contributing to the surface peat is lower than both BP and FL Figure 3.14. At this site, the majority of vegetation cover was from a very small range of plant species that consisted of non-*Sphagnum* mosses, which were found to contain very low levels of lignin derivatives, and *Molinia caerulea*. This, therefore, explains why this site was found to have the second lowest Λ concentrations instead of the highest (Figure 3.14). It can also account for the low carbohydrate concentrations at this site. The carbohydrate concentrations for the other sites were similar, with FL having the highest overall.

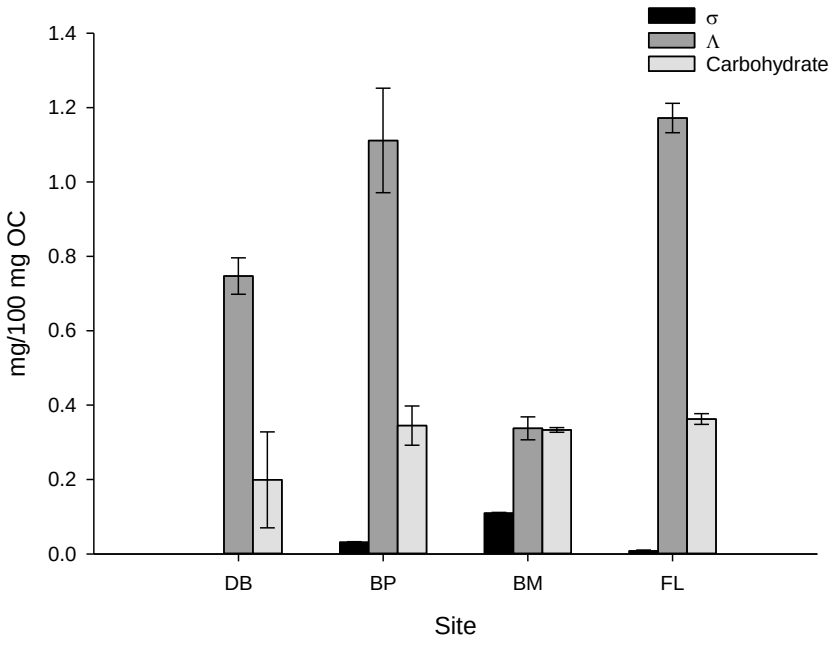

Figure 3.15: Total amounts of σ, Λ and carbohydrate in the surface peat (2-4 cm) at each coring site; Degraded bog (DB), Bog plateau (BP), Bog margin (BM) and Fen lagg (FL).

When the peat surface samples (2-4 cm) were analysed, results were similar for Λ and carbohydrate profiles, however differences can be seen for the σ profile. Figure 3.15 shows σ is absent from the surface peat at DB which matches with present-day vegetation assessments, however the highest levels of σ were present at BM which differs from the plant data in Figure 3.14. one reason for this is may be that the peat sample analysed covers a very small surface area of the peatland due to Russian corers being narrow, where as the vegetation assessment covered 3 m^2 of the peatland surface. If no *Sphagnum* mosses were growing on the top the the core taken then the σ signal will be low even if mosses were growing nearby as the σ signal is representative of the bound sphagnum acid in plant cell walls.

Λ follows the same trends in the surface peat with FL containing the highest concentrations and BM the lowest. As explained above, this is consistent with the diversity

of vascular plant species present at each site (Table 3.1). DB also contained the lowest carbohydrate concentrations with higher concentrations at all other sites.

3.4 Conclusions

The four coring sites identified at Butterburn Flow (DB, BP, BM and FL) represent a range of micro-habitats with different ecological signatures. DB was the only site that has no *Sphagnum* species growing in present-day conditions, and this should be reflected in the analysis of the surface peats. In contrast, BM had the largest diversity of *Sphagnum* species, however, the lowest species diversity overall demonstrating the competitive advantage of *Sphagnum* mosses at this site. Previous studies and vegetation surveys conducted on Butterburn Flow by Smith et al. (2003) and Yeloff et al. (2007a) suggest that vegetation composition has remained relatively stable for at least the last 30 years.

The *Sphagnum* biomarkers (I-III) were observed only in *Sphagnum* mosses, reinforcing their use as a reliable biomarker for this species. The σ and SR% proxies suggested by Abbott et al. (2013) are useful indicators of sphagnum moss abundance generally as well as in relation to vascular plants and are proxies that are in no way distorted by the presence of other species or below ground plant sections (e.g root systems).

The lignin proxy Λ still remains useful for vascular species, however, all bryophyte species observed in this study did contain low amounts of lignin phenols. The presence of lignin in mosses is a highly controversial topic, however, it is a possibility that water-soluble lignin phenols have been transported into the *Sphagnum* hyaline cells from DOM ((Abbott et al., 2013)). Future research should concentrate on determining the possibility of this further, however, which is the focus of Chapter 5. Although the levels of lignin observed in the bryophytes are not enough to distort lignin proxies, the concentrations of lignin found in vascular plant roots may be. The input of both lignin

and carbohydrate from root systems can be significant, with root based Λ concentrations exceeding levels found in above ground sections for *Calluna vulgaris*, and root based carbohydrate concentrations exceeding levels found in above ground sections for both *Calluna vulgaris* and *Vaccinium oxycoccos*. Further research to accurately quantify the effects of root systems on the carbon, lignin and carbohydrate content in peatland ecosystems, although difficult to carry out, is needed.

Chapter 4

Exploring the biogeochemistry of the peat across a range of environmental conditions at Butterburn Flow

4. Exploring the biogeochemistry of the peat across a range of environmental conditions at Butterburn Flow

4.1 Introduction

Northern peatlands cover around 4×10^6 km^2 and are a major carbon store, holding over one-third of global soil carbon as waterlogged peat (Gorham, 1991; Yu et al., 2010). Acidic and anoxic conditions, high water tables and frequent rainfall alongside dominant peat-forming vegetation such as *Sphagnum* mosses are key characteristics in sustaining a functioning peatland ecosystem (Charman et al., 2002). However, potentially detrimental environmental conditions are impacting on peatland ecosystems, e.g. greater fluctuations in precipitation regimes, together with intensification of the hydrological cycle which has already been reported in a 50-year observation (Durack et al., 2012).

Intensified drying and re-wetting of the peat may require these highly sensitive ecosystems to adapt to a new level of disturbance, resulting in a potential shift from carbon sink to carbon source (Freeman et al., 2004; Abbott et al., 2013). Water levels in ombrotrophic bogs are governed by the climate, and as such, are a key control on carbon input, decomposition, and sequestration (Belyea, 2009). Deeper water tables can lead to a range of changes in vegetation composition and therefore carbon input. In extreme cases, a moss-dominated carbon input can change to a system dominated by vascular plants, which can in turn significantly affect peat decomposition (Yeloff and Mauquoy, 2006; Potvin et al., 2015). Variations in climate can disrupt vegetation composition, altering the extent of peatland microhabitats (e.g bog plateau, bog margin, and fen lagg), and could lead to the development of new microhabitats (e.g degraded bog). Understanding the dynamics of carbon cycling and sequestration within such microhabitats is essential, and can provide insights into the fate of peatland carbon stocks resulting from a change in climate.

The ratio of carbon (C) to nitrogen (N) abundance has been shown to correlate with peat humification using colourimetric methods in North-West Scotland (Anderson, 2002), and as well as Infrared (FT-IR) measurements in Southern Patagonia (Broder et al., 2012). Alongside other geochemical proxies e.g. lignin proxies, C/N ratios provide a useful indicator of carbon and nitrogen cycling and sequestration in peatland habitats. Nitrogen concentration in peatlands is generally below 5%. Changes in nitrogen have been shown to negatively affect the growth of *Sphagnum* mosses which, long-term could lead to a positive feedback cycle and enable an ecological transition from a bog to a heathland or grassland ecosystem (Berendse et al., 2001). The C/N ratio should be interpreted with care, however, as vegetation input, and deep-reaching root systems can skew measurements for peat degradation and humification (Yeloff and Mauquoy, 2006; Broder et al., 2012).

Several studies have used thermally assisted hydrolysis and methylation (THM) in the presence of tetramethyammonium hydroxide (TMAH) to characterise a variety of bio- and geo-polymers. Specific examples include wood (del Rio et al., 1998; Vane et al., 2006), plants and river sediments (del Rio et al., 1998), grasslands (Mason et al., 2012), peats (Abbott et al., 2013), the fungal degradation of wheat straw (Robertson et al., 2008) and dissolved organic carbon (DOC) leached from soils (Williams et al., 2016*b*). TMAH thermochemolysis products have been identified from both lignin (vascular plant input) and sphagnum acid *(Sphagnum* input) in the same Swedish peat horizons (Abbott et al., 2013). Swain and Abbott (2013) demonstrated that the distributions of the individual thermochemolysis products derived from sphagnum acid can indicate redox conditions in young peats, and (Abbott et al., 2013) suggested a change in redox conditions could enhance peat degradation. Furthermore, (Hájek et al., 2011) have proposed cell wall polysaccharides in *Sphagnum* mosses contribute to the inhibition of microbial mineralization and decay resistance. Understanding the molecular chemistry, and degradation pathways of *Sphagnum* mosses and the peat they form are valuable for future predictions of peat accumulation, degradation, and carbon release,

particularly arising from climate change initiated by anthropogenic forcing.

The aim of the analyses described in this chapter is to use a multi-proxy approach to investigate the degree of organic matter decomposition as a function of water table depth across a variety of peatland microhabitats at Butterburn Flow, Cumbria. Eight 1 m peat cores from four sites covering a range of hydrological conditions and plant inputs were collected for this analysis. The specific objectives were;

1. To characterise the carbon storage and geochemical profile of each core

2. To investigate down core changes in THM product composition and degradation using lignin (Λ, $[Ad/Al]_G$) and *Sphagnum* proxies (σ, SR %)

3. To establish the persistence of *Sphagnum* thermochemolysates down core and whether their distribution can be used as an indicator for redox conditions.

4. To establish the effects of sphagnum acid degradation on the vulnerable carbohydrates and carbon contents of the peat.

4.2 Methods

4.2.1 Sample collection and preparation

Eight 1 m peat cores were collected from Butterburn Flow, Cumbria, the UK with the help of Dr. Chris Vane and Dr. Daren Berrio (British Geological Survey, Keyworth). The cores encompassed four microhabitats at Butterburn with varying hydrological conditions, placed along a 500 m transect. These habitats were; degraded bog (DB), bog plateau (BP), bog margin (BM) and fen lagg (FL). For a more detailed description of the site, see Chapter 2, section 2.1.

Bulk density measurements were taken using 10 cm whole core sections from each site. A second core for each site was sliced into 2 cm sections, freeze-dried and crushed, from which total organic carbon measurements were taken, and the OC profile deter-

mined. Samples were then solvent extracted, and analysed by on-line thermally assisted hydrolysis and methylation (THM) in the presence of tetramethylammonium hydroxide (TMAH). Both unlabelled and ^{13}C labelled TMAH was used so an intact lignin input could be distinguished from degraded and non-lignin inputs. For more information on how the chemical composition was determined, see Chapter 2, section 2.2.

Water table was recorded every 30 minutes continuously using pressure transducers, and a profile of mean, minimum and maximum water table depth was determined after 12 months of recording. The water table profile at each site is presented in each graph using a solid line for the mean level and dashed lines for minimum and maximum levels. For more information on water level recordings, see Chapter 2, section 2.1.

4.2.2 Chemical proxies

To investigate changes in down-core profiles of both *Sphagnum* biomarkers and lignin derivatives, different chemical proxies were used. σ represents a sum of the *Sphagnum* biomarkers I-III and the *Sphagnum* ratio (SR%) indicates the relative contributions of *Sphagnum* and lignin-derived products present in the peat. Calculations are shown in Chapter 3, section 3.2.3. Finally, the acid/aldehyde ratio $[\mathrm{Ad/Al}]_G$ is a proxy to indicate the level of oxidation of guaiacyl products G4 and G6. It is calculated using the following equation;

$$[Ad/Al]_G = G6/G4 \tag{4.1}$$

All products, and therefore proxies were normalised to mg/100 mg OC.

4.2.3 Core dating

A commonly used and precise method of dating peatcores is ^{14}C wiggle-match dating (WMD) (Speranza et al., 2000; Mauquoy et al., 2002; Yeloff et al., 2007b). As explained

by Blaauw et al. (2004), this method utilises a ^{14}C calibration curve constructed from the ^{14}C analysis of trees. It is assumed that plants growing on the surface of the bog recorded the same concentrations of atmospheric ^{14}C as the trees used to construct the calibration curve. Wiggles found in the calibrations curve, caused by changes in the atmospheric ^{14}C concentration should also be observable in the peat deposit. These wiggles can then be matched to those observed in the calibration curve to give an estimate of age. Due to how time-consuming and expensive ^{14}C WMD is, it may be possible to obtain only a few ^{14}C dates, however, if it is possible to obtain large numbers of closely spaced ^{14}C dates, it can give a reliable indicator of accumulation rates in peat deposits (Blaauw et al., 2004).

It was not possible in this study to date samples due to time and cost restraints, however, other studies have obtained dates from cores collected from Butterburn Flow (Yeloff et al., 2007b; McClymont et al., 2008). The ^{14}C dates obtained for a similar depth in this study that was estimated at 860 BP, with a primary mid-range date of 305 BP taken at 49.5 cm and a secondary midrange data of 235 BP at 43.5 cm depth. In addition, Yeloff et al. (2007b) obtained a ^{14}C date at 91.5 cm of approximately 830 BP. It can therefore be assumed the maximum age of the core in this study is approximately 900-1000 years BP with a mid-range estimate of around 250-300 BP.

4.2.4 Statistical analyses

All statistical analyses were carried out on IBM SPSS Statistics 23 software. All data were normalised to 100 mg OC and tested for normality using the Shapiro-wilk test as well as visual data assessments.

TOC data were first subjected to a Univariate Analysis of Variance (ANNOVA) with Fishers Least Significant Difference (LSD) *post-hoc* tests to evaluate differences in the TOC values of each core followed by a linear regression to investigate the relationship between TOC and core depth. All other data could not be made normal by

transformations and so non-parametric analyses were used throughout the remainder of this chapter.

TN, bulk density, OC storage, and chemical biomarker data (σ, SR%, $^{\sigma}$I-III, %$^{\sigma}$I-III, Λ, carbohydrates 1-5 and MC1-4, 1,2,4-TMB) were first subjected to generalized linear model (GZLM) with Fishers Least Significant Difference (LSD) *post-hoc* tests to evaluate overall differences between each core followed by a linear regression to investigate the relationship with core depth. For all elemental, bulk density, and OC storage analyses, including average values, the last 20 cm of data for DB were excluded, unless otherwise stated, as they reside in a clay layer with low levels of organic carbon and were therefore considered to no longer represent peat and were treated as anomalies.

The weight of organic carbon stored (t ha^{-1}) for Butterburn Flow as a whole, and per cm thickness of peat was calculated using the following method. Firstly, for each soil horizon, the total organic carbon content (%) was multiplied by the horizon depth (10 cm) and bulk density as outlined in Chapter 2, section 2.2.6, Equation 2.6 to give the organic carbon storage capacity (OCsc) per soil horizon. After this, the average for the OCsc (t ha^{-1}) across all cores was taken to give the average value for Butterburn Flow. Finally, to work out the amount of carbon stored (t ha^{-1})per cm thickness, this value was divided by 10.

Tannin data (gallic acid and 1,3,5-trimethoxybenzene (1,3,5-TMB)) were subjected first to a linear regression to investigate chemical behaviour as a function of depth, followed by Pearson's correlation to interpret the relationship between the two tannin derivatives. The last 20 cm of DB were included in all analyses on tannins. All analyses were considered to show significant differences if $p<0.05$

4.3 Results and discussion

4.3.1 Water table dynamics

Water table and temperature data were recorded over a 12 month period for each coring site are presented in Figure 4.1 and Table 4.1. Data for DB was recorded 12 months before the data at the rest of the sites. Gaps in the data at DB and BP reflect malfunctions with the level logger which resulted in recordings stopping. As remote monitoring was not possible, the malfunction could only be fixed once the field site was visited in person, and the level loggers checked which caused these gaps to be relatively large. The largest gap ($\sim$ 7 weeks) can be seen at BP, however, it should not have significantly affected the summary data, which is used for the remainder of this chapter. This data was recorded during the same time frame as BM and FL, and they show no significant wet or dry spells, and so the minimum and maximum water table levels are representative. The data gap observed at DB is much smaller, lasting only 3 weeks, and so the effect on the summary data for this site is considered negligible, and the data reliable.

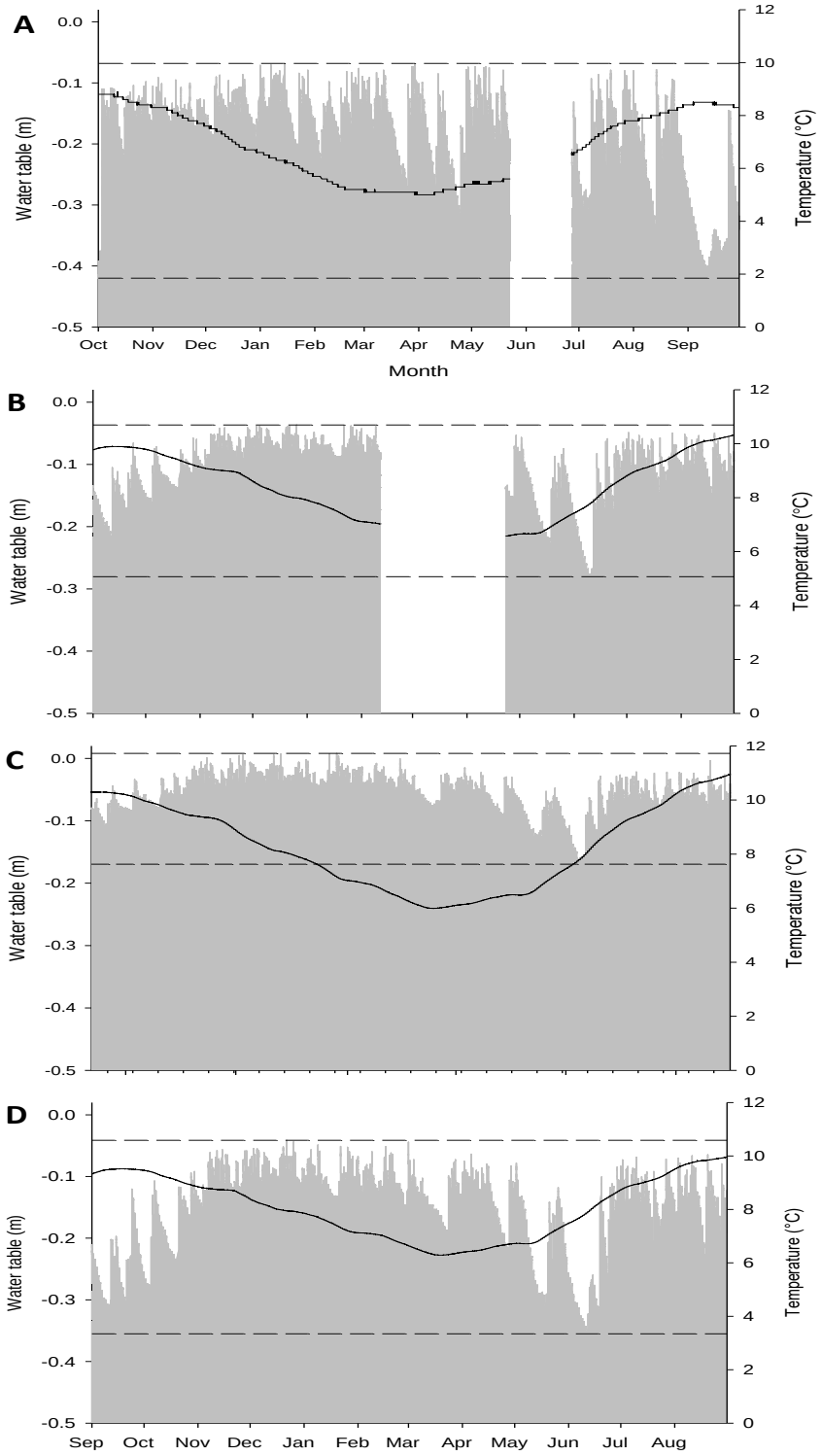

Figure 4.1: Water table (grey fill) and water temperature (solid black line) fluctuations over 12 months at Degraded Bog, DB (a), Bog Plateau, BP (b), Bog Margin, BM (c) and Fen Lagg, FL (d). The water table is presented as a distance from ground level (0 cm), dashed lines represent minimum and maximum values. Data for DB was recorded previous (Oct-Sep 2014-15) to the other 3 sites (Sep-Aug 2015-16).

The physical properties of peat such as temperature and water table dynamics have a significant effect on the ecology and carbon storage capacity of peatland ecosystems (Silvola et al., 1996*b*; Hargreaves and Fowler, 1998; Bubier et al., 2003; Lafleur et al., 2005; Ise et al., 2008). Both DB and FL have the deepest mean water table with the largest range resulting in a larger seasonally saturated zone. The highest water table is at BM where an oxic unsaturated layer is absent as the site becomes completely waterlogged during periods of intense rainfall (Figure 4.1, C and Table 4.1). Short-term fluctuations in water table can be seen which relate to precipitation events and demonstrates the self-regulating behaviour of peatlands in response to depth-dependent changes in hydraulic properties (Kettunen et al., 1999; Belyea, 2013). Peatlands naturally regulate their water levels causing these fluctuations, returning back to a natural mean due to the expulsion of water from the surface of the peat as well as through natural underground pipe systems. Temperatures, as shown in Figure 4.1, remain similar for BP, BM, and FL which were monitored during the same 12 month period, however, appear to be slightly lower at DB. This difference is likely due to the different monitoring times for this site.

Table 4.1: Mean, minimum and maximum water table (cm) as a function of distance from the bog surface (0 cm).

Coring site	Mean (cm)	minimum (cm)	maximum (cm)	range (cm)
DB	-18	-6	-42	36
BP	-11	-3	-28	25
BM	-5	+1	-17	18
FL	-15	-4	-36	32

Recorded temperatures reflect the temperature of the water as opposed to air temperatures at each site and range between 5-11 °C. The water temperature profile, as a function of time shows an apparent delay for the warming and cooling of water when considering typical air temperatures (Figure 4.1). For all sites, the lowest temperatures occur around April/May, a time when air temperatures would be rising, whereas the highest temperatures are recorded around September when air temperature would be

decreasing. Temperature down core can significantly change relative to surface temperatures. For example, Brown (1976) observed an average winter surface (2 cm depth) temperature of 3.1 °C and summer temperature of 15.2 °C at a bog in northern Minnesota. At 2 m depth, however, the winter temperature was 8.4 °C and the summer was 7.1 °C. The level loggers in the current study were placed at approximately 1 m depth, and so it is assumed here that the lower depth has resulted in a temperature lag, with deeper water taking longer to warm up and cool down than surface water.

4.3.2 Elemental analysis

TOC values for DB, BP, BM, and FL are displayed in Table 4.2 and Figure 4.2. All cores showed significant increases in TOC with depth (linear regression, $p<0.01$ for all), with DB and FL containing the highest average TOC (53.06 ± 0.40 and $52.83 \pm 0.37\%$ respectively) compared to BP and BM (50.72 ± 0.24 and $48.56 \pm 0.30\%$ for BP and BM respectively). Values ranged from 42.39-59.37% which are consistent with values obtained in other studies (Ran et al., 2002; Kechavarzi et al., 2010; Szajdak et al., 2010; Wellock et al., 2011). The change in TOC values observed in each of these cores suggests either a change in environmental conditions over time or a change in diagenesis resulting in increased carbon loss towards the surface of the peat. Further exploration of the geochemical composition of the peat, as provided throughout the remainder of this chapter, may provide some indication as to what the cause in carbon accumulation is.

A large drop in TOC from 49.22-1.80% was observed in the core from DB between 80-100 cm depth which reflects the transition from organic peat to a mineral clay substrate as seen in the stratigraphy (see Appendix A). Layers of clay minerals are not uncommon in peats, for example, Wellock et al. (2011) found a 15% drop in TOC values at the bottom of a peat profile due to mixing with underlying mineral layers. At DB, mixing occurs between 80-84 cm depth with TOC values of 49.22-15.14% respectively. For depths greater than 80 cm, the presence of organic peat material is minimal. TOC

values here fall within the range of 5.61-1.70% which is within the range observed by Moore and Turunen (2004) in four mineral subsoil profiles collected near Ramsay Lake, upper Michigan.

As a function of depth, TN remains stable for BP, BM and FL (linear regression, $p>0.05$ for all) and ranges between 0.99-3.94% for all cores (Table 4.2). However, at DB, TN declines as a function of depth (Linear regression, $R^2 = 0.40$, $p<0.05$), and ranges between 1.25-2.97% . Higher levels of N in the surface layers at this site could be a result of the abundant vascular plant species observed here that can provide a source of N through surface root systems and root litter (Malmer and Holm, 1984; Damman, 1988). In addition, these higher N values may also indicate an increase in microbial degradation in these surface layers, as mineralised nitrogen can be preserved within microbial biomass (Damman, 1988).

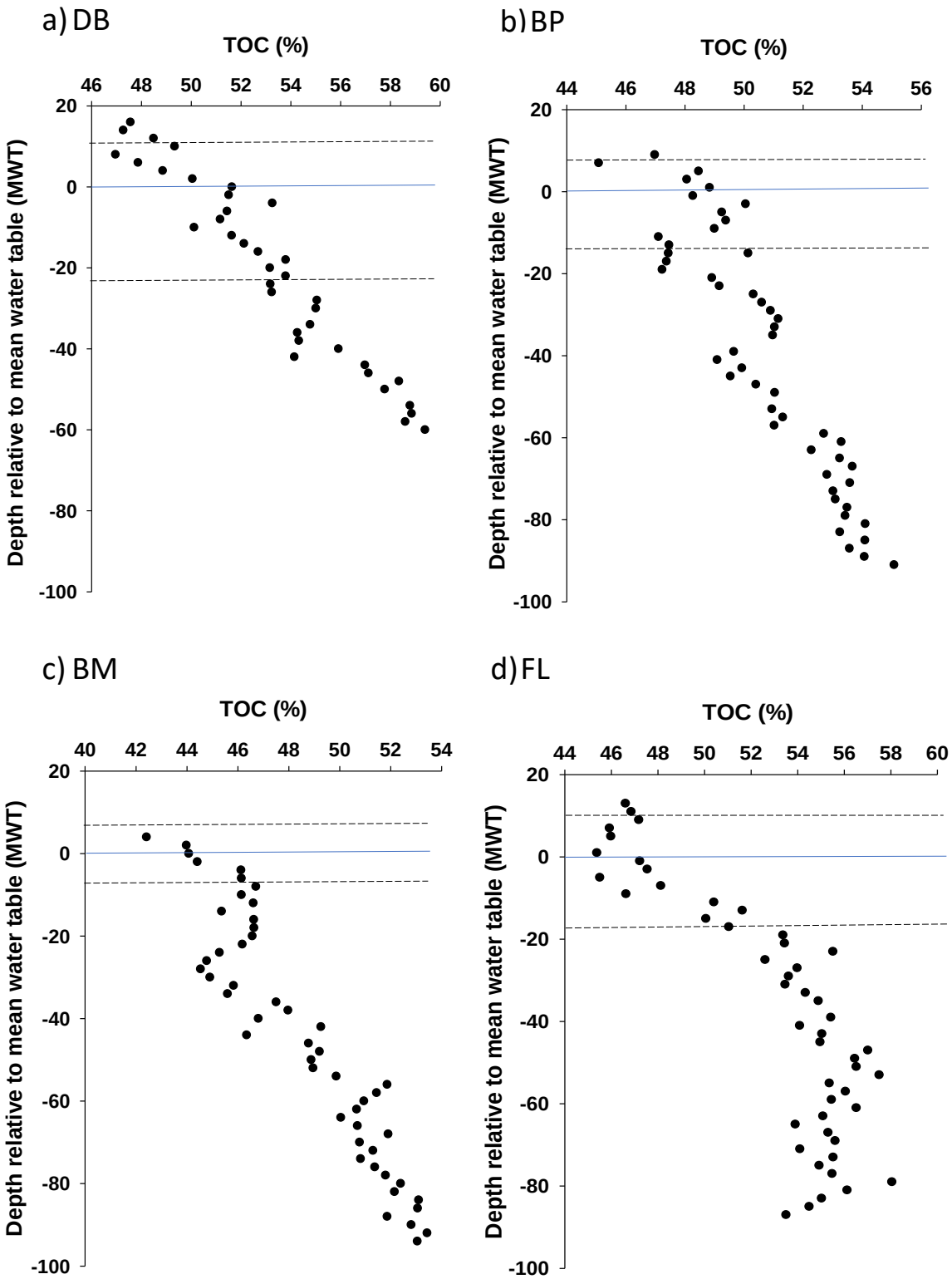

Figure 4.2: Linear regression showing changes in total organic carbon (%) as a function of depth from the mean water table (Solid blue line) for a) Degraded Bog, b) Bog Plateau, c) Bog Margin and d) Fen Lagg. Dashed lines represent the minimum and maximum water table

Overall, total nitrogen (TN) content was the lowest in BP and BM cores and highest at FL with average contents of 1.50 ± 0.04, 1.38 ± 0.05% and 2.20 ± 0.11% respectively (GZLM, $p<0.05$). TN at DB was significantly higher than BP and BM (average of 1.76 ± 0.10) but lower than FL (GZLM, $p<0.05$), with the highest values resting in the upper oxic layer of the core between 4-16 cm depth Table 4.2. This may be a result of increased microbial activity in this layer and rapid decomposition of the organic material (Damman, 1988; Berendse et al., 2001). Values are similar to those reported in other peatland studies. For example, Hornibrook et al. (2000) measured TN concentrations between 1.73-4.75 at Sifton Bog and 2.71-3.82% at Point Pelee Marsh in Ontario, Canada. The nitrogen content of ombrotrophic peat is determined by the properties of the organic matter, with poorly decomposed peat containing lower N levels than highly degraded peat (Damman, 1988; Berendse et al., 2001). This is reflected in the results of this study with BP and BM (the sites with better-preserved peat in relation to DB and FL) having lower overall N contents as a result.

Table 4.2: The downcore% TOC, TN and C:N values for Degraded Bog (DB), Bog Plateau (BP), Bog Margin (BM) and Fen Lagg (FL) sites. Bold values represent the mesotelm. Values represent a 2 cm thick slice of peat.

Depth	DB			BP			BM			FL		
(cm)	TOC (%)	TN (%)	C:N	TOC (%)	TN (%)	C:N	TOC (%)	TN (%)	C:N	TOC (%)	TN (%)	C:N
4	47.25	2.37	19.95	45.06	1.65	39.08	43.96	1.36	32.28	46.82	2.03	23.03
8	49.31	2.97	16.60	48.04	1.50	31.18	44.39	1.48	30.09	45.89	1.82	25.27
12	47.84	2.70	17.71	48.25	1.59	30.08	46.12	1.24	37.10	45.35	1.45	31.36
16	50.03	1.97	25.33	49.23	1.30	37.07	46.12	1.07	43.10	47.51	1.98	24.02
20	51.48	1.86	27.66	48.97	1.25	38.85	45.34	1.08	42.14	48.10	2.44	19.75
24	51.42	1.70	30.31	47.44	1.23	38.82	46.61	1.15	40.42	50.38	2.11	23.92
28	50.09	1.97	25.37	47.35	1.23	38.72	46.15	0.99	46.57	50.03	2.26	22.16
32	52.10	1.32	39.59	48.89	1.33	37.02	44.75	1.17	38.18	53.34	2.08	25.62
36	53.77	1.25	42.91	50.29	1.56	31.55	44.88	1.45	31.02	55.48	1.85	30.01
40	53.77	1.56	34.53	50.87	1.65	30.83	45.57	1.34	33.90	53.95	1.82	29.59
44	53.21	1.51	35.15	51.01	1.56	32.13	47.95	1.77	27.03	53.43	2.30	23.19
48	55.03	1.42	38.66	49.63	1.61	31.02	49.23	1.96	25.10	54.86	2.04	26.89
52	54.98	1.36	40.49	49.90	1.34	35.80	48.75	1.45	33.64	55.40	1.98	27.94
56	54.24	1.45	37.48	50.38	1.29	37.92	48.86	1.29	37.91	55.01	2.76	19.93
60	55.89	1.58	35.40	50.12	1.49	33.67	49.83	1.39	35.93	56.98	2.13	26.70
64	56.95	1.57	36.37	51.29	1.50	33.64	41.52	1.54	26.89	56.49	2.05	27.53
68	58.32	1.60	36.35	52.68	1.27	40.58	50.64	1.72	29.41	55.33	2.10	26.37
72	58.76	1.72	34.08	52.26	1.58	33.10	50.67	1.60	31.61	55.43	2.01	27.55
76	58.57	1.61	36.42	53.65	1.52	35.25	50.76	1.53	33.18	55.06	2.83	19.45
80	49.22	1.60	30.72	53.56	1.77	30.26	50.79	1.53	33.29	55.28	3.46	16.00
84	15.14	0.48	32.01	53.07	1.89	28.02	51.78	1.25	41.36	54.07	1.89	28.56
88	5.61	0.21	26.15	53.40	2.07	25.75	52.12	1.13	46.00	54.90	1.40	39.13
92	2.66	0.10	25.83	53.22	1.59	33.41	53.04	1.37	38.83	58.02	3.94	14.71
96	2.30	0.10	23.23	53.55	1.34	40.11	52.78	1.33	39.65	55.00	1.94	28.34
100	1.80	0.09	19.57	55.06	1.47	37.42	53.02	1.28	41.52	53.47	2.36	22.71
Mean	29.50 (53.06*) ± 3.61 (0.40*)	1.50 (1.77*) ± 0.11 (0.08*)	30.81 (32.00*) ± 1.12 (1.28*)	50.72 ± 0.24	1.50 ± 0.04	34.45 ± 0.81	48.56 ± 0.30	1.38 ± 0.05	35.85 ± 1.19	52.83 ± 0.37	2.20 ± 0.11	31.44 ± 1.03

* = mean and standard error for 1-80 cm depth only

The C/N ratios mirror the behaviour of TN values, with any increases in TN resulting in a decrease in the C/N ratio, as expected. C/N ratios show no change down core for BP, BM, or FL (linear regression, $p>0.05$ for all), however in contrast to TN,

an increase in the C/N ratio is observed at DB (linear regression, $R^2 = 0.45$, $p<0.01$). Average values were 30.71 ± 1.51, 34.45 ± 0.81, 35.85 ± 1.19 and, a lower, 25.19 ± 1.03% (GZLM, $P<0.05$) for DB, BP, BM, and FL respectively which appear to be slightly higher than values reported in other studies. For example, Hornibrook et al. (2000) observed C/N ratios between 11.5 and 24.3 for two Canadian bogs. However, results in the literature appear to be variable, as Malmer and Holm (1984) report C/N ratios of 86, 56 and 25 from four Swedish bogs. The lower C/N ratio observed for FL is likely a direct result of the higher TN values observed at this site, possibly as a result of a strong vascular plant input, increased microbial activity due to a large water table range, or possible nutrient input from the flow of the river, or bog water from the centre of the peat. The increase in C/N ratios at DB is unusual, as studies by Malmer and Holm (1984) and Hornibrook et al. (2000) both observed decreases in C/N with depth on various northern peatlands, however, the increasing carbon content with depth is a likely cause here.

4.3.3 Bulk density

Bulk density values ranged between 0.02-0.13 g cm^3 for the majority of samples with means of 0.15, 0.07, 0.06 and 0.12 g cm^3 for DB, BP, BM and FL respectively. Both BP and BM had significantly lower bulk density values than other sites ($p<0.05$ for both). These values show consistency with values observed by Holden (2005) collected from 8 UK blanket peat catchments as well as from 14 raised bogs in southern Sweden (Franzén, 2006). In addition, Lewis et al. (2012) observed similar peat densities from a pristine blanket bog in Ireland. Interestingly, Lewis et al. (2012) also observed densities from the centre of the peat where the water table was high to be approximately half that of the peat margin located near a stream. This is comparable with Butterburn Flow with both BP and BM, located in the centre of the peatland with higher mean water tables (11 and 5 cm below the surface respectively) having approximately half the average density (Figure 4.3) of FL located near the stream and with an average water table of 15 cm below the surface.

It has been widely accepted in the literature that bulk density increases with depth as a result of peat compaction (Milne and Brown, 1997; Cruickshank et al., 1998; Novák et al., 1999; Holden and Burt, 2003), though it should be noted that published data sets show this to be inconsistent (Weiss et al., 2002; Wellock et al., 2011). For example Wellock et al. (2011) sampled 24 Irish peats, covering a range of peatland types (e.g raised bog, high level blanket bog and low level blanket bog) and observed the bulk density of some peats to increase and others to decrease with depth, resulting in no overall change with depth. In addition, the upper 20 cm of peat tended to have a higher bulk density than that of lower depths. This study observed a general trend of increasing density with depth at each site except for FL. DB and BM show significant increases in density with depth (linear regression, $r^2 = 0.64$), 0.65 (for BM), $p <= < 0.05$ for all) with DB containing the highest density values between 80-100 cm of all cores (0.65-1.34 g cm^3) Figure 4.3. This increase corresponds to a decrease in TOC (Table 4.2) and reflects the transition of peat to a mineral clay substrate (see Appendix A, Table 4.2 and Figure 4.2). FL also contains a section of peat with higher density values reaching up to 0.18 g cm^3 between 20-40 cm, however, unlike DB, there is minimal change in the TOC values. In addition, no significant changes in stratigraphy were observed (Appendix A) and so the reason for this change remains unclear.

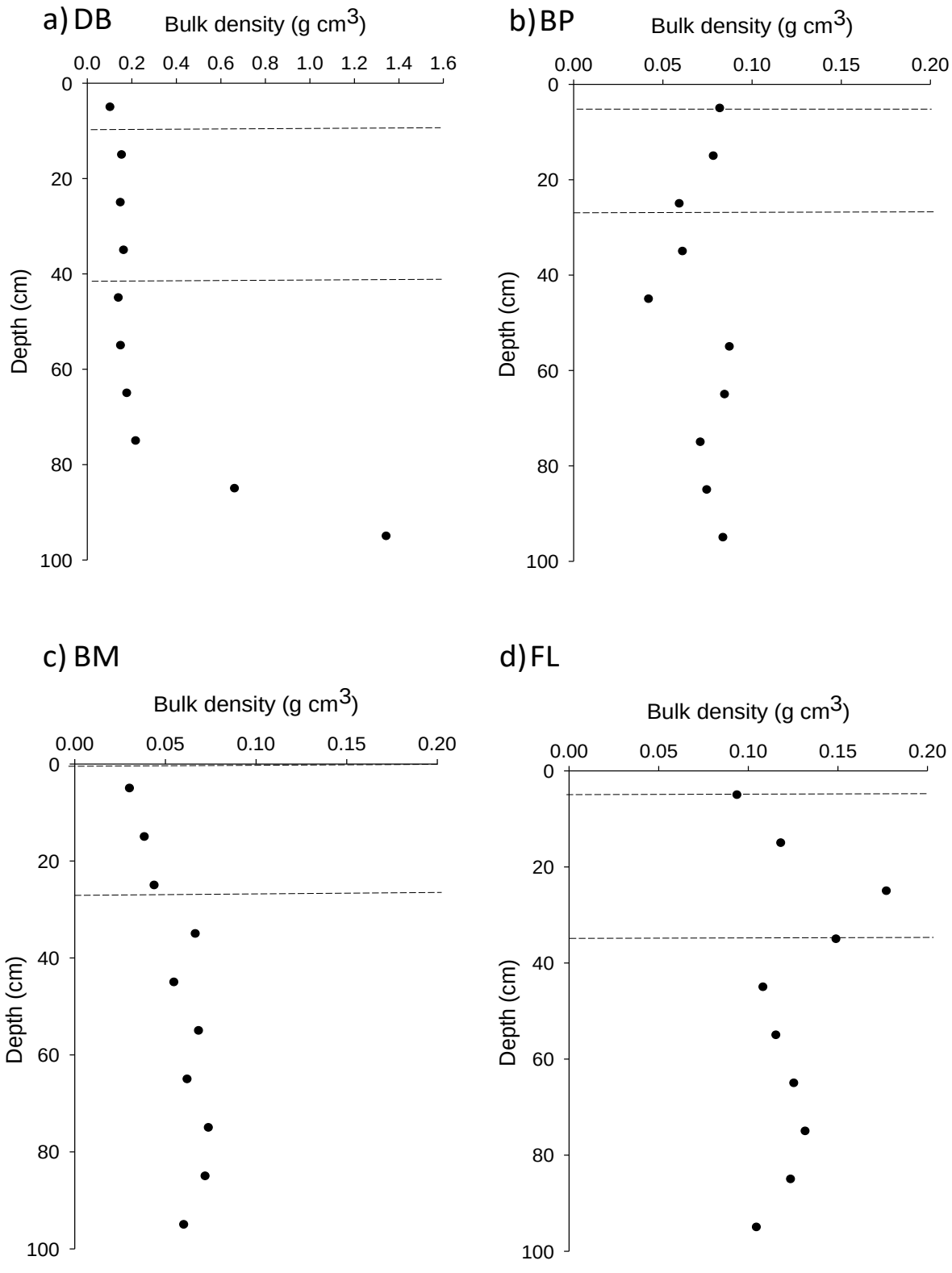

Figure 4.3: Bulk density profiles at (a) DB, (b) BP, (c) BM and (d) FL sites. Depth is from the surface, and water table range is indicated by the dotted lines. Note the different scale used for DB

As the peat decomposes, there are significant changes to its physical properties (Kechavarzi et al., 2010), which could account for a change in density. However, for peat so close to the surface, extensive decomposition is unlikely to be responsible. Another explanation could be dehydration of the peat due to agricultural drainage or climatic changes. Kechavarzi et al. (2010) demonstrated that less decomposed (or more pristine) peat both retains and loses more water than peat that has experienced extensive levels of decomposition. This causes pristine peat to have a higher propensity to drain faster. Once drained, significant changes in soil structure occur. It may be possible that in its recent history this site has undergone shrinkage due to water-table drawdown and drying of the peat. Land use change such as agricultural or forestry activity can lead to sudden changes in water-table dynamics if occurring in close proximity (Shotbolt et al., 1998; Bonn et al., 2016). Sheep have access to the peatland for grazing and the site is surrounded by a large forestry plantation, so whether this drying occurred due to agricultural activity/drainage, or anthropogenic climate change is impossible to tell. This theory is further supported by the plant species composition at this site, which, except for the presence of *Sphagnum* mosses, is most similar to DB. This could suggest that this site is in a transition from a water saturated area with a high water table to one that is much drier.

Overall, these measurements highlight the variation in peat bulk density both laterally and vertically on a UK peatland, which should be taken into account when estimating carbon stocks not only for individual sites but for national and global estimations as well. Peatland history is an important factor to consider as subsurface layers may change rapidly due to past land use changes.

4.3.4 Organic carbon storage

Organic carbon storage showed a large variation between cores, ranging from 13.22-122.36 t ha^{-1}, with means of 75.70, 36.57, 27.79 and 74.76 t ha^{-1} for DB, BP, BM, and FL respectively. Trends closely followed bulk density profiles (Figure 4.3) with the exception of DB, where the increase in bulk density from 80-100 cm corresponded to

a decrease in OC storage due to a reduction in TOC (See Table 4.2, Figure 4.3 and Figure 4.4).

Cumulative carbon stocks for each core show a linear increase with depth for all cores (Figure 4.4) with the exception of DB where storage slows considerably at 80-100 cm. As discussed in the sections above, this reflects the transition of organic-rich peat to a mineral clay substrate with low TOC content. Due to the higher bulk densities and higher TOC values, DB and FL hold the largest carbon stocks over a 1 m depth reaching 756.98 (659.72 with last 2 samples removed) and 657.35 t ha^{-1} respectively. In comparison, BP and BM hold considerably smaller amounts of 365.66 and 277.88 t ha^{-1} respectively.

As mentioned above, the estimated age of these cores is assumed to be around 900-1000 BP, with a mid-range age of 305 BP. At 1000 BP, the carbon stocks for each core are stated above, with mid range (at 50 cm depth) stock of 357.38, 157.27,106.62 and 324.93 t ha^{-1} for DB, BP, BM and FL respectively. These values further highlight the linear increase in carbon storage as displayed in Figure 4.4 and give a carbon accumulation rate of 0.76, 0.37, 0.28, and 0.66 t ha^{-1} per year for DB, BP, BM and FL respectively.

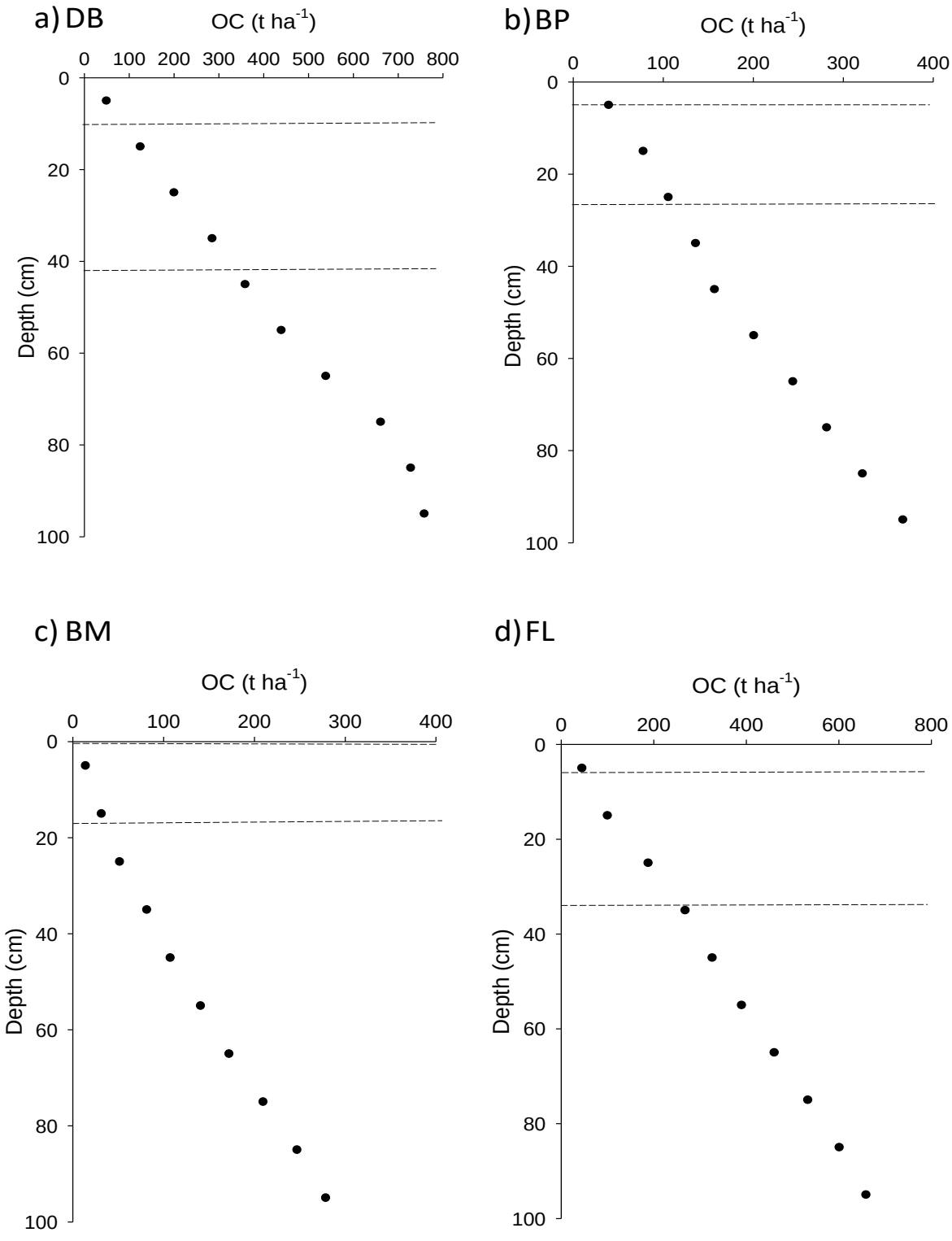

Figure 4.4: Cumulative organic carbon storage profiles at (a) Degraded Bog, DB, (b) Bog Plateau, BP, (c) Bog Margin, BM and (d) Fen Lagg, FL sites. Depth is from the surface, and water table range is indicated by the dotted lines. Note the different scales used.

Carbon storage across Butterburn Flow can be averaged at 51.45 t ha^{-1} $\pm$ 3.94 including the last 20 cm at DB, or 51.60 t ha^{-1} $\pm$ 4.09 excluding these samples, for a 10 cm section of peat. This is equivalent to an average of 5.1 t ha^{-1} per cm thickness of peat, which is slightly higher than the 4.7 t ha^{-1} estimated by Cannell et al. (1993) for British peats. This may be because this average was taken from an average peat depth of 2.43 m as opposed to the 1 m used here. However, deeper peats are expected to have higher bulk density values, leading to an increase in the carbon storage capacity of the peat and so this value should be higher than that obtained from Butterburn Flow. More recently Ostle et al. (2009) estimated British bog habitats contain 5.18 t ha per cm of peat from a 50 cm average, which matches the estimate found here, although from half the depth. This highlights the large capacity for carbon storage that Butterburn Flow and all northern peatlands possess, making them incredibly important resources in the face of climate change.

4.3.5 THM in the presence of TMAH

The range of THM products identified and their peak assignments are presented in Table 4.3. The naming system used for lignin- derived compounds is the same as that used in works by del Rio et al. (1998); Clifford et al. (1995); Chefetz et al. (2000); Vane et al. (2001) and Frazier et al. (2003))

Table 4.3: The main thermochemolysis products

Peak label	Tentative assignment
P1	methoxybenzene
P2	4-methoxytoluene
G1	1,2-dimethoxybenzene
P3	4-methoxybenzeneethylene
1	methylated isosaccharinic acid
2	methylated isosaccharinic acid
G2	3,4-dimethoxytoluene
4	methylated isosaccharinic acid
I	4-isopropenylphenol
P4	4-methoxybenzaldehyde
S1	1,2,3-trimethoxybenzene
P5	4-methoxyacetophenone
P6	4-methoxybenzoic acid methyl ester
1,2,4-TMB	1,2,4-trimethoxybenzene
S2	3,4,5-trimethoxytoluene
1,3,5-TMB	1,3,5-trimethoxybenzene
1,2,3,4-TETMB	1,2,3,4-tetramethoxybenzene
G4	3,4-dimethoxybenzaldehyde
5	methylated isosaccharinic acid
MC1	methylated metasaccharninc acid
MC2	methylated metasaccharninc acid
MC3	methylated metasaccharninc acid
MC4	methylated metasaccharninc acid
G5	3,4-dimethoxyacetophenone
P17	*cis*-3-(4-dimethoxyphenyl)-3-propenoic acid methyl ester
G6	3,4-dimethoxybenzoic acid methyl ester
S4	3,4,5-trimethoxybenzaldehyde
IIa	*cis*-3-(4-hydroxyphen-1-yl)but-2-enoic acid methyl ester
III	3-(4-hydroxyphen-1-yl)but-3-enoic acid methyl ester
G7	*cis* 1-(3,4-dimethoxyphenyl)-2-methoxyethylene
G8	*trans* 1-(3,4-dimethoxyphenyl)-2-methoxyethylene
P18	*trans*-3-(4-dimethoxyphenyl)-3-propenoic acid methyl ester
IIb	*trans*-3-(4-hydroxyphen-1-yl)but-2-enoic acid methyl ester
S5	3,4,5-trimethoxyacetophenone
S6	3,4,5-benzoic acid methyl ester
S7	*cis* 1-(3,4,5-trimethoxyphenyl)-2-methoxyethylene
S8	*trans* 1-(3,4,5-trimethoxyphenyl)-2-methoxyethylene
G14	*threo/erythro* 1-(3,4-dimethoxyphenyl)-1,2,3-trimethoxypropane
S10	*cis*-1-(3,4,5-trimethoxyphenyl)-methoxyprop-1-ene
G15	*threo/erythro* 1-(3,4-dimethoxyphenyl)-1,2,3-trimethoxypropane
S11	*trans*-1-(3,4,5-trimethoxyphenyl)-methoxyprop-1-ene
G18	*trans*-3-(3,4-dimethoxyphenyl)-3-propenoic acid methyl ester
G19	*trans* 1-(3,4-dimethoxyphenyl)-1,3-dimethoxyprop-1-ene
S14	*threo/erythro* 1-(3,4,5-trimethoxyphenyl)-1,2,3-trimethoxybenzene
$C_{16:0}$ FAME	C_{16} fatty acid methyl ester
S15	*threo/erythro* 1-(3,4,5-trimethoxyphenyl)-1,2,3-trimethoxybenzene
IS	5α-androstane
S17	*cis* 3-(3,4,5-trimethoxyphenyl)-3-propenoic acid methyl ester

The surface of the peat (2-4 cm) generally reflects the present day vegetation contributing to each site (see chapter 3, section 3.3). DB was the only site where sphagnum acid pyrolysis products (I-III) were absent in the surface layers of the peat (Figure 4.5), which is consistent with our vegetation survey which showed no *Sphagnum* mosses are present at this site (see Chapter 3, section 3.3). The increased abundance of *p*-courmaric acid (P18) and ferulic acid (G18) at this site reflects the significant contribution of the grass *Molinia caerulea* to the surface peat. Higher abundances of all four sphagnum acid products were observed at BM relative to lignin-derived phenols (Figure 4.6c) which reflects the higher diversity and abundance of *Sphagnum* mosses observed at this site (see Chapter 3, section 3.3).

The most abundant of the phenols identified across all cores include the *p*-hydroxyl phenols 4-methoxytoluene (P2) and 4-methoxybenzeneethylene (P3) in addition to the vascular plant-derived guaiacyl lignin phenols 3,4-dimethoxytoluene (G2), 3,4-dimethoxybenzaldehyde (G4), 3,4-dimethoxyacetophenone (G5), 3,4-dimethoxybenzoic acid methyl ester (G6) and the cinnamyl phenols *p*-courmaric acid (P18) and ferulic acid (G18). These products contained degraded and non-lignin phenols with an average of 48% derived from intact lignin across all sites.

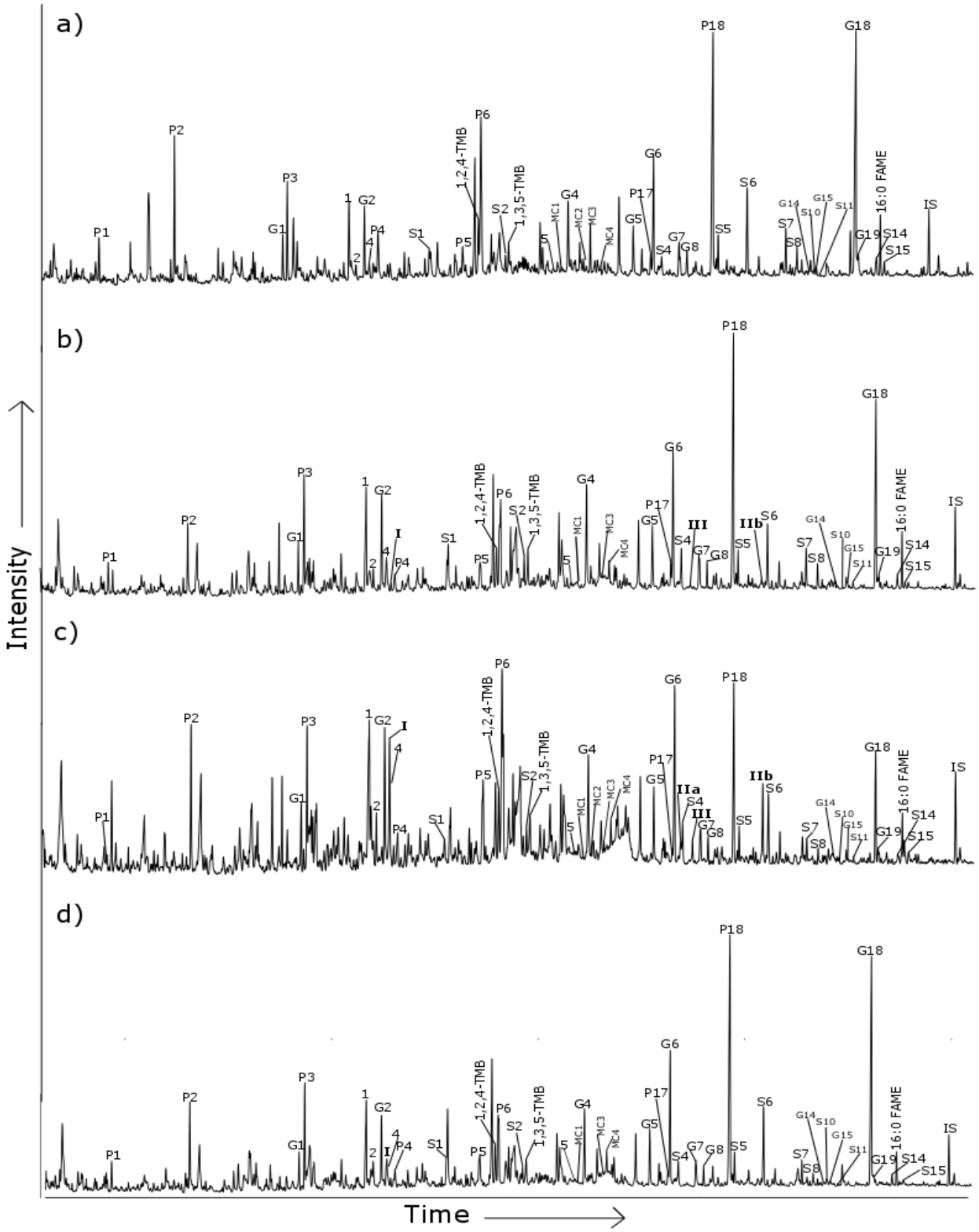

Figure 4.5: Partial chromatogram for the total ion current (TIC) of the thermochemolysis products from DB (a), BP (b), BM (c) and FL (d) at 2-4 cm depth. Peak identities are listed in Table 4.3

4.3.5.1 *Sphagnum* biomarkers

Sphagnum acid derivatives (I-III) were identified in all cores (Figure 4.6) Minimum-maximum values for the sum of these products (σ) include 0.000-0.010, 0.000-0.163, 0.016-0.174 and 0.002-0.036 mg/100 mg OC with an average of 0.0004, 0.049, 0.077 and 0.008 mg/100 mg OC for DB, BP, BM and FL respectively. BM contained the highest concentrations ($p<0.05$). DB contained the lowest concentrations ($p<0.05$), with only products I and/or IIb identified between 14-16 cm and 24-52 cm only below the MWT. Increases in concentration occurred at 14 and 26 cm below the mean water table (MWT). This suggests a historical re-wetting of the peat with an increase in the water table resulting in the growth of *Sphagnum* mosses. Therefore, significant changes in water table and the growth of *Sphagnum* mosses at this site are not unusual, but conditions appear to change quickly allowing only a small *Sphagnum* population to develop over a short timescale. A complete absence of this species, indicating a dry and degraded area, is common for this site. I-III were consistently seen throughout all other cores, with BM generally containing higher concentrations of these products relative to lignin-derived phenols.

In contrast to DB, the strong and consistent presence of these products at BM suggests a historically high water table with a *Sphagnum* rich vegetation cover not unlike what exists today (Chapter 3, section 3.3). Persistence of these products down core also confirms they are stable under oxic and anoxic conditions, making them an ideal chemical biomarker for *Sphagnum* mosses, particularly when the plant material and macro-fossils can no longer be reliably identified.

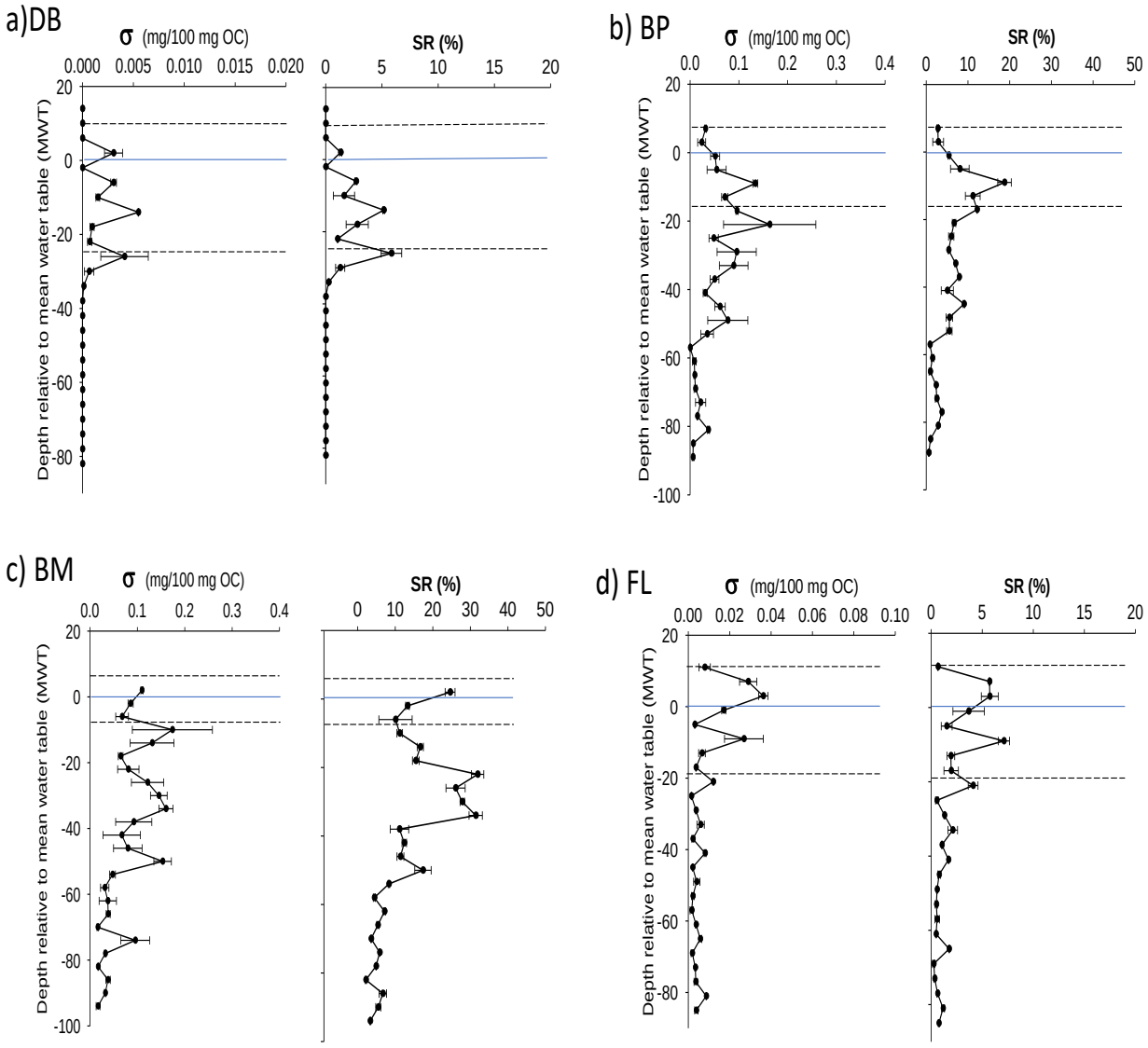

Figure 4.6: Depth profiles of σ and SR% relative to the mean water table (MWT) for Degraded bog (a), Bog plateau (b), Bog margin (c) and Fen lagg (d) sites. Negative values on the y-axis indicate samples below the MWT, positive values indicate samples above the MWT. 0 and the solid blue lines indicate the MWT, with the dashed lines indicating the minimum and maximum water table levels. Note the different scale used. Error bars represent standard error for two analytical replicates.

The yield of *Sphagnum* biomarkers (σ) and the *Sphagnum* ratio (SR %) are displayed in Figure 4.6. As a function of depth from the mean water table (MWT) both σ and SR % display decreasing concentrations from the surface to the base of the core

(linear regression, $p<0.05$ for all) with the exception of DB where very few biomarkers were identified. For most cores, oscillations in concentration appear to occur in the seasonally saturated zone, between the minimum and maximum water table levels, and at the very top of the permanently saturated zone. Below this, concentrations become more stable, gradually decreasing from 50 cm below the MWT to the base of the core (Figure 4.6).

DB contained only a small range and quantity of sphagnum thermochemolysis products with only products I and IIb identified. This is reflected in the σ yield which was only identified in the seasonally saturated zone, and the very top of the permanently saturated zone. Several small changes in concentration can be seen with the maximum of 0.005 mg/100 mg OC at 14 cm below the MWT in the seasonally saturated zone. At peat layers lower than 38 cm below the MWT, no sphagnum acid thermochemolysis products were detected. The SR% for this site follows the same trend with the largest value of 5.84% reached at the very top of the permanently saturated zone at 26 cm below the MWT. Again, at 38 cm, the values can be seen to drop to 0 mg/100 mg OC where they remain.

Both BP and FL show maxima in σ and SR% from the surface and into the seasonally saturated layer, showing peaks in σ concentration of 0.13 and 0.36 mg/100 mg OC for BP and FL respectively (Figure 4.6b and 4.6d respectively). For FL, this peak occurs just above the MWT and represents the highest concentration at this site, which then declines slowly to 0.002 mg/100 mg OC at 45 cm below the MWT. Below this, σ is stabilised at this low concentration to the deepest section of the core. At BP, σ oscillates between 0.03-0.16 mg/100 mg OC just below the MWT and into the permanently saturated zone (from 5-49 cm) before dropping to 0.01 mg/100 mg OC for the remainder of the core. These results support the findings of Schellekens et al. (2015a) that *Sphagnum* phenols are degraded rapidly in aerobic conditions.

The SR% for these cores mirror the σ depth profiles, with SR% at BP increasing

to 18.76% in the seasonally saturated zone, and dropping to 6.67% in the permanently saturated zone (21 cm below MWT). The ratio remains stable between here and 53 cm below the MWT. Further drops are seen for the remainder of the core before reaching a base value of 0.62%. At FL, the seasonally saturated zone contains a changeable ratio of 4.11% between -7 and 21 cm depth relative to the MWT. After this depth, stabilisation is seen at a lower value of around 0.5% in the permanently saturated zone, reaching a base value of 0.75%.

The strong contribution from the full range of sphagnum acid thermochemolysis products observed in the BM core is reflected in the σ and SR% profiles (Figure 4.6c). However, unlike the other cores, there is a decrease in concentration from the surface to below the MWT (-2-6 cm depth) at this site. Below 6 cm, concentrations oscillate between 0.06-0.17 mg/100 mg OC between 10-50 cm depth in the permanently saturated zone. Values fall to 0.03 mg/100 mg OC where they remain to the base of the core reaching a value of 0.02 mg/100 mg OC. The SR% at this site shows a continuous decrease throughout the seasonally saturated zone from 24.60-10.06% after which there is an increase up to 31.92% at 22 cm below the MWT which remains relatively stable until 34 cm below the MWT, and suggests a smaller contribution from vascular plants during this time as this change is not seen in the σ profile. After this depth, there is a large drop to 11.4%, and the values continue to decrease until they reach a base value of 3.31%.

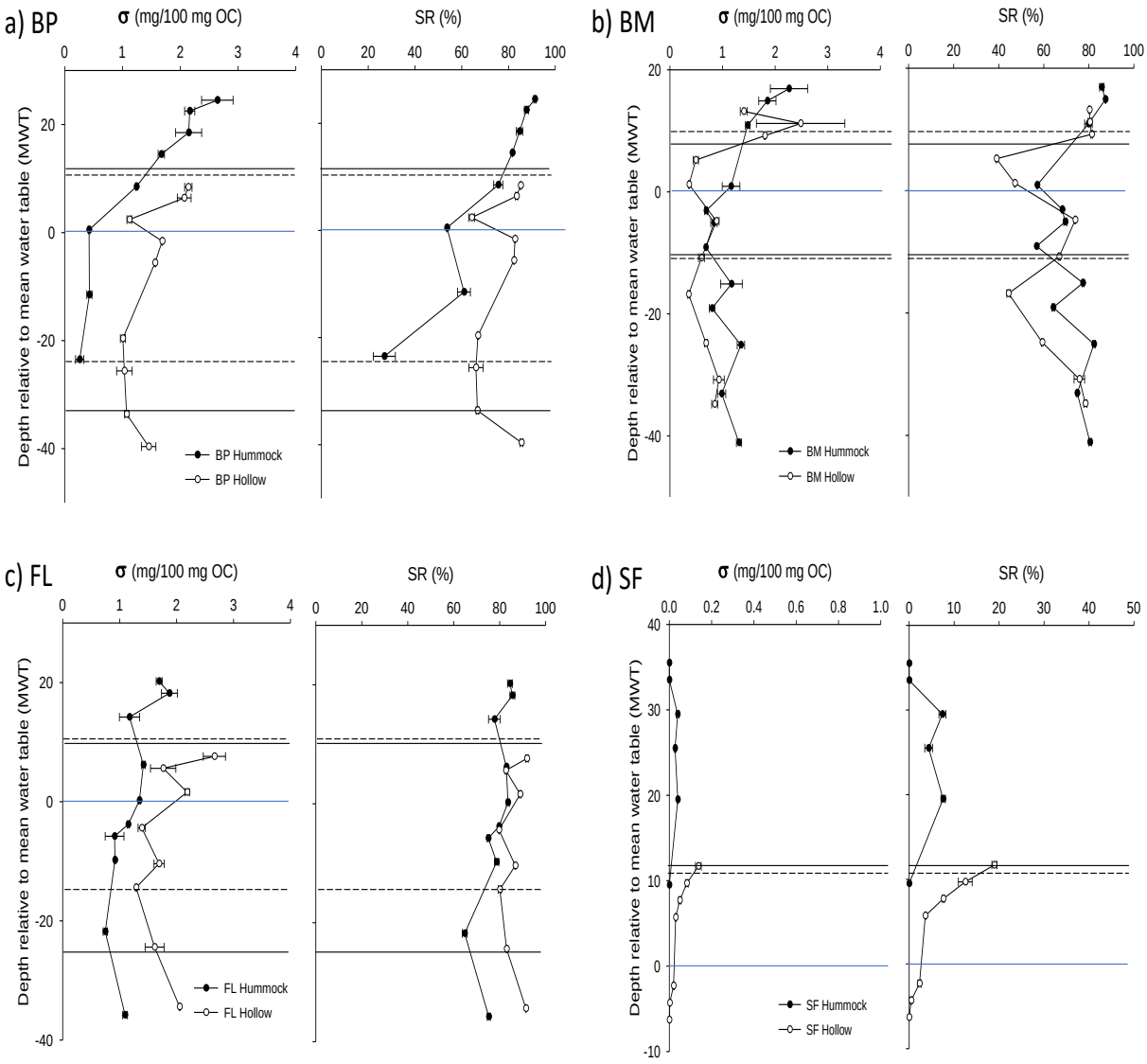

Figure 4.7: Depth profiles of σ and SR% relative to the mean water table (MWT) for both hummock and hollow cores from (a), Bog plateau (a), Bog margin (b), Fen lagg (c) and Swamp forest (d) sites at Rygmossen, Sweden. Negative values on the y-axis indicate samples below the MWT, positive values indicate samples above the MWT. 0 and the solid blue lines indicate the MWT, with minimum and maximum water table levels indicated by the dashed lined for hollows and the solid black lines for hummocks. Error bars represent standard error for two analytical replicates. Adapted from Abbott et al. (2013)

.

Abbott et al. (2013) first proposed and utilised σ and the SR% to investigate the degradation of bound sphagnum acid in the peat layers of Rygmossen peatland, Sweden. The data collected from Rygmossen is shown in Figure 4.7. Eight 50 cm cores, one from a hummock and one from a hollow were collected from 4 different sites namely; Bog plateau (BP), Bog margin (BM), Fen lagg (FL) and Swamp forest (SF) and analysed for sphagnum phenols. The values obtained from Butterburn for both σ and SR% appear to be significantly lower than the majority of those observed in the Ryggmossen peat (Figure 4.6 and 4.7). In the Swedish peatland σ values of around 2.0 mg/100 mg OC were observed in cores from all sites except SF, almost double some of the highest values obtained from Butterburn Flow. The SR% for these sites on average fell between 60-90%. In addition, both BP and BM at Rygmossen, showed a marked decrease in σ from the surface, through both the unsaturated and seasonally saturated layers, before reaching a minimum at the transition point into the permanently saturated zone. Below this, concentrations appear to increase for the hollow core at BP and both the hummock and hollow core at BM Figure 4.7a and 4.7b. Such a trend is absent in the results obtained from Butterburn with base values for all cores smaller than surface values.

One explanation for such a discrepancy could be the vast difference in the quantity of *Sphagnum* mosses observed in the present-day vegetation between Ryggmossen and Butterburn Flow. % *Sphagnum* coverage varied between 3-95% for the Swedish peat, however, at Butterburn the majority of quadrats contained between 1-9% (see Chapter 3, section 3.3 for vegetation survey). Although at Ryggmossen SF was obtained from a vascular plant dominated area that was completely unsaturated for part of the year. For the cores collected from this site, a much lower σ of 0.04 and 0.03 mg/100 mg OC and SR% of around 10% were observed, which match more closely with the values obtained from Butterburn.

Overall, the results both from Ryggmossen and Butterburn Flow demonstrate that micro-habitats within a peatland ecosystem will not always respond in the same way to climate-induced changes. In addition, they illustrate the extreme sensitivity of Sphag-

num peat to water table characteristics, which may differ greatly between sites. It would be highly beneficial for more cores around the border mires in the UK, and around Ryggmossen in Sweden to be investigated in the same way, and comparisons made.

The depth profile of each individual *Sphagnum* biomarker (σ_{I-III}) displayed a gradual increase from the surficial layers through the unsaturated and seasonally saturated layers until the top of the permanently saturated zone below which there is a gradual decrease to the base of the core. σ_I was the dominant product with the highest concentrations in BP and BM and the lowest concentrations in DB and FL ($P<0.05$). σ_{IIa} and σ_{III} were least abundant in all cores. Where σ_{IIa} and σ_{III} were identified, changes in the $\sigma_{IIa/b}$ and σ_{III} profiles occurred simultaneously and were consistently high in BM and low in DB and FL (<0.05).

DB contained the lowest total amounts of sphagnum acid products followed by FL ($P<0.05$), with highest abundances in the seasonally saturated layer. At DB, I and IIb reached a maximum of 0.003 mg/100 mg OC and were absent in the unsaturated and permanently saturated zone, whilst IIa and III were completely absent. FL displayed a similar trend, however, contained higher amounts of products with an absence of IIa only. III and IIb were present above the mean water table in the seasonally saturated zone only, reaching a maximum of 0.03 and 0.08 mg/100 mg OC respectively. I was present throughout the whole core, oscillating between 0.003 and 0.03 mg/100 mg OC in the seasonally saturated zone before dropping to a stabilised level of around 0.004 mg/100 mg OC throughout the permanently saturated zone.

In contrast, both BP and BM contained all four pyrolysis products with an obvious dominance of I (Figure 4.8b and 4.8c). IIa/b and III at BP increased in concentration through the seasonally saturated zone, reaching a maximum of 0.008, 0.011 and 0.046 mg/100 mg OC for IIa, III and IIb respectively at the beginning of the permanently saturated zone Figure 4.8b). For the remainder of the core, levels decreased and were

no longer present at the base. I was much more abundant displaying a similar trend, however, reached a maximum of 0.10 mg/100 mg OC both in the seasonally saturated zone, just beneath the mean water table as well as the beginning of the permanently saturated zone. From here, concentrations oscillate until 49 cm below the mean water table, after which there is a significant drop to a lower, more stabilized level before reaching a base value of 0.01 mg/100 mg OC Figure 4.8c).

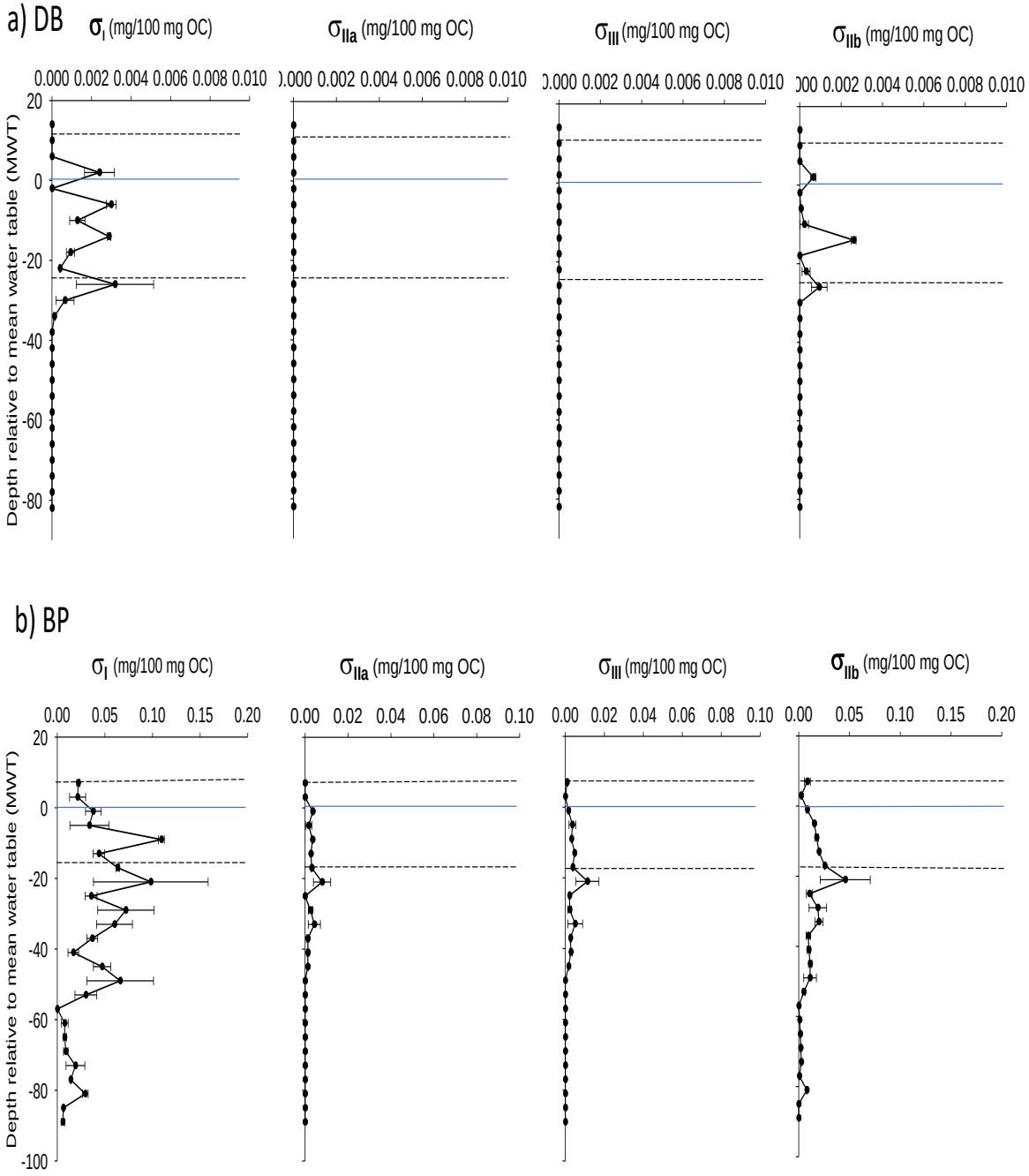
a) DB
σI (mg/100 mg OC)
σIIa (mg/100 mg OC)
σIII (mg/100 mg OC)
σIIb (mg/100 mg OC)
0.000 0.002 0.004 0.006 0.008 0.010
Depth relative to mean water table (MWT)
20
0
-20
-40
-60
-80
b) BP
σI (mg/100 mg OC)
σIIa (mg/100 mg OC)
σIII (mg/100 mg OC)
σIIb (mg/100 mg OC)
0.00 0.05 0.10 0.15 0.20
0.00 0.02 0.04 0.06 0.08 0.10
Depth relative to mean water table (MWT)
20
0
-20
-40
-60
-80
-100

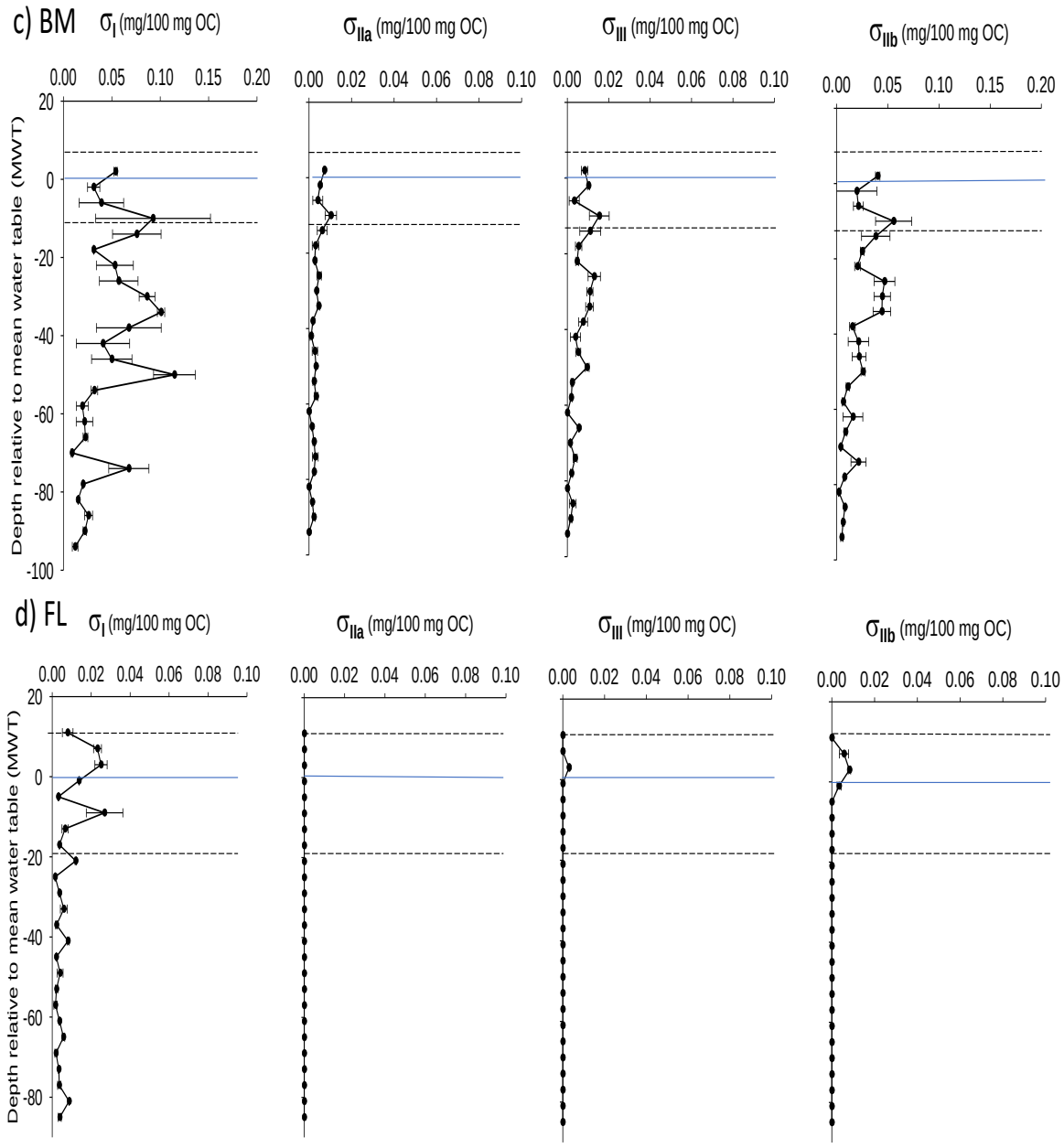

Figure 4.8: Depth profiles relative to mean water table (MWT) of individual σ component yields (mg/100 mg OC) for Degraded bog (a), Bog plateau (b), Bog margin (c) and Fen lagg (d). Negative values on the y-axis indicate samples below the MWT, positive values indicate samples above the MWT. 0 and the solid blue lines indicate the MWT, with the dashed lines indicating the minimum and maximum water table levels. Note the different scales used. Error bars represent standard error of two analytical replicates.

BM contained the highest concentrations of all products ($P<0.05$) with IIa, III and IIb remaining relatively constant in the seasonally saturated layer, reaching a maximum of 0.01, 0.02 and 0.06 mg/100 mg OC respectively immediately before the permanently saturated layer (Figure 4.8c). In this layer, at 50 cm below the MWT, III and IIb concentrations begin to drop to lower more stable value of 0.003 and 0.010 mg/100 mg OC respectively. I presents a slightly increasing trend with oscillations throughout the seasonally saturated, and into the permanently saturated zone, reaching a maximum value of 0.11 mg/100 mg OC at 50 cm below the MWT. Below this point, concentrations drop to around 0.02 mg/100 mg OC. There is a noticeable increase at 74 cm below the MWT after which levels drop again, reaching a base value of 0.01 mg/100 mg OC.

A similar analysis of these sphagnum acid products in relation to water table was investigated by Swain and Abbott (2013) on Ryggmosssen, a peatland in central Sweden. Their analysis shows markedly different trends for the yields of the individual sphagnum acid products to Butterburn. At Ryggmossen, all four products were identified in the majority of samples and decreased simultaneously in the unsaturated and seasonally layers. In the permanently saturated layer, increases in I were observed whilst IIa/b and III remained relatively constant. However, there are several significant differences that should be noted between this study and the one conducted here on Butterburn FLow. Firstly, significantly higher abundances of each product were found, which is likely a reflection of the significantly larger % of *Sphagnum* cover observed in the present day vegetation. Observations of up to 95% were recorded, as opposed to the 1-9% observed from the majority of surveys at Butterburn. Moreover, a comparison of the present day vegetation at Ryggmossen with a survey conducted in 1925 revealed historically, very little vegetational change. Such a comparison cannot be made here, and so the changes in product composition may indeed be a result of changing vegetation cover rather than diagenetic changes. The fact that no *Sphagnum* species were observed in the vegetation survey (see chapter 3, section 3.3) at DB, and yet small amounts of sphagnum acid phenolics were detected in the peat further illustrates this point. Secondly, water tables at Rygmossen appear to be lower, allowing several samples to sit in an unsaturated, very

oxic layer. This may allow initial degradation to begin, which then continues rapidly into the seasonally saturated layer. The only core that extends into an unsaturated zone here is DB, where no *Sphagnum* phenolics were identified in the surficial layers. Finally, samples collected from Ryggmossen only represent the top 50 cm of peat as opposed to the 100 cm represented here. If only the top 50 cm is considered, product yields, particularly for I, appear to be more stable, as it is after 40 cm below the MWT where all products begin to decrease to the lowest levels. Unlike at Ryggmossen, increases in I throughout the permanently saturated zone could only be considered for BM, however.

In contrast, when considering the proportion of individual *Sphagnum* biomarkers ($\%\sigma_{I-III}$) to the total *Sphagnum* yield (σ), the findings presented in Swain and Abbott (2013) correlate more closely with the data obtained from Butterburn. I and IIb were the dominant compounds contributing an average of 66.6 $\pm$ 3.3 and 13.4 $\pm$ 1.4% respectively to the total *Sphagnum* yield across all four sites. BP and BM both show similar trends with IIa and III remaining relatively constant in the in the seasonally saturated layer and the top half of the permanently saturated layer. At BP IIa and III cease to contribute to the total yield from 49 cm below the MWT to the base of the core, whereas at BM the opposite occurs, and contributions begin to oscillate before reaching a base value of 0%. Both I and IIb fluctuate in the seasonally saturated layer, remaining relatively constant. Once in the permanently saturated zone, however, I begins to increase at the expense of III, confirming that the distribution of these four products could potentially be used as a proxy for redox conditions in young peats as suggested by Swain and Abbott (2013).

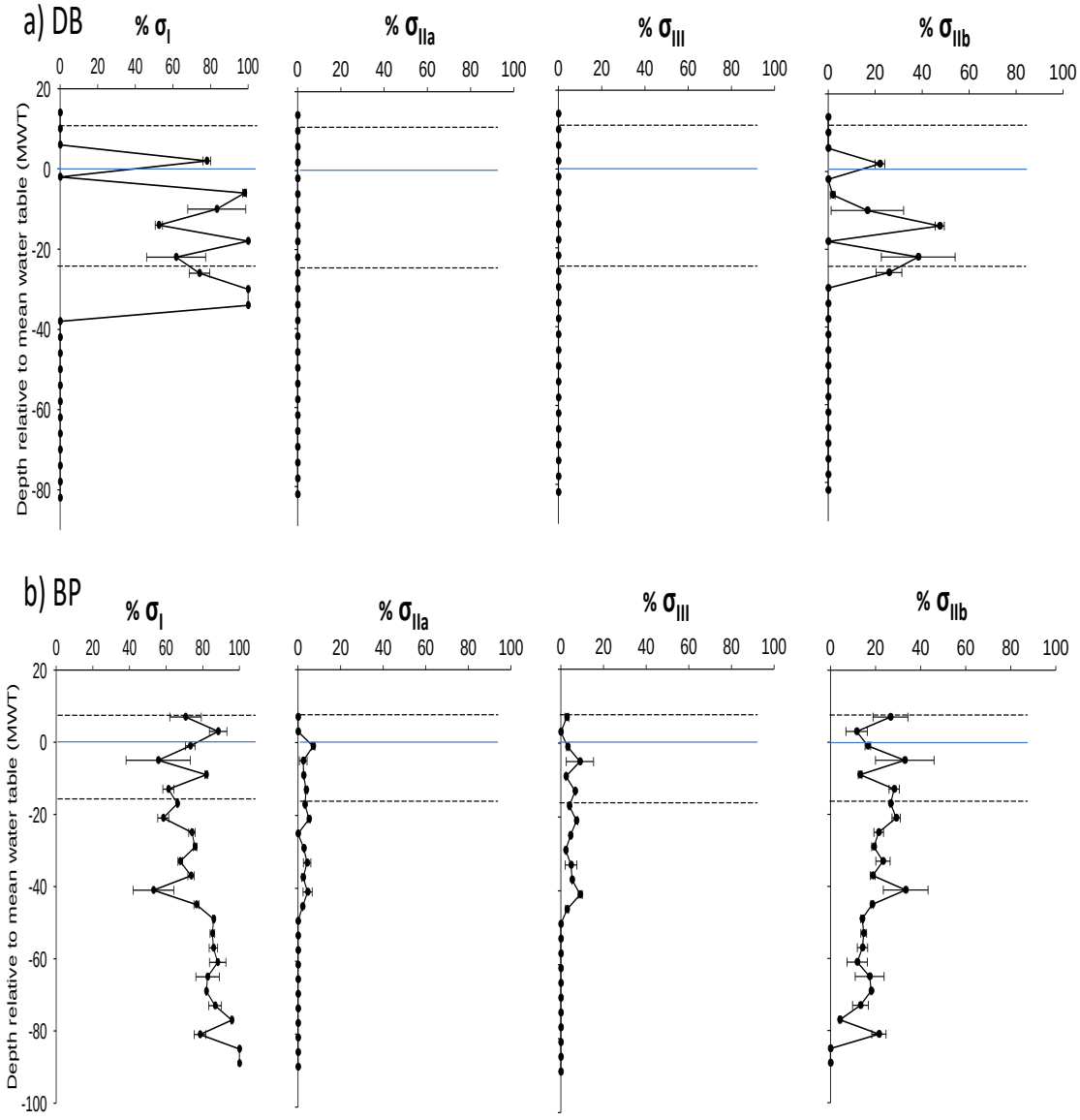
a) DB
% σI
% σIIa
% σIII
% σIIb
0 20 40 60 80 100
20 0 -20 -40 -60 -80
Depth relative to mean water table (MWT)
b) BP
% σI
% σIIa
% σIII
% σIIb
0 20 40 60 80 100
20 0 -20 -40 -60 -80 -100
Depth relative to mean water table (MWT)

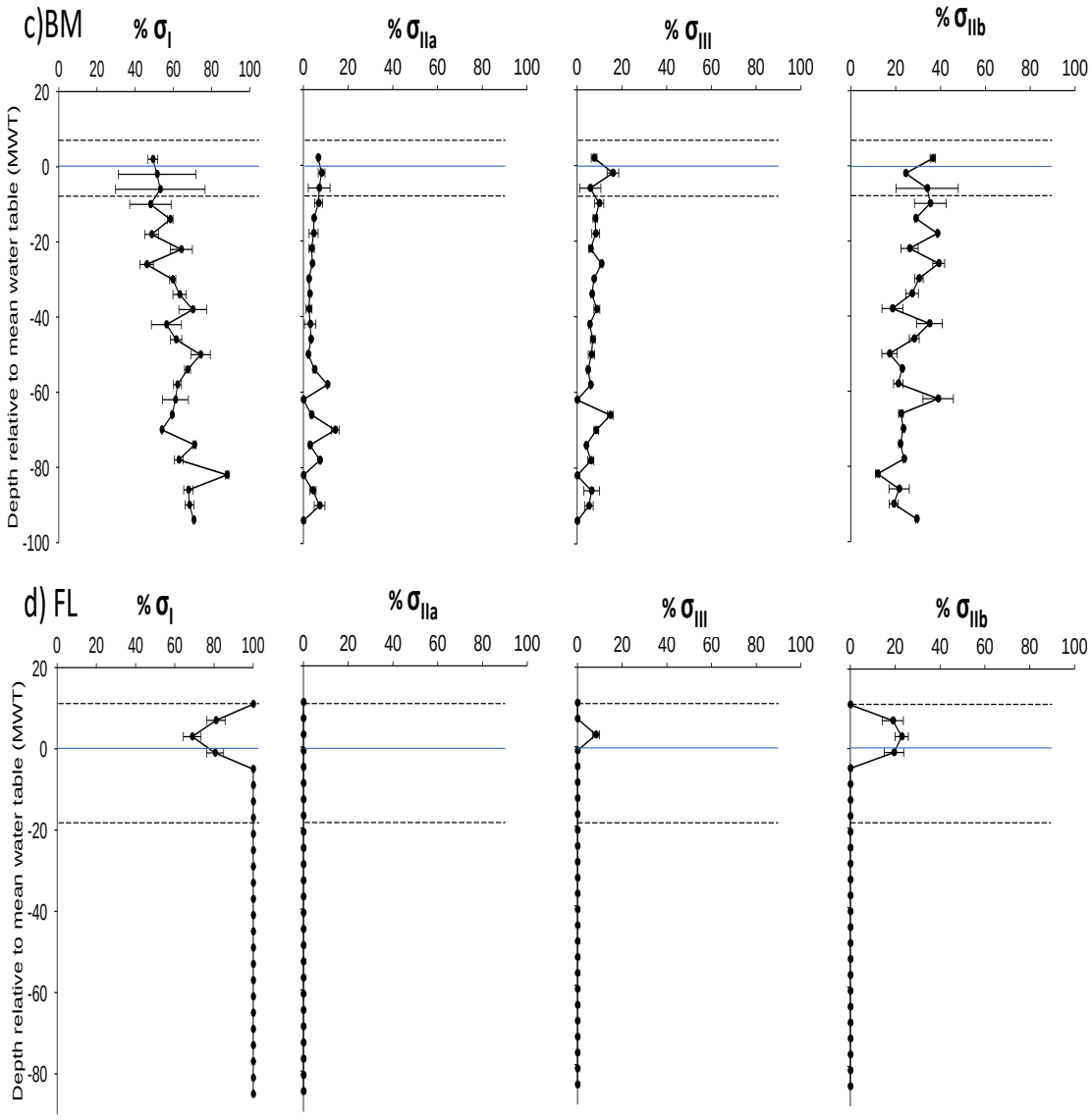

Figure 4.9: Depth profiles relative to mean water table (MWT) of individual σ component yields relative to total σ (%) for Degraded bog (a), Bog plateau (b), Bog margin (c) and Fen lagg (d). Negative values on the y-axis indicate samples below the MWT, positive values indicate samples above the MWT. 0 and the solid blue lines indicate the MWT, with the dashed lines indicating the minimum and maximum water table levels. Note the different scale used. Error bars represent standard error for two analytical replicates.

Such a proxy could only be adopted however in peats that have a considerable sphagnum input. The product distributions from both DB and FL do not match those from BP and BM which have a higher *Sphagnum* input. At DB, the majority of products were identified in the seasonally saturated layer, whereas in the other cores, products extend into the permanently saturated layer. An inverse relationship between I and III occurs below the mean water table at BP and BM. FL shows a decrease in I, and an increase in IIb in the seasonally saturated layer above the MWT, which is then reversed below the MWT resulting in the presence of I only in the permanently saturated layer. Such an increase in IIb may indicate a relatively recent increased input of fresh *Sphagnum* moss, which has not yet begun diagenetic change. The application of the $\%\sigma_{I-III}$ may, therefore, only be advantageous when there is a strong input from *Sphagnum* mosses, and all four sphagnum acid derivatives can be identified in the peat.

4.3.5.2 Lignin biomarkers

Vascular plant-derived phenols, including intact, degraded and non-lignin products, were identified at each site in consistently higher concentrations than sphagnum acid derivatives. Minimum-maximum values for the sum of intact lignin derivatives (Λ) include 0.000-0.747, 0.000-2.204, 0.169-1.544 and 0.207-1.172 mg/100 mg OC with an average of 0.095, 0.831, 0.601 and 0.488 mg/100 mg OC for DB, BP, BM and FL respectively. A continuous lignin input can be seen throughout each core with the exception of DB. At this site, there is a complete absence of lignin-derived products between 88-100 cm depth, where the organic-rich peat is replaced with a dense, inorganic clay layer (See Appendix A).

Figure 4.10 shows the downcore profiles for the lignin yield Λ and the acid/aldehyde ratios for guaiacyl derivatives $[Ad/Al]_G$ as an indicator of oxidative stress at each site. There was no significant change in Λ with depth, the exception being DB, where Λ decreased (Linear regression, R^2=0.46, $p<0.01$) before falling below the limits of detection as the peat transitioned into the clay fraction. This suggests a relatively rapid decay of

the lignin bipolymer with increasing burial at this site. The notion that lignin decomposition may differ between individual environments has been suggested by Hackett et al. (1977) who observed significant differences in the degree of lignin degradation depending upon the nature of material studied. In addition, Kirk and Farrell (1987) discuss the increased microbial degradation of lignin under aerobic conditions. The result observed here at DB further supports these theories, as DB is the only site in which lignin decreased with depth, and the most rapid decreases can be seen above the mean water table where oxygen will be more readily available. The results also support the theory proposed by Schellekens et al. (2015b) of lignin decay as a surface process. Polysaccharides were preferentially degraded over lignin during the first stage of decay and resulted in minor effects of depth related anaerobic decay on lignin parameters. In the anaerobic peatland environment, this first stage of decay is extended and may account for the stabilisation of Λ in the permanently saturated zone for the majority of cores analysed.

For the remainder of the cores, the lignin phenols appear to be stable with depth with average yields of 0.12 (0.09 including last 20 cm), 0.83, 0.60 and 0.49 $\pm$ 0.04 (0.03), 0.08, 0.05 and 0.04 mg/100 mg OC for DB, BP, BM and FL respectively. DB contained the lowest amounts of Λ and BP contained the highest (GZLM, $p<0.05$). Products that were consistently dominant in all cores included the *p*-hydroxyl phenols; 4-methoxytoluene (P2) and 4-methoxybenzeneethylene (P3) as well as the methyl esters of the cinnamyl phenols *p*-coumaric (P18) and ferulic acid (G18). Dominant guaiacyl lignin derivatives included; 1,2-dimethoxybenzene (G1), 3,4-dimethoxytoluene (G2), 3,4-dimethoxybenzaldehyde (G4), 3,4-dimethoxyacetophenone (G5), 3,4-dimethoxybenzoic acid methyl ester (G6) and *trans* 3-(3,4-dimethoxyphenyl)-3-propenoic aid methyl ester (G18). The syringyl derivative 3,4,5-trimethoxybenzoic acid methyl ester (S6) was also dominant in most samples. There are some small oscillations in Λ for most cores which may reflect a build-up of monomers due to selective preservation of lignin phenols (Cerli et al., 2008), changes in vegetation or input from root systems, which may therefore change the phenolic input (see Chapter 3, section 3.3.2.4).

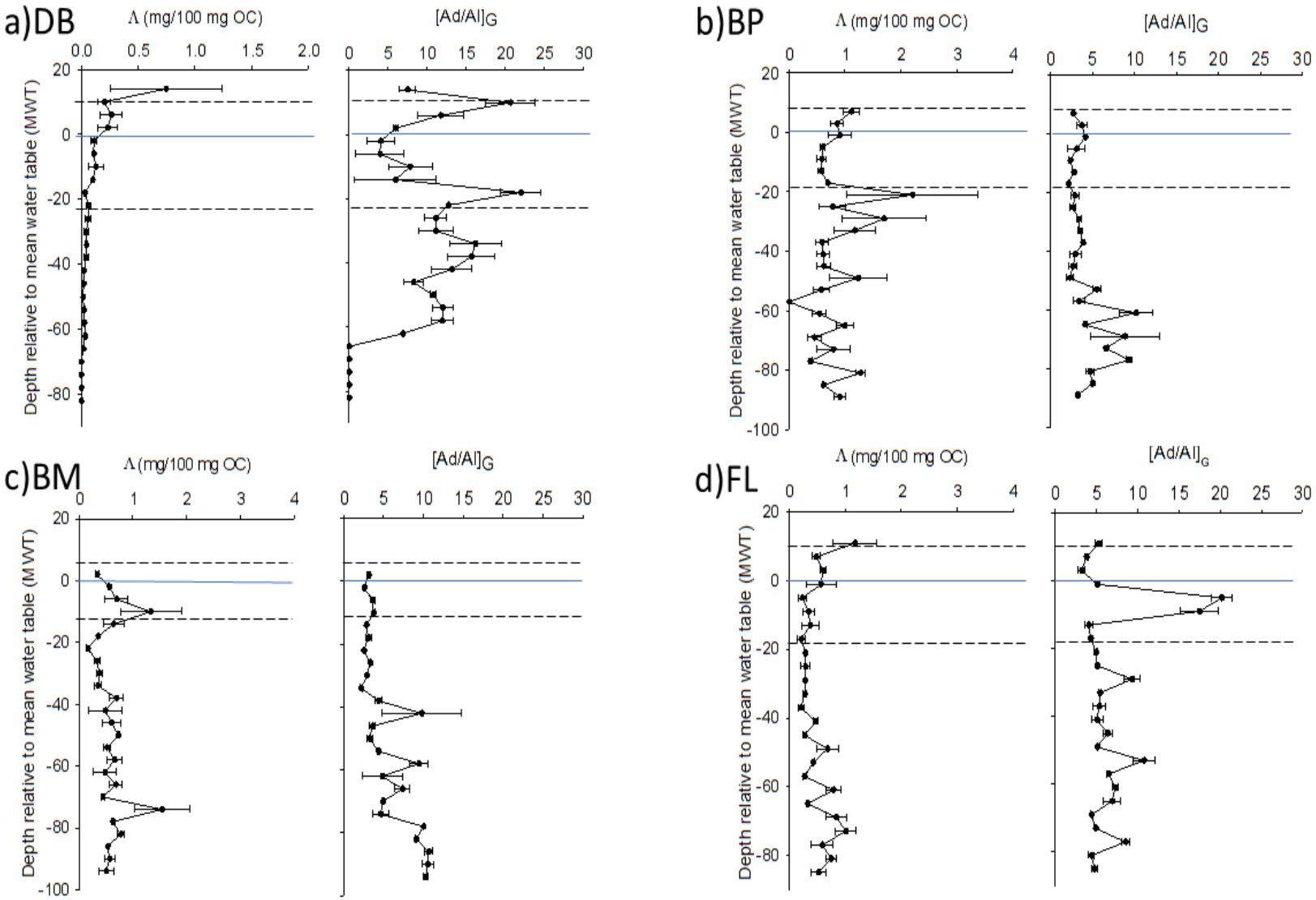

Figure 4.10: Depth profiles for Λ (mg/100 mg OC) and $[Ad/Al]_G$ ratios at DB (a), BP (b), BM (c) and FL (d). Negative values on the y-axis indicate samples below MWT and positive values above MWT. Solid blue lines indicates the MWT, dashed lines indicate the minimum and maximum water table levels. Error bars represent the standard error from two analytical replicates.

The $[Ad/Al]_G$ was highest at DB and overall showed stability as a function of depth at both DB (linear regression, R^2=0.01, p=0.69) and FL (linear regression, R^2=0.02, p=0.50), although large oscillations can be observed at DB (Figure 4.10a). The two peaks in the $[Ad/Al]_G$ ratio around the minimum and maximum water levels, as well as the large oscillation in the ratio throughout the seasonally saturated layer, is interesting and such a phenomenon is not observed in any other core. This unusual $[Ad/Al]_G$ profile at DB may reflect historically significant changes in water table regime at this site, which is further supported by the presence of *Sphagnum* biomarkers at selective points down the core.

FL shows a large increase in the $[Ad/Al]_G$ in the seasonally saturated layer (Figure 4.10d), between 1-13 cm below the MWT, which also corresponds to an increase in bulk density at this site (section 4.3.3, Figure 4.3), lending further support to the idea of a recent drop in water level and a 'shrinking' of the peat, as previously discussed. At BP, the $[Ad/Al]_G$ ratio showed an increase as a function of depth (linear regression, R^2=0.29, p<0.01) and the same was observed at BM (linear regression, R^2=0.60, p<0.01), indicating the progressive oxidation of lignin with increasing depth at these sites (Huang et al., 1998; Vane et al., 2001). These results are unexpected as BP and BM are the sites where the water table is highest, and therefore where lignin decomposition and alteration should be lowest. Perhaps at these sites, historic drops in water table have occurred resulting in the increased $[Ad/Al]_G$ downcore. Such a change would not be limited to a single site, however, and if this happened, a similar tend should be seen at other sites.

As illustrated by Nierop et al. (2005*a*), tannin compounds can be a significant component of natural samples, and therefore distort the Λ yield. Table 4.4 illustrates the considerable and varied effects of non-lignin and de-methylated lignin phenols on the yields of lignin derivatives that contribute to the Λ proxy, with G4, G5, S4 and particularly S6 being most affected. There were also differences between sites with DB consistently having the lowest yields of intact lignin monomers. All sites were

significantly affected by hydroxyl species (Table 4.4) as has been observed in other studies (Nierop and Filley, 2008).

Table 4.4: The average percentage yield of intact lignin (1 %OH), degraded lignin (2 %OH) and non-lignin (3 %OH) for the guaiacyl monomers G4, G5, G6 and G18 and the syringyl monomers S4, S5 and S6 at each site

Coring site	%OH G4	%OH G5	%OH G6	%OH G18	1%OH S4	2%OH S4	3%OH S4
DB	27.53	11.22	73.35	73.11	3.11	8.00	68.89
	±	±	±	±	±	±	±
	3.16	1.37	6.97	6.61	0.84	2.06	7.52
BP	44.27	16.93	85.70	86.95	23.00	30.78	46.23
	±	±	±	±	±	±	±
	1.90	1.19	1.00	0.76	2.98	2.97	5.41
BM	55.44	19.78	78.86	78.37	13.69	17.31	69.01
	±	±	±	±	±	±	±
	1.84	1.77	1.25	0.66	1.53	1.99	3.44
FL	37.64	16.78	90.29	89.54	19.10	32.48	48.42
	±	±	±	±	±	±	±
	1.74	0.91	0.39	0.30	1.84	3.03	4.33
Mean	41.22	16.16	82.05	81.99	14.73	22.14	58.13
	±	±	±	±	±	±	±
	2.15	1.31	2.40	2.08	1.80	5.81	6.26
	1%OH S5	2%OH S5	3%OH S5	1%OH S6	2%OH S6	3%OH S6	
DB	71.04	8.91	4.05	7.48	63.54	12.98	
	±	±	±	±	±	±	
	6.38	0.96	0.58	1.15	5.75	1.39	
BP	86.35	9.70	3.96	18.30	70.39	11.31	
	±	±	±	±	±	±	
	0.70	0.52	0.25	1.17	1.27	0.46	
BM	83.75	12.59	3.66	18.56	69.62	11.82	
	±	±	±	±	±	±	
	0.86	0.62	0.28	0.69	0.90	0.46	
FL	82.53	12.98	4.49	12.12	73.93	13.94	
	±	±	±	±	±	±	
	0.78	0.59	0.26	0.84	0.83	0.65	
Mean	50.92	11.05	4.04	14.12	69.37	12.51	
	±	±	±	±	±	±	
	2.18	1.02	0.17	0.96	2.16	0.59	

4.3.5.3 Lignin source proxies

The ratios between S/G and C/G lignin monomers can be used to assess vegetation input and change downcore. The relative abundance of angiosperms can be determined if S/G > 0 as well as the abundance of gymnosperms if S/G = 0 or non-woody tissue if C/G > 0. The ratios themselves are calculated using the following equations, with all compound abundances corrected for non-lignin inputs and normalised to mg/100 mg OC before being used in the equations;

$$S/G = \frac{(S4 + S5 + S6)}{(G4 + G5 + G6)} \tag{4.2}$$

$$C/G = \frac{(P18 + G18)}{(G4 + G5 + G6)} \tag{4.3}$$

The S/G and C/G profiles down core can be seen in Figure 4.11 and Figure 4.12. Overall, there was no significant change in either the S/G or C/G profile as a function of depth (linear regression, p>0.05 for all), however, small changes in the profiles can still be observed (Figure 4.11 and Figure 4.12). All cores displayed S/G and C/G values above 0, indicating a consistent angiosperm and non-woody input, as is seen in the vegetation assemblage today (See vegetation survey in Chapter 3, section 3.3).

The S/G ratio was similar for all cores with averages of 0.18 ± 0.01 (0.23 ± 0.08 including last 20 cm), 0.22 ± 0.01, 0.18 ± 0.01 and 0.21 ± 0.02 for DB, BP, BM and FL respectively. At DB, a large increase in the S/G ratio can be seen at 66 cm below the MWT which is as a result of the increasing syringyl and decreasing guaiacyl monomers as the peat begins to transition into the clay fraction (Figure 4.11). This suggests that during initial peat formation, there was a significant input from grasses and heather vegetation, although potential mixing of sediment during this section of the core may be the reason for the unusually high value observed here. The S/G profile at FL appears to slowly increase downcore, however, as noted above, these changes are not significant. As at DB, there appears to be a brief spike in the S/G ratio, reaching 0.51 at 29 cm

below the MWT and may indicate a more grassy or heather rich vegetation cover during this time, and values return back to 0.24, which is similar to the rest of the values obtained throughout the core.

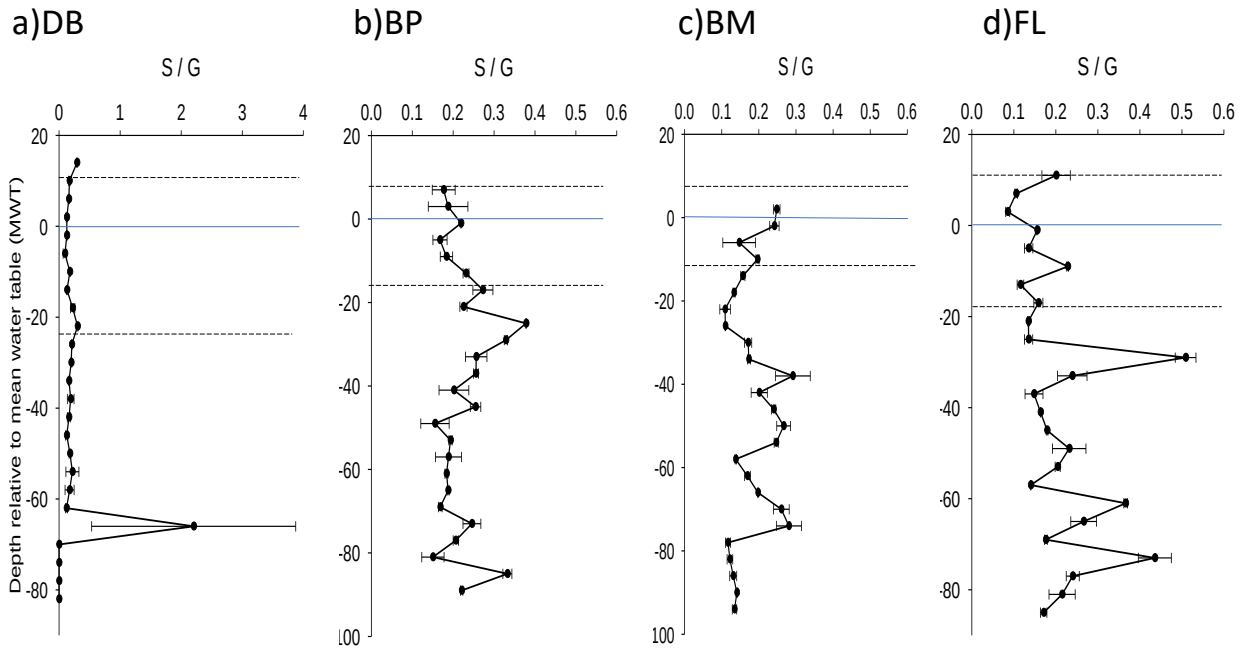

Figure 4.11: S/G ratios as a function of depth from the mean water table (MWT) for DB (a), BP (b), BM (c) and FL (d). Negative values on the y-axis indicate samples below MWT and positive values above MWT. Solid blue lines indicates the MWT, dashed lines indicate the minimum and maximum water table levels. Error bars represent the standard error from two analytical replicates.

Like the S/G ratio, the values obtained from the C/G ratio appear to be similar for all cores with average values of 1.42 (1.38 $\pm$ 0.28), 3.46, 3.00 and 1.89 $\pm$ 0.21, 0.23, 0.22 and 0.12 for DB, BP, BM and FL respectively. Both DB and FL show slightly lower values than BP and BM due to the decrease in C and increase in G monomers (Figure 4.12) at these sites. The same peak observed at DB for the S/G ratio can be observed here in the C/G ratio at 66 cm below the MWT which does suggest that possible mixing of sediment as the peat transitions into the clay fraction may be causing this (Figure 4.12). At BP, the C/G ratio declines throughout the permanently saturated zone, due to the decline in C and increase in G monomers. This is also the reason for the steep

decline that can be observed at the surface of FL where values drop from 0.2 to 0.09 between 11-3 cm above the mean water table.

The increase in G relative to C monomers is unusual, as the conversion of G structures to C during degradation through demethylation, is a common process that occurs during the diagenesis of lignin (Ertel and Hedges, 1984). This has been illustrated during a study by Huang et al. (1998) who observed the preferential removal S>G>C type units during lignin degradation in grassland soils. In contrast, however, Bahri et al. (2006) investigated the transformation and decomposition of lignin monomers in proportion to total lignin yield in a soil over 9 years and found guaiacyl type monomers had slower accumulation and turnover rates than the S- and C-type, which may be what is happening here. One possible explanation for this was the different spatial arrangement of the monomers with C-types located on the periphery of the lignin polymer (Scalbert et al., 1985; Opsahl and Benner, 1995), and S and G types embedded within the lignin structure. Therefore C-type monomers may be more accessible for degradation than other lignin types.

It should be noted, however, that the studies mentioned above used the CuO method as opposed to THM in the presence of labelled and unlabelled TMAH. Few studies (e.g Mason et al., 2009, 2012; Abbott et al., 2013) have used THM in the presence of TMAH to eliminate the distortion of Λ by non-lignin sources in peats and this is something that needs to be investigated further. Therefore the studies which utilise the CuO method are observing changes in phenolic monomers as opposed to specific lignin-derived units as presented here as Λ will be distorted by non-lignin sources.

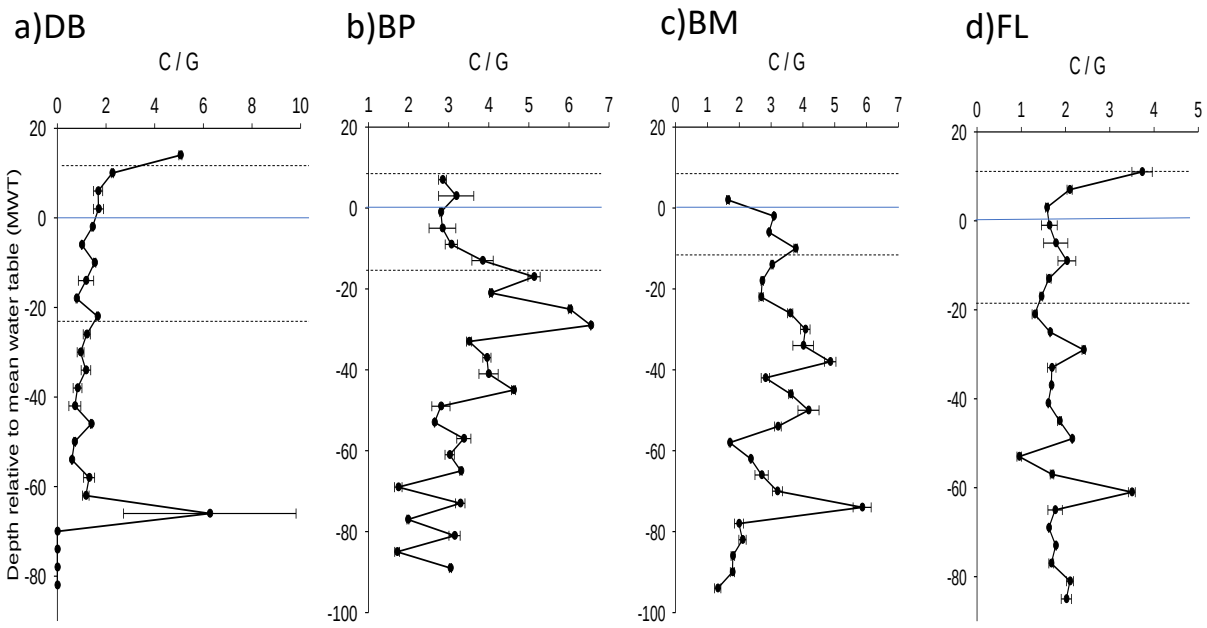

Figure 4.12: C/G ratios as a function of depth from the mean water table (MWT) for DB (a), BP (b), BM (c) and FL (d). Negative values on the y-axis indicate samples below MWT and positive values above MWT. Solid blue lines indicates the MWT, dashed lines indicate the minimum and maximum water table levels. Error bars represent the standard error from two analytical replicates.

4.3.5.4 Carbohydrate analyses

Fabbri and Helleur (1999) identified pairs of methylated carbohydrate (metasaccharinic acid) isomers when analysing a series of monosaccharide hexose standards, and the same can be seen in this study with two pairs identified; MC1 & 3 and MC2 & 4. The mass spectra of these compounds are shown in Chapter 3, Figure 3.5.

The second set of carbohydrate derived compounds (1-5), also known as isosaccharinic acids, originate from polysaccharides such as cellulose (Abbott et al., 2013) and were identified in the peat samples analysed in this study. Mass spectra are shown in Chapter 3, Figure 3.4. These match the spectra obtained from the thermochemolysis of cellulose by Schwarzinger et al. (2002), Abbott et al. (2013) and Swain (2013) with the exception of compound 6, a fully methylated version of compound 5, which was

not detected in these samples. For a more detailed description on the origin of these compounds can be found in Chapter 3, section 3.2.4.

1,2,4-trimehtoxybenzene (1,2,4-TMB) has also been identified in the analysis of carbohydrates (Fabbri and Helleur, 1999; Schwarzinger et al., 2002) and was major component identified in all samples. In this study, therefore, 1,2,4-TMB has been compared with both the methylated carbohydrate and polysaccharides (down core profiles). However, 1,2,4-TMB has multiple origins and had been identified in analyses of monosaccharides, polysaccharides, tannins and amino sugars (Fabbri and Helleur, 1999; Schwarzinger et al., 2002; Black, 2016). Findings should, therefore, be interpreted with care.

For the remainder of this section, concentrations for the total carbohydrate pool (compounds 1-5 and MC1-4), cellulose derivatives (compounds 1-5), methylated carbohydrate derivatives (compounds MC1-4) and 1,2,4-trimethoxybenzene (1,2,4-TMB) were compared as a function of depth from the mean water table (MWT). Results are displayed in Figure 4.13.

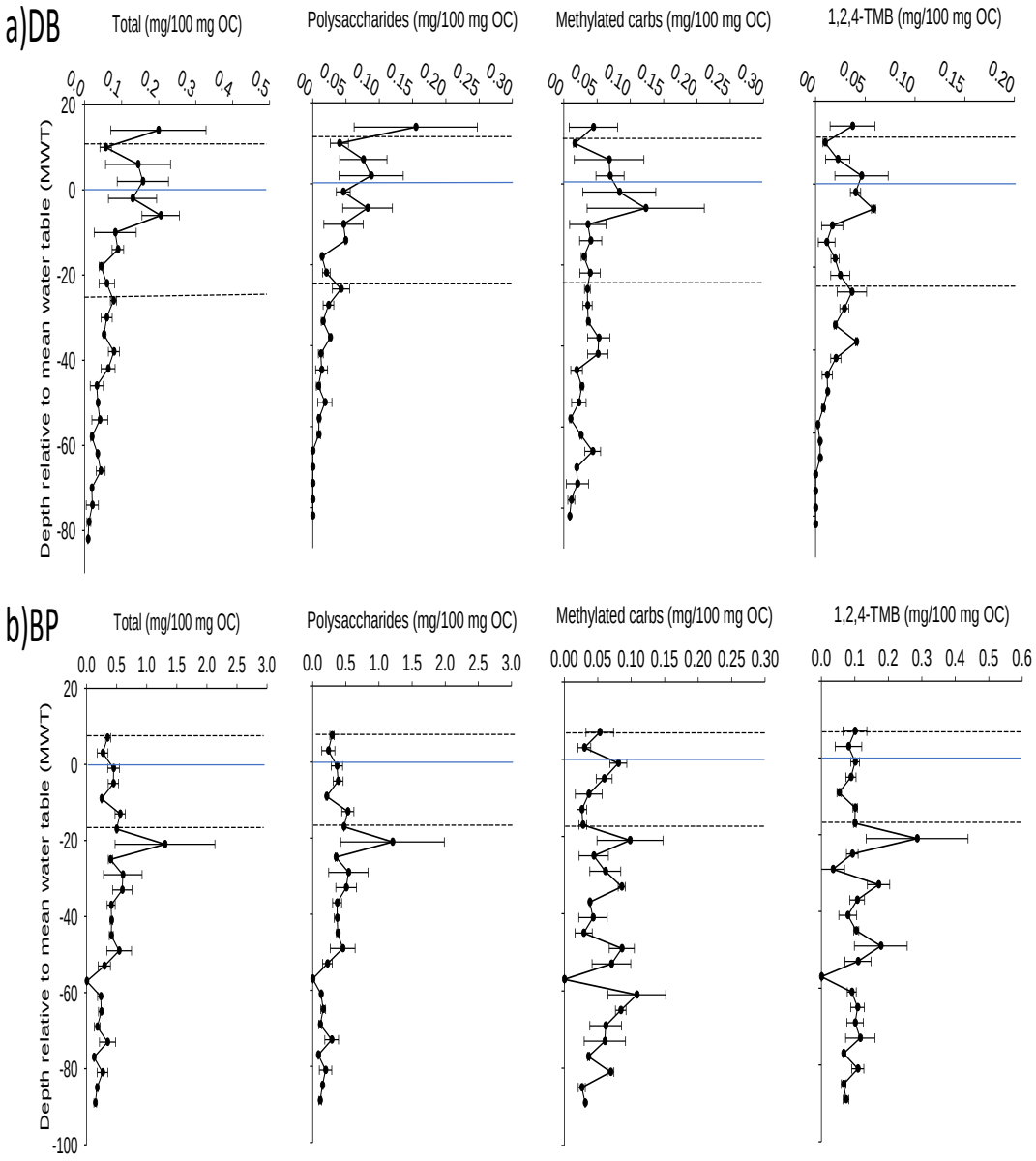
a)DB
Total (mg/100 mg OC)
Polysaccharides (mg/100 mg OC)
Methylated carbs (mg/100 mg OC)
1,2,4-TMB (mg/100 mg OC)
Depth relative to mean water table (MWT)
b)BP
Total (mg/100 mg OC)
Polysaccharides (mg/100 mg OC)
Methylated carbs (mg/100 mg OC)
1,2,4-TMB (mg/100 mg OC)
Depth relative to mean water table (MWT)

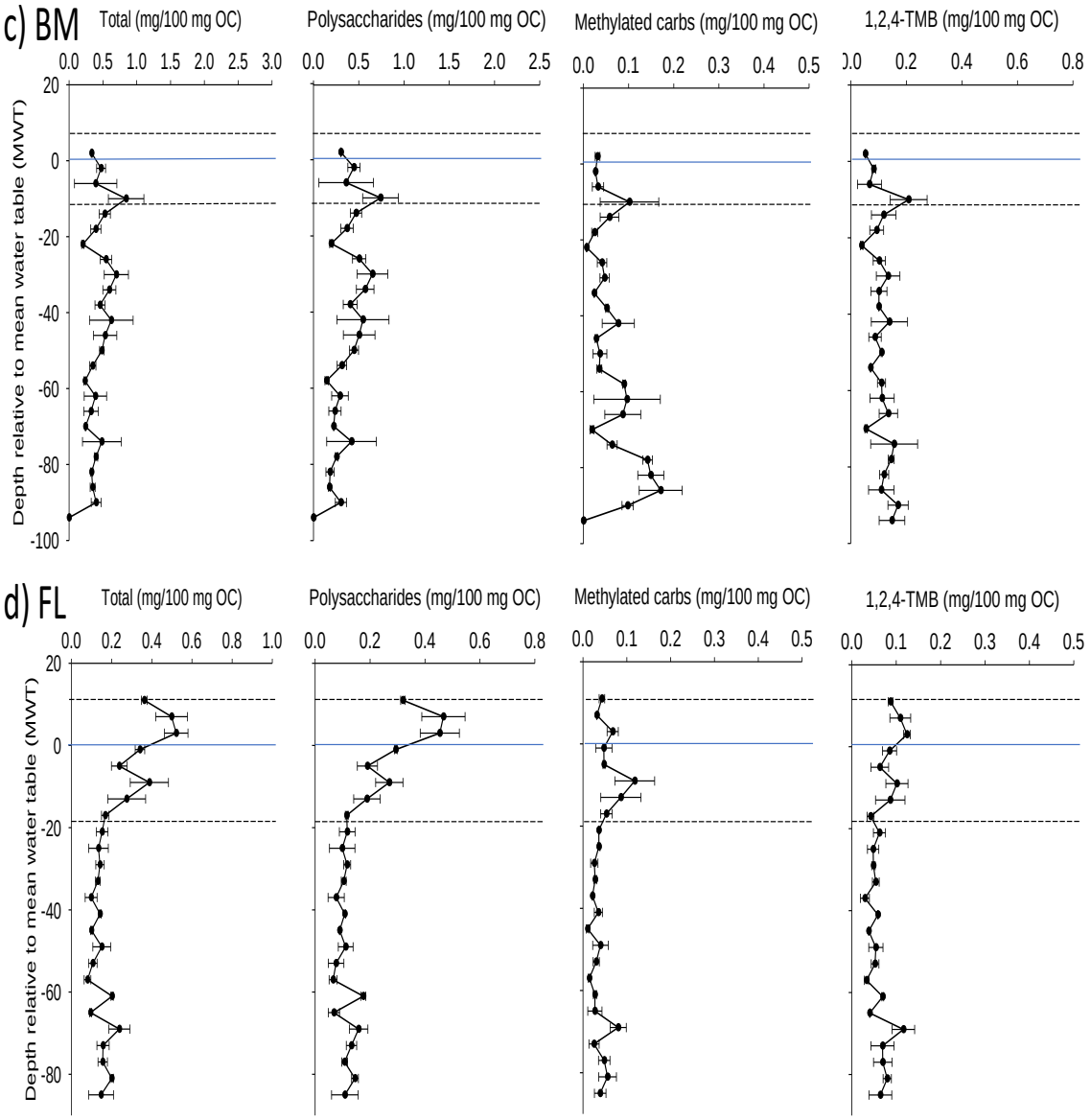

Figure 4.13: Depth profiles relative to mean water table (MWT) of concentrations (mg/100 mg OC) of total carbohydrate pool, polysaccharide (cellulose) derived products, methylated carbohydrates and 1,2,4-trimethoxybenzene for a) DB, b) BP, c) BM and d) FL. Negative values on the y-axis indicate samples below MWT and positive values above MWT. Solid blue lines indicates the MWT, dashed lines indicate the minimum and maximum water table levels. Error bars represent the standard error of two analytical replicates.

For all cores, the THM thermochemolysis of both the total accessible carbohydrate pool and the polysaccharide derivatives are strongly correlated (Pearsons correlation, $P<0.01$ for all cores) and display a decreasing trend in abundance from the surface of the core to the base (linear regression, $p<0.05$ for all). On average, DB contained the lowest concentrations of total carbohydrate (0.07 ± 0.01 mg/100 mg OC) and polysaccharide derived (0.03 ± 0.01 mg/100 mg OC) compounds of all the cores. BM displayed the highest concentrations containing 0.42 ± 0.03 and 0.36 ± 0.03 mg/100 mg OC for the total carbohydrate and polysaccharide derived compounds respectively. Profiles differ within the different hydrological layers between sites. DB displays a rapid decrease from the unsaturated layer into the seasonally saturated layer, where concentrations appear to stabilise until 6 cm below the MWT, after which concentrations continue to decrease to the base of the core. In contrast, concentrations increase through the seasonally saturated layer at both BP and BM, and appear more stable, with a slight decrease downcore to the base. At FL, increases are also seen in the seasonally saturated layer, however, once the MWT is reached, concentrations drop before becoming stable in the permanently saturated layer. These results agree with work by Schellekens et al. (2015b) where depth related anaerobic decay resulted in preferential degradation of polysaccharides over the more recalcitrant lignin phenols present in the peat.

Correlations between σ and carbohydrate and polysaccharide compounds can be seen, with the exception of DB, where very few *Sphagnum* biomarkers were identified. This agrees with findings from Swain (2013) that both carbohydrates and sphagnum acid products are involved with decay resistance, however, in this study, correlation was also observed between these carbohydrate profiles and the lignin yield Λ at DB and BP. The most likely reason for this is the high lignin input at both sites. The majority of phenolics identified at DB were lignin-derived, with only a few samples containing *Sphagnum* biomarkers, and BP contained the highest average Λ yield of all cores ($p<0.05$). No correlation was observed with Λ for BM and FL.

As described in section 4.3.5.1 above, BM contained the highest concentrations of

sphagnum acid derivatives (σ), whereas BP contained the highest concentrations of lignin-derived phenolics (Λ)(section 4.3.5.2). Total carbohydrate and polysaccharide concentrations are also highest at these sites. This could suggest that both *Sphagnum* and lignin derivatives play a role in the decay resistance of peat. However, the lower levels of σ present at FL, and the strong correlation observed with the carbohydrate derivatives demonstrate that even when the input is relatively low, these recalcitrant phenolics can still have a considerable influence on the preservation or degradation of carbohydrates buried within the peat.

Although there is a clear relationship between carbohydrate content and σ, it should also be noted that carbohydrate content was highest at the sites with the highest MWT and smallest seasonally saturated layer. Water table dynamics have a strong relationship with vegetation cover and species dynamics, with *sphagnum* species struggling for survival in areas with lower water tables. It could, therefore, be concluded that a mixture of water table drawdown and change in vegetation species composition an have a significant impact on OC storage in peatland ecosystems.

THM thermochemolysis released very small amounts of the methylated carbohydrate products (MC1-4) and were consistently dominated by the polysaccharide markers. There were no significant differences in concentration between cores or as a function of depth at BP or FL, however, concentrations decreased with depth at DB and increased at BM ($p<0.05$). Relatively weak correlations between the methylated carbohydrates and polysaccharide markers at DB and FL were seen ($P=<0.05$) demonstrating these compounds play different roles in the turnover of organic matter in peatland ecosystems. Further research is needed on this.

Finally, 1,2,4-TMB concentrations were highest at BP and BM with averages of 0.10 ± 0.01 and 0.11 ± 0.01, respectively. Concentrations decreased as a function of depth at DB only ($p<0.05$). Profiles appear to be a mixture of the polysaccharide and methylated carbohydrate profiles and correlate with each across all cores ($p<0.05$), with

the exception of the polysaccharide compounds at BM (p= 0.20). Further research is clearly needed to pinpoint the origin of this compound and its role within peatland OC cycle.

At this point, it is interesting to note that throughout this chapter, DB has had consistently low values for all compounds measured thus far (Sections 4.3.5.1, 4.3.5.2 and 4.3.5.3), however, the TOC values remain the highest of all sites at 53.06% (Section 4.3.2, Table 4.2). A possible explanation for this is offered by Dignac et al. (2005) who observed a 47% removal of soil lignin in contrast to only a 9% decrease in soil organic carbon (SOC) over 9 years. The authors propose that the long-term storage plant molecules may occur, however, these molecules are transformed before storage occurs, and are subsequently not detected using lignin-focussed analytical methods that are focussed on in-tact lignin identification.

4.3.5.5 Non-lignin phenols

Thermochemolysis with ^{13}C TMAH allows the assessment of the non-lignin contribution to the peat. Gallic acid (3,4,5-trihydroxybenzene) is a hydrolysable tannin which, following methylation with TMAH mimics the lignin-derived syringyl compound 3,4,5-trimethoxybenzoic acid methyl ester (S6). However, the application of ^{13}C TMAH to a sample allows us to differentiate between the methylated tannin molecule and the lignin derivative due to a distinct change in the molecular weight of gallic acid after methylation with the heavier methyl groups. It should be noted, however, that this method does not allow us to distinguish microbially degraded, fully de-methylated S6 from gallic acid. It is assumed, however, that in young surficial peats, the contribution from the fully de-methylated syringic acid would be negligible, and therefore has a predominantly tannin source. Assigned as a product the A-ring of condensed tannins, 1,3,5-trimethoxybenzene can also be considered as a useful marker for a tannin input to soils and vegetation (Nierop et al., 2005*a*). Contributions of both gallic acid and 1,3,5-TMB to the OM displayed in Figure 4.14.

Gallic acid decreases through all layers as a function of depth at DB (linear regression, $R^2 = 0.63$, $p<0.01$, all samples included), whereas at BM, gallic acid remains relatively stable in the seasonally saturated layer, and once into the permanently saturated layer, begins to accumulate (linear regression, $R^2 = 0.21$, $p<0.05$) (Figure 4.14). The same accumulation can also be seen at FL (linear regression, $R^2 = 0.32$, $p<0.05$), however in the seasonally saturated layer, concentrations decrease (linear regression, $R^2 = 0.75$, $p<0.01$) before reaching the permanently saturated zone. Large oscillations in gallic acid are seen at BP, and with a slight accumulation beginning in the last 20 cm of the core. If deeper samples were analysed, this accumulation may become statistically significant (linear regression, $R^2 = 0.10$, $p= 0.186$).

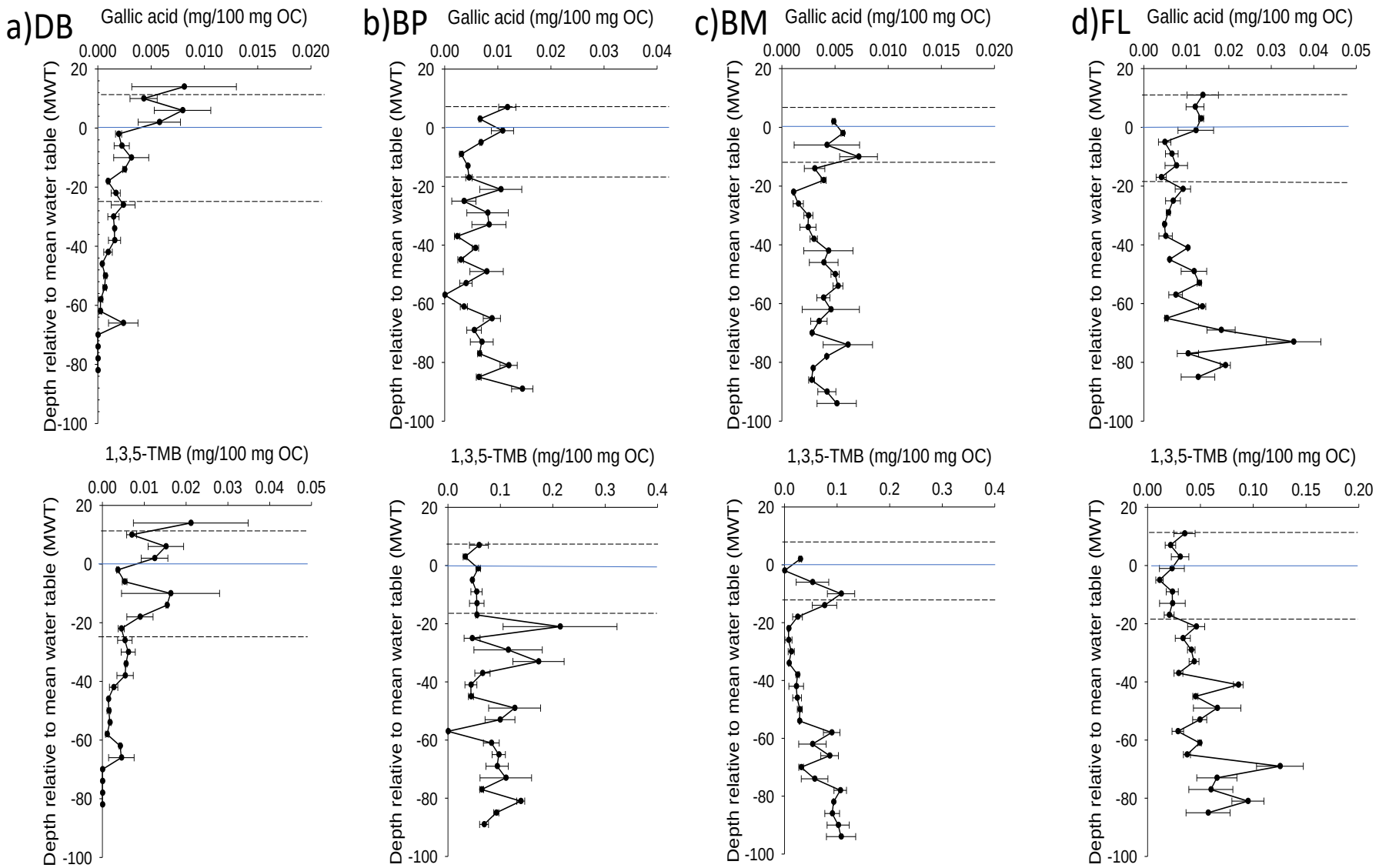

Figure 4.14: Depth profiles relative to mean water table (MWT) of gallic acid and 1,3,5-trimethoxybenzene for a) DB, b) BP, c) BM and d) FL. Negative values on the y-axis indicate samples below MWT and positive values above MWT. Solid blue lines indicates the MWT, dashed lines indicate the minimum and maximum water table levels.

1,3,5-TMB is present in low concentrations at DB, and shows strong correlations with gallic acid (Pearsons correlation, $R^2 = 0.79$, $p<0.01$) with concentrations decreasing as a function of depth (linear regression, $R^2 = 0.6054$, $P<0.01$, all samples included). At BM 1,3,5-TMB accumulates in the permanently saturated layer (linear regression, $R^2 = 0.21$, $p<0.05$) and shows a similar profile to gallic acid. Profiles of both compounds show strong correlations at FL (Pearsons correlation, $R^2 = 0.56$, $p<0.01$) however, in contrast to gallic acid, 1,3,5-TMB does not accumulate in the permanently saturated layer (linear regression, $R^2 = 0.21$,$p= 0.06$). At BP, 1,3,5-TMB oscillates throughout the permanently saturated zone, however, concentrations overall appear to be more stable in comparison to gallic acid.

The accumulation of tannins in the permanently saturated layers could indicate preservation of these phenolic compounds in anoxic environments, however, it should be noted that gallic acid is a water-soluble molecule, and so the leaching of hydrolysable tannins and movement down the profile could also be the cause (Nierop and Filley, 2007). The strong correlation of the two phenols at sites where the MWT is lowest (DB and FL) is interesting and suggests these compounds can provide some indication of hydrolysable and condensed tannin input. However, the absence of such a correlation at BP and BM (Pearsons correlation, $R^2 = 0.25$, $p= 0.23$ for BP and $R^2 = 0.34$, $p= 0.10$ for BM) demonstrates that under different environmental conditions, the role of these phenolic compounds in the cycling of OM can differ and further investigation into the causes and consequences of this is needed. Tannins undergo structural changes with time (Nierop and Filley, 2008) and environmental conditions and initial tannin input has been shown to have a significant impact on tannin decomposition in spruce soils and litter (Lorenz et al., 2000). However, more research into the cycling of these phenols in peat based ecosystems is needed.

4.4 Conclusions

The TOC content of all cores increased as a function of depth, with the exception of DB where TOC declined at depths greater than 80 cm (Table 4.2). This was due to the core transitioning from a carbon-rich peat into a carbon-poor clay layer. DB and FL had a higher average TOC value than BP and BM which is interesting as these sites, particularly DB contained significantly lower Λ, σ and carbohydrate concentrations. It is unknown what chemical compounds are contributing to this higher TOC value, and is something that will need further research. The possibility that these compounds have been produced by transformed phenolics, some of which may have originally been lignin-derived monomers, that are undetectable using analytical methods focussed on intact lignin identification, as suggested by Dignac et al. (2005), remains an untested possibility and is something that should be considered in future research concerning peatland carbon dynamics.

TN remained stable in all cores except DB where it declined after 80 cm. Overall, TN content was highest at DB and FL with an average of 1.77 ± 0.08 and $2.20 \pm 0.11\%$ respectively compared to BP and BM which contained an average TN content of 1.50 and 1.38 ± 0.04 and 0.05% respectively. These results may reflect increased microbial activity due to a low water table at these sites or may be a result of the higher vascular plant input. Lower TN was observed at BP and BM where *Sphagnum* mosses were more dominant and the peat was better preserved. Bulk density was highest at the sites where the water table was lowest (DB and FL), resulting in higher OC being stored in these cores. Bulk density in the centre of the mire was also found to be approximately half that at the mire edge, a phenomenon also observed by Lewis et al. (2012) in an Atlantic blanket bog in the southwest of Ireland. Overall, it was estimated that Butterburn Flow has an average OC storage capacity of 5.1 t ha^{-1}, which is similar to the estimate of 5.18 t ha^{-1} made by Ostle et al. (2009) for British bog habitats.

The lowest concentrations of σ were identified at DB as the majority of layers in

this core had no *Sphagnum* biomarkers, and BM the highest. Sphagnum acid pyrolysis products were only identified within the seasonally saturated zone at DB, suggesting historic changes in the water-table regime and a brief encroachment of *Sphagnum* species from the surrounding peat. σ concentrations remained consistent down core at BM suggesting this site has always experienced relatively high water tables and a healthy *Sphagnum* moss community. Generally, concentrations of the individual biomarkers I-III decreased with depth in contrast to the findings of Abbott et al. (2013), however the fact that peat samples at a depth greater than 50 cm were analysed in this study may be one reason for this. The consistent decrease of σ and the individual sphagnum acid biomarkers downcore suggests that this compound may not remain in the peat long-term (e.g 10,000 years), undergoing continuous degradation in anoxic conditions. However, the presence of the biomarkers throughout BM, and the predicted age of the peat as suggested by Yeloff et al. (2007b), does suggest these biomarkers can survive diagenesis in the medium term (around 900-1000 years). Future research should focus on the fate of these biomarkers within deeper sections of the peat.

When looking at the proportion of individual biomarkers (% I-III) to the total *Sphagnum* yield, results matched those of Swain and Abbott (2013) with I increasing at the expense of IIb in the permanently saturated layer. This lends further support to these biomarkers being used as indicators for redox conditions. This was only observed when there was a significant input of all four sphagnum acid pyrolysis products, however, and so if *Sphagnum* input is low, these biomarkers may not be as useful.

With the exception of DB, Λ did not change as a function of depth. DB had the lowest Λ concentrations, which declined as a function of depth, and the highest $[\mathrm{Ad/Al}]_G$ ratios indicating high levels of oxidation throughout the core. At FL a spike in the $[\mathrm{Ad/Al}]_G$ ratios can be seen in the seasonally saturated layer, which coincides with an increase in bulk density which is thought to correspond to a recent water table drop, peat shrinkage and therefore increased density. The Λ proxy at each site was dominated by cinnamyl and guaiacyl monomers, with a smaller input from syringyl type lignin.

This is a common observation due to the preferential removal of S>G>C type units (Huang et al., 1998). In contrast to this degradation paradigm, however, there were often increases in guaiacyl as opposed to cinnamyl type units. Such a phenomenon could be due to the increased accessibility for degradation of C-type monomer which are located on the periphery of the lignin polymer (Scalbert et al., 1985; Opsahl and Benner, 1995).

The presence of deep-reaching root systems may also be a contributor to increased guaiacyl lignin or the leaching of these phenols from the peat above (See Chapter 3, section 3.3.2.4). Further research is needed to clarify this, particularly using THM in the presence of TMAH to eliminate the effects of non-lignin products. In this study, contamination from non-lignin phenolic products was substantial and would have significantly affected the Λ proxy had they not been excluded. The guaiacyl monomers G4 and G5, and syringyl monomers S4 and S6 were most affected across all sites (Table 4.4).

Total carbohydrate concentrations decreased with depth in all cores and strongly correlated with σ, suggesting that increased degradation of *Sphagnum* biomarkers results in increased degradation of carbohydrates in *Sphagnum*-dominated peats. At DB where σ was minimal, carbohydrate content was also lowest of all cores but correlated strongly with lignin content suggesting that lignin can influence degradation in peatland ecosystems where the contribution from *Sphagnum* mosses is not significant. Overall, the sites with the lowest water table tended to have lower phenolic content, particularly those derived from *Sphagnum* mosses, higher oxidative stress and lower carbohydrate content. Therefore, for greater preservation of the carbon stored within peatlands, water tables need to be kept high with an abundance of *Sphagnum* mosses contributing to the peat.

In light of these results, in a future with an intensified hydrological cycle, chemical degradation of ombrotrophic northern peat is likely to increase and phenolic content decrease. Both DB and FL are sites with the lowest average water table and largest

water table range. These sites also had the lowest σ, Λ, and total carbohydrate content along with the highest lignin oxidation ratios.

Chapter 5

An investigation into the presence of lignin-derived phenolics in *Sphagnum* mosses

5. An investigation into the presence of lignin-derived phenolics in *Sphagnum* mosses

5.1 Introduction

Currently, there are around 300 species of *Sphagnum* moss worldwide, the majority of which can be found in the northern hemisphere, dominating peatland ecosystems (Clymo and Hayward, 1982; Rydin et al., 2013). They thrive in these environments due to the fully water saturated and highly acidic conditions which *Sphagnum*'s unique physiology and chemistry are well adapted to, but which remain unfavourable for most other plant species and microbes (Clymo and Hayward, 1982; Rydin et al., 2013).

Sphagnum mosses, also known as peat mosses, belong to the class Sphagnopsida within the division Bryophyta (Shaw, 2000; Shaw et al., 2003*b*). There are numerous morphological and developmental features which set *Sphagnum* apart from other mosses (Shaw et al., 2003*b*). For example, *Sphagnum* species are often determined by the shape and eminence of the capitulum, a cluster of branches near the stem apex (Eddy, 1977; Andrus, 1980; Flatberg, 2002; Shaw et al., 2003*b*). In addition to the distinctive capitulum, *Sphagnum* mosses also have large hyaline water-holding cells which are decorated with fibrils, a unique characteristic of *Sphagnum* mosses (Warnstorf, 1911; Holcombe, 1984; Shaw et al., 2003*b*). The water that these cells hold can account for up to 90% of the *Sphagnum* carpet (Clymo and Hayward, 1982).

Sphagnum consist of a suite of secondary metabolites which have no direct involvement with plant metabolism (Baas, 1989; Verhoeven and Liefveld, 1997). An example of such metabolites includes 'sphagnol', a polymeric network first identified by (Czapek, 1899, Czapek, 1913). This chemical network consists of *p*-hydroxyl (e.g 4-methoxybenzaldehyde, 4-hydroxybenzoic acid) and cinnamyl (*p*-coumaric and ferulic acid) phenols in addition to sphagnum acid, a unique and dominant phenolic in *Sphagnum* mosses (von Rudolph, 1972; Rasmussen et al., 1995; Verhoeven and Liefveld, 1997;

van der Heijden et al., 1997).

Although it has been established that *Sphagnum* mosses contain phenolic compounds, the presence of lignin-derived phenolics is a topic which is currently under debate. In a review of lignin biosynthesis by Weng and Chapple (2010), it is stated that the development of lignin synthesis began with the evolution of the vascular plants, which may have taken place around 700 million years ago (Heckman et al., 2001), and therefore lignin phenolics should be absent from mosses. However, several studies have identified the presence of lignin derivatives in *Sphagnum* species (Bland et al., 1968; Smeerdijk and Boon, 1987; Schellekens et al., 2009; McClymont et al., 2011; Swain, 2013; Schellekens et al., 2015a). One reason for this may be the solubility of vascular plant phenols (Hernes and Benner, 2003) coupled with the sponge-like quality of *Sphagnum* mosses. Previous studies have suggested that these soluble phenols become incorporated into *Sphagnum* tissue via the dissolved organic carbon (DOC) stored within the large hyaline cells of *Sphagnum* mosses (Abbott et al., 2013; Schellekens et al., 2015a). This is a likely possibility as *Sphagnum* mosses do not have a root system, and therefore directly absorb peat surface water which contains a large amount of dissolved organic carbon leached from the peat (Fenner et al., 2005). *Sphagnum* is widely recognised as a biosorbent, efficient at absorbing a variety of inorganic compounds, including heavy metals, and so the absorption of lignin monomers from surrounding water is quite plausible (Zhang and Banks, 2005, Zhang and Banks, 2006). However, some research has identified a genetic ability for mosses to synthesise lignin, suggesting this ability may not be limited to higher plants (Xu et al., 2009). In addition, Ligrone et al. (2008) demonstrated epitopes asociated with condensed homoguaiacyl (G) polymers and condensed, mixed guaiacyl-syringyl (GS) polymers were present in the cell walls of several bryophyte species and one species of green algae. In vascular plants, such polymers serve a structural role, however, Ligrone et al. (2008) suggests that in bryophytes, their role is likely to be a protective one against microbial attack or UV radiation. Therefore, the ability for these plants to incorporate G or GS moieties into cell walls is a primitive character of land plants, and allowed the evolution of lignin in vascular plants. Given

this conflicting body of research, it is currently unknown whether these phenols are indeed synthesised internally, or incorporated into *Sphagnum* tissues externally via DOC.

The most commonly used method to analyse lignin is via cupric oxidation (CuO), however, this method has a variety of drawbacks including it being a very time-consuming method, and inefficient for use on samples with a high carbon content (e.g peat and plant samples)(See Chapter 1, section 1.2.5 for more information)(Wysocki et al., 2008). Due to such drawbacks, thermally assisted hydrolysis and methylation (THM) in the presence of tetratmethylammonium hydroxide (TMAH) is increasingly employed (Shadkami and Helleur, 2010). This method requires little sample preparation, is well suited to samples that contain high levels of organic carbon. In addition, when ^{13}C-labelled TMAH is employed, the method allows differentiation between intact, degraded and non-lignin products which can make a significant contribution to peat and plant samples (Filley et al., 1999, Filley et al., 2006). Whichever method is used, however, the sum of eight main monomers is used to provide information on lignin yield, and these include; the cinnamyl phenols *p*-courmaric acid (P18) and ferulic acid (G18), three guaiacyl phenols; 3,4-dimethoxybenzaldehyde (G4), 3,4-dimethoxyacetophenone (G5) and 3,4-dimethoxybenzoic acid methyl ester (G6)) and three syringyl phenols; 3,4,5-trimethoxybenzaldehyde (S4), 3,4,5-trimethoxyacetophenone (S5) and 3,4,5-trimethoxybenzoic acid methyl ester (S6)) (Hedges and Parker, 1976).

The aim of this chapter is to establish whether *Sphagnum* mosses are able to incorporate lignin-derived phenols into their tissue via external water sources. The species *Sphagnum capillifolium* collected from a carpet at Moor House Natural Nature Reserve (NNR), North Yorkshire were used to test this. The specific objectives were:

1. To understand the effects of exposing *Sphagnum* moss to lignin-derived phenol enriched water on the concentrations of lignin-derived phenols identified in *Sphagnum* tissue

2. To understand the effects of exposing *Sphagnum* moss to phenol-free water on the concentrations of lignin-derived phenols identified in *Sphagnum* tissue

3. To establish whether this provides further support to the theory of the uptake of lignin-derived phenols via external water sources.

5.2 Methods

This experiment, as described below, was designed to mimic a peatland environment as much as possible. The treatment solution was added to a set volume to mimic water table with sand pre-saturated with treatment solution added to the base of cellulose extraction thimbles to mimic peat. Sand was chosen as it would remain wet throughout the experiment providing a moist and more realistic environment for the mosses to be placed in.

5.2.1 Field site and sample collection

A sample of *Sphagnum capillifolium* was taken from a large carpet at Moor House National Nature Reserve (NNR) and placed into plastic bags to be brought back to Newcastle University. Whole plant sections (i.e capitulum, stems and branches) were collected. Once returned to Newcastle University, the vegetation was thoroughly rinsed in deionised water and plants were separated and checked for contamination from other plant sections (e.g leaves, roots and seeds) or fungi. It should be noted that although the samples were rigorously cleaned, it is still possible that traces of other plants and fungi remained.

Moor House is an upland blanket peat, forming part of the Trout Beck catchment, situated in the North Pennines, UK. The mean annual temperature (1991–2006) is 5.8 °C and mean annual precipitation (1953–2006) is 2012 mm (Holden and Rose, 2011). The nature reserve is used by the UK Environmental Change Network (ECN) to collect hydrological data from the Tout Beck catchment, which is a primary headwater tributary of the River Tees. The underlying geology of Moor House has previously been described by Johnson (1963) and consists of Carboniferous limestones, sandstones, and shales with intrusions of the doleritic whin sill. This is covered with glacial till which

provides poor drainage and allowed the development of the ombrotrophic peat present today. Dominant vegetation at the site consists of *Eriophorum* species such as cotton grass, *Calluna vulgaris* or common heather as well as a diversity of *Sphagnum* mosses. See Worrall et al. (2003) for site descriptions and catchment map and Figure 5.1 for sitemap.

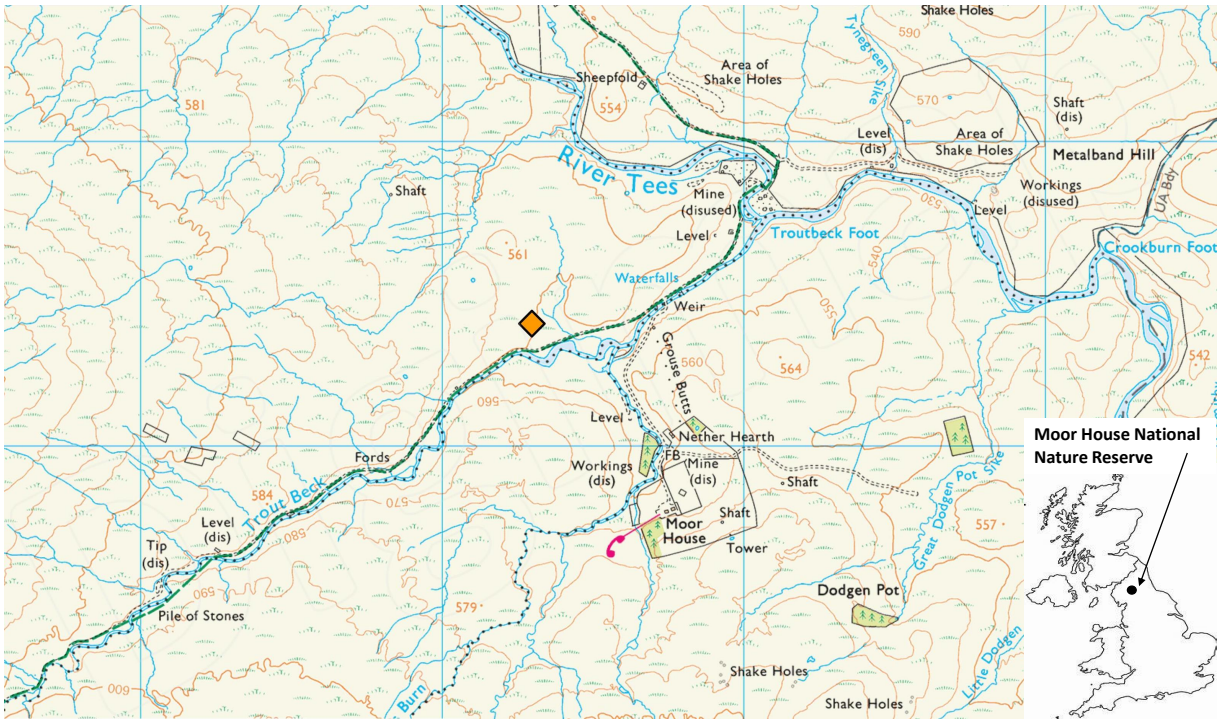

Figure 5.1: Map of Moor House National Nature Reserve. Sampling point represented by the orange diamond. Grid reference NY7527833361.

5.2.2 Sample preparation and experimental design

Figure 5.2 illustrates the experimental design as described below. Eight individual *Sphagnum* plants (including capitulum, stem and branches) were picked, and stems were cut to 2 cm lengths. These eight plants were then placed upright into a soxhlet pre-extracted Whatman cellulose extraction thimble (22 mm x 80 mm internal diameter x external length). The thimbles contained approximately 2 cm of soxhlet pre-extracted Merck Sea Sand (VWR) which the *Sphagnum* was placed on top of.

Four of these thimbles were then placed in a 250 mL glass beaker and filled up to 50 mL with one of 3 treatment solutions. Each of the four thimbles in the beaker had the respective treatment solution poured over to saturate the sand in the bottom before being topped up to the 50 mL mark on the glass beaker. The treatment solutions were; 1) Milli-Q water, 2) Bog water collected from a pool at Moor House and 3) Bog water with added lignin phenols at a total concentration of 1 mg/L^{-1} (referred to in the text as Milli-Q, bog water, and phenols treatment respectively). This specific concentration was chosen to match real-world concentrations as shown by Fenner et al. (2005) who measured phenolic compound concentrations between 0.6-3.2 mg/L^{-1} in the pore water of control and manipulated peatlands. The individual phenolic compounds that were added include; 4-methoxyacetophenone (P5), *p*-courmaric acid (P18), (3,4-dimethoxybenzaldehyde (G4) and 3,4-dimethoxyacetophenone (G5) and well as the two syringyl phenols (3,4,5-trimethoxybenzaldehyde (S4) and 3,4,5-trimethoxyacetophenone (S5). The beakers were then placed near a window for sunlight, ready for the experiment to begin.

The first samples were taken from each treatment as soon as the experiment was set up, and is referred to in this study as the week 0 sample. Vegetation was washed with deionised water to wash off treatment solutions before being place in a glass jar and then stored in the freezer at -20 °C. The remaining vegetation in the thimbles was washed daily with 5 mL of treatment solution for four weeks. This time frame was chosen after (Anii et al., 2009) observed accumulation of various elements in samples of *Sphagnum girgensohnii* after 1 month of exposure. It was therefore assumed that 1 month is long enough to observe accumulation of organic compounds as well. At the end of four weeks, each treatment was sampled again and these are referred to as the week 4 samples. Like the week 0 samples, they were washed in deionised water to rinse off any external treatment solution, placed in a glass jar and stored at -20 °C. Each treatment was repeated three times to ensure the accuracy of results and enable statistical interpretation. Throughout the experiment, all treatment solutions were stored in the fridge at 4 °C and out of direct sunlight. Control samples were run

alongside vegetation samples, and glass wool was used as the control medium.

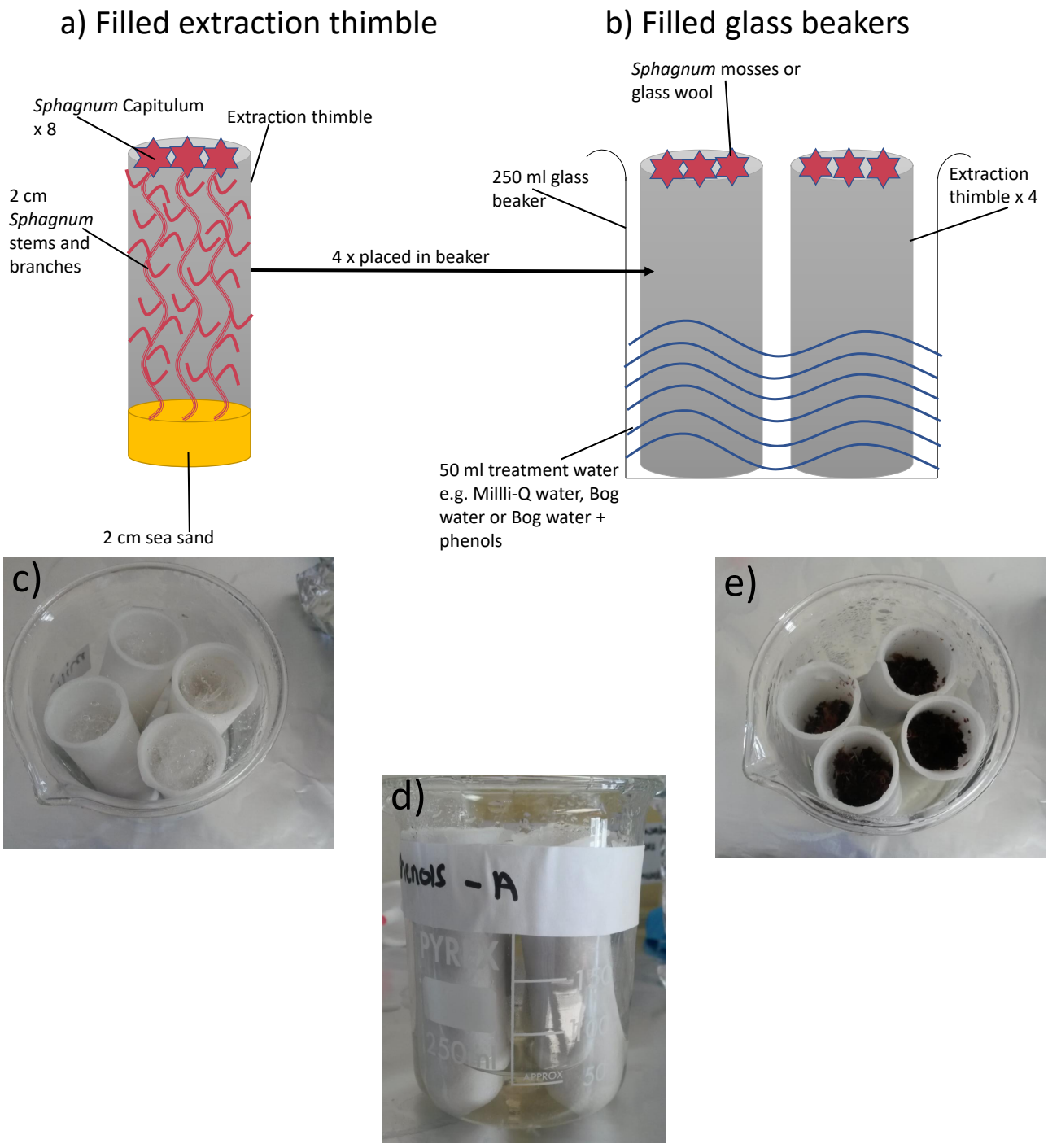

Figure 5.2: Pictures illustrating the experimental design. a) cross section of an extraction thimble filled with *Sphagnum* mosses, b) beakers filled with thimbles and treatment water c) aerial view of the extracted cellulose thimbles containing the glass wool control, d) aerial view of the extracted thimbles containing eight *Sphagnum capillifolium* plants each and e) illustrates how the thimbles were placed in the beaker and topped up to 50 mL with the treatment solution.

5.2.3 Chemical extraction and analytical analysis of the plants

After sampling, the vegetation was freeze-dried and crushed to a fine powder following methods previously described in Chapter 2, section 2.2. 18 total organic carbon (TOC) measurements were taken before samples were extracted with a 1 : 1 DCM : MeOH solution. Extracts were stored in the freezer for later analysis whilst around 1 mg of the insoluble *Sphagnum* residues were placed into a quartz tube plugged with extracted glass wool. On-line THM was carried out at 610 °C for 10 s. 5α-androstane was used as an internal standard for the quantification of compounds, and the NIST 98 library was used for compound identification. For more detailed descriptions of the analytical methods, see Chapter 2, section 2.2

5.2.4 Chemical extraction and analytical analysis of the bog water

Along with the vegetation, analysis of the water-soluble organic matter (OM) within the bog water prior to pouring it on the plants was conducted. Three separate water samples that were collected from the same pool at Moor House were extracted following the methods outlined in Williams et al. (2016*a*) and are outlined below.

500 mL of unfiltered bog water was extracted using reversed phase C_{18} end capped solid phase extraction (SPE) cartridges (Agilent, 60 mL, 10 g megabond elut flash cartridge). Cartridges were connected to a vacuum pump (Heidolph Rotavac vario control) which allowed the sample to be drawn through the cartridge at a rate of 20 mL/min before passing into a liquid trap (1 L glass bottle). Each cartridge was pre-conditioned with 100 mL MeOH followed by 50 mL distilled water acidified to pH2 using 37% HCl acid (Fisher Scientific). After extraction, cartridges were rinsed with 50 mL acidified water to remove residual salts. Finally, a glass beaker was placed under the cartridge for the collection of the water-soluble organic matter. Elution was conducted in a single fraction using 50 mL of MeOH, which was passed slowly through the cartridge. To do this, a rubber bung was placed in the top of the cartridge to seal it, which contained a

glass rod in the middle. This rod was connected to a nitrogen tap via plastic tubing. The cartridge became pressurised as the N_2 was allowed to flow through, slowly pushing the MeOH and extracted OM into the glass beaker. The MeOH was rotary evaporated (Heidolph Laborota 4003, Rotavac vario control) down to $\sim$ 1 mL and then transferred into a 10 mL glass vial. The sample was then evaporated to dryness under N_2.

Around 1 mg of the dried sample was then placed in a quartz tube plugged with extracted glass wool and analysed using THM in the presence of TMAH as described in Chapter 2, section 2.2. On-line THM was carried out at 610 °C for 10 s. 5α-androstane was used as an internal standard for quantification of compounds. For more detail, see Chapter 2, section 2.2.

A second aliquot of the dried sample was analysed for total organic carbon (TOC) content using a LECO-CS230 Carbon - Sulphur analyser (Leco Corporation, USA). The analyser was calibrated using 1 g standard steel rings of certified carbon content (Leco Corporation, USA) and evolved CO2 was quantified using infrared detection. A reference soil (ISE reference soil 999) was analysed periodically to confirm the accuracy of measurements. For more information on TOC analysis, see Chapter 2, section 2.2.6.

5.2.5 Statistical analyses

All statistical analyses were carried out on IBM SPSS Statistics 23 software. All data were normalised to 100 mg OC and corrected for non-lignin and degraded lignin phenols before being tested for normality using the Shapiro-wilk test as well as visual data assessments. For the mosses, data across all treatments at both week 0 and week 4 was not normal, and could not be made normal via transformations and so non-parametric analyses were used throughout this chapter. Firstly, Λ concentrations between week 0 and week 4 for all treatments were tested using a generalized linear model (GZLM) with Fishers Least Significant Difference (LSD) *post-hoc* tests. Both the main effects of 'treatment' and 'time' were explored as well as the interaction of treatment*time.

The results of this interaction were the main focus of this study, and so main effects are only briefly mentioned where considered necessary. The same statistical method was then used independently for each of the lignin phenols added to the 'phenols' treatment that were identified in the moss (P5, P18, G4, G5) as well as the naturally occurring phenols that contribute to the Λ proxy (G6, G18 and S6). S4 and S5 were also added to the 'phenols' treatment, however, these compounds were not identified in any of the mosses analysed, and so could not be included in any statistical analyses. Finally, this same statistical method was used to investigate whether concentrations of σ changed in each treatment between week 0 and week 4.

For the bog water, differences between the bog water and moss (at time 0) Λ and σ concentrations were tested using the non-parametric Mann-Whitney U statistical test. All three extracted water samples were included in this analysis as well as the nine moss samples analysed at time 0 (i.e 3 samples from each treatment). For all tests, results were considered significant if $p<0.05$

5.3 Results and discussion

THM thermochemolysis of the water-soluble organic matter in the bog water and the solvent-extracted *Sphagnum capillifolium* samples yielded a range of methylated phenolic products alongside other oxygenated compounds as listed in Table 5.1. The naming system used for lignin derived compounds follows the work by Clifford et al. (1995); del Rio et al. (1998); Chefetz et al. (2000); Vane et al. (2001) and Frazier et al. (2003).

Table 5.1: The main thermochemolysis products observed in all samples

Peak label	Tentative assignment
P1	methoxybenzene
P2	4-methoxytoluene
G1	1,2-dimethoxybenzene
P3	4-methoxybenzeneethylene
1	methylated isosaccharinic acid
2	methylated isosaccharinic acid
3	methylated isosaccharinic acid
I	4-isopropenylphenol
P4	4-methoxybenzaldehyde
S1	1,2,3-trimethoxybenzene
P5	4-methoxyacetophenone
1,2,4-TMB	1,2,4-trimethoxybenzene
G4	3,4-dimethoxybenzaldehyde
5	methylated isosaccharinic acid
MC2	methylated metasaccharninc acid
MC3	methylated metasaccharninc acid
MC4	methylated metasaccharninc acid
G5	3,4-dimethoxyacetophenone
G6	3,4-dimethoxybenzoic acid methyl ester
IIa	*cis*-3-(4-hydroxyphen-1-yl)but-2-enoic acid methyl ester
III	3-(4-hydroxyphen-1-yl)but-3-enoic acid methyl ester
P18	*trans*-3-(4-dimethoxyphenyl)-3-propenoic acid methyl ester
IIb	*trans*-3-(4-hydroxyphen-1-yl)but-2-enoic acid methyl ester
S6	3,4,5-benzoic acid methyl ester
G18	*trans*-3-(3,4-dimethoxyphenyl)-3-propenoic acid methyl ester
$C_{16:0}$ FAME	C_{16} fatty acid methyl ester
IS	5α-androstane

5.3.1 Lignin composition of the bog water

The carbon contained within dissolved organic matter (DOM) is an important and rather understudied part of the carbon cycle, affecting carbon cycling in both terrestrial and aquatic environments (Bolan et al., 2011). The chemical composition of this dissolved organic carbon includes lignin-, carbohydrate-derived compounds and n-alkanes (Williams et al., 2016a). A significant amount of lignin is leached in oligomeric form as well as monomers (Williams et al., 2016a), and lignin phenol concentrations have been reported to range between 0.07 mg/100 mg OC from a river delta in Northern

California (Eckard et al., 2007) up to 8.13 mg/100 mg OC from a forest watershed in California (Dalzell et al., 2005).

Using SPE extraction, a total of 7.4 mg/L of organic matter was extracted from the water, which is similar to the values obtained by Williams et al. (2016*a*) from the waterborne material from a woodland in Devon, UK. TOC concentrations reached 3.09%, however, it should be noted that the SPE method of extraction excludes particulate matter, and so may greatly underestimate the amount of carbon exported by peatland waters. The bog water contained a range of thermochemolysis products including lignin-derived phenols which were dominant products in each sample Figure 5.3. The range of lignin phenols was limited when compared to lignin-rich peat samples analysed throughout Chapter 4, however, those that were present included the cinnamyl phenols P18 and G18, the Guaiacyl phenols G1, G2, G4, G5, G6 and G18 as well as the syringyl phenols S1, S5 and S6 Figure 5.3. This product range is very similar to the range of products observed in *Sphagnum* mosses, which lends further support to the absorption of these phenols from the bog water via the *Sphagnum*'s hyaline cells. The Phenolic composition of dissolved organic matter (DOM) is often specific to the phenolic composition of the litter and soils that the water is sourced from (Williams et al., 2016*a*). The range of phenolic products observed here is therefore not surprising as it reflects the significant lignin content of the peat from which the water has been sourced as well as the vegetation growing there.

The most dominant phenolic products observed in the water samples included G1, G6 and S6 which agrees with the findings of Williams et al. (2016*a*). In that study, the water-borne organic matter was analysed from a range of different land uses using TMAH thermochemolysis. *p*-hydroxyl, as well as the lignin-derived guaiacyl and syringyl phenols, were all detected with compounds G6, P6 and S6 dominating. THe *p*-hydroxyl units identified here included P1, P2, P3, P5 and P6, with additional products of the sphagnum acid derived I, as well as 1,2,4-trimethoxy benzene and 1,3,5-trimethoxy benzene which may be either tannin or carbohydrate derived. For more

discussion on these products, see Chapter 4, section 4.3.5.4.

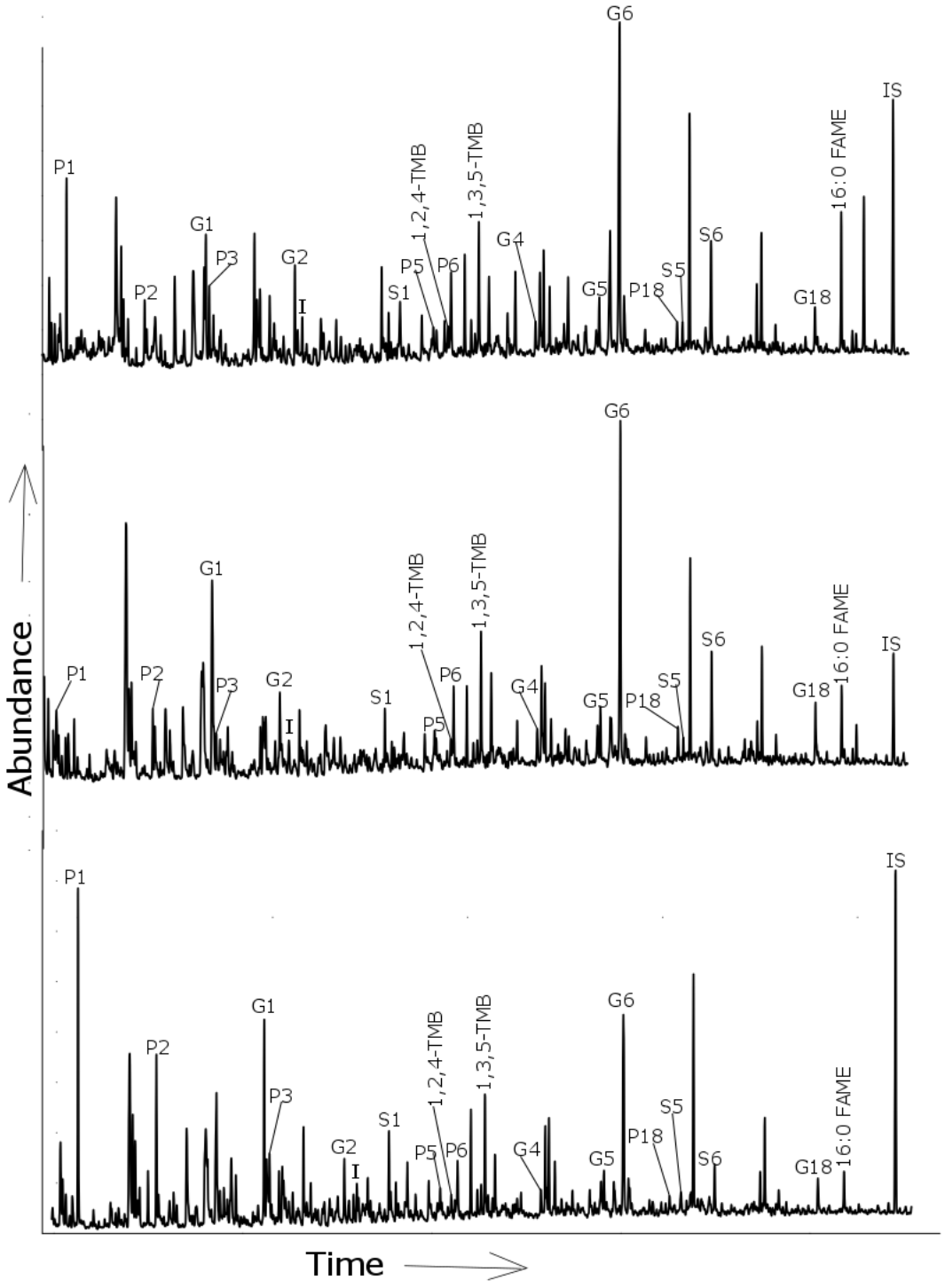

Figure 5.3: Partial total ion chromatogram (TIC) of the thermochemolysis products from bog water samples collected from Moor House peatland. Peak identities are listed in Table 5.1

On average, Λ concentrations reached 3.27 ± 0.88 mg/100 mg OC, which is significantly higher than the amounts observed in the *Sphagnum* mosses which only reached 0.12 ± 0.02 mg/100 mg OC (Mann Whitney, p<0.05)(Figure 5.4). It is also considerably higher than the 0.09 and 0.82 mg/100 mg OC of total phenols detected by Williams et al. (2016*a*) in the dissolved organic matter from grasslands, woodlands, and a river system. In contrast to Λ concentrations, σ was much higher in the mosses with I being the only biomarker identified in the water (Mann Whitney, p<0.05) (Figure 5.4 and Figure 5.3). The low levels of sphagnum acid biomarkers in the peat water are not unusual, as sphagnum acid is known to break down rapidly in the bog water of the acrotelm through peroxidative degradation (Verhoeven and Liefveld, 1997).

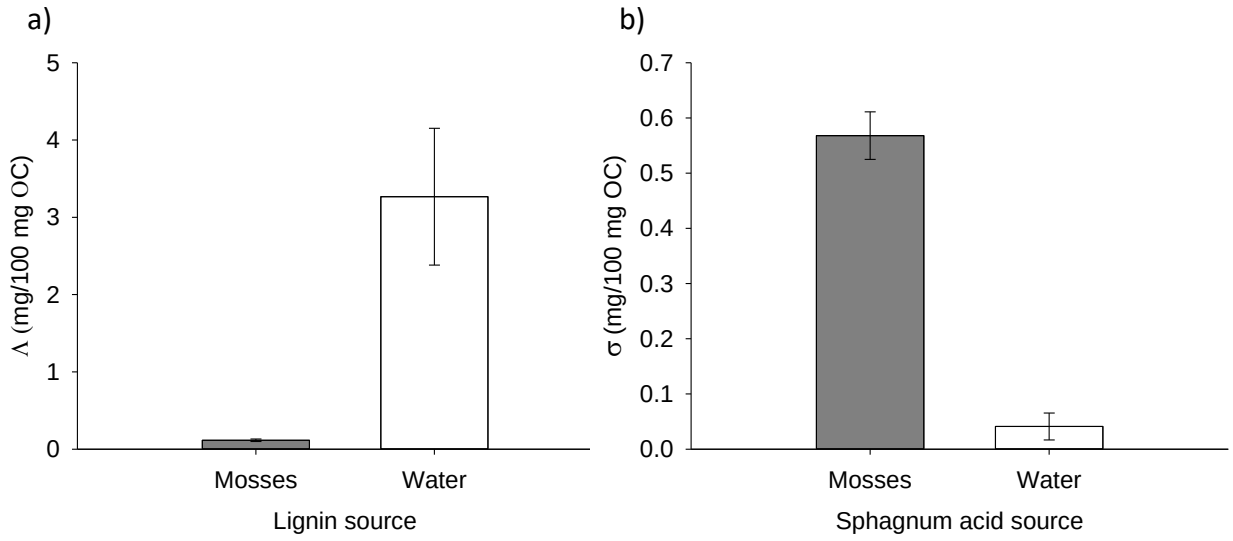

Figure 5.4: The concentrations of Λ (a) and σ (b) in *Sphagnum* mosses and the bog water sampled at Moor House

5.3.2 Chemical composition of the *Sphagnum* mosses

There was no significant effect of treatment or time on Λ, however, Figure 5.5 shows a significant difference was found for the interaction between treatment*time (p=0.01). The difference was only found for the bog water treatment between week 0 and week 4

with the other treatments showing no significant difference ($p>0.05$). As can be seen in Figure 5.5 there was an increase in Λ by week 4 in the bog water treatment, changing from the lowest concentrations at week 0 (mean values of 0.11, 0.07 and 0.16 $\pm$ 0.01, 0.01 and 0.03 for Milli-Q, bog and phenols treatment respectively) to the highest at week 4 (0.08, 0.15 and 0.12 $\pm$ 0.01, 0.05 and 0.01 for Milli-Q, bog and phenols treatment respectively). This result can, therefore, confirm the hypothesis that *Sphagnum* mosses can take up lignin-derived phenolics from the surrounding bog water that they are exposed to and surrounded by. The addition of lignin phenolics to the bog water had no significant effect on Λ ($p>0.05$). In addition, it appears that the addition of phenols beyond their natural concentrations prevented the mosses from taking up the phenols and they perhaps may have lost previously present phenols as well. This is an unexpected result and the reasons for which remain unclear. The observed drop in phenols for both the Milli-Q and Phenols treatment could be explained by the growth of the Sphagnum plants whilst the experiment was running. If new growth occurred that contained no lignin-derived phenols, it could lead to a drop in overall concentrations. Unfortunately plant growth was not measured in this study, however, this provides a possible explanation for the observed drop rather than the leaching of phenols from the plant into the water.

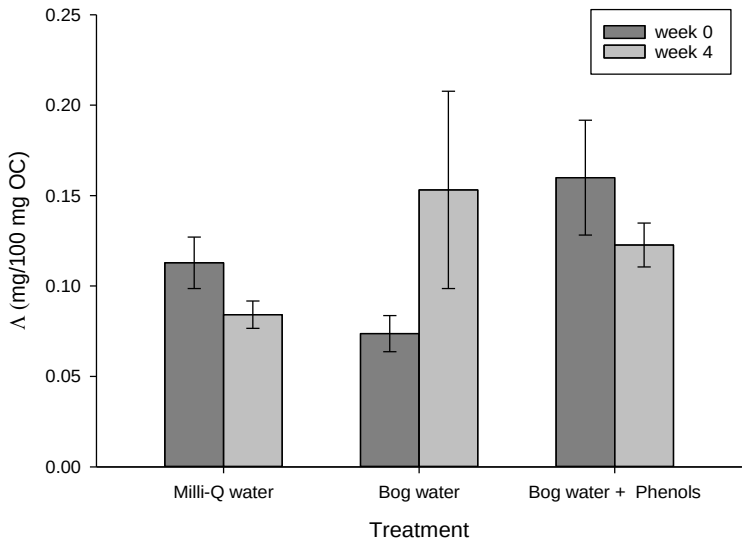

Figure 5.5: Changes in Λ concentrations in the *Sphagnum* mosses between the Milli-Q, bog water and additional phenols treatments as measured at week 0 and week 4

For the individually added or lignin-derived phenols , there was no difference for the interaction between treatment*time for the added phenols P5 and P18 or the naturally occurring S6, although all compounds showed borderline significance (p=0.06, p=0.07 and p=0.06 for P5, P18 and S6 respectively)(Figure 5.6). In contrast, the added phenols G4 and G5, as well as the naturally occurring G18, showed a significant difference for the bog water treatment ($p<0.05$ for all) with increased concentrations in week 4 relative to week 0. Therefore, these lignin-derived phenols are preferentially selected. One reason for this may be the species-specific endophytic bacterial communities present in *Sphagnum* mosses (Opelt et al., 2007). These endophytes could be responsible for the selective transport of lignin phenols and their incorporation into *Sphagnum* tissues. Differences in these bacterial communities between moss species and peatlands could also explain why slight chemical differences are observed between plant species collected from different peatlands. For example, Figure 5.7 shows the partial total ion chromatogram for a *Sphagnum capillifolium* sample taken from Moor House National

Nature reserve and a sample of the same moss species taken from Butterburn Flow. Slight chemical variation can be seen between the two samples, with the Moor House samples containing the *p*-hydroxyl phenol P6 and syringyl lignin derivative S6 which are absent from the sample collected from Butterburn Flow. It could be possible that the endophytic bacterial communities differ between these two samples, with the bacteria present at Moor House specifically selecting and transporting these phenols into the *Sphagnum* tissue. The mechanisms for this are unknown and to test such a hypothesis, the phenolic and biological composition of both the peat water and the *Sphagnum* itself needs further investigation.

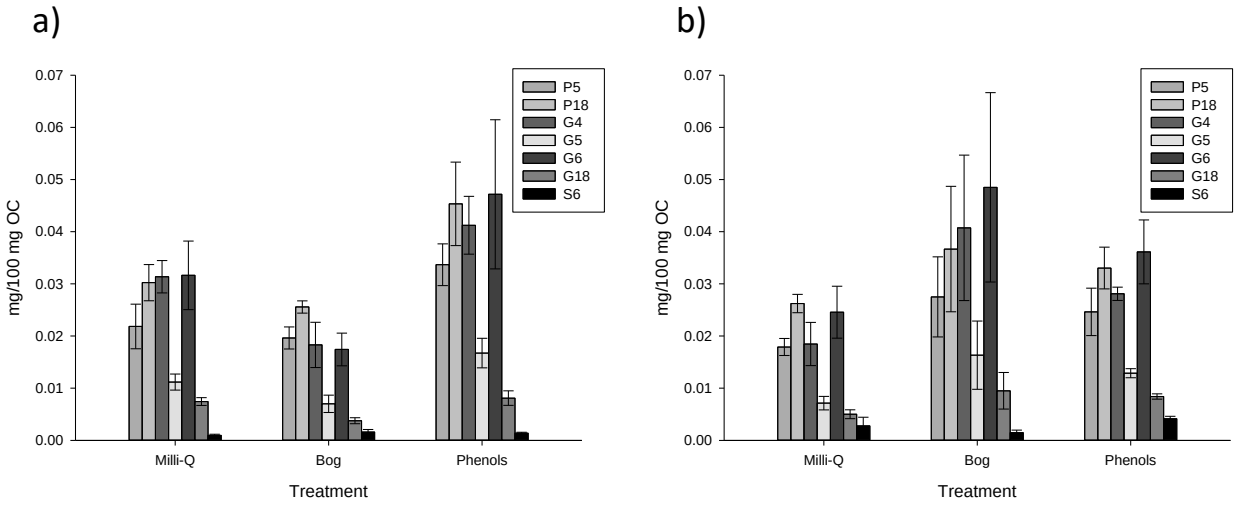

Figure 5.6: Changes in concentrations of the phenols that were specifically added to the phenols treatment (P5, P18, G4 and G5) as well as the phenols that contribute to the Λ proxy (G6, G18 and S6) for the Milli-Q, bog water and additional phenols treatments as measured at week 0 (a) and week 4 (b)

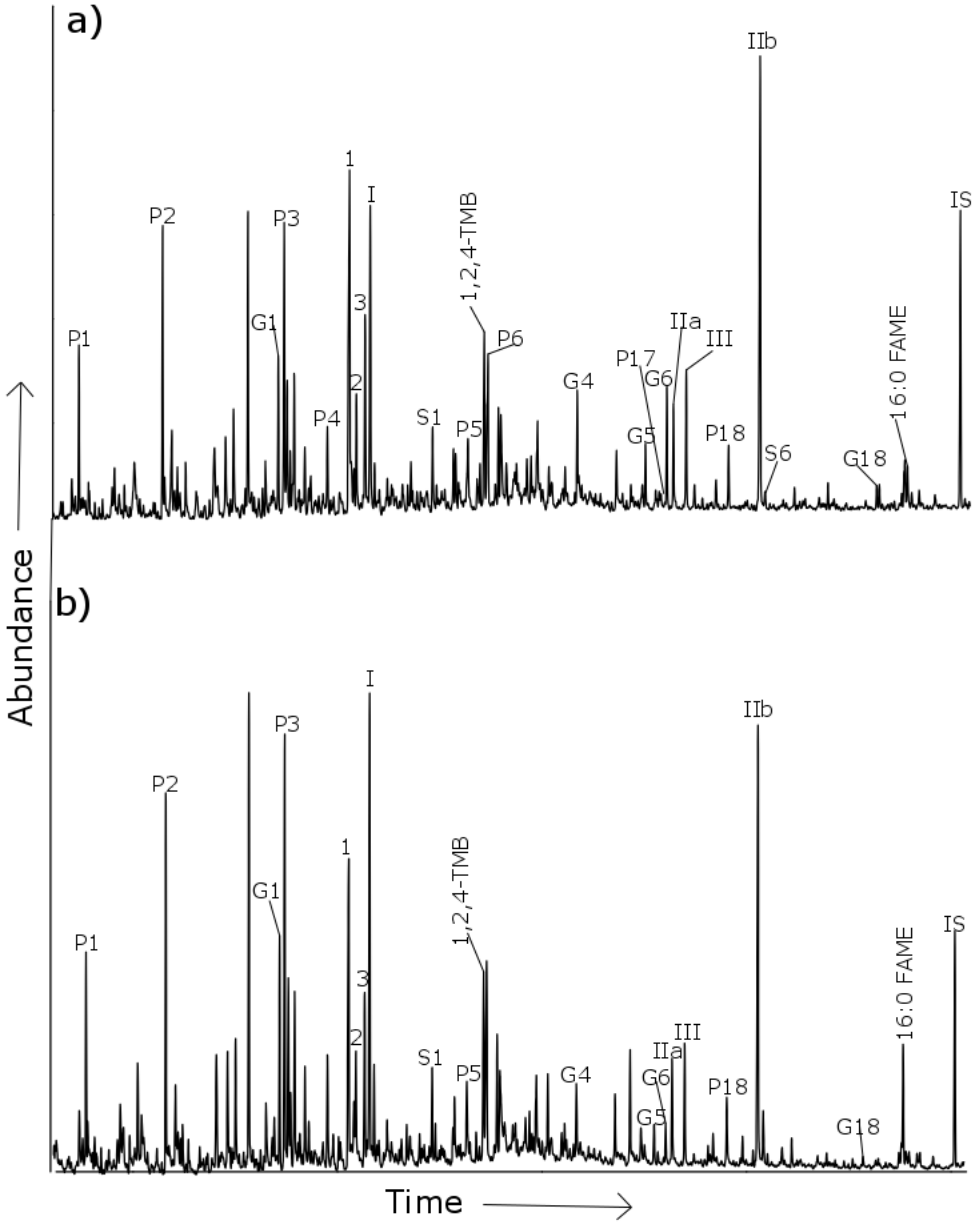

Figure 5.7: Partial total ion chromatogram (TIC) of the thermochemolysis products from *Sphagnum capillifolium* samples collected from Moor House (a) and Butterburn Flow (b). The Moor House sample used here is from the Milli-Q water treatment collected at week 0. IS denotes internal standard. Peak identities are listed in Table 5.1

.

The guaiacyl phenols G4, G5, G6 and G18 in the plants were significantly higher in the phenols treatment compared to the bog water treatment at week 0 Figure 5.8-5.9. By week 4 this difference is no longer observed. This demonstrates the variability of *Sphagnum* chemistry as, at week 0 the plants were collected at the very beginning of the experiment, and had minimal exposure to the treatment solutions. It would, therefore, be expected for all samples to contain the same amount of phenolic compounds. Such a result is very surprising given the individual plants were collected from not only the same peatland, but also the same lawn, and so individual plants were growing in close proximity. This observation lends further support to the possibility of a bacterial mechanism for lignin incorporation. It is suggested that due to changes in endophytic bacterial diversity, the chemistry of *Sphagnum* mosses can not only change based on their external environment, and between countries and peatlands, but also within peatlands, and within a single lawn (Figure 5.6-5.9).

To date, this study is the first to show the chemical alteration of *Sphagnum* mosses tissue via the uptake of externally available organic compounds. This may be important to consider when using chemical proxies in the analysis of peat. If phenolic content can be altered, perhaps lipid content can also be altered, which may significantly affect paleoclimate reconstructions. Further research is needed on the chemical composition of peatland waters, and the effects of this chemistry on the moss communities present.

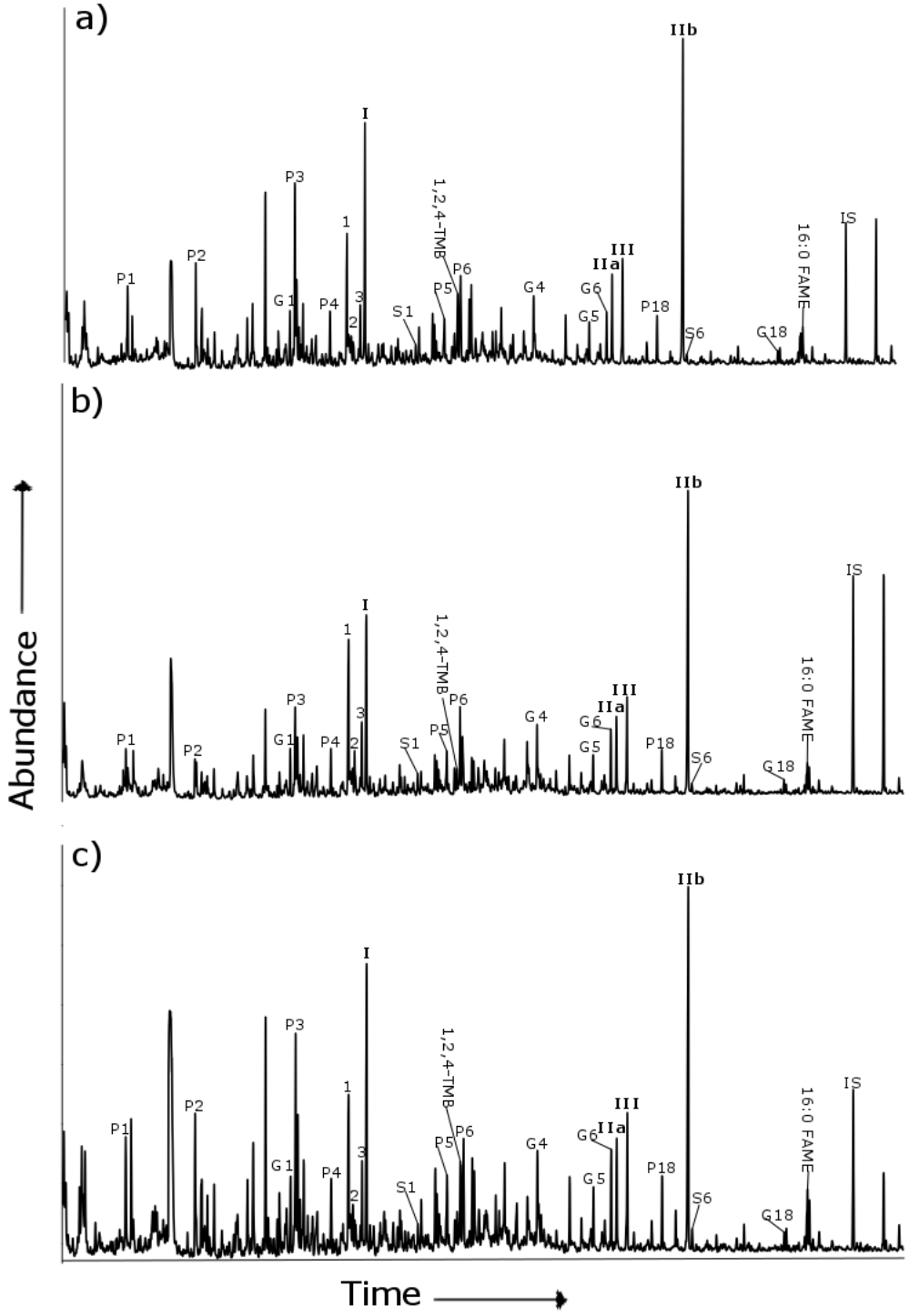

Figure 5.8: Partial total ion chromatogram (TIC) of the thermochemolysis products from *Sphagnum capillifolium* samples after 0 weeks in the Milli-Q water (a), bog water only (b), or bog water with additional phenols (c) treatment. IS denotes internal standard. Peak identities are listed in Table 5.1

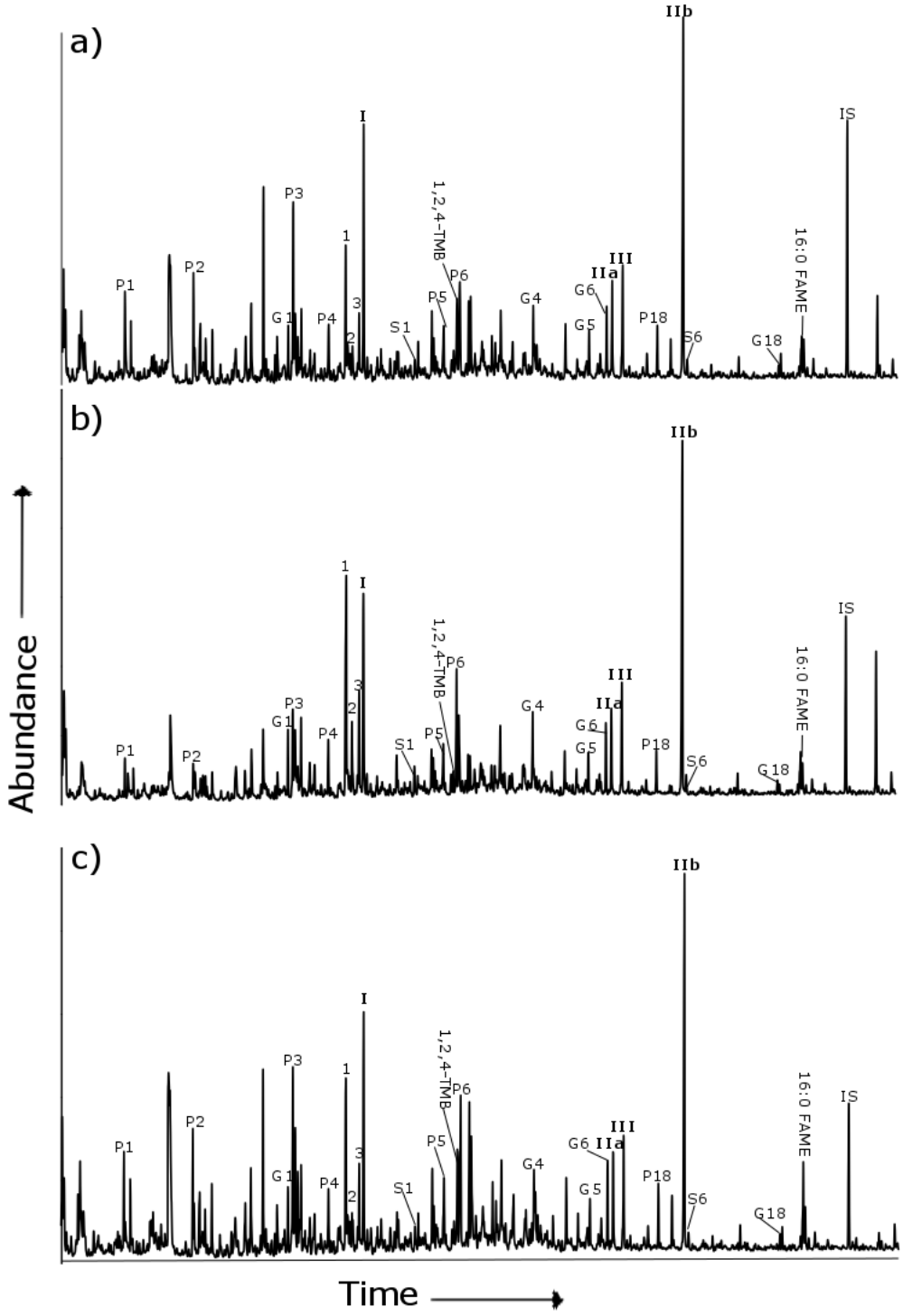

Figure 5.9: Partial total ion chromatogram (TIC) of the thermochemolysis products from *Sphagnum capillifolium* samples after 4 weeks in the Milli-Q water (a), Bog water only (b), or Bog water with additional phenols (c) treatment. IS denotes internal standard. Peak identities are listed in Table 5.1

Finally, changes in the sphagnum acid content (σ) was explored, however, no significant differences were observed ($p>0.05$). Nonetheless, it should be noted that the interaction between treatment*time showed borderline significance ($p=0.054$). Although changes were not statistically significant, Figure 5.10 shows there is a decrease in σ for the phenols treatment and an increase in the bog water treatment. Perhaps if a larger sample size was used, or if the experiment was left to run for a longer time, this interaction would indeed become significant. This could, therefore, suggest that the environment within which the *Sphagnum* mosses preside is not only important for the survival of the species, but also for the production of sphagnum acid by the mosses. Previous studies have shown that the sphagnum acid content of *Sphagnum* species can vary seasonally (Rudolph and Samland, 1985), and further work is needed to establish whether the chemistry of the water surrounding these plants may have an effect on the sphagnum acid content of these species. Climate change models predict both an increase in summer droughts and increased rainfall, depending on region, which can significantly change the phenolic content of peatland pore water, and may, therefore, affect sphagnum acid production in the long term (Fenner et al., 2005). Sphagnum acid has been shown to have a preservative effect on peatland litter and therefore contributes to the high carbon storage capacity of peatland ecosystems (Verhoeven and Toth, 1995; Bragazza et al., 2007). Any decrease in the production of sphagnum acid could, therefore, affect the carbon storage capacity by enhancing decay rates and resulting in the loss of carbon directly to the atmosphere in the form of carbon dioxide as well as via dissolved organic carbon into river and the ocean systems (Freeman et al., 2001a; Glatzel et al., 2003).

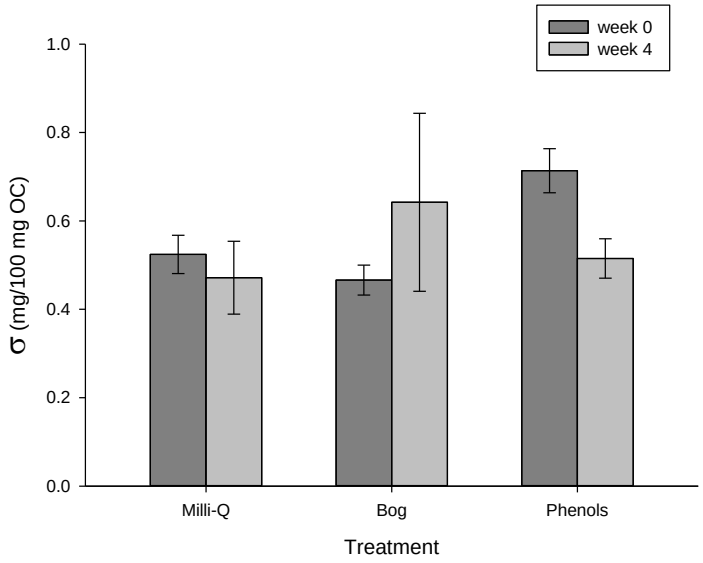

Figure 5.10: Changes in σ concentrations between the Milli-Q, bog water and additional phenols treatments as measured at week 0 and week 4

5.4 Conclusions

The results of this study show that the presence of lignin-derived phenols in *Sphagnum* tissues is likely a result of their exposure to the phenolic-rich bog water from which the phenols are extracted, and incorporated into *Sphagnum* tissue, possibly via bacterial mechanisms. The permanent saturation of *Sphagnum capillifolium* with water from the bog where samples were collected resulted in an increase in Λ concentrations mainly as a result of increased amounts of the guaiacyl phenols G4, G5 and G18. Neither phenol free water nor the enrichment of lignin phenols above those naturally found in bog water had a significant effect on either Λ or the amounts of individual lignin derivatives. Further work is needed to establish the mechanisms for lignin uptake by *Sphagnum* mosses and the effects of bog water chemistry on the sphagnum acid content of *Sphagnum* species long term. In addition, the chemical and biological composition

of both the peat water and the *Sphagnum* itself needs further investigation to establish how the interaction between mosses and the water surrounding them can affect chemical signatures.

This chapter presents the first evidence of organic compound uptake by *Sphagnum caplillifolium* in the short term. Further work is needed to establish whether these results can be applied to other *Sphagnum* species and whether such results remain consistent over the long term. Although this study does not rule out the possibility of the synthesis of such phenols by *Sphagnum* mosses as suggested by Ligrone et al. (2008) and Xu et al. (2009), it does provide evidence that the chemistry of these plants can be significantly altered by the chemical environment within which they preside. The uptake of other organic compounds by such species e.g lipids used in palaeoclimate reconstructions should also be explored and their effects upon important chemical proxies evaluated.

Chapter 6

General discussion and future work

6. General discussion and future work

6.1 Discussion and conclusions

This study was conducted to better understand the carbon dynamics and cycling of a northern peatland under future climate conditions. Both above and below ground carbon has been taken into consideration to understand carbon cycling and the future of peatland organic carbon stocks on a wider ecosystem level. Surface vegetation, as well as a 1 metre core of peat, were analysed using thermally assisted hydrolysis and methylation (THM) in the presence of both unlabelled and ^{13}C-labelled tetramethylammonium hydroxide (TMAH). This study has mainly focused on the peat itself from both a bulk (TOC, bulk density and OC) level as well as an in depth molecular level (sphagnum acid, lignin, carbohydrates and tannins). Four sites were sampled over a 500 metre transect on Butterburn Flow, a Northern peatland located on the border between Cumbria and Northumberland in the UK. Each site differed in terms of its hydrological and environmental conditions. The chemical signatures of the dominant plant species at each site along with the peat itself has enabled a greater understanding of the long-term stability and turnover of macromolecules such as lignin under different hydrological regimes. Changes in the carbon storage capacity of the peat at each site were also investigated to understand the effects of climate change on northern peatland organic carbon stocks.

The key molecular biomarkers utilised throughout this study include lignin and *Sphagnum* biomarkers which allowed the unambiguous identification of both vascular and non-vascular species and their diagenesis during burial across a range of environmental conditions. The continuous use of ^{13}C-labelled TMAH throughout the study allowed the differentiation between intact, degraded and non-lignin products such as gallic acid that can significantly contribute to lignin signals. This methodology has therefore ensured that the results presented are a true reflection of lignin diagenesis in a northern peatland has also allowed the percentage contribution of intact, degraded

and non-lignin products to the lignin signal downcore to be better understood.

6.1.1 Peatland vegetation

The aim of Chapter 3 was to explore the chemical composition of the dominant peat-forming plant species across various microhabitats at Butterburn Flow. All dominant plant species identified at each site were analysed along with the root systems of four plant species. Plant species diversity and composition at each site differed, with DB and FL being most similar. This is most likely a result of the similarities identified in the water table dynamics observed at these sites. *Sphagnum* species diversity was highest where the mean water table was highest, reinforcing the competitive advantage of these mosses in wetter climates. Dryer sites consisting mostly of non-*Sphagnum* mosses and grasses.

Different plant types contained different amounts of σ, Λ and carbohydrate thermochemolysis products. The sphagnum acid thermochemolysis products; (I) methylated 4-isopropenylphenol (IUPAC: 1-methoxy-4-(prop-1-en-2-yl)benzene), (IIa/b) methylated *cis*- and *trans*-3-(4-hydroxyphen-1-yl)but-2-enoic acid (IUPAC: (E/Z)-methyl 3-(4-methoxyphenyl)but-2-enoate), and (III) methylated 3-(4-hydroxyphen-1-yl)but-3-enoic acid (IUPAC: methyl 3-(4-methoxyphenyl)but-3-enoate), previously confirmed by (Abbott et al., 2013), have been identified in all *Sphagnum* moss species. These biomarkers were absent from all non-*Sphagnum* mosses and vascular plants. In all instances, I and IIb were present in significantly higher concentrations than IIa and III, and concentrations were similar to those reported in other studies.

Very small quantities of lignin thermochemolysis products were identified in *Sphagnum* and non-*Sphagnum* mosses, however, not enough to distort the lignin signal from vascular species, as these contained significantly larger quantities, with grasses having the highest quantities of all. These results authenticate the validity of Λ as a vascular plant proxy and σ and a *Sphagnum* moss proxy. Vascular plants showed large, but sim-

ilar, distributions of thermochemolysis products, however concentrations of *p*-hydroxy, guaiacyl and syringyl structures varied between species and plant type. Angiosperms contained a mixture of guaiacyl and syringyl phenols, and grasses showed a specific dominance of thermochemolysis products *p*-courmaric acid (*trans* 3-(4-methoxyphenyl)-3-propenoic acid methyl ester (P18)) and ferulic acid (*trans* 3-(3,4-dimethoxyphenyl)-3-propenoic acid methyl ester (G18)).

The phenolic content of root systems was also investigated. This study demonstrates that the input of both lignin and carbohydrate from root systems can be significant, with root based Λ concentrations exceeding levels found in above ground sections for *Calluna vulgaris* (Table 6.1). *Vaccinium oxycoccos* showed a dominance of the *p*-hydroxy phenols P3 and P18 as well as the guaiacyl monomer G18 when compared to the roots, whereas the roots contained increased concentrations of the guaiacyl monomers G2, G4 and G6. In fact, many of the monomers that contribute to the Λ signal (e.g P18, G6 and G18) have been observed as dominant products in all root samples. These results highlight the need for careful interpretation of lignin THM product concentrations in the peat, particularly when dense root systems are present. For example in the upper and surface layers of the peat, or in drier areas with a stronger vascular plant input, the Λ proxy could be significantly distorted in the surface peat where root systems make a significant contribution to the organic matter.

Table 6.1: The Λ concentrations (mg/100 mg OC) observed in above ground (shoot) and below ground (root) sections of *Calluna vulgaris*, *Erica tetralix*, *Vaccinium oxycoccos* and *Molinia caerulea*

Species	Shoot Λ (mg/100 mg OC)	Root Λ (mg/100 mg OC)
Calluna vulgaris	0.78 ± 0.20	1.27 ± 0.11
Erica tetralix	0.31 ± 0.02	0.55 ± 0.35
Vaccinium oxycoccos	1.10 ± 0.21	0.51 ± 0.01
Molinia caerulea	2.07 ± 0.64	0.89 ± 0.10

Overall, the distribution of plant types, and species, will differ depending on the water-table characteristics of the peat. Plant biodiversity has been shown to have a significant effect on the peat SOM and can change chemical biomarker presence, distribution and concentration.

6.1.2 Peat chemistry and carbon storage

Chapter 4 is a comprehensive exploration into the OC and phenolic content of the peat in relation to water table dynamic at Butterburn Flow. ^{13}C-labelled TMAH was employed throughout the study to ensure contamination of the lignin signal from non-lignin phenolic products was prevented. In this study, contamination from degraded lignin and non-lignin phenolic products was substantial and would have significantly affected the Λ proxy had they not been excluded. The guaiacyl monomers G4 and G5, and syringyl monomers S4 and S6 were most affected across all sites and from these, only S4 was impacted by non-lignin sources with the others mainly affected by oxidised and degraded lignin inputs.

Overall, BP and FL contained lower Λ, σ and carbohydrate concentrations. The organic carbon accumulation rates were higher in these cores as a direct result of increased bulk density, however, average TOC content at these sites was also higher. The reason for this unexpected result is something that needs further research. However, as suggested by Dignac et al. (2005), it could be possible that the compounds contributing to the TOC maybe lignin-derived monomers that have undergone transformation and are no longer identifiable using analytical methods focussed on intact lignin identification. This theory fits well given the low phenolic content observed in these cores and may be a process requiring oxygen, given that these sites also had the lowest water tables. The higher N levels, possibly reflecting increased microbial activity at DB and FL, also supports the theory of lignin transformation. An overall estimate of an average OC storage capacity of 5.1 t ha^{-1} is made for Butterburn Flow, which is similar to the estimate of 5.18 t ha^{-1} made by Ostle et al. (2009) for British bog habitats. OC storage

was linear in all cores with an accumulation rate of 0.76, 0.37, 0.28, and 0.66 t ha^{-1} per year for DB, BP, BM and FL respectively.

σ concentrations decreased down core, which differs from results obtained by Abbott et al. (2013) from the Swedish Bog, Rygmossen peatland. However, there are several key differences between the current study and the one conducted on Rygmossen that might explain this difference. Firstly, Rygmossen contained significantly higher abundances of each of the sphagnum acid thermochemolysis products, which is likely a reflection of the significantly larger % of *Sphagnum* cover observed in the present day vegetation. Moreover, a comparison of the present day vegetation at Ryggmossen with a survey conducted in 1925 revealed historically, very little vegetational change. Such a comparison cannot be made here, and so the changes in product composition may indeed be a result of changing vegetation cover rather than diagenetic changes. The fact that no *Sphagnum* species were observed in the vegetation survey (see chapter 3, section 3.3) at DB, and yet small amounts of sphagnum acid phenolics were detected in the peat further illustrates this point. Secondly, only 50 cm of peat were analysed in the study as opposed to the 100 cm analysed here, and so this may be one reason for the discrepancy. If only the top 50 cm of the peat at Butterburn is considered, product yields, particularly for I, appear to be more stable, as it is after 40 cm below the MWT where all products begin to decrease to the lowest levels. Without accurate dating to establish the time period that the 50 cm of peat at Rygmossen and the 100 cm of peat at Butterburn represent we cannot say the core depth is definitely a reason for the differences seen, but it is considered here as a possibility. The consistent decrease of these biomarkers down core also suggest that these biomarkers may not remain in the peat long-term, particularly IIa and III which were consistently lower in concentration than I and IIb for all cores.

In all cores where *Sphagnum* input was significant and all four sphagnum acid pyrolysis products could be identified, I increased at the expense of IIb in the permanently saturated layer of the peat. Therefore, the proportion of individual biomarkers (% I-III)

to the total *Sphagnum* yield (σ) could be used as an indicator for redox conditions as suggested by Swain and Abbott (2013).

In contrast to σ, Λ remained stable as a function of depth in all cores except DB where increased lignin oxidation was observed. A common observation of lignin-degradation is the preferential removal of S>G>C type units (Huang et al., 1998). However, in this study, increases in guaiacyl, as opposed to cinnamyl type units, were observed in all cores. This could potentially be due to the increased accessibility of the C-type monomer which are located on the periphery of the lignin polymer, resulting in increased degradation (Scalbert et al., 1985; Opsahl and Benner, 1995). In addition, the cinnamyl phenols are weakly bound to the lignin matrix by ester linkages (Opsahl and Benner, 1995) making them more susceptible to both degradation and leaching processes (Hernes et al., 2007).

Overall, this chapter demonstrated that an intensified hydrological cycle where mean water tables may be lower with a larger range between minimum and maximum levels, chemical degradation of ombrotrophic northern peat is likely to increase and phenolic content decrease. Due to lower water tables, there will be more oxygen available for increased degradation and lignin oxidation, which will lead to the loss of lignin from the peat in deeper layers.

6.1.3 *Sphagnum* mosses

The aim of Chapter 5 was to establish whether *Sphagnum* mosses are able to incorporate lignin into their tissues via external water sources. This was achieved by regularly exposing the *Sphagnum* only to either lignin-derived phenol-enriched water, natural bog water or Milli-Q water for 4 weeks. The consistent exposure of the plants to the natural bog water resulted in an increase in Λ concentrations, confirming *Sphagnum* mosses can take up lignin-derived phenolics though the bog water that they are exposed to. This is likely to be done via the large water-holding hyaline cells. The range of

products identified in the bog water was very similar to the range of products observed in *Sphagnum* mosses, lending further support to the absorption of these phenols from the bog water via the *Sphagnum*'s hyaline cells.

When the plants were analysed at week 0, differences in guaiacyl lignin concentration were also observed which demonstrates the variability of *Sphagnum* moss chemistry. These plants were collected from the same lawn, and therefore growing in close proximity to each other and exposed to the same environmental conditions, thus it is very surprising to see significant differences in compound concentrations. This variability is important to consider when comparing analytical products within the scientific community as changes in analytical products will vary even if studies are conducted in the same location and time.

The experiment was designed as a short-term trial study focussed on a single *Sphagnum* species and changes in Λ and σ thermochemolysis products. Other organic compounds such as lipids, and their effects upon important chemical proxies, now needs to be explored as these are commonly used in palaeoclimate reconstruction studies.

6.1.4 Recommendations for future work

The results presented in this thesis have highlighted some areas in which further work is required. The following section will outline specific recommendations for future research.

Root systems play an important role in the C cycle (Silvola et al., 1992, Silvola et al., 1996*a*; Joabsson et al., 1999; Kögel-Knabner, 2002; Zerva et al., 2005; Wiesenberg et al., 2010) and can therefore significantly influence the carbon balance within soils and peat. The chemical composition of above and below ground sections of peatland plants varies between plant type and species (Chapter 3). A larger scale study into the chemical composition of peatland roots systems, concentrating on all dominant

northern peatland plant species is required. This will allow a greater understanding of how roots may affect the chemical signatures and organic carbon content of peat layers. From this, work can then focus on trying to quantify the relative contribution of root-derived material to the peat with the aim of developing a more refined analysis of carbon cycling and the fate of plant-derived phenolics such as Λ and σ within the peat itself.

As demonstrated in this study, there is high spatial variability of peat organic matter within a peatland ecosystem (Chapter 4). Due to this, future research needs to turn away from single core analysis, and instead look towards multi-core analysis that allows the spatial variability within micro-habitats to be quantified as well as powerful statistical analysis such as multivariate analysis to be employed. Longer-term studies also require more focus in peatland studies to account for temporal differences that may be present. Peatlands are complex ecosystems that have developed over thousands of years and are very gradual in their reactions to environmental changes. Long-term studies with a carefully considered experimental design are therefore essential if long-term changes to the peatland carbon cycling are to be fully understood.

The maximum age of the peat in this study is assumed to be around 900-1000 BP, an assumption derived from the dates recorded in paleoclimate studies by Yeloff et al. (2007b) and McClymont et al. (2008) at Butterburn Flow. For example, McClymont et al. (2008) reports a mid-range date of 305 BP taken at 49.5 cm and a mid-range data of 235 BP at 43.5 cm depth. In addition, Yeloff et al. (2007b) obtained a ^{14}C date at 91.5 cm of approximately 830 BP. It was therefore assumed the maximum age of the core in this study is approximately 900-1000 years BP with a mid-range estimate of around 250-300 BP. If large numbers of closely spaced samples could be analysed using ^{14}C wiggle-match dating (WMD) it can give a reliable indicator of accumulation rates in peat deposits (Blaauw et al., 2004). Such a method, although expensive and time-consuming, applied to the cores analysed in this study would be highly beneficial to confirm that all cores represent the same time period, as DB contained 20 cm of clay

material which was unobserved in any other core, and likely to be older than 1000 BP. Such analysis would also help establish the stability of the *Sphagnum* biomarkers in the longer-term.

The composition of the dissolved organic matter and particulate organic matter in the water of the peat could be another interesting avenue of research to further understand carbon cycling in peatlands. The leaching and sorption of lignin and non-lignin phenols is a process that can significantly affect lignin signatures in soils and sediments (Hernes et al., 2007) particularly if minerals are present and may determine the length of time organic matter can be sequestered (Hernes et al., 2007). Understanding the fractionation and phase changes of lignin and non-lignin phenols that occur under different environmental conditions is essential to fully understand the fate of the compounds within peatland ecosystems and the resulting effect on the OC storage capacity of the peat. This research may also shed light on the unexpected higher TOC values obtained at DB and FL in Chapter 4, despite low concentrations of Λ, σ and carbohydrates.

Finally, an extension of the work carried out in Chapter 5 should also be considered. Chapter 5 was designed to be a short-term trial study, however, a long term experiment which included several *Sphagnum* species would be highly beneficial, giving further support to the uptake of lignin phenols in the *Sphagnum* tissues through direct contact with the phenol-rich bog water. The analysis of other compounds such as lipids should also be considered given abundance of studies that place a strong reliance on changing *n*-alkane distributions to indicate climatic change in paleoclimate reconstructions (Nott et al., 2000; Xie et al., 2000; Charman et al., 2004; Nichols et al., 2006).

References

Abbott, G. D., Swain, E. Y., Muhammad, A. B., Allton, K., Belyea, L. R., Laing, C. G. and Cowie, G. L. (2013), 'Effect of water-table fluctuations on the degradation of *Sphagnum* phenols in surficial peats', *Geochimica et Cosmochimica Acta* **106**, 177 – 191.

Adler, E. (1977), 'Lignin chemistry—past, present and future', *Wood Science and Technology* **11**(3), 169–218.

Agarwal, U. P. and Ralph, S. A. (1997), 'FT-Raman spectroscopy of wood: identifying contributions of lignin and carbohydrate polymers in the spectrum of black spruce *(Picea mariana)*', *Applied spectroscopy* **51**(11), 1648–1655.

Ahmad, M., Taylor, C. R., Pink, D., Burton, K., Eastwood, D., Bending, G. D. and Bugg, T. D. (2010), 'Development of novel assays for lignin degradation: comparative analysis of bacterial and fungal lignin degraders', *Molecular Biosystems* **6**(5), 815–821.

Alves, A., Schwanninger, M., Pereira, H. and Rodrigues, J. (2006), 'Analytical pyrolysis as a direct method to determine the lignin content in wood: Part 1: Comparison of pyrolysis lignin with klason lignin', *Journal of analytical and applied pyrolysis* **76**(1), 209–213.

Amelung, W. (2001), Methods using amino sugars as markers for microbial residues in soil, *in* 'Assessment methods for soil carbon', Vol. 100, Lewis Publishers Boca Raton, pp. 233–270.

Amelung, W., Cheshire, M. V. and Guggenberger, G. (1996), 'Determination of neutral and acidic sugars in soil by capillary gas-liquid chromatography after trifluoroacetic acid hydrolysis', *Soil Biology and Biochemistry* **28**(12), 1631 – 1639.

Amelung, W., Miltner, A., Zhang, X. and Zech, W. (2001), 'Fate of microbial residues during litter decomposition as affected by minerals', *Soil Science* **166**(9), 598–606.

Amelung, W., Zhang, X., Zech, W. and Flach, K. W. (1999), 'Amino sugars in native grassland soils along a climosequence in north america', *Soil Science Society of America Journal* **63**(1), 86–92.

Ander, P., Stoytschev, I. and Eriksson, K.-E. (1988), 'Cleavage and metabolism of methoxyl groups from vanillic and ferulic acids by brown-rot and soft-rot fungi', *Cellulose chemistry and technology* **22**(2), 255–266.

Anderson, D. E. (2002), 'Carbon accumulation and C/N ratios of peat bogs in northwest scotland', *Scottish Geographical Journal* **118**(4), 323–341.

Andersson, R. A., Kuhry, P., Meyers, P., Zebhr, Y., Crill, P. and Mrth, M. (2011), 'Impacts of paleohydrological changes on n-alkane biomarker compositions of a holocene peat sequence in the eastern European Russian Arctic', *Organic Geochemistry* **42**(9), 1065 – 1075.

Andrus, R. E. (1980), *Sphagnaceae (peat moss family) of New York State*, 442, University of the State of New York, State Education Department.

Angers, D., Nadeau, P. and Mehuys, G. (1988), 'Determination of carbohydrate composition of soil hydrolysates by high-performance liquid chromatography*', *Journal of Chromatography A* **454**, 444 – 449.

Anii, M., Tomaevi, M., Tasi, M., Raji, S., Popovi, A., Frontasyeva, M., Lierhagen, S. and Steinnes, E. (2009), 'Monitoring of trace element atmospheric deposition using dry and wet moss bags: Accumulation capacity versus exposure time', *Journal of Hazardous Materials* **171**(1), 182 – 188.

Antai, S. P. and Crawford, D. L. (1981), 'Degradation of softwood, hardwood, and grass lignocelluloses by two streptomyces strains', *Applied and environmental microbiology* **42**(2), 378–380.

Baas, W. J. (1989), 'Secondary plant compounds, their ecological significance and consequences for the carbon budget', *Causes and consequences of variation in growth rate and productivity of higher plants* pp. 313–340.

Bahri, H., Dignac, M.-F., Rumpel, C., Rasse, D. P., Chenu, C. and Mariotti, A. (2006), 'Lignin turnover kinetics in an agricultural soil is monomer specific', *Soil Biology and Biochemistry* **38**(7), 1977 – 1988.

Baird, A. J. (1997), 'Field estimation of macropore functioning and surface hydraulic conductivity in a fen peat', *Hydrological Processes* **11**(3), 287–295.

Baird, A. J., Comas, X., Slater, L. D., Belyea, L. R. and Reeve, A. (2009), 'Understanding carbon cycling in northern peatlands: recent developments and future prospects', *Carbon cycling in northern peatlands* pp. 1–3.

Bardy, M., Derenne, S., Allard, T., Benedetti, M. F. and Fritsch, E. (2011), 'Podzolisation and exportation of organic matter in black waters of the Rio Negro (upper Amazon basin, Brazil)', *Biogeochemistry* **106**(1), 71–88.

Bashir, F. (1999), Molecular characterization of sedimentary organic matter., PhD thesis, Newcastle University, Newcastle Upon Tyne, UK.

Bate-Smith, E. (1977), 'Astringent tannins of acer species', *Phytochemistry* **16**(9), 1421 – 1426.

Belyea, L. R. (2009), *Nonlinear Dynamics of Peatlands and Potential Feedbacks on the Climate System*, American Geophysical Union, pp. 5–18.

Belyea, L. R. (2013), *Nonlinear Dynamics of Peatlands and Potential Feedbacks on the Climate System*, American Geophysical Union, pp. 5–18.

Berendse, F., Van Breemen, N., Rydin, H., Buttler, A., Heijmans, M., Hoosbeek, M. R., Lee, J. A., Mitchell, E., Saarinen, T., Vasander, H. et al. (2001), 'Raised atmospheric CO_2 levels and increased N deposition cause shifts in plant species composition and production in *Sphagnum* bogs', *Global Change Biology* **7**(5), 591–598.

Blaauw, M., Van Geel, B., Mauquoy, D. and Van Der Plicht, J. (2004), 'Carbon-14 wiggle-match dating of peat deposits: advantages and limitations', *Journal of Quaternary Science* **19**(2), 177–181.

Black, J. E. (2016), Soil organic carbon and molecular characterisation of soils and vegetation inputs along a Savannah-rainforest boundary in Central Guyana, South America, PhD thesis, School of Civil Engineering and Geosciences.

Bland, D., Logan, A., Menshun, M. and Sternhell, S. (1968), 'The ligning of *Sphagnum*', *Phytochemistry* **7**(8), 1373 – 1377.

Boelter, D. H. (1969), 'Physical Properties of Peats as Related to Degree of Decomposition', *Soil Science Society of America Journal* **33**(4), 606.

Boerjan, W., Ralph, J. and Baucher, M. (2003), 'Lignin biosynthesis', *Annual review of plant biology* **54**(1), 519–546.

Bolan, N. S., Adriano, D. C., Kunhikrishnan, A., James, T., McDowell, R. and Senesi, N. (2011), 'Dissolved organic matter: biogeochemistry, dynamics, and environmental significance in soils', *Advances in agronomy* **110**, 1.

Bonn, A., Allott, T., Evans, M., Joosten, H. and Stoneman, R. (2016), *Peatland Restoration and Ecosystem Services: Science, Policy and Practice*, Cambridge University Press.

Bourdon, S., Laggoun-Dfarge, F., Disnar, J.-R., Maman, O., Guillet, B., Derenne, S. and Largeau, C. (2000), 'Organic matter sources and early diagenetic degradation in a tropical peaty marsh (Tritrivakely, Madagascar). implications for environmental reconstruction during the sub-atlantic', *Organic Geochemistry* **31**(5), 421 – 438.

Bragazza, L., Siffi, C., Iacumin, P. and Gerdol, R. (2007), 'Mass loss and nutrient release during litter decay in peatland: The role of microbial adaptability to litter chemistry', *Soil Biology and Biochemistry* **39**(1), 257 – 267.

Brett, C. T. and Waldron, K. W. (1996), *Physiology and biochemistry of plant cell walls*, Vol. 2, Springer Science & Business Media.

Broder, T., Blodau, C., Biester, H. and Knorr, K. H. (2012), 'Peat decomposition records in three pristine ombrotrophic bogs in southern Patagonia', *Biogeosciences* **9**(4), 1479–1491.

Brown, J. M. (1976), 'Peat temperature regime of a Minnesota bog and the effect of canopy removal', *Journal of Applied Ecology* **13**(1), 189–194.

Bubier, J. L., Bhatia, G., Moore, T. R., Roulet, N. T. and Lafleur, P. M. (2003), 'Spatial and temporal variability in growing-season net ecosystem carbon dioxide exchange at a large peatland in Ontario, Canada', *Ecosystems* **6**(4), 353–367.

Cajnder, A. (1913), 'Studien uber moore finnlands', *Acta forest. fenn* **3**(2), 3.

Cannell, M., Dewar, R. and Pyatt, D. (1993), 'Conifer plantations on drained peatlands in britain: a net gain or loss of carbon?', *Forestry* **66**(4), 353–369.

Cavers, F. (1911), 'The inter-relationships of the bryophyta', *New Phytologist* **10**(1-2), 1–21.

Cerli, C., Celi, L., Kaiser, K., Guggenberger, G., Johansson, M.-B., Cignetti, A. and Zanini, E. (2008), 'Changes in humic substances along an age sequence of norway spruce stands planted on former agricultural land', *Organic Geochemistry* **39**(9), 1269 – 1280.

Chabannes, M., Ruel, K., Yoshinaga, A., Chabbert, B., Jauneau, A., Joseleau, J.-P. and Boudet, A.-M. (2001), 'In situ analysis of lignins in transgenic tobacco reveals a differential impact of individual transformations on the spatial patterns of lignin deposition at the cellular and subcellular levels', *The Plant Journal* **28**(3), 271–282.

Challinor, J. (1989), 'A pyrolysis-derivatisation-gas chromatography technique for the structural elucidation of some synthetic polymers', *Journal of Analytical and Applied Pyrolysis* **16**(4), 323–333.

Challinor, J. (1991), 'The scope of pyrolysis methylation reactions', *Journal of Analytical and Applied Pyrolysis* **20**, 15–24.

Challinor, J. M. (2001), 'Review: the development and applications of thermally assisted hydrolysis and methylation reactions', *Journal of Analytical and Applied Pyrolysis* **61**(12), 3 – 34.

Chambers, F., Beilman, D. and Yu, Z. (2011), 'Determining peat humification and for quantifying peat bulk density, organic matter and carbon content for palaeostudies of climate and peatland carbon dynamics.', *Mires and Peat* **7**, 1 – 10.

Charman, D., Brown, A., Hendon, D. and Karofeld, E. (2004), 'Testing the relationship between holocene peatland palaeoclimate reconstructions and instrumental data at two european sites', *Quaternary Science Reviews* **23**(1), 137 – 143.

Charman, D. et al. (2002), *Peatlands and environmental change.*, John Wiley and Sons Ltd.

Chefetz, B., Chen, Y., Clapp, C. E. and Hatcher, P. G. (2000), 'Characterization of organic matter in soils by thermochemolysis using tetramethylammonium hydroxide (TMAH)', *Soil Science Society of America Journal* **64**(2), 583–589.

Chiavari, G., Montalbani, S., Prati, S., Keheyan, Y. and Baroni, S. (2007), 'Application of analytical pyrolysis for the characterisation of old inks', *Journal of Analytical and Applied Pyrolysis* **80**(2), 400–405.

Clark, J., Billett, M., Coyle, M., Croft, S., Daniels, S., Evans, C., Evans, M., Freeman, C., Gallego-Sala, A., Heinemeyer, A., House, J., Monteith, D., Nayak, D., Orr, H., Prentice, I., Rose, R., Rowson, J., Smith, J., Smith, P. and Tun, Y. (2010), 'Model inter-comparison between statistical and dynamic model assessments of the long-term stability of blanket peat in Great Britain (19402099)', *Climate research* **45**, 227–248.

Clark, J., Gallego-Sala, A., Allott, T., Chapman, S., Farewell, T., Freeman, C., House, J., Orr, H., Prentice, I. and Smith, P. (2010), 'Assessing the vulnerability of blanket peat to climate change using an ensemble of statistical bioclimatic envelope models', *Climate research* **45**, 131–150.

Clifford, D. J., Carson, D. M., McKinney, D. E., Bortiatynski, J. M. and Hatcher, P. G. (1995), 'A new rapid technique for the characterization of lignin in vascular plants: thermochemolysis with tetramethylammonium hydroxide (TMAH)', *Organic Geochemistry* **23**(2), 169 – 175.

Clymo, R. S. (1963), 'Ion exchange in *Sphagnum* and its relation to bog ecology', *Annals of Botany* **27**(2), 309–324.

Clymo, R. S. (1984), 'The limits to peat bog growth', *Philosophical Transactions of the Royal Society of London. Series B, Biological Sciences* **303**(1117), 605–654.

Clymo, R. S. and Hayward, P. M. (1982), The ecology of *Sphagnum*, *in* A. J. E. Smith, ed., 'Bryophyte Ecology', Springer Netherlands, Dordrecht, pp. 229–289.

Coq, S., Souquet, J.-M., Meudec, E., Cheynier, V. and Hättenschwiler, S. (2010), 'Interspecific variation in leaf litter tannins drives decomposition in a tropical rain forest of french guiana', *Ecology* **91**(7), 2080–2091.

Crawford, D. L., Pometto, A. L. and Crawford, R. L. (1983), 'Lignin degradation by *Streptomyces viridosporus*: isolation and characterization of a new polymeric lignin degradation intermediate', *Applied and Environmental Microbiology* **45**(3), 898–904.

Crawford, R. L. et al. (1981), *Lignin biodegradation and transformation.*, John Wiley and Sons.

Cruickshank, M., Tomlinson, R., Devine, P. and Milne, R. (1998), Carbon in the vegetation and soils of Northern Ireland, *in* 'Biology and Environment: Proceedings of the Royal Irish Academy', JSTOR, pp. 9–21.

Czapek, F. (1899), 'Zur chemie der zellmembranen bei den laub-und lebermoosen', *Flora* **86**, 361–381.

Czapek, F. (1913), Zellmembranen bei moosen und farnen, *in* 'Z. Biochem. d. Pflanzen', Vol. 1, G. Fischer Jena.

Dallinga, J., Nibbering, N. and Boerboom, A. a. (1984), 'Curie-ponit pyrolysis of saturated and unsaturated dicarboxylic acids studied by tandem mass spectrometry', *Journal of the Chemical Society, Perkin Transactions 2* pp. 1065–1076.

Dalzell, B. J., Filley, T. R. and Harbor, J. M. (2005), 'Flood pulse influences on terrestrial organic matter export from an agricultural watershed', *Journal of Geophysical Research: Biogeosciences* **110**(G2).

Damman, A. W. (1988), 'Regulation of nitrogen removal and retention in *Sphagnum* bogs and other peatlands', *Oikos* pp. 291–305.

de Leeuw, J. and Largeau, C. (1993), A review of macromolecular organic compounds that comprise living organisms and their role in kerogen, coal, and petroleum formation, *in* 'Organic Geochemistry', Vol. 11, Springer US, pp. 23–72.

del Rio, J., Martin, F. and Gonzalez-Vila, F. (1996), 'Thermally assisted hydrolysis and alkylation as a novel pyrolytic approach for the structural characterization of natural biopolymers and geomacromolecules', *TrAC Trends in Analytical Chemistry* **15**(2), 70–79.

del Rio, J., McKinney, D., Knicker, H., Nanny, M., Minard, R. and Hatcher, P. (1998), 'Structural characterization of bio- and geo-macromolecules by off-line thermochemolysis with tetramethylammonium hydroxide', *Journal of Chromatography A* **823**(12), 433 – 448.

Derrien, D., Marol, C., Balabane, M. and Balesdent, J. (2006), 'The turnover of carbohydrate carbon in a cultivated soil estimated by ^{13}C natural abundances', *European Journal of Soil Science* **57**(4), 547–557.

Dignac, M.-F., Bahri, H., Rumpel, C., Rasse, D., Bardoux, G., Balesdent, J., Girardin, C., Chenu, C. and Mariotti, A. (2005), 'Carbon-13 natural abundance as a tool

to study the dynamics of lignin monomers in soil: an appraisal at the Closeaux experimental field (France)', *Geoderma* **128**(1), 3 – 17.

Dijkstra, E., Boon, J., Van Mourik, J. et al. (1998), 'Analytical pyrolysis of a soil profile under scots pine', *European Journal of Soil Science* **49**(2), 295–304.

Dorrestijn, E., Laarhoven, L. J., Arends, I. W. and Mulder, P. (2000), 'The occurrence and reactivity of phenoxyl linkages in lignin and low rank coal', *Journal of Analytical and Applied Pyrolysis* **54**(1), 153 – 192.

Dungait, J. A. J., Hopkins, D. W., Gregory, A. S. and Whitmore, A. P. (2012), 'Soil organic matter turnover is governed by accessibility not recalcitrance', *Global Change Biology* **18**(6).

Durack, P. J., Wijffels, S. E. and Matear, R. J. (2012), 'Ocean salinities reveal strong global water cycle intensification during 1950 to 2000', *Science* **336**, 455–458.

Eckard, R. S., Hernes, P. J., Bergamaschi, B. A., Stepanauskas, R. and Kendall, C. (2007), 'Landscape scale controls on the vascular plant component of dissolved organic carbon across a freshwater delta', *Geochimica et Cosmochimica Acta* **71**(24), 5968 – 5984.

Eddy, A. (1977), 'Sphagnales of tropical asia', *Bull. Br. Mus. Nat. Hist.(Bot.)* **5**, 357–445.

Ertel, J. R. and Hedges, J. I. (1984), 'The lignin component of humic substances: distribution among soil and sedimentary humic, fulvic, and base-insoluble fractions', *Geochimica et Cosmochimica Acta* **48**(10), 2065–2074.

Espiñeira, J., Novo Uzal, E., Gómez Ros, L., Carrión, J., Merino, F., Ros Barceló, A. and Pomar, F. (2011), 'Distribution of lignin monomers and the evolution of lignification among lower plants', *Plant Biology* **13**(1), 59–68.

Estournel-Pelardy, C., Delarue, F., Laurent, Laggoun-Dfarge, F. and Ambls, A. (2011), 'Tetramethylammonium hydroxide thermochemolysis for the analysis of cellulose

and free carbohydrates in a peat bog', *Journal of Analytical and Applied Pyrolysis* **92**(2), 401 – 406.

Fabbri, D., Chiavari, G. and Galletti, G. (1996), 'Characterization of soil humin by pyrolysis(/methylation)-gas chromatography/mass spectrometry: structural relationships with humic acids', *Journal of Analytical and Applied Pyrolysis* **37**(2), 161 – 172.

Fabbri, D. and Helleur, R. (1999), 'Characterization of the tetramethylammonium hydroxide thermochemolysis products of carbohydrates', *Journal of Analytical and Applied Pyrolysis* **49**(12), 277 – 293.

Farmer, V. and Morrison, R. (1964), 'Lignin in *Sphagnum* and phragmites and in peats derived from these plants', *Geochimica et Cosmochimica Acta* **28**(10), 1537 – 1546.

Fenner, N., Freeman, C. and Reynolds, B. (2005), 'Hydrological effects on the diversity of phenolic degrading bacteria in a peatland: implications for carbon cycling', *Soil Biology and Biochemistry* **37**(7), 1277 – 1287.

Filley, T., Cody, G., Goodell, B., Jellison, J., Noser, C. and Ostrofsky, A. (2002), 'Lignin demethylation and polysaccharide decomposition in spruce sapwood degraded by brown rot fungi', *Organic Geochemistry* **33**(2), 111 – 124.

Filley, T., Hatcher, P., Shortle, W. and Praseuth, R. (2000), 'The application of ^{13}C-labeled tetramethylammonium hydroxide (^{13}C-TMAH) thermochemolysis to the study of fungal degradation of wood', *Organic Geochemistry* **31**(2), 181 – 198.

Filley, T., Minard, R. and Hatcher, P. (1999), 'Tetramethylammonium hydroxide (TMAH) thermochemolysis: proposed mechanisms based upon the application of ^{13}C-labeled TMAH to a synthetic model lignin dimer', *Organic Geochemistry* **30**(7), 607–621.

Filley, T. R., Nierop, K. G. J. and Wang, Y. (2006), 'The contribution of polyhydroxyl aromatic compounds to tetramethylammonium hydroxide lignin-based proxies', *Organic Geochemistry* **37**(6), 711–727.

Flatberg, K. I. (2002), 'The Norwegian Sphagna: a field colour guide'.

Franzén, L. (2006), 'Increased decomposition of subsurface peat in Swedish raised bogs: are temperate peatlands still net sinks of carbon', *Mires and Peat* **1**(03), 1–16.

Frazier, S. W., Kaplan, L. A. and Hatcher, P. G. (2005), 'Molecular characterization of biodegradable dissolved organic matter using bioreactors and [^{12}C/^{13}C] tetramethylammonium hydroxide thermochemolysis GC-MS', *Environmental science & technology* **39**(6), 1479–1491.

Frazier, S. W., Nowack, K. O., Goins, K. M., Cannon, F. S., Kaplan, L. A. and Hatcher, P. G. (2003), 'Characterization of organic matter from natural waters using tetramethylammonium hydroxide thermochemolysis GC-MS', *Journal of Analytical and Applied Pyrolysis* **70**(1), 99 – 128.

Freeman, C., Evans, C., Monteith, D., Reynolds, B. and Fenner, N. (2001a), 'Export of organic carbon from peat soils', *Nature* **412**(6849), 785.

Freeman, C., Ostle, N., Fenner, N. and Kang, H. (2004), 'A regulatory role for phenol oxidase during decomposition in peatlands', *Soil Biology and Biochemistry* **36**(10), 1663–1667.

Freeman, C., Ostle, N. and Kang, H. (2001), 'An enzymic'latch'on a global carbon store', *Nature* **409**(6817), 149–149.

Freudenberg, K., Neish, A. C. et al. (1968), 'Constitution and biosynthesis of lignin.', *Constitution and biosynthesis of lignin.* .

Gallet, C. and Lebreton, P. (1995), 'Evolution of phenolic patterns in plants and associated litters and humus of a mountain forest ecosystem', *Soil Biology and Biochemistry* **27**(2), 157 – 165.

Geib, S. M., Filley, T. R., Hatcher, P. G., Hoover, K., Carlson, J. E., del Mar Jimenez-Gasco, M., Nakagawa-Izumi, A., Sleighter, R. L. and Tien, M. (2008), 'Lignin degradation in wood-feeding insects', *Proceedings of the National Academy of Sciences* **105**(35), 12932–12937.

Gill, R. A. and Jackson, R. B. (2000), 'Global patterns of root turnover for terrestrial ecosystems', *New phytologist* **147**(1), 13–31.

Glaser, B., Turrin, M.-B. and Alef, K. (2004), 'Amino sugars and muramic acidbiomarkers for soil microbial community structure analysis', *Soil Biology and Biochemistry* **36**(3), 399 – 407.

Glatzel, S., Kalbitz, K., Dalva, M. and Moore, T. (2003), 'Dissolved organic matter properties and their relationship to carbon dioxide efflux from restored peat bogs', *Geoderma* **113**(3), 397–411.

Godden, B., Ball, A. S., Helvenstein, P., Mccarthy, A. J. and Penninckx, M. J. (1992), 'Towards elucidation of the lignin degradation pathway in actinomycetes', *Microbiology* **138**(11), 2441–2448.

Goi, M. A. and Hedges, J. I. (1990), 'Potential applications of cutin-derived cuo reaction products for discriminating vascular plant sources in natural environments', *Geochimica et Cosmochimica Acta* **54**(11), 3073 – 3081.

Gold, M. H., Wariishi, H. and Valli, K. (1989), *Extracellular Peroxidases Involved in Lignin Degradation by the White Rot Basidiomycete Phanerochaete chrysosporium*, American Chemical Society, chapter 9, pp. 127–140.

Goñi, M. A. and Hedges, J. I. (1992), 'Lignin dimers: structures, distribution, and potential geochemical applications', *Geochimica et Cosmochimica Acta* **56**(11), 4025–4043.

Gorham, E. (1991), 'Northern peatlands: Role in the carbon cycle and probable responses to climatic warming', *Ecological Applications* **1**(2), 182–195.

Grasset, L., Rovira, P. and Ambls, A. (2009), 'TMAH-preparative thermochemolysis for the characterization of organic matter in densimetric fractions of a mediterranean forest soil', *Journal of Analytical and Applied Pyrolysis* **85**(12), 435 – 441.

Grigal, D. F. (1989), 'Forest Floor and Mineral Samples', *Canadian Joiurnal of Soil Science* **90**, 895–900.

Hackett, W., Connors, W., Kirk, T. and Zeikus, J. (1977), 'Microbial decomposition of synthetic 14C-labeled lignins in nature: lignin biodegradation in a variety of natural materials', *Applied and environmental microbiology* **33**(1), 43–51.

Haider, K. and Trojanowski, J. (1980), Comparison of the degradation of ^{14}C-labeled DHP and corn stalk lignins by micro-and macrofungi and bacteria, *in* 'Lignin biodegradation: microbiology, chemistry, and potential applications', CRC Press, Inc.

Hájek, T., Ballance, S., Limpens, J., Zijlstra, M. and Verhoeven, J. T. A. (2011), 'Cell-wall polysaccharides play an important role in decay resistance of *Sphagnum* and actively depressed decomposition in vitro', *Biogeochemistry* **103**(1), 45–57.

Harborne, J. B. (1997), 'Recent advances in chemical ecology', *Natural product reports* **14**, 83–98.

Hargreaves, K. and Fowler, D. (1998), 'Quantifying the effects of water table and soil temperature on the emission of methane from peat wetland at the field scale', *Atmospheric Environment* **32**(19), 3275 – 3282.

Haslam, E. (1988), 'Plant polyphenols (syn. vegetable tannins) and chemical defense—a reappraisal', *Journal of Chemical Ecology* **14**(10), 1789–1805.

Hatakka, A. (1994), 'Lignin-modifying enzymes from selected white-rot fungi: production and role from in lignin degradation', *FEMS Microbiology Reviews* **13**(2-3).

Hatcher, P. G. and Minard, R. D. (1995), 'Comment on the origin of benzenecarboxylic acids in pyrolysis methylation studies', *Organic Geochemistry* **23**(10), 991 – 994.

Hatcher, P. G., Nanny, M. A., Minard, R. D., Dible, S. D. and Carson, D. M. (1995), 'Comparison of two thermochemolytic methods for the analysis of lignin in decomposing gymnosperm wood: the cuo oxidation method and the method of thermochemolysis with tetramethylammonium hydroxide (TMAH)', *Organic Geochemistry* **23**(10), 881–888.

Hättenschwiler, S. and Vitousek, P. M. (2000), 'The role of polyphenols in terrestrial ecosystem nutrient cycling', *Trends in Ecology and Evolution* **15**(6), 238 – 243.

Heckman, D. S., Geiser, D. M., Eidell, B. R., Stauffer, R. L., Kardos, N. L. and Hedges, S. B. (2001), 'Molecular evidence for the early colonization of land by fungi and plants', *Science* **293**(5532), 1129–1133.

Hedges, J. I. and Ertel, J. R. (1982), 'Characterization of lignin by gas capillary chromatography of cupric oxide oxidation products', *Analytical Chemistry* **54**(2), 174–178.

Hedges, J. I. and Mann, D. C. (1979), 'The characterization of plant tissues by their lignin oxidation products', *Geochimica et Cosmochimica Acta* **43**(11), 1803 – 1807.

Hedges, J. I. and Parker, P. L. (1976), 'Land-derived organic matter in surface sediments from the Gulf of Mexico', *Geochimica et Cosmochimica Acta* **40**(9), 1019 – 1029.

Heim, A. and Schmidt, M. W. I. (2007), 'Lignin turnover in arable soil and grassland analysed with two different labelling approaches', *European Journal of Soil Science* **58**(3), 599–608.

Hendon, D. and Charman, D. (2004), 'High-resolution peatland water-table changes for the past 200 years: the influence of climate and implications for management', *The Holocene* **14**(1), 125–134.

Hendon, D., Charman, D. and Kent, M. (2001), 'Palaeohydrological records derived from testate amoebae analysis from peatlands in northern england: within-site variability, between-site comparability and palaeoclimatic implications', *The Holocene* **11**(2), 127–148.

Hernes, P. J. and Benner, R. (2003), 'Photochemical and microbial degradation of dissolved lignin phenols: Implications for the fate of terrigenous dissolved organic matter in marine environments', *Journal of Geophysical Research: Oceans* **108**(C9).

Hernes, P. J. and Hedges, J. I. (2004), 'Tannin signatures of barks, needles, leaves, cones, and wood at the molecular level', *Geochimica et Cosmochimica Acta* **68**(6), 1293 – 1307.

Hernes, P. J., Robinson, A. C. and Aufdenkampe, A. K. (2007), 'Fractionation of lignin during leaching and sorption and implications for organic matter freshness', *Geophysical Research Letters* **34**(17), L17401.

Hogg, E. H. (1993), 'Decay potential of hummock and hollow *Sphagnum* peats at different depths in a Swedish raised bog', *Oikos* pp. 269–278.

Holcombe, J. W. (1984), 'Morphogenesis of branch leaves of *Sphagnum magellanicum* brid', *Journal of the Hattori Botanical Laboratory* **57**, p179–240.

Holden, J. (2005), 'Controls of soil pipe frequency in upland blanket peat', *Journal of Geophysical Research: Earth Surface* **110**(F1), 1–11.

Holden, J. and Burt, T. P. (2003), 'Hydraulic conductivity in upland blanket peat: measurement and variability', *Hydrological Processes* **17**(6).

Holden, J. and Rose, R. (2011), 'Temperature and surface lapse rate change: a study of the UK's longest upland instrumental record', *International Journal of Climatology* **31**(6), 907–919.

Hon, D. N.-S. (1995), *Chemical modification of lignocellulosic materials*, CRC Press.

Hornibrook, E. R., Longstaffe, F. J., Fyfe, W. S. and Bloom, Y. (2000), 'Carbon-isotope ratios and carbon, nitrogen and sulfur abundances in flora and soil organic matter from a temperate-zone bog and marsh', *Geochemical Journal* **34**(3), 237–245.

Hu, S., Coleman, D., Beare, M. and Hendrix, P. (1995), 'Soil carbohydrates in aggrading and degrading agroecosystems: influences of fungi and aggregates', *Agriculture, Ecosystems & Environment* **54**(1), 77 – 88.

Huang, X., Wang, C., Zhang, J., Wiesenberg, G. L., Zhang, Z. and Xie, S. (2011), 'Comparison of free lipid compositions between roots and leaves of plants in the Dajiuhu Peatland, central China', *Geochemical Journal* **45**(5), 365–373.

Huang, Y., Eglinton, G., Van Der Hage, E. R. E., Boon, J. J., Bol, R. and Ineson, P. (1998), 'Dissolved organic matter and its parent organic matter in grass upland soil

horizons studied by analytical pyrolysis techniques', *European Journal of Soil Science* **49**(1), 1–15.

International Peat Society, I. (2001), 'Peat as an energy resource'. [Accsessed: 29/06/17].
URL: *http://www.peatsociety.org/peatlands-and-peat/peat-energy-resource*

IPCC (2014), Climate change 2014: Synthesis report. contribution of working groups I, II and III to the fifth assessment report of the intergovernmental panel on climate change, Technical report, [Core Writing Team, R.K. Pachauri and L.A. Meyer (eds.)] IPCC, Geneva, Switzerland, 151 pp.

Ise, T., Dunn, A. L., Wofsy, S. C. and Moorcroft, P. R. (2008), 'High sensitivity of peat decomposition to climate change through water-table feedback', *Nature Geoscience* **1**(11), 763–766.

Jackson, R. B., Canadell, J., Ehleringer, J. R., Mooney, H. A., Sala, O. E. and Schulze, E. D. (1996), 'A global analysis of root distributions for terrestrial biomes', *Oecologia* **108**(3), 389–411.

Janssens, I., Freibauer, A., Schlamadinger, B., Ceulemans, R., Ciais, P., Dolman, A., Heimann, M., Nabuurs, G., Smith, P., Valentini, R. and Schulze, E. (2006), 'The carbon budget of terrestrial ecosystems at country-scale–a european case study', *Biogeosciences* **2**, 15–26.

Jia, G., Dungait, J. A., Bingham, E. M., Valiranta, M., Korhola, A. and Evershed, R. P. (2008), 'Neutral monosaccharides as biomarker proxies for bog-forming plants for application to palaeovegetation reconstruction in ombrotrophic peat deposits', *Organic Geochemistry* **39**(12), 1790 – 1799.

JNCCC (2011), 'Towards an assessment of the state of uk peatlands', *Joint Nature Conservation Committee report* **445**(445).

Joabsson, A., Christensen, T. R. and Walln, B. (1999), 'Vascular plant controls on

methane emissions from northern peatforming wetlands', *Trends in Ecology and Evolution* **14**(10), 385 – 388.

Johnson, G. A. L. (1963), *The geology of Moor House: a national nature reserve in north-east Westmorland*, 2, HM Stationery Office.

Johnson, L. C. and Damman, A. W. (1991), 'Species-controlled *Sphagnum* decay on a south swedish raised bog', *Oikos* pp. 234–242.

Kaal, E. and Janssen, H.-G. (2008), 'Extending the molecular application range of gas chromatography', *Journal of Chromatography A* **1184**(1), 43 – 60.

Kandeler, E., Tscherko, D., Bruce, K. D., Stemmer, M., Hobbs, P. J., Bardgett, R. D. and Amelung, W. (2000), 'Structure and function of the soil microbial community in microhabitats of a heavy metal polluted soil', *Biology and Fertility of Soils* **32**(5), 390–400.

Kechavarzi, C., Dawson, Q. and Leeds-Harrison, P. (2010), 'Physical properties of low-lying agricultural peat soils in England', *Geoderma* **154**(34), 196 – 202.

Kettunen, A., Kaitala, V., Lehtinen, A., Lohila, A., Alm, J., Silvola, J. and Martikainen, P. J. (1999), 'Methane production and oxidation potentials in relation to water table fluctuations in two boreal mires', *Soil Biology and Biochemistry* **31**(12), 1741 – 1749.

Kiem, R. and Kögel-Knabner, I. (2003), 'Contribution of lignin and polysaccharides to the refractory carbon pool in C-depleted arable soils', *Soil Biology and Biochemistry* **35**(1), 101 – 118.

Kirk, T. K. and Farrell, R. L. (1987), 'Enzymatic" combustion": the microbial degradation of lignin', *Annual Reviews in Microbiology* **41**(1), 465–501.

Kirk, T. K., Higuchi, T. and Chang, H. (1980), *Lignin biodegradation: microbiology, chemistry, and potential applications*, CRC Press, Inc.

Kishimoto, T., Chiba, W., Saito, K., Fukushima, K., Uraki, Y. and Ubukata, M. (2010), 'Influence of syringyl to guaiacyl ratio on the structure of natural and synthetic lignins', *Journal of Agricultural and Food Chemistry* **58**(2), 895–901.

Klingberg, A., Odermatt, J. and Meier, D. (2005), 'Influence of parameters on pyrolysis-GC/MS of lignin in the presence of tetramethylammonium hydroxide', *Journal of Analytical and Applied Pyrolysis* **74**(1), 104 – 109.

Knill, C. J. and Kennedy, J. F. (2003), 'Degradation of cellulose under alkaline conditions', *Carbohydrate Polymers* **51**(3), 281 – 300.

Kögel, I. (1986), 'Estimation and decomposition pattern of the lignin component in forest humus layers', *Soil Biology and Biochemistry* **18**(6), 589–594.

Kögel-Knabner, I. (2002), 'The macromolecular organic composition of plant and microbial residues as inputs to soil organic matter', *Soil Biology and Biochemistry* **34**(2), 139 – 162.

Kraus, T. E. C., Dahlgren, R. A. and Zasoski, R. J. (2003), 'Tannins in nutrient dynamics of forest ecosystems - a review', *Plant and Soil* **256**(1), 41–66.

Kraus, T. E., Zasoski, R. J., Dahlgren, R. A., Horwath, W. R. and Preston, C. M. (2004), 'Carbon and nitrogen dynamics in a forest soil amended with purified tannins from different plant species', *Soil Biology and Biochemistry* **36**(2), 309–321.

Kuroda, K.-I. and Nakagawa-izumi, A. (2006), 'Tetramethylammonium hydroxide (TMAH) thermochemolysis of lignin: Improvement of the distribution profile of products derived from -aryl ether subunits', *Journal of Analytical and Applied Pyrolysis* **75**(2), 104 – 111.

Lafleur, P., Moore, T., Roulet, N. and Frolking, S. (2005), 'Ecosystem respiration in a cool temperate bog depends on peat temperature but not water table', *Ecosystems* **8**(6), 619–629.

Lehtonen, T., Peuravuori, J. and Pihlaja, K. (2003), 'Comparison of quaternary methyl-, ethyl-and butylammonium hydroxides as alkylating reagents in pyrolysis-GC/MS studies of aquatic fulvic acid', *Journal of analytical and applied pyrolysis* **68**, 315–329.

Lewis, C., Albertson, J., Xu, X. and Kiely, G. (2012), 'Spatial variability of hydraulic conductivity and bulk density along a blanket peatland hillslope', *Hydrological Processes* **26**(10), 1527–1537.

Ligrone, R., Carafa, A., Duckett, J. G., Renzaglia, K. S. and Ruel, K. (2008), 'Immunocytochemical detection of lignin-related epitopes in cell walls in bryophytes and the charalean alga *Nitella*', *Plant Systematics and Evolution* **270**(3), 257–272.

Lindsay, R., Campus, S. and Lane, W. (2010), 'Peatbogs and carbon: a critical synthesis to inform policy development in oceanic peat bog conservation and restoration in the context of climate change', *RSPB Scotland* **315**.

Loranger, G., Ponge, J.-F., Imbert, D. and Lavelle, P. (2002), 'Leaf decomposition in two semi-evergreen tropical forests: influence of litter quality', *Biology and Fertility of Soils* **35**(4), 247–252.

Lorenz, K., Preston, C. M., Raspe, S., Morrison, I. K. and Feger, K. H. (2000), 'Litter decomposition and humus characteristics in canadian and german spruce ecosystems: information from tannin analysis and ^{13}C CPMAS NMR', *Soil Biology and Biochemistry* **32**(6), 779–792.

Lunn, A. and Burlton, B. (2010), The border mires: A conservation history, Technical report, UK,.
URL: *http://www.iucn-uk-peatlandprogramme.org/files/borderMireshistory0.pdf*

Malmer, N. and Holm, E. (1984), 'Variation in the C/N-quotient of peat in relation to decomposition rate and age determination with 210 Pb', *Oikos* pp. 171–182.

Mason, S. (2009), Polyphenolic degradation and turnover in model and natural systems., PhD thesis, Newcastle University, Newcastle Upon Tyne, UK.

Mason, S. L., Filley, T. R. and Abbott, G. D. (2009), 'The effect of afforestation on the soil organic carbon (SOC) of a peaty gley soil using on-line thermally assisted hydrolysis and methylation (THM) in the presence of ^{13}C-labelled tetramethylammonium hydroxide (TMAH)', *Journal of Analytical and Applied Pyrolysis* **85**(12), 417 – 425.

Mason, S. L., Filley, T. R. and Abbott, G. D. (2012), 'A comparative study of the molecular composition of a grassland soil with adjacent unforested and afforested moorland ecosystems', *Organic Geochemistry* **42**(12), 1519 – 1528.

Mauquoy, D., van Geel, B., Blaauw, M. and van der Plicht, J. (2002), 'Evidence from northwest european bogs shows little ice age climatic changes driven by variations in solar activity', *The Holocene* **12**(1), 1–6.

McClymont, E. L., Bingham, E. M., Nott, C. J., Chambers, F. M., Pancost, R. D. and Evershed, R. P. (2011), 'Pyrolysis GCMS as a rapid screening tool for determination of peat-forming plant composition in cores from ombrotrophic peat', *Organic Geochemistry* **42**(11), 1420 – 1435.

McClymont, E. L., Mauquoy, D., Yeloff, D., Broekens, P., van Geel, B., Charman, D. J., Pancost, R. D., Chambers, F. M. and Evershed, R. P. (2008), 'The disappearance of *Sphagnum imbricatum* from Butterburn Flow, UK', *The Holocene* **18**(6), 991–1002.

McKinney, D., Bortiatynski, J., Carson, D., Clifford, D., de Leeuw, J. and Hatcher, P. (1996), 'Tetramethylammonium hydroxide (TMAH) thermochemolysis of the aliphatic biopolymer cutan: insights into the chemical structure', *Organic Geochemistry* **24**(6), 641 – 650.

McKinney, D. and Hatcher, P. (1996), 'Characterization of peatified and coalified wood by tetramethylammonium hydroxide (TMAH) thermochemolysis', *International Journal of Coal Geology* **32**(1), 217 – 228.

Milne, R. and Brown, T. (1997), 'Carbon in the vegetation and soils of Great Britain', *Journal of Environmental Management* **49**(4), 413–433.

Moore, P. D. (1989), 'The ecology of peat-forming processes: a review', *International Journal of Coal Geology* **12**(1), 89 – 103.

Moore, T. R. and Turunen, J. (2004), 'Carbon accumulation and storage in mineral subsoil beneath peat', *Soil Science Society of America Journal* **68**(2), 690–696.

Murata, T., Tanaka, H., Yasue, S., Hamada, R., Sakagami, K. and Kurokawa, Y. (1999), 'Seasonal variations in soil microbial biomass content and soil neutral sugar composition in grassland in the japanese temperate zone', *Applied Soil Ecology* **11**(2), 253 – 259.

Nichols, J., Booth, R. K., Jackson, S. T., Pendall, E. G. and Huang, Y. (2010), 'Differential hydrogen isotopic ratios of *Sphagnum* and vascular plant biomarkers in ombrotrophic peatlands as a quantitative proxy for precipitationevaporation balance', *Geochimica et Cosmochimica Acta* **74**(4), 1407 – 1416.

Nichols, J. E., Booth, R. K., Jackson, S. T., Pendall, E. G. and Huang, Y. (2006), 'Paleohydrologic reconstruction based on n-alkane distributions in ombrotrophic peat', *Organic Geochemistry* **37**(11), 1505 – 1513.

Nierop, K. G. (2001), 'Temporal and vertical organic matter differentiation along a vegetation succession as revealed by pyrolysis and thermally assisted hydrolysis and methylation', *Journal of Analytical and Applied Pyrolysis* **61**(1), 111 – 132.

Nierop, K. G. and Filley, T. R. (2007), 'Assessment of lignin and (poly-) phenol transformations in oak (*Quercus robur*) dominated soils by ^{13}C-TMAH thermochemolysis', *Organic Geochemistry* **38**(4), 551–565.

Nierop, K. G. and Filley, T. R. (2008), 'Simultaneous analysis of tannin and lignin signatures in soils by thermally assisted hydrolysis and methylation using ^{13}C-labeled {TMAH}', *Journal of Analytical and Applied Pyrolysis* **83**(2), 227 – 231.

Nierop, K. G. J., Preston, C. M. and Kaal, J. (2005*a*), 'Thermally assisted hydrolysis and methylation of purified tannins from plants', *Analytical Chemistry* **77**(17), 5604–5614.

Nierop, K. G., Preston, C. M. and Kaal, J. (2005*b*), 'Thermally assisted hydrolysis and methylation of purified tannins from plants', *Analytical chemistry* **77**(17), 5604–5614.

Nierop, K. G., van Lagen, B. and Buurman, P. (2001), 'Composition of plant tissues and soil organic matter in the first stages of a vegetation succession', *Geoderma* **100**(1), 1 – 24.

Nikitina, D. L., Kemp, A. C., Horton, B. P., Vane, C. H., van de Plassche, O. and Engelhart, S. E. (2014), 'Storm erosion during the past 2000 years along the north shore of Delaware Bay, {USA}', *Geomorphology* **208**, 160 – 172.

Nott, C. J., Xie, S., Avsejs, L. A., Maddy, D., Chambers, F. M. and Evershed, R. P. (2000), '*n*-Alkane distributions in ombrotrophic mires as indicators of vegetation change related to climatic variation', *Organic Geochemistry* **31**(2), 231–235.

Novák, M., Buzek, F. and Adamová, M. (1999), 'Vertical trends in 13C, 15N and 34S ratios in bulk *Sphagnum* peat', *Soil Biology and Biochemistry* **31**(9), 1343 – 1346.

Opelt, K., Chobot, V., Hadacek, F., Schönmann, S., Eberl, L. and Berg, G. (2007), 'Investigations of the structure and function of bacterial communities associated with *Sphagnum* mosses', *Environmental microbiology* **9**(11), 2795–2809.

Opsahl, S. and Benner, R. (1995), 'Early diagenesis of vascular plant tissues: Lignin and cutin decomposition and biogeochemical implications', *Geochimica et Cosmochimica Acta* **59**(23), 4889 – 4904.

Ostle, N., Levy, P., Evans, C. and Smith, P. (2009), 'UK land use and soil carbon sequestration', *Land Use Policy* **26, Supplement 1**, S274 – S283.

Painter, T. J. (1991), 'Lindow man, tollund man and other peat-bog bodies: the preservative and antimicrobial action of sphagnan, a reactive glycuronoglycan with tanning and sequestering properties', *Carbohydrate Polymers* **15**(2), 123–142.

Pancost, R., Baas, M., Van Geel, B. and Damsté, J. (2002), 'Biomarkers as proxies for plant inputs to peats: an example from a sub-boreal ombrotrophic bog', *Organic Geochemistry* **33**(7), 675 – 690.

Park, J., Meng, J., Lim, K. H., Rojas, O. J. and Park, S. (2013), 'Transformation of lignocellulosic biomass during torrefaction', *Journal of Analytical and Applied Pyrolysis* **100**, 199–206.

Peberdy, J. F. (1990), *Fungal Cell Walls — A Review*, Springer Berlin Heidelberg, Berlin, Heidelberg, pp. 5–30.

Potvin, L. R., Kane, E. S., Chimner, R. A., Kolka, R. K. and Lilleskov, E. A. (2015), 'Effects of water table position and plant functional group on plant community, aboveground production, and peat properties in a peatland mesocosm experiment (peatcosm)', *Plant and soil* **387**(1-2), 277–294.

Prietzel, J., Dechamps, N. and Spielvogel, S. (2013), 'Analysis of non-cellulosic polysaccharides helps to reveal the history of thick organic surface layers on calcareous alpine soils', *Plant and Soil* **365**(1/2), 93–114.

Ran, Y., Huang, W., Rao, P., Liu, D., Sheng, G. and Fu, J. (2002), 'The role of condensed organic matter in the nonlinear sorption of hydrophobic organic contaminants by a peat and sediments', *Journal of environmental quality* **31**(6), 1953–1962.

Rasmussen, S., Wolff, C. and Rudolph, H. (1995), 'Compartmentalization of phenolic constituents in *Sphagnum*', *Phytochemistry* **38**(1), 35 – 39.

Reddy, K. R. and DeLaune, R. D. (2008), *Biogeochemistry of wetlands: science and applications*, CRC press.

Robertson, S. A., Mason, S. L., Hack, E. and Abbott, G. D. (2008), 'A comparison of lignin oxidation, enzymatic activity and fungal growth during white-rot decay of wheat straw', *Organic Geochemistry* **39**(8), 945 – 951.

Rochefort, L., Vitt, D. H. and Bayley, S. E. (1990), 'Growth, production, and decomposition dynamics of *Sphagnum* under natural and experimentally acidified conditions', *Ecology* **71**(5), 1986–2000.

Ronkainen, T., McClymont, E. L., Vliranta, M. and Tuittila, E.-S. (2013), 'The n-alkane and sterol composition of living fen plants as a potential tool for palaeoecological studies', *Organic Geochemistry* **59**, 1 – 9.

Ros, L., Gabaldón, C., Pomar, F., Merino, F., Pedreño, M. A. and Barceló, A. R. (2007), 'Structural motifs of syringyl peroxidases predate not only the gymnosperm–angiosperm divergence but also the radiation of tracheophytes', *New Phytologist* **173**(1), 63–78.

Rovira, P. and Vallejo, V. R. (2007), 'Labile, recalcitrant, and inert organic matter in mediterranean forest soils', *Soil Biology and Biochemistry* **39**(1), 202 – 215.

Rudolph, H. and Samland, J. (1985), 'Occurrence and metabolism of sphagnum acid in the cell walls of bryophytes', *Phytochemistry* **24**(4), 745–749.

Rumpel, C. and Dignac, M.-F. (2006), 'Gas chromatographic analysis of monosaccharides in a forest soil profile: Analysis by gas chromatography after trifluoroacetic acid hydrolysis and reductionacetylation', *Soil Biology and Biochemistry* **38**(6), 1478 – 1481.

Rydin, H. (1985), 'Effect of water level on desiccation of *Sphagnum* in relation to surrounding *Sphagna*', *Oikos* **45**(3), 374–379.

Rydin, H., Jeglum, J. K. and Jeglum, J. K. (2013), *The biology of peatlands*, Oxford university press.

Saariaho, A.-M., Jääskeläinen, A.-S., Nuopponen, M. and Vuorinen, T. (2003), 'Ultra violet resonance raman spectroscopy in lignin analysis: determination of characteristic vibrations of p-hydroxyphenyl, guaiacyl, and syringyl lignin structures', *Applied spectroscopy* **57**(1), 58–66.

Saiz-Jimenez, C. (1994), 'Analytical pyrolysis of humic substances: Pitfalls, limitations, and possible solutions', *Environmental Science & Technology* **28**(11), 1773–1780.

Sarkanen, K. V. and Ludwig, C. H. (1971), *Lignins. Occurrence, formation, structure, and reactions*, New York.; Wiley-Interscience.

Scalbert, A., Monties, B., Lallemand, J.-Y., Guittet, E. and Rolando, C. (1985), 'Ether linkage between phenolic acids and lignin fractions from wheat straw', *Phytochemistry* **24**(6), 1359–1362.

Schellekens, J., Bindler, R., Martnez-Cortizas, A., McClymont, E. L., Abbott, G. D., Biester, H., Pontevedra-Pombal, X. and Buurman, P. (2015a), 'Preferential degradation of polyphenols from *Sphagnum* 4-isopropenylphenol as a proxy for past hydrological conditions in *Sphagnum*-dominated peat', *Geochimica et Cosmochimica Acta* **150**, 74 – 89.

Schellekens, J., Buurman, P., Kuyper, T. W., Abbott, G. D., Pontevedra-Pombal, X. and Martnez-Cortizas, A. (2015b), 'Influence of source vegetation and redox conditions on lignin-based decomposition proxies in graminoid-dominated ombrotrophic peat (Penido Vello, NW Spain)', *Geoderma* **237-238**, 270 – 282.

Schellekens, J., Buurman, P. and Pontevedra-Pombal, X. (2009), 'Selecting parameters for the environmental interpretation of peat molecular chemistry a pyrolysis-GC/MS study', *Organic Geochemistry* **40**(6), 678 – 691.

Schipperges, B. and Rydin, H. (1998), 'Response of photosynthesis of *Sphagnum* species from contrasting microhabitats to tissue water content and repeated desiccation', *New Phytologist* **140**(4), 677–684.

Schulten, H. R. and Sorge, C. (1995), 'Pyrolysis methylationmass spectrometry of whole soils', *European Journal of Soil Science* **46**(4), 567–579.

Schwarzinger, C. (2004), 'Identification of methylated saccharinolactones and partially methylated saccharinic acids in the thermally assisted hydrolysis and methylation of carbohydrates', *Journal of analytical and applied pyrolysis* **71**(2), 501–514.

Schwarzinger, C., Tanczos, I. and Schmidt, H. (2002), 'Levoglucosan, cellobiose and their acetates as model compounds for the thermally assisted hydrolysis and methylation of cellulose and cellulose acetate', *Journal of Analytical and Applied Pyrolysis* **62**(2), 179 – 196.

Shadkami, F. and Helleur, R. (2010), 'Recent applications in analytical thermochemolysis', *Journal of Analytical and Applied Pyrolysis* **89**(1), 2–16.

Shaw, A. J. (2000), 'Phylogeny of the sphagnopsida based on chloroplast and nuclear dna sequences', *The bryologist* **103**(2), 277–306.

Shaw, A. J., Cox, C. J. and Boles, S. B. (2003*a*), 'Global patterns in peatmoss biodiversity', *Molecular Ecology* **12**(10), 2553–2570.

Shaw, A. J., Cox, C. J. and Boles, S. B. (2003*b*), 'Polarity of peatmoss (*Sphagnum*) evolution: who says bryophytes have no roots?', *American journal of botany* **90**(12), 1777–1787.

Shotbolt, L., Anderson, A. and Townend, J. (1998), 'Changes to blanket bog adjoining forest plots at Bad a Cheo, Rumster Forest, Caithness', *Geoderma* **71**(4), 311 – 324.

Silvola, J., Alm, J. and Ahlholm, U. (1992), 'The effect of plant roots on CO_2 release from peat soil', *Suo* **43**(4-5), 259 – 262.

Silvola, J., Alm, J., Ahlholm, U., Nykänen, H. and Martikainen, P. J. (1996*a*), 'The contribution of plant roots to CO_2 fluxes from organic soils', *Biology and Fertility of Soils* **23**(2), 126–131.

Silvola, J., Alm, J., Ahlholm, U., Nykanen, H. and Martikainen, P. J. (1996*b*), 'CO_2 fluxes from peat in boreal mires under varying temperature and moisture conditions', *Journal of Ecology* **84**(2), 219–228.

Smeerdijk, D. G. V. and Boon, J. J. (1987), 'Characterisation of subfossil *Sphagnum* leaves, rootlets of ericaceae and their peat by pyrolysis-high-resolution gas chromatography-mass spectrometry', *Journal of Analytical and Applied Pyrolysis* **11**, 377 – 402.

Smith, R., Charman, D., Rushton, S., Sanderson, R., Simkin, J., Shiel, R. and Marrs, R. (2003), 'Vegetation change in an ombrotrophic mire in northern england after excluding sheep', *Applied Vegetation Science* **6**(2), 261–270.

Solomon, D., Lehmann, J. and Zech, W. (2001), 'Land use effects on amino sugar signature of chromic luvisol in the semi-arid part of northern tanzania', *Biology and Fertility of Soils* **33**(1), 33–40.

Sørensen, H. (1962), 'Decomposition of lignin by soil bacteria and complex formation between autoxidized lignin and organic nitrogen compounds', *Microbiology* **27**(1), 21–34.

Spearing, A. M. (1972), 'Cation-exchange capacity and galacturonic acid content of several species of *Sphagnum* in Sandy Ridge Bog, central New York state', *The Bryologist* **75**(2), 154–158.

Speranza, A., van der Plicht, J. and van Geel, B. (2000), 'Improving the time control of the subboreal/subatlantic transition in a czech peat sequence by 14C wiggle-matching', *Quaternary Science Reviews* **19**(16), 1589 – 1604.

Srebotnik, E., Jensen, K., Kawai, S. and Hammel, K. E. (1997), 'Evidence that *Ceriporiopsis subvermispora* degrades nonphenolic lignin structures by a one-electron-oxidation mechanism.', *Applied and environmental microbiology* **63**(11), 4435–4440.

Stewart, D., Yahiaoui, N., McDougall, G. J., Myton, K., Marque, C., Boudet, A. M. and Haigh, J. (1997), 'Fourier-transform infrared and raman spectroscopic evidence for the incorporation of cinnamaldehydes into the lignin of transgenic tobacco (*Nicotiana tabacum L.*) plants with reduced expression of cinnamyl alcohol dehydrogenase', *Planta* **201**(3), 311–318.

Sutherland, W. J. (2006), *Ecological census techniques: a handbook*, Cambridge University Press.

Swain, E. Y. (2013), Molecular characterization of terrestrial organic carbon in some organic-rich soils in the northern latitudes, PhD thesis, Newcastle University.

Swain, E. Y. and Abbott, G. D. (2013), 'The effect of redox conditions on sphagnum acid thermochemolysis product distributions in a northern peatland', *Journal of Analytical and Applied Pyrolysis* **103**, 2 – 7.

Szajdak, L., Szatylowicz, J. et al. (2010), 'Impact of drainage on hydrophobicity of fen peat-moorsh soils', *Mires Peat* **6**, 158–174.

Tanczos, I., Rendl, K. and Schmidt, H. (1999), 'The behavior of aldehydesproduced as primary pyrolysis productsin the thermochemolysis with tetramethylammonium hydroxide', *Journal of Analytical and Applied Pyrolysis* **49**(1), 319–327.

Tanczos, I., Schwarzinger, C., Schmidt, H. and Balla, J. (2003), 'THM-GC/MS analysis of model uronic acids of pectin and hemicelluloses', *Journal of analytical and applied pyrolysis* **68**, 151–162.

Tarnocai, C. and Stolbovoy, V. (2006), 'Chapter 2 northern peatlands: their characteristics, development and sensitivity to climate change', *Developments in Earth Surface Processes* **9**, 17 – 51.

Troels-Smith, J. (1955), 'Karakterisering af lose jordarter. characterization of unconsolidated sediments'.

Trojanowski, J. (2001), 'Biological degradation of lignin', *International Biodeterioration & Biodegradation* **48**(1-4), 213–218.

Turrión, M.-B., Glaser, B. and Zech, W. (2002), 'Effects of deforestation on contents and distribution of amino sugars within particle-size fractions of mountain soils', *Biology and Fertility of Soils* **35**(1), 49–53.

Umezawa, T. and Higuchi, T. (1987), 'Mechanism of aromatic ring cleavage of -o-4 lignin substructure models by lignin peroxidase', *FEBS Letters* **218**(2), 255 – 260.

UNFCCC (2008), Kyoto protocol reference manual on accounting of emissions and assigned amounts, Technical report, United Nationts Framework Convention on Climate Change (UNFCCC).

UNFCCC (2017), 'The paris agreement'. [Accsessed: 29/06/17].
URL: *http://unfccc.int/parisagreement/items/9485.php*

van Breemen, N. (1995), 'How *Sphagnum* bogs down other plants', *Trends in Ecology and Evolution* **10**(7), 270 – 275.

Van Campenhout, K., Wouters, K., De Vos, B., Buurman, P., Swennen, R. and Deckers, J. (2009), 'Differences in chemical composition of soil organic matter in natural ecosystems from different climatic regions–a pyrolysis–GC/MS study', *Soil Biology and Biochemistry* **41**(3), 568–579.

van der Heijden, E., Boon, J. and Rassmussen, S. (1997), 'Sphagnum acid and it decarboxylation product isopropenylphenol as biomarkers for fossilised *Sphagnum* in peats', *Ancient Biomolecules* **12**, 93–107.

van der Heyden, E. (1994), A combined anatomical and pyrolysis mass spectrometric study of peatified plant tissues, PhD thesis, University of Amsterdam, Amsterdam.

Vane, C. H., Drage, T. C. and Snape, C. E. (2006), 'Bark decay by the white-rot fungus lentinula edodes: Polysaccharide loss, lignin resistance and the unmasking of suberin', *International Biodeterioration and Biodegradation* **57**(1), 14 – 23.

Vane, C. H., Martin, S. C., Snape, C. E. and Abbott, G. D. (2001), 'Degradation of lignin in wheat straw during growth of the oyster mushroom (*Pleurotus ostreatus*) using off-line thermochemolysis with tetramethylammonium hydroxide and solid-state 13C NMR', *Journal of Agricultural and Food Chemistry* **49**(6), 2709–2716.

Verhoeven, J. and Liefveld, W. (1997), 'The ecological significance of organochemical compounds in *Sphagnum*', *Acta Botanica Neerlandica* **46**(2), 117–130.

Verhoeven, J. and Toth, E. (1995), 'Decomposition of carex and *Sphagnum* litter in fens: Effect of litter quality and inhibition by living tissue homogenates', *Soil Biology and Biochemistry* **27**(3), 271 – 275.

von Rudolph, H. (1972), 'Identifikation der czapek schen sphagnolkristalle', *Biochemie und Physiologie der Pflanzen* **163**(1), 110–112.

Warnstorf, C. (1911), *Sphagnales-Sphagnaceae (Sphagnologia universalis)...*, Vol. 51, Engelmann.

Weber, C. A. (1902), *Über die vegetation und entstehung des hochmoors von Augstumal: im memeldelta mit vergleichenden ausblicken auf andere hochmoore der erde; eine formationsbiologisch-historische und geologische studie*, P. Parey.

Weiss, D., Shotyk, W., Rieley, J., Page, S., Gloor, M., Reese, S. and Martinez-Cortizas, A. (2002), 'The geochemistry of major and selected trace elements in a forested peat bog, kalimantan, SE asia, and its implications for past atmospheric dust deposition', *Geochimica et Cosmochimica Acta* **66**(13), 2307 – 2323.

Wellock, M. L., Reidy, B., Laperle, C. M., Bolger, T. and Kiely, G. (2011), 'Soil organic carbon stocks of afforested peatlands in ireland', *Forestry* **84**(4), 441–451.

Weng, J.-K. and Chapple, C. (2010), 'The origin and evolution of lignin biosynthesis', *New Phytologist* **187**(2), 273–285.

Wiesenberg, G. L., Gocke, M. and Kuzyakov, Y. (2010), 'Fast incorporation of root-derived lipids and fatty acids into soil evidence from a short term multiple pulse labelling experiment', *Organic Geochemistry* **41**(9), 1049 – 1055.

Williams, C. J., Yavitt, J. B., Wieder, R. K. and Cleavitt, N. L. (1998), 'Cupric oxide oxidation products of northern peat and peat-forming plants', *Canadian Journal of Botany* **76**(1), 51–62.

Williams, J. S., Dungait, J. A., Bol, R. and Abbott, G. D. (2016*a*), 'Comparison of extraction efficiencies for water-transportable phenols from different land uses', *Organic Geochemistry* **102**, 45 – 51.

Williams, J. S., Dungait, J. A. J., Bol, R. and Abbott, G. D. (2016*b*), 'Contrasting temperature responses of dissolved organic carbon and phenols leached from soils', *Plant and Soil* **399**(1), 13–27.

Worrall, F., Reed, M., Warburton, J. and Burt, T. (2003), 'Carbon budget for a british upland peat catchment', *Science of The Total Environment* **312**(1), 133 – 146.

Wysocki, L. A., Filley, T. R. and Bianchi, T. S. (2008), 'Comparison of two methods for the analysis of lignin in marine sediments: Cuo oxidation versus tetramethylammonium hydroxide (TMAH) thermochemolysis', *Organic Geochemistry* **39**(10), 1454 – 1461.

Xie, S., Nott, C., Avsejs, L., Volders, F., Maddy, D., Chambers, F. M., Gledhill, A., Carter, J. and Evershed, R. (2000), 'Palaeoclimate records in compound-specific δd values of a lipid biomarker in ombrotrophic peat', *Organic Geochemistry* **31**(10), 1053–1057.

Xu, Z., Zhang, D., Hu, J., Zhou, X., Ye, X., Reichel, K. L., Stewart, N. R., Syrenne, R. D., Yang, X., Gao, P., Shi, W., Doeppke, C., Sykes, R. W., Burris, J. N., Bozell, J. J., Cheng, M. Z.-M., Hayes, D. G., Labbe, N., Davis, M., Stewart, C. N. and Yuan, J. S. (2009), 'Comparative genome analysis of lignin biosynthesis gene families across the plant kingdom', *BMC Bioinformatics* **10**(11), S3.

Yeloff, D., Charman, D., van Geel, B. and Mauquoy, D. (2007a), 'Reconstruction of hydrology, vegetation and past climate change in bogs using fungal microfossils', *Review of Palaeobotany and Palynology* **146**(1), 102 – 145.

Yeloff, D. and Mauquoy, D. (2006), 'The influence of vegetation composition on peat humification: implications for palaeoclimatic studies', *Boreas* **35**(4), 662–673.

Yeloff, D. and Van Geel, B. (2007), 'Abandonment of farmland and vegetation succession following the eurasian plague pandemic of AD 1347–52', *Journal of Biogeography* **34**(4), 575–582.

Yeloff, D., van Geel, B., Broekens, P., Bakker, J. and Mauquoy, D. (2007b), 'Mid- to late-Holocene vegetation and land-use history in the Hadrian's Wall region of northern England: the record from Butterburn Flow', *Holocene* **17**(4), 527–538.

Younes, K. and Grasset, L. (2017), 'Analysis of molecular proxies of a peat core by thermally assisted hydrolysis and methylation-gas chromatography combined with

multivariate analysis', *Journal of Analytical and Applied Pyrolysis* **124**(Supplement C), 726 – 732.

Yu, Z., Loisel, J., Brosseau, D. P., Beilman, D. W. and Hunt, S. J. (2010), 'Global peatland dynamics since the last glacial maximum', *Geophysical Research Letters* **37**(13).

Zerva, A., Ball, T., Smith, K. A. and Mencuccini, M. (2005), 'Soil carbon dynamics in a sitka spruce (*Picea sitchensis* (bong.) carr.) chronosequence on a peaty gley', *Forest Ecology and Management* **205**(13), 227 – 240.

Zhang, X., Amelung, W., Yuan, Y., Samson-Liebig, S., Brown, L. and Zech, W. (1999), 'Land-use effects on amino sugars in particle size fractions of an argiudoll', *Applied Soil Ecology* **11**(2), 271–275.

Zhang, Y. and Banks, C. (2005), 'Factors affecting the removal of selected heavy metals using a polymer immobilised *Sphagnum* moss as a biosorbent', *Environmental Technology* **26**(7), 733–744.

Zhang, Y. and Banks, C. (2006), 'A comparison of the properties of polyurethane immobilised *Sphagnum* moss, seaweed, sunflower waste and maize for the biosorption of Cu, Pb, Zn and Ni in continuous flow packed columns', *Water Research* **40**(4), 788 – 798.

Zigang, L. and Xintu, L. (2009), *The Global Distribution of Peat*, Vol. 2, EOLSS Publications, pp. 166–402.

Zimmermann, W. (1990), 'Degradation of lignin by bacteria', *Journal of biotechnology* **13**(2-3), 119–130.

Appendices

Appendix A

Description of stratigraphy using Troels-Smith (1955) method and photos of cores for each site (0-50 cm top photo, 50-100 cm bottom photo). Stratigraphy was physically assessed on cores in 5 cm increments.

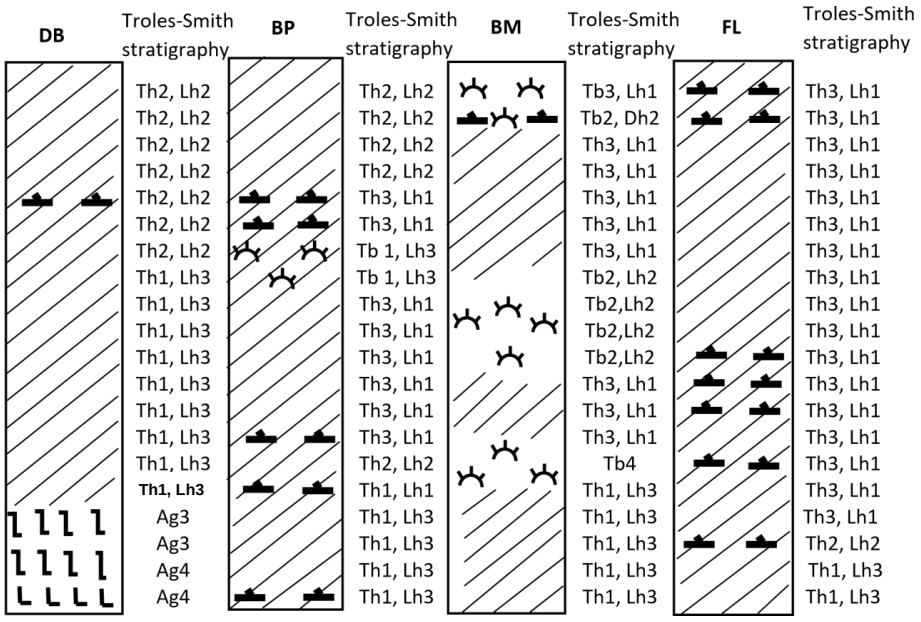

Rooted and herbaceous peat

Moss dominated peat

Peat-clay mixture

Clay

Wood fragments

Core	Notes
DB	0-80 cm dark brown peat, occasional black banding at 59, 66, 70, 76.5, 79, 80 cm. 80-90 cm beige clay, 90-100 cm grey clay
BP	0-100 cm black herbaceous except 30-40 cm light brown peat with mosses, 40-45 dark brown peat, 65-75 cm dark brown peat. 0-65 cm roots tightly packed, 25-30, 45-75 cm roots densely packed, 75100 cm roots and crumbly peat.
BM	0-100 cm black peat except for 65-75 cm gradual change from black to light brown peat and 85-90 cm light brown peat. 0-25cm living roots present, 10-40 cm root systems dense, 80-100 cm root systems loosely packed. Moss peat sections were spongy and loose.
FL	0-75 cm dense root systems, 75-90 cm roots are tightly packed, and 90-100 cm roots become loosely packed and are small fragments. Some living roots located near the top between 0-30 cm. and this area is dark brown in colour. Colour changes to black peat gradually over 30-35 cm and remains black peat for the rest of the core.

a)DB

b) BP

c)BM

d) FL

Appendix B

The equations used to determine percentage hydroxyl content of guaiacyl (1 and 2), syringyl (3 and 4) and sphagnum acid (5) thermochemolysis compounds. Equations 1-4 taken from Filley et al. (2006) with the correction highlighted in Mason et al. (2009). These equations have been applied in previous works (e.g Abbott et al. (2013) and Swain and Abbott (2013)). A table listing the thermochemolysis products as observed in the equations can be seen below;

Table 6.2: The main thermochemolysis products

Peak Label	Compound name
G5	3,4-dimethoxyacetophenone
G6	3,4-dimethoxybenzoic acid methyl ester
G18	*trans*-3-(3,4-dimethoxyphenyl)-3-propenoic acid methyl ester
G4	3,4-dimethoxybenzaldehyde
S5	3,4,5-trimethoxyacetophenone
S6	3,4,5-benzoic acid methyl ester
S4	3,4,5-trimethoxybenzaldehyde
I	4-isopropenylphenol
IIa	*cis*-3-(4-hydroxyphen-1-yl)but-2-enoic acid methyl ester
IIb	*trans*-3-(4-hydroxyphen-1-yl)but-2-enoic acid methyl ester
III	3-(4-hydroxyphen-1-yl)but-3-enoic acid methyl ester

Hydroxyl equations

1. Used to determine the original % 3-methoxyl, 4-hydroxyl content of G5, G6 and G18

$$= 100 \times \left[\frac{(M_{L+1} \; - \; (M_{L+1})_{calc})}{(M_L + M_{L+1} \; - \; (M_{L+1})_{calc}}\right]$$

where

$$(M_{L+1})_{calc} = M_L \times \left(\frac{M_{UL+1}}{M_{UL}}\right) \times \left(\frac{N_L}{N_{UL}}\right)$$

2. Used to determine the original % 3-methoxyl, 4-hydroxyl content of G4

$$= 100 \times \left[\frac{(M_{L+2})_{calc}}{(M_L)_{calc} \; + \; (M_{L+2})_{calc}}\right]$$

where

$$(M_L)_{calc} = M_{L-1} \times \left(\frac{M_{UL}}{M_{UL-1}}\right) \times \left(\frac{N_L}{N_{UL}}\right)$$

where

$$(M_{L+1})_{calc} =$$
$$\left(\left(M_L - \left(M_{L-1} \times \frac{M_{UL+1}}{M_{UL}} \times \frac{N_L}{N_{UL}}\right)\right) - \left(\left(M_{L+1} - \left(M_{L+2} \times \frac{M_{UL-1}}{M_{UL}}\right)\right) \times \frac{M_{UL-1}}{M_{UL}}\right) \frac{N_{L+1}}{N_{UL}}\right) \frac{M_{UL+1}}{M_{UL}}$$

where

$$(M_{L+2})_{calc} = \left(M_{L+1} - \left(M_{L+2} \times \frac{M_{UL-1}}{M_{UL}} \times \frac{N_{L+1}}{N_{UL}}\right)\right) - (M_{L+1})_{calc}$$

3. Used to determine the original relative amount of 1, 2, or 3 hydroxyls in S5 and S6

$$\% \text{ 1 OH} = 100 \times \frac{M_L}{M_L + [M_{L+1} - (M_{L+1})_{calc}] + [M_{L+2} - (M_{L+2})_{calc}]}$$
$$\% \text{ 2 OH} = 100 \times \frac{M_{L+1} - (M_{L+1})_{calc}}{M_L + [M_{L+1} - (M_{L+1})_{calc}] + [M_{L+2} - (M_{L+2})_{calc}]}$$
$$\% \text{ 3 OH} = 100 \times \frac{M_{L+2} - (M_{L+2})_{calc}}{M_L + [M_{L+1} - (M_{L+1})_{calc}] + [M_{L+2} - (M_{L+2})_{calc}]}$$

where

$$(M_{L+1})_{calc} = M_L \times \frac{M_{UL+1}}{M_{UL}} \times \frac{N_L}{N_{UL}}$$

where

$$(M_{L+2})_{calc} = [M_{L+1} - (M_{L+1})_{calc}] \times \frac{M_{UL+1}}{M_{UL}} \times \frac{N_{L+1}}{N_{UL}}$$

4. Used to determine the original relative amount of 1, 2, or 3 hydroxyls in S4

$$\% \text{ 1 OH} = 100 \times \frac{(M_{L-1})}{(M_{L-1}) + [(M_{L+1})_{calc}] + [(M_{L+2})_{calc}]}$$
$$\% \text{ 2 OH} = 100 \times \frac{(M_{L+1})_{calc}}{(M_{L-1}) + [(M_{L+1})_{calc}] + [(M_{L+2})_{calc}]}$$
$$\% \text{ 3 OH} = 100 \times \frac{(M_{L+2})_{calc}}{(M_{L-1}) + [(M_{L+1})_{calc}] + [(M_{L+2})_{calc}]}$$

where

$$(M_{L+1})_{calc} = M_{L+1} - \left[\left(M_L - M_{L-1} \times \frac{M_{UL}}{MUL-1}\right) \times \frac{M_{UL}}{M_{UL-1}} \times \frac{N_L}{N_{UL}} + \left(M_{L+2} - M_{L+3} \times \frac{M_{UL+1}}{M_{UL}}\right) \times \frac{M_{UL+1}}{M_{UL}} \times \frac{N_{L+1}}{N_{UL}}\right]$$

where

$$(M_{L+2})_{calc} = M_{L+2} - \left[M_{L+1} - \left(M_{L+2} - M_{L+3} \times \frac{M_{UL+1}}{M_{UL}}\right) \times \frac{M_{UL+1}}{M_{UL}} \times \frac{N_{L+1}}{N_{UL}}\right] \times \frac{M_{UL}}{M_{UL-1}}$$

5. Used to determine the original relative amount of hydroxyls/methoxyl content of the sphagnum acid products I, IIa, IIb and III

$$= 100 \times \left[\frac{(M_{L+1} - (M_{L+1})_{calc})}{(M_L + M_{L+1} - (M_{L+1})_{calc}} \right]$$

where

$$(M_{L+1})_{calc} = M_L \times \left(\frac{M_{UL+1}}{M_{UL}} \right) \times \left(\frac{N_L}{N_{UL}} \right)$$

It should be noted that in all the equations listed here, it is assumed the methoxyl carbon atom at position 4 in both the guaiacyl and syringyl thermochemolysis products is always derived from the ^{13}C-labelled methyl group as it is the location of the binding site in the -O-4 lignin linkage, which is broken during thermochemolysis, and therefore does not contain an original methoxyl group.

ML refers to abundance of the molecular ion/fragment ion of the labelled monomer contains the aryl methoxyl groups.

ML + 1 refers to abundance of the molecular ion/fragment ion of the labelled monomer that is +1 mass unit higher than ML.

NL refers to the number of C atoms in a specific ^{13}C-labelled permethylated lignin monomer that contribute to ML + 1 and M + 1.

NUL refers to the number of C atoms in a specific unlabelled permethylated lignin monomer that contribute to ML + 1 and M + 1

(ML + 1)calc refers to the calculated intensity of the molecular ion/fragment ion which is +1 mass unit higher than ML and is determined by the multiplication of ML by the ratio (M + 1)/M of the same compound obtained from unlabelled TMAH thermochemolysis, then normalized by multiplication of the ratio of NL/NUL.

(ML + 2)calc refers to the calculated intensity of the molecular ion/fragment ion which is +2 mass unit higher than ML. The difference between ML + 1 and (ML + 1)calc is used to determine the value for (ML + 2)calc and the multiplication of this difference by the ratio of (M + 1)/M, then normalized by the ratio of NL+1/NUL is the value of (ML + 2)calc.

Specifically for the G4 and S4 thermochemolysis products, the aldehyde group on the ring can also be methylated by ^{13}C-TMAH. We can get the contribution of normalized effect between ML and ML l to ML + 1, the contribution of normalized effect between ML + 2 and ML + 3 to ML + 1. (ML + 1)calc value is obtained by subtracting these two contributions from measured abundance of ML + 1. The same principles can be used in calculating (ML + 2)calc value.

Appendix C

Schematic of the methylation process of gallic acid (3,4,5-trihydroxybenzoic acid) using both ^{12}C TMAH and ^{13}C TMAH, demonstrating the purity of the synthesised ^{13}C-labelled TMAH and the successful methylation of the hydroxy groups.